



University
of Glasgow

Galban Horcajo, Francesc (2014) *The application of glycosphingolipid arrays to autoantibody detection in neuroimmunological disorders.*
PhD thesis.

<http://theses.gla.ac.uk/5030/>

Copyright and moral rights for this thesis are retained by the author

A copy can be downloaded for personal non-commercial research or study, without prior permission or charge

This thesis cannot be reproduced or quoted extensively from without first obtaining permission in writing from the Author

The content must not be changed in any way or sold commercially in any format or medium without the formal permission of the Author

When referring to this work, full bibliographic details including the author, title, awarding institution and date of the thesis must be given

The application of glycosphingolipid arrays to autoantibody detection in neuroimmunological disorders

Francesc Galban Horcajo

BSc (Hons) MSc

Thesis submitted for the degree of PhD
to the University of Glasgow,
Institute of Infection, Immunity and Inflammation.

March 2014

Author's Declaration

All experiments and results presented in this thesis are my own work unless specifically stated otherwise within the text.

Francesc Galban Horcajo, BSc (Hons) MSc

Dedication

I dedicate this thesis to my parents, Alfons and Pilar, my sister, Raquel and my mentor and friend Jesús Batlle.

*Whoever you are, I fear you are walking the walks of dreams,
I fear these supposed realities are to melt from under your feet and hands;
Whoever you are, now I place my hand upon you, that you be my poem;
I whisper with my lips close to your ear,
I have loved many women and men, but I love none better than you.*

Walt Whitman

Table of Contents

Author's Declaration	2
Dedication	3
Abstract	7
List of Tables.....	8
List of Figures	9
Definitions/Abbreviations	11
1 Chapter 1. Introduction	13
1.1 Lipids	13
1.1.1 Lipids and cell activity	15
1.1.2 Lipids and cell membrane structure	15
1.1.3 Gangliosides	17
1.2 Domain organization and Membrane Rafts.....	19
1.3 Lipids and disease	24
1.3.1 Guillain-Barré syndrome (GBS)	25
1.3.2 Multifocal Motor Neuropathy (MMN)	28
1.3.3 Chronic Inflammatory demyelinating polyneuropathy (CIDP)	30
1.4 The application of glycosphingolipid arrays to autoantibody detection in neuroimmunological disorders	31
1.4.1 Introduction	31
1.4.2 The use of covalent carbohydrate arrays for autoantibody detection	34
1.4.3 The biophysical basis for arrays of heteromeric lipid complexes ...	35
1.4.4 Conformational modulation of GSLs	36
1.4.5 <i>Cis</i> -interactions between GSLs result in the formation of neoepitopes or introduce steric hindrance	39
1.4.6 Methodological developments of combinatorial glycoarrays	40
1.5 Summary	42
2 Chapter 2. Materials and Methods	44
2.1 Monoclonal antibody production from existing cell lines	44
2.1.1 Antibody purification	45
2.2 Preparation of liposomes	46
2.3 Quantification of antibody binding to liposomes using flow cytometry .	47
2.4 Affinity Purification using liposomes	48
2.5 Enzyme linked immunosorbant assay (ELISA).....	49
2.6 Glycoarray	50
2.6.1 Slide preparation	50
2.6.2 Lipid preparation	50
2.6.3 TLC Printing and program preparation	51

2.6.4	Array probing and Analysis	53
2.7	Microarray	55
2.7.1	Microarray generation	55
2.7.2	Microarray probing	55
2.8	Mass spectrometry.....	56
2.9	Statistical methodologies	57
2.9.1	Normality test.....	57
2.9.2	Receiver Operator Characteristic (ROC) analysis	57
2.9.3	Heat map analysis	58
2.9.4	Clinical correlation studies.....	58
3	Chapter 3. Anti-GM1 antibody diversity.	59
3.1	Introduction	59
3.2	Aims	60
3.3	Results	60
3.3.1	Antibody binding to liposomes containing gangliosides.....	60
3.3.2	Affinity purification of anti-GM1 antibodies from a GBS patient (BTN) serum 68	
3.4	Discussion.....	74
3.4.1	Future technical improvements	74
3.4.2	Future prospectives	74
3.4.3	Conceptual development.....	75
4	Chapter 4. Antibodies to heteromeric glycolipid complexes in Multifocal Motor Neuropathy.	80
4.1	Introduction	80
4.2	Chapter aims	80
4.3	Southern General Hospital serology study	80
4.3.1	Study aims	80
4.3.2	Study design	81
4.3.3	Results.....	82
4.3.4	Study remarks.....	97
4.4	Cryptic behaviour of GBS/MMN-derived human monoclonal antibodies. 98	
4.4.1	Study aims	98
4.4.2	Results.....	98
4.5	Dutch MMN validation cohort (first screen).....	103
4.5.1	Results.....	103
4.5.2	Summary	113
4.5.3	Future recommendations.....	113
4.6	GalC investigations	114
4.6.1	Qualitative differences	114

4.6.2	Quantitative differences	118
4.6.3	Future recommendations.....	122
4.7	Dutch MMN validation cohort (repeat)	123
4.7.1	Study design	123
4.7.2	Results.....	123
4.7.3	Summary	127
4.7.4	Future recommendations.....	127
4.8	Discussion	128
5	Chapter 5. Antibodies to heterotrimeric glycolipid complexes in Chronic Inflammatory Demyelinating Polyradiculoneuropathy.	131
5.1	Introduction	131
5.2	Aims	131
5.2.1	Conceptual aims	131
5.2.2	Experimental aims.....	131
5.3	Study design.....	132
5.4	Results	133
5.4.1	Pilot Studies	133
5.4.2	CIDP cohort screening.....	136
5.5	Future work	146
5.6	Discussion	147
6	Chapter 6. Discussion.....	149
6.1	Modulation of antibody binding to GM1	149
6.1.1	GM1:GD1a complex inhibition as potential modulator of clinical phenotypes.....	152
6.1.2	Molecular ratios of GalC as modulators of antibody binding to GM1 156	
6.1.3	Cholesterol as potential modulator of GM1 antibody binding.....	158
6.1.4	Standardisation of the GM1:GalC assay	159
6.2	Antibodies to heterotrimeric glycolipid complexes in CIDP	162
6.3	Final remarks.....	163
6.4	In conclusion	165
7	Appendices.....	166
7.1	Buffers and solutions.....	166
7.2	Methodological development	167
7.2.1	Fluorescent slides development	167
7.2.2	Fluorescence-ECL comparison	167
7.3	Publications	170
	Bibliography	172

Abstract

Serum autoantibodies directed towards a wide range of single glycosphingolipids, especially gangliosides, in humans with autoimmune peripheral neuropathies have been extensively investigated since the 1980s and these are widely measured both in clinical practice and research. It has been recently appreciated that glycosphingolipid and lipid complexes, formed from 2 or more individual components, can interact to create molecular shapes capable of being recognised by autoantibodies that do not bind the individual components. Conversely, 2 glycosphingolipids may interact to form a heteromeric complex that inhibits binding of an antibody known to bind one of the partners. As a result of this, previously undiscovered autoantibodies have been identified, providing substantial new insights into disease pathogenesis and diagnostic testing. In particular, this newly-termed 'combinatorial glycomic' approach has provided the impetus to redesigning the assay methodologies traditionally used in the neuropathy-associated autoantibody field. Combinatorial glycoarrays can be readily constructed in house using any lipids and glycosphingolipids of interest, and as a result many new antibody specificities to gangliosides and other glycosphingolipid complexes are being discovered in neuropathy subjects. Herein we also highlight the role of the neutral lipids cholesterol and galactocerebroside in modifying glycosphingolipid orientation as two critical components of the molecular topography of target membranes in nerves that might favour or inhibit autoantibody binding.

List of Tables

Table 1.1. Milestones in lipid research.	14
Table 1.2. Enzymes involved in the biosynthetic pathway of gangliosides	19
Table 2.1. Lipids used in ELISA, Array and liposome experiments.	44
Table 4.1. Sensitivity and specificity values for GM1, GM2, GA1 and representative complexes.	87
Table 4.2. Top markers.	124
Table 5.1. Comparison of CIDP and Control populations.	140
Table 7.1. Coefficient of variation (CV) for Fluorescence and ECL.	169

List of Figures

Figure 1.1. Structure of representative sterols and GSLs.	16
Figure 1.2. Structure and biosynthetic pathway of gangliosides.	18
Figure 1.3. Top view of cell membrane bilayers.....	22
Figure 1.4. Antibody screening of MFS patient sera.	27
Figure 1.5. MMN Ab binding fingerprint.	30
Figure 1.6 Anti-glycolipid antibody binding to glycolipid complexes analysed by combinatorial glycoarray and in live tissue.....	33
Figure 1.7. Inter- and intra-molecular modulation of GSL conformation.	38
Figure 2.1. Diagram illustrating the formation of GM1-containing multilamellar vesicles (MLVs).	47
Figure 2.2. Diagramme illustrating the liposome-based methodology for antibody affinity purification from patient sera.	49
Figure 2.3. Chromacol vials illustrating the different lipid preparations.	51
Figure 2.4. Example of a programme listing the coordinates for 10 single lipids and methanol only controls on the first slide.	52
Figure 2.5. Glycoarray slide holder for TLC dispensing.....	53
Figure 2.6. TotalLab software lay out depicting the measurement of a 9x9 lipid grid.	54
Figure 2.7. Diagram illustrating the process of printing, probing with the FAST Frame and scanning the arrays.	56
Figure 3.1. Histogram representing OVA-488 positive liposomes.....	62
Figure 3.2. Cholesteryl BODIPY and liposome's fluorescence intensity.	63
Figure 3.3. Flow Cytometry data corresponding to stained GM1-liposomes.	64
Figure 3.4. Analysis of GM1:GD1a IgG antibodies in the patient JK.....	66
Figure 3.5. Histograms depicting DG1 and DG2 binding to liposomes.	67
Figure 3.6. Array illustrating the IgG antibody binding profile of BTN serum. ...	68
Figure 3.7. Affinity purification process.	70
Figure 3.8. Liposomes spotted using microarray.....	71
Figure 3.9. Glycoarray blots depicting GM1:Cholesterol mole to mole heteromeric complexes and singles lipids.	72
Figure 3.10. Arrays containing GM1 complexes with cholesterol variants probed with purified IgG GM1:Cholesterol antibody.	73
Figure 3.11. Diagram illustrating the Hypothesis of "GM1 structure change".	77
Figure 3.12. Two hypothesis for multivalent binding molecules.	79
Figure 4.1. Representative blots from glycoarray.	83
Figure 4.2. Quantitative and statistical analysis of glycoarray data.	86
Figure 4.3. Diagram illustrating Ab binding profiles found in MMN sera.....	88
Figure 4.4. Patterns of antibody binding in MMN sera.	89
Figure 4.5. Analysis of positive controls.	92
Figure 4.6. Regression analysis of GM1 and/or GM1:GalC for both glycoarray and ELISA.....	94
Figure 4.7. Comparative data of ELISA and glycoarray performance for MMN serum binding to GM1:GalC.	96
Figure 4.8. Glycoarray binding fingerprint of human mAb SM1.	99
Figure 4.9. Diagramme illustrating ganglioside molecular mimicry.....	100
Figure 4.10. Human monoclonal antibodies binding profile.....	102
Figure 4.11. Quantitative analysis of glycoarray data.	104
Figure 4.12. Statistical analysis of best performing biomarkers.....	106
Figure 4.13. Heat map representation of Dutch serology data.	108
Figure 4.14. Analysis of negative patients for overall markers.	109

Figure 4.15. Representative glycoarray blots.	110
Figure 4.16 Glycoarray and ELISA performance comparison.	111
Figure 4.17. Inter-assay variability of a control sera used during a serology study.	112
Figure 4.18. Phrenosin and Kerasin content of commercial GalC stocks.	116
Figure 4.19. Kerasin and Phrenosin structure.	117
Figure 4.20. Monoclonal antibody binding profile on ELISA.	118
Figure 4.21. The effect of GalC concentration and solubilisation in GM1:GalC complexes.	120
Figure 4.22. Comparison of different GM1 and GalC concentration.	122
Figure 4.23. Quantitative and statistical analysis of glycoarray data.	125
Figure 4.24. First and second screening correlation studies.	126
Figure 5.1. Array lay out for CIDP cohort screen.	133
Figure 5.2. Ganglioside complexes containing different GalC ratios.	133
Figure 5.3 Patterns of antibody binding in CIDP sera.	135
Figure 5.4. Galnglioside complexes with different adjuvant molecules.	136
Figure 5.5. Data from the CIDP population presented as a clustered Heat map.	137
Figure 5.6. Data from the control population presented as a clustered Heat map.	138
Figure 5.7. Representative blots from glycoarray.	139
Figure 5.8. Statistical analysis of glycoarray data for top markers.	141
Figure 5.9. Characteristic blots depicting enhanced or complex specific GM3:Sulph:Phre reactivities.	143
Figure 5.10. Heat map depicting the top markers.	144
Figure 5.11. Statistical analysis of glycoarray data for overall markers.	145
Figure 5.12. Ab binding fingerprint after the inclusion of Phre.	146
Figure 7.1. Arrays showing the differential auto fluorescent profile of two commercial 3M glues.	167
Figure 7.2. Experimental outline of combinatorial arrays using Chemoluminescence or Fluorescence as detection systems.	168
Figure 7.3. Fluorescence and ECL assay variability.	169
Figure 7.4 Detection methods employed in combinatorial glycoarrays.	170

Definitions/Abbreviations

AI - arbitrary intensity

AIDP - acute inflammatory demyelinating polyradiculopathy

BSA - bovine serum albumin

BSA bovine serum albumin

Cardio cardiolipin

Cer - ceramide

Cer ceramides

Chol cholesterol

CI - confidence interval

CIDP chronic inflammatory demyelinating polyradiculoneuropathy

CTB - cholera toxin B subunit

CV - coefficient of variation

DGG digalactosyl diglyceride

DMEM - Duplecco's Modified Eagle's medium

ECL - enhanced chemiluminescence

ELISA - enzyme linked immunosorbent assay

FBS - foetal bovine serum

GA1 - asialo-ganglioside GM1

Gal - galactose

GalC - galactocerebroside (galactosylceramide)

GalC galactocerebroside

GBS - Guillain-Barré syndrome

GD1a - disialoganglioside GD1a (Cer-Glc-Gal(NeuAc)-GalNAc-Gal-NeuAc)

GD1b - disialoganglioside GD1b (Cer-Glc-Gal(NeuAc-NeuAc)-GalNAc-Gal)

GD3 - disialoganglioside GD3 (Cer-Glc-Gal-NeuAc-NeuAc)

Glc - glucose

GM1 - monosialoganglioside GM1 (Cer-Glc-Gal(NeuAc)-GalNAc-Gal)

GM2 - monosialoganglioside GM2 (Cer-Glc-Gal(NeuAc)-GalNAc)

GM3 - monosialoganglioside GM3 (Cer-Glc-Gal-NeuAc)

GQ1b - tetrasialoganglioside GQ1b (Cer-Glc-Gal(NeuAc-NeuAc)-GalNAc-Gal-NeuAc-NeuAc)

HC healthy controls

HRP horseradish peroxidase

IgG immunoglobulin

IVIG intravenous immunoglobulin

LOS lipo-oligosaccharide

LPS lipopolysaccharide

MAG myelin associated glycoprotein

MMN multifocal motor neuropathy

NeuAc sialic acid, N-acetylneuraminic acid
OND other neurological disease
ONLS overall neuropathy limitation scale
PBS phosphate buffered saline
PC L alphaphosphatidylcholine
PNS peripheral nervous system
PVDF polyvinylidene fluoride
PVDF-Fl low fluorescence polyvinylidene fluoride
rAb recombinant antibody
SEM standard error of the mean
SM sphingomyelin
SS sphingosine
Sulph sulfatide
TLC Thin layer chromatography
w:w weight:weight

1 Chapter 1. Introduction

1.1 Lipids

Lipids were first identified in 1673 by Tachenius Otto who suggested that an acid compound was hidden in fat since the strength of alkali disappeared when making soap. Lipids were then defined as fatty acids and their derivatives, and substances related biosynthetically or functionally to these compounds.

We now know that lipids are crucial elements of the eukaryotic cell, approximately 5% of their genes being occupied directly or indirectly in lipid synthesis (van et al. 2008), making them capable of generating more than 9,000 different molecular species that actively contribute to crucial cellular activities (van, Voelker, & Feigenson 2008). Lipids can be sub-divided into different groups including: fatty acyls, glycerolipids, glycerophospholipids, sphingolipids, sterol lipids, prenol lipids, saccharolipids and polyketides (Degroote et al. 2004). Each of these groups will fulfil a different general function in the eukaryotic cell for example triacylglycerols and steryl esters act in energy storage due to their relatively reduced state, whereas polar lipids are involved in conformation of cellular membranes or acting as first and second messengers in signal transduction (Spiegel et al. 1996).

Table 1.1. Milestones in lipid research.

From the first description of lipids to the fluid mosaic model.

1673	Tachenius Otto suggested for the first time the existence of fatty acids.
1783	Fourcroy AF introduced alcohol to extract brain lipids.
1811	Vauquelin LN described the presence of phosphorus bound to fat in the brain.
1818	Chevreul ME characterizes cholesterol in bile stones .
1834	Couerbe J P Reported the first composition of the brain lipids.
1846	Claude Bernard reported lipase activity in the pancreas.
1848	Saalmüller L isolated for the first time a hydroxy fatty acid.
1895	Overton C First proposed that the cell membranes were made of lipids.
1906	Wassermann A first described an antiphospholipid antibody.
1924	Lieb H described cerebrosides as the stored glycolipids in Gaucher's disease.
1925	Bloor WR First classification of lipids.
1926	Sperry WM first cited the word Lipid in a paper.
1932	Windaus A described the full structure of cholesterol.
1933	Blix G isolated sulfatide from human brain.
1936	Thannhauser SJ chloroform:methanol (2:1) effective method for phospholipid extraction.
1938	First description of thin layer chromatography (TLC).
1941	Pangborn MC first isolates cardiolipin and described its antigenic properties.
	Klenk E first isolated and named neuraminic acid from a cerebroside fraction.
1942	Klenk E first describes gangliosides, named substance x in 1935.
	Smith EL first liquid chromatography separations of fatty acids.
1947	Carter HE first names sphingolipide to lipids containing sphingosine.
1951	Kirchner JG first time application of TLC on silica to lipidic compounds.
	Yamakawa T isolated a ganglioside containing galactose and neuraminic (GM3).
1960	Kaufmann HP described the separation of fatty acids by TLC.
1961	Shapiro D the first complete synthesis of a cerebroside reported.
1972	Bretscher MS first characterization of the membrane lipid bilayer as an asymmetric structure.
	Singer S J proposed for the first time the fluid mosaic model for membrane lipid bilayer.

1.1.1 Lipids and cell activity

From the expanding list of cellular activities in which lipids are involved signal transduction and receptor modulation are possibly the main ones.

Lipids have been described as first and secondary messengers in several studies (Carlson et al. 1994; Spiegel, Foster, & Kolesnick 1996). The process of lipid degradation is involved in signalling within the cell membrane by the action of hydrophobic lipid portions or in the case of soluble portions of the lipid molecule through the cytosol (van, Voelker, & Feigenson 2008). As first and secondary messengers lipids can regulate cellular activities and modulate receptor activation. An example of lipid-mediated receptor modulation is the close interaction of sphingolipids and cholesterol with ligand-gated ion channels and G protein-coupled receptors (eg. acetylcholine and serotonin receptors) which can lead to a major change in the receptor conformation therefore directly regulating its functionality (Fantini and Barrantes 2009). These receptors in the form of integral membrane proteins would be directly affected by the lipid environment serving as a receptor regulatory system.

1.1.2 Lipids and cell membrane structure

Although the content of lipids and variety of lipid species in cells can vary from tissue to tissue the major structural lipids in eukaryotic membranes are the glycerophospholipids including phosphatidylcholine (pc), phosphatidylethanolamine (pe), phosphatidylserine (ps), phosphatidylinositol (pi) and phosphatidic acid (pa).

Another less abundant class of structural lipids are the sphingolipids. These lipids are composed of a common backbone of ceramide (cer) which by addition of a sugar based head group forms glycosphingolipids (GSLs) the most common being galactose (galactosylceramide), sulphated galactose (sulfatide) or glucose (glucosylceramide).

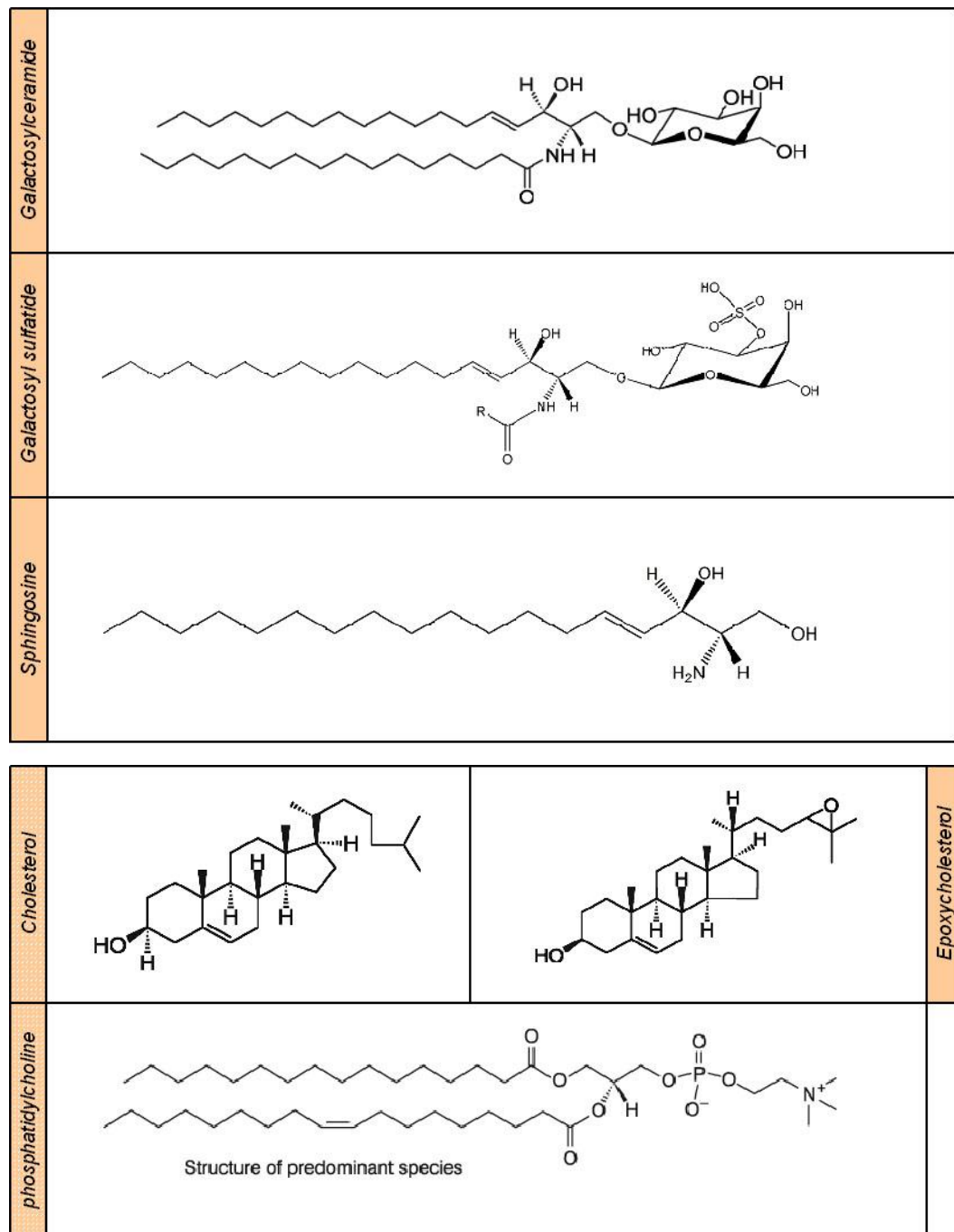


Figure 1.1. Structure of representative sterols and GSLs.

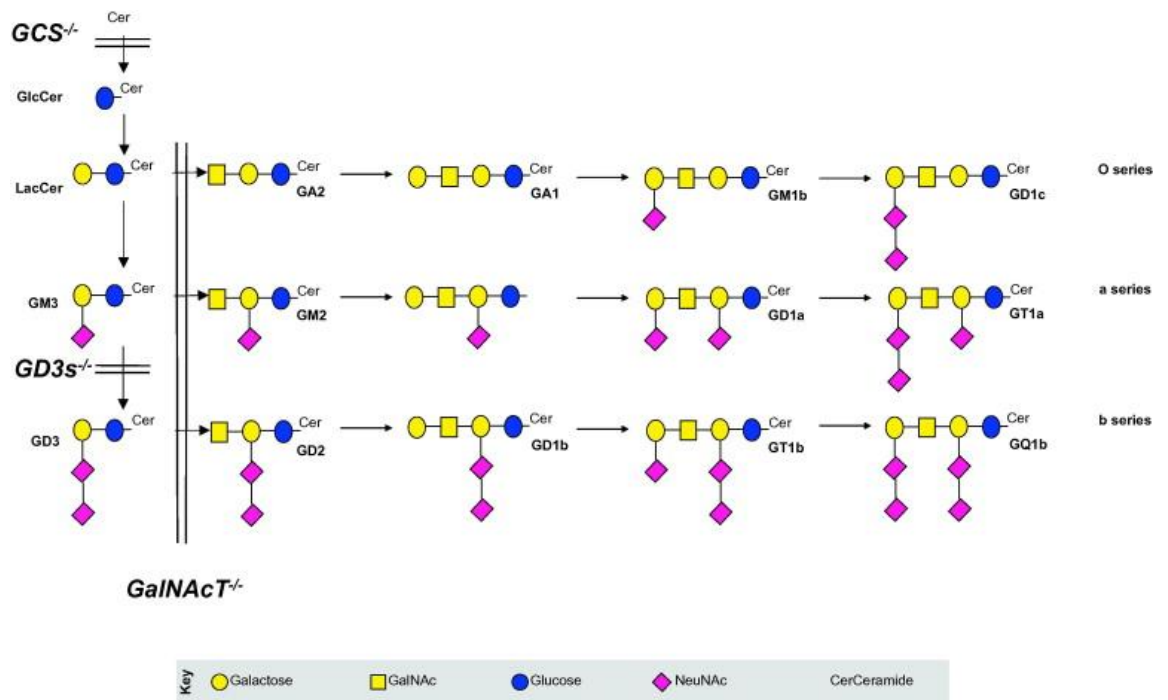
1.1.3 Gangliosides

Another highly relevant group of GSLs are the gangliosides. Gangliosides firstly described and named by Ernst Klenk in 1942 (Klenk 1970) are GSLs with terminal sialic acids and are mainly found in vertebrate peripheral nervous system (PNS) and central nervous system (CNS) tissue. The content and quantification of gangliosides in brain was first reported by Svennerholm and co-workers in 1956 establishing the relevance of these GSLs (Svennerholm 1956a;Svennerholm 1956b). In later studies the amount of ganglioside in both PNS and CNS tissue was established as 10% to 12% of the overall lipid content (Gong et al. 2002;Tettamanti et al. 1973a;Tettamanti et al. 1973b).

Chemically, gangliosides are defined as amphipathic molecules containing both a hydrophobic and a hydrophilic fraction. This ambivalent nature determines the way they are displayed within the lipid membrane. The carbohydrate moiety of the molecule protrudes into the exoplasmic surface of the cell membrane with the ceramide tail anchored within the membrane bilayer (Sonnino et al. 2007).

Gangliosides are classified according to the profile of sugars attached to the ceramide tail (Figure 1.2 A) a system of nomenclature first described by Svennerholm. This nomenclature designates an initial G indicating gangliosides, followed by the number of sialic acid residues (M=1, D=2, T=3 and Q=4) and the length of the carbohydrate sequence expressed as five minus the number of residues. The final part corresponded to the isomeric form of the sialic acid residues as a, b or c (svennerholm 1994). So, as an example, GM1b (Figure 1.2 B) would refer to a ganglioside , containing one sialic acid molecule, with 4 carbon residues and the sialic acid in conformation b.

A



B

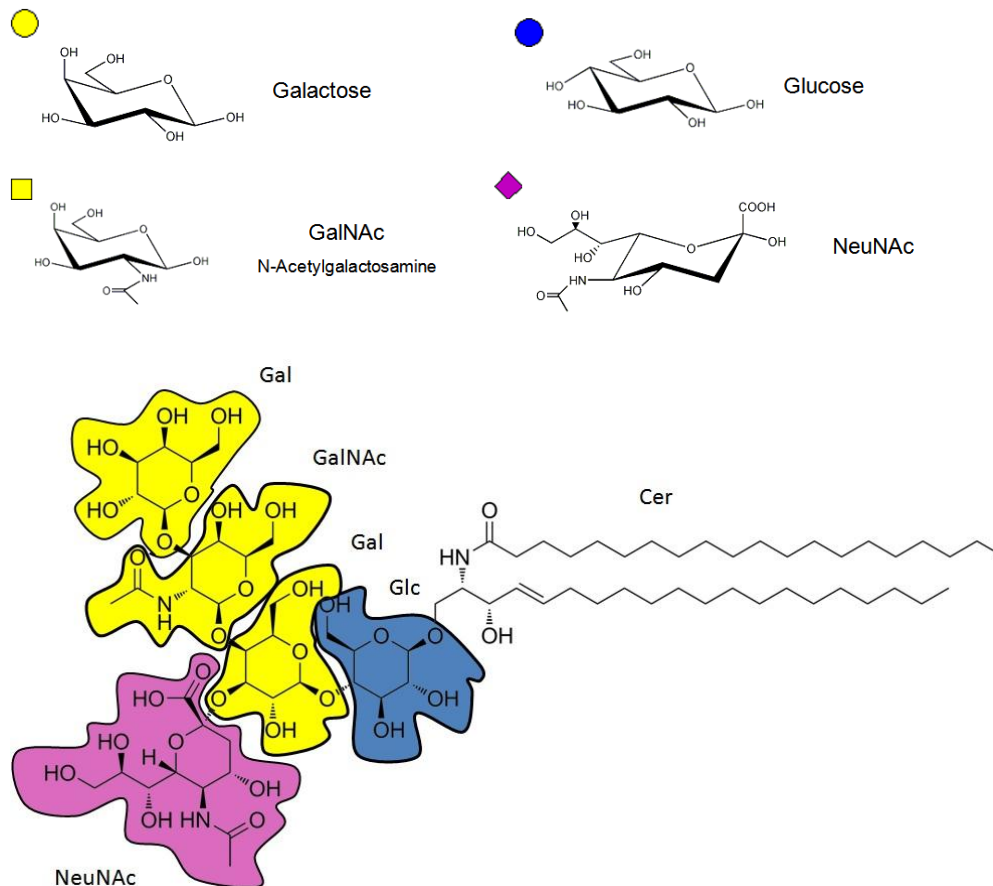


Figure 1.2. Structure and biosynthetic pathway of gangliosides.

A. Ganglioside biosynthetic pathway (adapted from (Rinaldi and Willison 2008)). B. GM1 ganglioside structure containing Galactose (Gal), Glucose (Glc), N-Acetylgalactosamine (GalNAc) and Neuraminic acid (NeuNAc).

The synthesis of gangliosides within the Golgi apparatus consists of the sequential addition of sialic acids and saccharide polymers. The addition of these molecules is catalysed by and dependent on a series of specific glycotransferases listed in Table 1.2.

Table 1.2. Enzymes involved in the biosynthetic pathway of gangliosides

Enzymes	Molecule added and position
Ceramide glucosyltransferase	Glucose
β 1,4 galactosyltransferase	β 4 Galactose
α 2,3 sialtransferase	α 3 NeuAc
α 2,8 sialtransferase	α 8 NeuAc
N-acetylgalactosaminyltransferase	β 4 GalNac
β 1,3 galactosyltransferase	β 3 Galactose

1.2 Domain organization and Membrane Rafts

The lateral organization of biomembranes has become a recurrent topic of discussion since the fluid mosaic model postulated by Singer and Nicolson in 1972 (Singer and Nicolson 1972) was challenged by the “lipid rafts” model. However, due to the heterogeneity and diversity of the field of lipid research, a clear and common definition for “lipid raft” was still the main challenge. It was not until the Keystone symposium on lipid rafts and cell function which took place on March 2006 that the research community agreed on one consistent definition for “lipid raft”. First the terminology “lipid raft” was discarded in favour of the term “membrane raft” due to the fact that the formation of these domains was not exclusively determined by lipids but by a cooperative contribution of lipids and proteins. These “membrane rafts” were then defined as “small (10-200 nm), heterogeneous, highly dynamic, sterol- and sphingolipid-enriched domains that compartmentalize cellular processes. Small rafts can sometimes be stabilized to form larger platforms through protein-protein and protein-lipid interactions” (Munro 2003). This definition introduced the necessity of establishing the key molecules intervening in raft formation, trying to elucidate the nature of their lateral organization and interactions within the domain thus opening a new line of research, lipidomics.

The road to defining membrane rafts and realising their implications has been a long one. The first studies in the early 1970s served as preliminary evidences of the existence of membrane rafts and their composition; some of these described the tendency of cholesterol (Chol) and sphingolipids to preferentially interact with each other (Oldfield and Chapman 1971; Oldfield and Chapman 1972). These results complemented data obtained from x-ray diffraction and polarized light studies of the myelin sheath of nerve suggesting that chol molecules complex with phospholipids and/or cerebroside (Finean 1954a; Finean 1954b). However, it was not until later that the presence and composition of these platforms in cell membranes was confirmed; the results of the study showed that the solubilisation of cell membranes at 4°C by non-ionic detergents such as Triton X-100 results in two clearly defined fractions: a detergent-resistant membrane fraction (DRM) rich in sphingolipids and chol and a detergent-soluble fraction, suggesting the DRM as a membrane raft domain (Simons and Ikonen 1997). Although the conclusions extracted from the “detergent-based” studies have been widely criticized and finally defeated, for being a highly artificial and subjective approach which could even induce the formation of membrane domains (Fastenberg et al. 2003; Shogomori and Brown 2003), it was these results and some others (Kenworthy and Edidin 1998) which first suggested the existence of small dynamic entities in cell membranes controlled and regulated by the presence of chol and sm (sphingomyelin). Therefore, it was assumed that lipids were structural building elements involved in maintaining cell membrane consistency. Although this definition for the purpose of the lipid presence in cell membranes explained their relevance in cellular physiology it did not suggest the direct intervention of lipids in cellular activities. However, we now know that lipids can act as functional entities in cellular functions. Evidence suggested that lipids can play a major role as cell surface receptors (Fishman et al. 1980; Fishman and Atikkan 1980), precursors of bioactive molecules (Koumanov et al. 2002) or function as secondary messengers (Hakomori and Igarashi 1995).

One example of membrane rafts are the glycosphingolipid (GSL) enriched microdomains. GSLs due to their high melting temperature tend to cluster forming ordered subcellular domains (Fantini et al. 2000; Fantini 2003). The possible functional implications of these GSL platforms and their role as surface receptors in cell recognition has been widely studied. A good example is the

characterization in the early 80s of a GSL domain as a binding site for cholera toxin; the study described the affinity of this bacterial toxin for GM1 (monosialotetrahexosylganglioside) ganglioside included in the membrane raft (Fishman, Pacuszka, Hom, & Moss 1980; Fishman & Atikkan 1980).

In order to exert any of the biological functions specified above lipids need to be organized in dynamic microdomains. These subcellular domains are created by the association of particular molecular species of membrane lipids, more ordered than the surrounding lipids composing the cell membrane. This specific domain composition will consist of lipids acting as stabilizer components of the membrane raft and lipids directly intervening in biological processes such as cell to cell recognition. Initial studies pointed to the role of chol and sm acting as a raft stabilizer (Wolf et al. 2001). Wolf and co-workers described in their work how a hydrogen bond network was established between the 3 β -OH group of chol and the amide-linkage in sm. These results supported those of Bittman and co-workers (Bittman et al. 1994). This work used the substitution of the amide-linked fatty acid in sm for a carbonyl ester-linked acyl chain in a chol/sm subdomain to confirm the looseness of domain integrity. In addition to this, data indicating that chol interacted favourably with all the physiologically relevant forms of sm (eg. 16:0, 18:0, 24:0 as well as 24:1 fatty acids in the N-linked position) implied that other forces other than Van der Waals attractive forces and hydrophobic interactions were involved in the formation of a chol:sm dynamic interaction within the raft (Ramstedt and Slotte 1999). The hydrogen bond network was then elucidated as the most plausible explanation for the domain stability and dynamics.

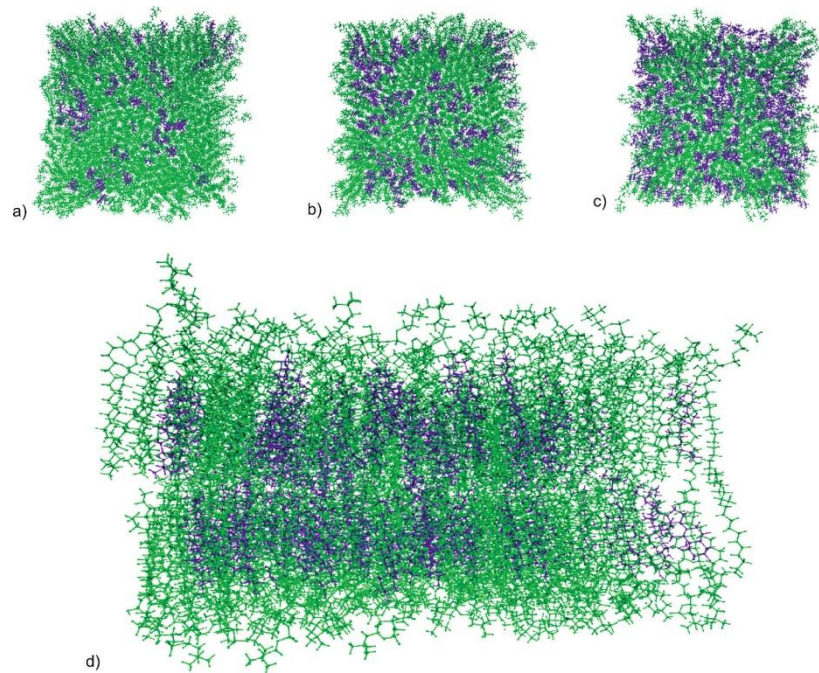


Figure 1.3. Top view of cell membrane bilayers

including different Chol (violet)/sm (18:0) (green) molar ratios (a) 20/80, (b) 35/65, and (c) 40/60. (d) Side view of (b) (Zidar et al. 2009).

Although the interaction between chol and sm was accepted by some in the formation and long-term maintenance of subcellular raft domains, several studies argued with the hypothetical involvement of chol in the formation of sm domains highlighting a possible lateral demixing effect exerted by chol within the raft (Radhakrishnan 2010). Therefore, chol would be having an attenuating effect on domain formation; this chol-induced negative effect on raft formation was observed by Milhiet and co-workers on domain formation for renal brush border membranes (Milhiet et al. 2001; Milhiet et al. 2002). Other studies tried to define the role of chol in raft formation by extracting it from the domains. Veatch & Keller found that chol exclusion from the domain instead of disrupting the raft structure tended to increase its size, demonstrating that the generation of functional domains is possible in the absence of high concentrations of chol (Veatch and Keller 2005a; Veatch and Keller 2005b).

After shifting from the idea of Chol as an essential building block in the sm containing microdomains, the majority of the research then focussed on finding another element which could stabilize the rafts by establishing a partnership with sm. The generation of membrane domains was finally observed in lipid bilayer models containing different ratios of sm and phosphatidylcholine (pc) even without the presence of chol (Prenner et al. 2007). Furthermore, this study

reiterated the importance of Sm:pc molar ratios within the domain as a critical factor in defining the formation and functional properties of the subcellular domain. The molar threshold for domain formation in a liquid ordered phase (l_0) was then established for lipid mixtures containing sm and pc molar % above 30 mol % (Prenner, Honsek, Honig, Mobius, & Lohner 2007) and mixtures including sm and/or chol molar % above 30 mol % (Zidar, Merzel, Hodoscek, Rebolj, Sepcic, Macek, & Janezic 2009). It would seem that the studies so far had not managed to give a conclusive answer to the minimum requirements to form a functional GSL raft. A deeper insight into the chol role in GSL domains was achieved when the cytolytic activity of a protein, Ostreolysin, isolated from the fruiting bodies of the mushroom *Pleurotus ostreatus* was found to be directly affected by the content and accessibility of chol in a sm:chol membrane domain (Rebolj et al. 2006). Overall, it would seem that cholesterol instead of directly regulating the formation of sm domains could be regulating the raft functionality and influencing the physical state and packing density of phospholipids (Bjorkbom et al. 2007; Bjorkbom et al. 2010). In terms of internal raft networking and lipid-lipid interactions it could be concluded that Van der Waals' forces could be established between the saturated acyl-chains of the sphingolipids and possible hydrogen bonding in the head group between sphingolipids and/or chol (Dobrowsky 2000; Dobrowsky and Gazula 2000).

So far the composition and distribution of lipids within the rafts has been discussed with the understanding that the membrane domains are three-dimensional entities. Although membrane domains are relatively stable, evidence has shown that they are dynamic structures (Pike 2006). Taking into account the dynamic nature of membrane rafts some research groups pointed out the necessity to introduce a fourth dimension in the domain's composition, time. This fourth dimension would define rafts not as static functional entities localized on a specific cell fraction but as dynamic domains whose appearance would be subjected to cell membrane composition and lipid fluctuations (Pike 2006).

I have described what it is known about the formation and stability of the rafts and how critical they are in the raft-dependent cellular activities and tissue integrity, but what would happen if the membrane microdomain architecture

was somehow disrupted, what would be the implications of losing membrane raft consistency in terms of cellular activity and homeostasis?

1.3 Lipids and disease

Lipids belonging to the same group can have internal subtle variation in structure and composition. This variation can be due to changes following lipid synthesis, for example differential hydroxylation patterns on the fatty acid chain forming the ceramide (cer) in glycolipids (Sandhoff and Kolter 2003). It is known that in the case of galactosylceramide (galC), hydroxylation is a highly recurrent modification. The most abundant form of hydroxylation in galC occurs at the α -Carbon atom of the fatty acid moiety (Degroote, Wolthoorn, & van 2004). The enzyme responsible for the formation of α -hydroxylated galc is called fatty acid 2-hydroxylase (FA2H) (Eckhardt et al. 2005). Research in mice lacking 2-hydroxylated sphingolipids has shown that up to 5 months the presence of hydroxylated sphingolipids is not necessary for the development of normal compacted myelin. However, mice up to 18 months old lacking 2-hydroxylated sphingolipids presented severe myelin sheath degeneration in the spinal cord and a pronounced loss of consistency of myelin in sciatic nerve (Zoller et al. 2008). In addition to this, Dick and co-workers associated severe neurodegeneration in patients suffering a progressive spasticity and weakness of the lower limbs included in the diagnostic group of Hereditary spastic paraplegia (HSP) to a mutation in the gene encoding FA2H (Dick et al. 2010). These results together suggested that the hydrogen bonding network created by lateral interaction of hydroxylated lipids is a key mediator of long term maintenance of domain stability (Zoller, Meixner, Hartmann, Bussow, Meyer, Gieselmann, & Eckhardt 2008).

Although lipid accumulation in motor and sensory nerve cell membranes has been identified as an important mechanism in the cause and progression of several neurodegenerative diseases such as Niemann-Pick and metachromatic leukodystrophy (MLD) (Gieselmann et al. 2003) there are other mechanisms which dramatically disrupt membrane domain architecture causing disorganization of myelin components and causing demyelination and neurodegeneration. One of these demyelinating mechanisms is based on auto-antibody recognition of lipid-based structures localized in membrane domains of

peripheral nerves; this mechanism seems to be involved in the progression of a particular group of disorders known as Guillain-Barré syndrome (GBS) and another neuropathy known as Multifocal Motor Neuropathy (MMN). In the case of neurons, the antibody targeting of lipids causes cell death via the complement-induced formation of MAC (membrane attack complex) pores causing a wide range of neuropathies. The involvement of antibodies targeting lipids in some neuropathies was described more than 20 years ago (Ilyas et al. 1988b). However, the way in which lipids behave in the cellular membrane was poorly understood. Lipids were still considered as individual entities forming an exclusive individual epitope. It was not until 2004 that Kaida and co-workers described lipid complexes originating from cis-interactions of two different lipid species as novel targets for antibodies involved in neural injury (Kaida et al. 2004). The definition of antibody lipid targets as possible heteromeric complexes was an important breakthrough in understanding a group of neuropathies which are more closely aligned to the complex arrangement of lipids found in the cell membrane.

1.3.1 Guillain-Barré syndrome (GBS)

1.3.1.1 Introduction

The characteristic phenotype of this neuropathy consists of: peripheral sensory symptoms and ascending motor weakness with loss of tendon reflexes.

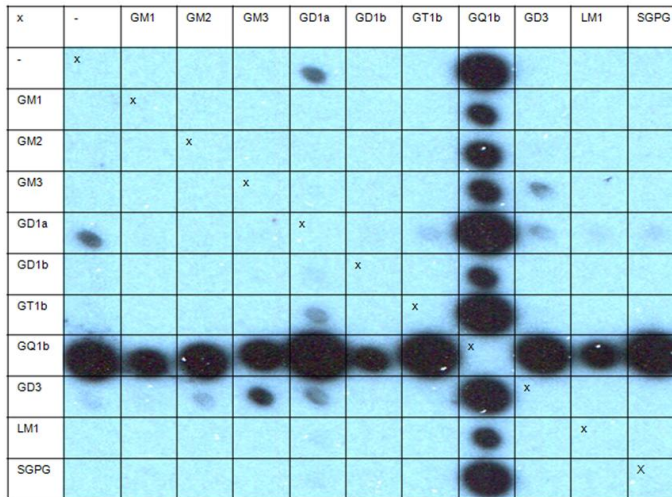
It has been reported that approximately two thirds of GBS patients develop the disease following an infection with a pathogen, the most common being *Campylobacter jejuni* enteritis (Ang et al. 2004;van Doorn et al. 2008).

GBS has been characterised as presenting a wide variety of clinical subtypes. All these subtypes are defined according to their differential clinical phenotypes and pathology. These include: acute inflammatory demyelinating polyneuropathy (AIDP), acute motor and axonal neuropathy (AMSAN), acute motor axonal neuropathy (AMAN) and Miller-Fisher Syndrome (MFS) (Kaida and Kusunoki 2010;Plomp and Willison 2009).

1.3.1.2 GBS phenotypes and anti-ganglioside antibodies

Clinically, the presentation of different GBS phenotypes correlates with differential antibody profiling in patient sera (Kaida & Kusunoki 2010). It has been suggested that this is due to ganglioside distribution across the PNS and the specific site of injury which then leads to a specific disease phenotype. One well defined example would be that of MFS. MFS which has been associated with IgG antibodies against GQ1b ganglioside is clinically characterised by ataxia, areflexia and ophthalmoplegia (Chiba et al. 1993). Lipid profiling of cranial nerves and spinal nerve roots revealed that GQ1b was characteristically enriched in the oculomotor, trochlear and abducens nerves. This lipid profiling correlates with the specific sites of injury required for the development of MFS. In addition to this, anti-GQ1b mAb binding revealed specific localised binding to the paranodes of these nerves (Chiba, Kusunoki, Obata, Machinami, & Kanazawa 1993; Chiba et al. 1997). Subsequent work by Halstead and co-workers (Halstead et al. 2004) demonstrated anti-GQ1b binding to motor nerve terminals in tissue preparations and the capability of these antibodies to fix complement. Other studies confirmed the existing link of IgG antibodies against GM1, GD1a or GalNAc GD1a and their combinations with the motor axonal forms of GBS (AMAN and AMSAN) (Hadden and Hughes 1998).

ACUTE



CONVALESCENT

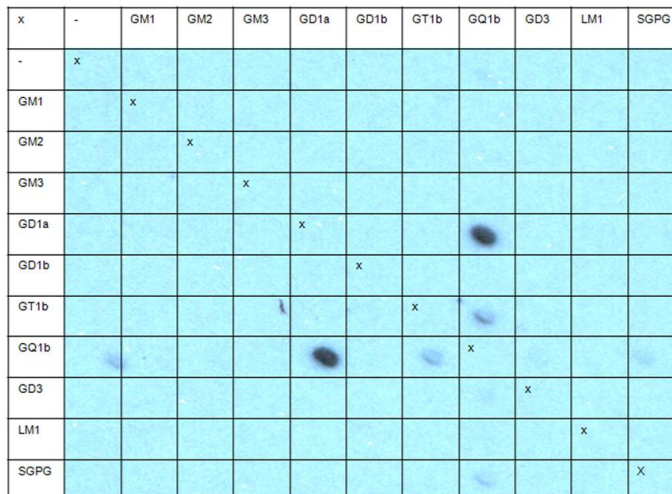


Figure 1.4. Antibody screening of MFS patient sera.

Combinatorial glycoarray demonstrating the anti-GQ1b IgG reactivity of patient serum (1:100) in the acute and convalescent phase of the illness. Combinatorial glycoarrays are designed to identify antibody reactivity to single glycolipids (duplicated in top row and left-hand row) and 1:1 glycolipid complexes (remainder of grid). A line of symmetry runs top left to bottom right, representing analysis in duplicate. In the acute phase serum, strong reactivity to GQ1b is seen that is not substantially enhanced or inhibited when in complex with other glycolipids. In the convalescent serum, anti-GQ1b antibody activity is no longer detectable, except for a low antibody signal for the complex of GQ1b with GD1a.

This evidence, in addition to the recovery after IVIG and/or plasma exchange (PE) treatment, would suggest the direct implication of antibodies in the development of the disease.

Among the different variants of GBS, AIDP is the only one which has not been associated with a significant anti-ganglioside antibody reactivity (Kusunoki et al. 2008; Plomp & Willison 2009).

1.3.1.3 Antibodies against heterodimeric complexes

In an attempt to elucidate the antibody profile of GBS patients negative for Abs binding to single ganglioside epitopes, Kaida and co-workers explored the existence of heterodimeric complexes of gangliosides as targets for neuropathy related antibodies.

The screening of a population consisting of 100 GBS patients revealed 8% of cases presenting IgG antibodies directed against a ganglioside complex formed by GD1a and GD1b but not to the gangliosides alone (Kaida, Morita, Kanzaki, Kamakura, Motoyoshi, Hirakawa, & Kusunoki 2004). This study helped to redefine GBS cases thought to be antibody negative, and strengthened the idea of GBS as an Ab driven disease.

A subsequent study on a cohort of 234 GBS patients found 17% of patients with a detectable IgG reactivity against GSL complexes such as GD1:GD1b, GM1:GD1a, GD1b:GT1b, GM1:GT1b and GM1:GD1b. Among these complexes, GD1a:GD1b and GD1b:GT1b were associated with a characteristic disease phenotype consisting of disability and the requirement for mechanical ventilation (Kaida et al. 2007).

1.3.2 Multifocal Motor Neuropathy (MMN)

MMN was first described by three different research groups (Parry and Clarke 1988) (Roth et al. 1986) (Chad et al. 1986). These groups reported the existence of a cohort of patients presenting a pure motor neuropathy, electrophysiologically characterized by the presence of multifocal persistent conduction blocks on motor but not sensory nerves.

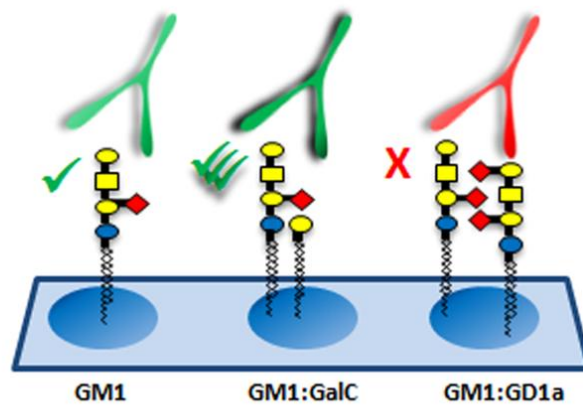
Antibodies to GM1 ganglioside were first identified in multifocal motor neuropathy (MMN) sera by Pestronk and colleagues almost 25 years ago (Pestronk et al. 1988). Since then, extensive studies have examined the sensitivity and specificity of anti-GM1 IgM antibody detection in MMN in contrast to related neurological disorders and healthy control populations (Adams et al. 1991; Kornberg and Pestronk 1994; Pestronk and Li 1991), using a wide range of different assay methodologies (Alaadini and Latov 2000; Bech et al. 1994; Carpo et al. 1999; Chabraoui et al. 1993; Willison et al. 1999). Studies including MMN diagnosed patients have found variable proportions of patients with anti-GM1

antibodies ranging from 31% (Kinsella et al. 1994;Sadiq et al. 1990) to 78% (Chaudhry 1998). Although no uniform consensus on methodology has been achieved, in part due to differences in defining patient populations and the lack of standardised assay guidelines, it is widely accepted that IgM antibodies to GM1 do occur in a significantly higher proportion of MMN cases compared with control groups (Baumann et al. 1998;Nobile-Orazio et al. 2005). Therefore, due to the potential implication of antibodies in the development of the disease, patients diagnosed with MMN were first successfully treated with immune therapy (Pestronk, Cornblath, Ilyas, Baba, Quarles, Griffin, Alderson, & Adams 1988;van Asseldonk et al. 2005).

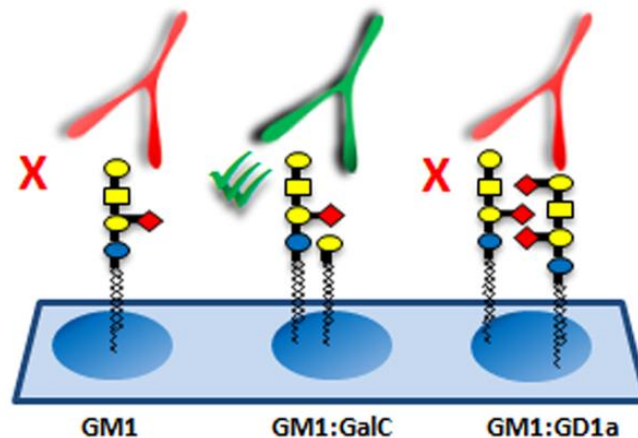
However, the clinical utility of antibody testing and its predictive value in clinical course and treatment responsiveness remain debated. In the case of MMN, the lack of a definitive antibody marker, defining the majority of disease cases, and the absence of a differential disease phenotype between antibody-positive and negative cases has fed this debate.

One long-standing consideration in assay design has been varying the antigen composition to include ‘accessory’ lipids that might enhance or attenuate the detection of anti-GM1 antibody binding revealing a new binding ‘fingerprint’. Many studies have shown that accessory lipids or liposomal GM1 preparations markedly affect anti-GM1 antibody detection exerting an epitope unmasking effect (Willison et al. 1994). Pestronk previously detected enhanced MMN antibody binding to GM1 in the presence of galactocerebroside (GalC) (Pestronk et al. 1997), results recently validated by two independent laboratories (Galban-Horcajo et al. 2013;Nobile-Orazio et al. 2013), and Greenshields observed inhibition of anti-GM1 binding to GM1 in the presence of GD1a using MMN-derived human monoclonal antibodies (Greenshields et al. 2009;Paterson et al. 1995), a finding subsequently confirmed using MMN patient sera (Nobile-Orazio et al. 2010). In addition to previous findings by Pestronk, the recent observations by Kaida on ganglioside complexes has led to renewed interest in the roles of accessory lipids and glycolipids in influencing antibody binding to GM1 (Kaida, Morita, Kanzaki, Kamakura, Motoyoshi, Hirakawa, & Kusunoki 2004;Kaida & Kusunoki 2010).

A

MMN Antibody binding fingerprint

B

**Figure 1.5. MMN Ab binding fingerprint.**

Two potential Ab-GSL binding scenarios characteristic of MMN patients. A. In the first example, the anti-GM1Abs bind GM1 as a single GSL (green ticks), binding to GM1 is affected by the presence of a second GSL (red ticks for the GM1:GD1a complex) and thus exhibits complex-inhibition. In contrast, in the presence of GalC, binding to GM1 is cis-enhanced (green ticks). B. In the second example, binding to GM1 solely occurs in the presence of GalC but not when presented as a single epitope (GM1:GalC green tick).

These data suggest the potentially cryptic nature of glycolipid epitopes bound by anti-GM1 antibodies, thus offering a new line of investigation attempting to re-define the presence of anti-glycolipid antibodies in the ‘antibody-negative’ MMN cases.

1.3.3 Chronic Inflammatory demyelinating polyneuropathy (CIDP)

CIDP is an acquired disease affecting the PNS characterised by demyelination. The disease phenotype consists of progressive or relapsing weakness and impaired sensory function in the upper and lower limbs (McCombe et al. 1987).

To a significant extent CIDP patients respond well to immunotherapies. Among these therapies the most efficient are intravenous immunoglobulin (IVIG) and plasma exchange (PE) (Dyck et al. 1986;Lunn and Willison 2009). These empirical observations give support to the idea that CIDP is an autoimmune condition with myelin as the likely antibody target.

Another indication of the antibody-mediated nature of CIDP was the generation of a chronic experimental autoimmune neuritis CIDP (CIDP-EAN) model after immunising rabbits with bovine galactocerebroside (Saida et al. 1979). After localised injection of the resulting anti-galactosylcerebroside sera, demyelinating lesions localised within the PNS started appearing in rabbit sciatic nerve (Saida, Saida, Brown, & Silberberg 1979). These observations were further supported by the inhibition of the demyelinating process in the CIDP-EAN model following complement inactivation (Sumner et al. 1982). Antibodies against galactosylcerebroside have not been found in serology studies in CIDP patients, however an early study suggested the presence of antibodies against sulphated galactosylcerebroside in a significant proportion (Fredman et al. 1991). Other major GSL antibody targets have been found in serology studies LM1, GD1a and SGPG (Fredman, Vedeler, Nyland, Aarli, & Svennerholm 1991;Ilyas et al. 1992;Willison and Yuki 2002).

1.4 The application of glycosphingolipid arrays to autoantibody detection in neuroimmunological disorders

1.4.1 Introduction

A significant number of human subjects with autoimmune peripheral neuropathy harbour serum IgG and IgM autoantibodies (neuropathy-associated antibodies, N-Abs) to glycosphingolipids (GSLs) which are present in peripheral nerves (Kaida & Kusunoki 2010;Rinaldi 2013;Rinaldi & Willison 2008;Willison & Yuki 2002). In the acute disorder termed Guillain-Barré syndrome (GBS), the anti-GSL antibodies cause patterns of paralysis that can be recapitulated in animal models, attesting to their clinical and pathological significance(Plomp & Willison 2009). Over 20 individual GSL species have been reported as antigens in GBS and allied chronic disorders; for example the GBS variant termed acute motor axonal neuropathy is

highly associated with anti-GM1 and -GD1a N-Abs, and the Miller Fisher syndrome variant with anti-GQ1b and -GT1a N-Abs. Despite this major advance in knowledge, in many neuropathy cases anti-GSL autoantibodies remain undiscovered, although there are strong hypothetical grounds for assuming their presence. Measuring N-Abs is widespread for diagnostic purposes, notwithstanding methodological shortcomings. Conventionally, in house or commercially available enzyme linked immunosorbent assays (ELISAs, usually 96 well plate format) or nitrocellulose dot blots or strip assays are used, in which a small range of 6-10 purified GSLs as the adhered antigens are probed with neuropathy sera. Until recently, the emphasis has been on analyzing N-Ab reactivity to highly purified, single species of GSLs. Although longstanding studies have highlighted the importance of accessory lipids and liposomal environments in influencing GSL antibody binding, incorporating the necessary modifications to achieve multimeric composition in routine assays has not been widely implemented in reproducible protocols (Rinaldi et al. 2012). Recent observations have led to a renaissance of interest in this area of multimeric lipid complexes as N-Ab targets (Kaida and Kusunoki 2013). Firstly, it was discovered that pairs of GSL can interact in 1:1 molar ratios to form heteromeric complexes that enhance binding of N-Abs (Kaida, Morita, Kanzaki, Kamakura, Motoyoshi, Hirakawa, & Kusunoki 2004; Kaida et al. 2008; Mauri et al. 2012). Secondly, it was discovered that GSL complexes that form naturally in live nerve membranes can inhibit binding of certain N-Abs to single GSLs, rendering them pathologically harmless, as summarised in Figure 1.6 (Greenshields, Halstead, Zitman, Rinaldi, Brennan, O'Leary, Chamberlain, Easton, Roxburgh, Padiani, Furukawa, Furukawa, Goodyear, Plomp, & Willison 2009). These enhancing and inhibiting GSL complexes form on solid phase matrices such as microtitre wells, thin layer chromatography plates and nitrocellulose or polyvinylidene difluoride (PVDF) membranes, and can thereby be analysed using modified immunoassay techniques (Kusunoki et al. 2007). When considering the potentially vast combinatorial diversity of heteromeric or multimeric GSL and lipid targets, these new perspectives open up substantial challenges that impact on the design and detection methodologies for N-Abs, on which this thesis is focussed.

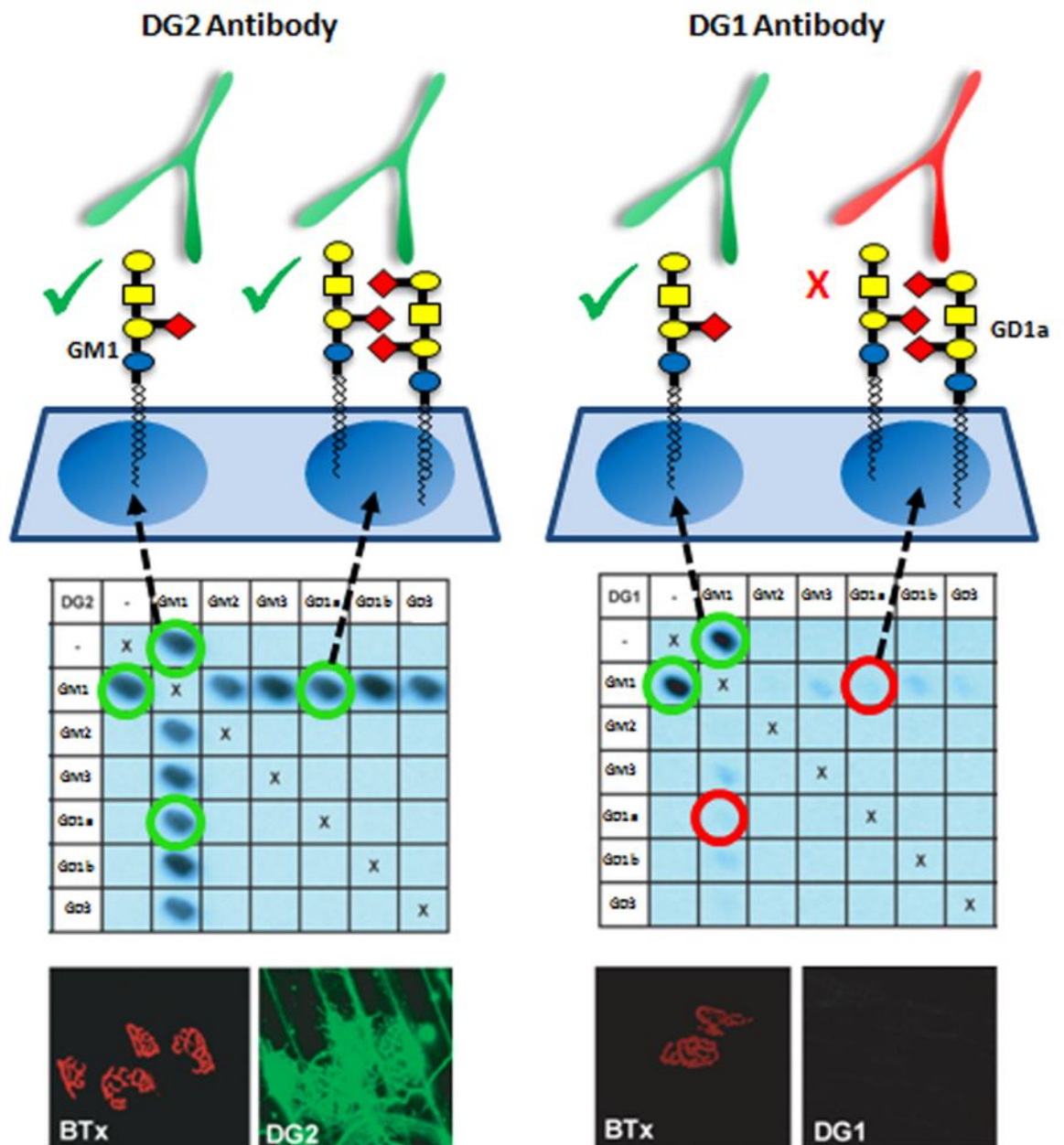


Figure 1.6 Anti-glycolipid antibody binding to glycolipid complexes analysed by combinatorial glycoarray and in live tissue.

Combinatorial glycoarray grids are printed in duplicate with single GSLs and their 1:1 heteromeric complexes. In each 6x6 grid, a diagonal line of symmetry runs from top left to bottom right, with the single GSLs printed in the outermost left hand column and uppermost row and the complexes duplicated at two unique XY coordinates within the grid. The mouse anti-GM1 mAbs, DG1 and DG2 both bind GM1 as a single GSL (green circles in outermost rows/columns). DG2 binding to GM1 is unaffected by the presence of a second GSL (circled in green for the GM1:GD1a complex) and thus exhibits complex-independent binding. In contrast, DG1 is inhibited from binding GM1 by the presence of GD1a (circled in red) and all other GSLs depicted.

In live nerve-muscle tissue preparations (bottom row, 4 panels), fluorescently conjugated bungarotoxin (BTx, red) was used to delineate the region of the neuromuscular synapse and the presence of DG1 or DG2 antibody binding was detected with fluorescently conjugated anti-mouse IgG antibody (green). DG2 readily binds to GM1-containing membranes in the synaptic region, whereas DG1 does not. These data indicate that although both DG1 and DG2 bind GM1 as a single GSL, cis-interactions between GM1 and other GSLs are capable of masking the target epitope within GM1 for DG1, but do not interfere with the epitope for DG2 (adapted from (Greenshields, Halstead, Zitman, Rinaldi, Brennan, O'Leary, Chamberlain, Easton, Roxburgh, Pediani, Furukawa, Furukawa, Goodyear, Plomp, & Willison 2009)). Epitope masking by GSL cis-interactions thus occurs for DG1 both in solid phase assay and biologically intact membranes.

1.4.2 The use of covalent carbohydrate arrays for autoantibody detection

Many carbohydrate arrays have been developed for high-throughput screening (HTS) of autoantibody responses in recent decades. Each approach is methodologically varied to achieve array designs that are tailored to specific research field perspectives, including immune response profiling (Oyelaran et al. 2009b), drug development (Kaufmann et al. 2011) and detection of viral (de Geus et al. 2013) and parasite (Aranzamendi et al. 2011) infection in sera. A key distinguishing feature of assay platforms has been the application of covalent or non-covalent binding methodology for glycan immobilisation. Covalent immobilisation arrays employ a derivatized solid surface, either containing hydrophobic linkers or photo-labile groups, to achieve the immobilisation of modified (Harris et al. 2009) or unmodified (Wang et al. 2007) glycans. These arrays have the advantage of probing a fixed amount of glycan at pre-determined, variable density (Disney and Seeberger 2004). This approach is highly applicable to areas such as IgM antibody and toxin profiling where multivalent binding plays a major role in amplifying the avidity of interaction (Godula and Bertozzi 2012; Wehner et al. 2013). The binding of lectins is also dependent upon the density and molecular distribution of their glycan ligand, lending them well to analysis by covalent glycan arrays where density of binding to protein supports such as BSA can be controlled (Narla and Sun 2012; Oyelaran et al. 2009a; Zhang et al. 2010). With respect to N-Abs, covalent linkage of GM1 to ELISA plates has been used to detect anti-GM1 IgM antibodies, but with conflicting data on improvements in sensitivity and specificity achieved in comparison with conventional non-covalent ELISA methods (Carpo, Allaria, Scarlato, & Nobile-Orazio 1999; Pestronk and Choksi 1997). GM1-sepharose and disialylgalactose-sepharose (NeuAc(α 2-8)NeuAc(α 2-3)Gal-sepharose) conjugates have also been shown to bind anti-GM1 and GQ1b IgG and IgM N-Abs respectively, although some N-Abs that bind the native GSL appear unable to bind the glycan-sepharose conjugate, indicating that the display of the sepharose-conjugated glycan may not be optimal in comparison with non-covalently adhered GSLs (Townson et al. 2007; Willison et al. 2004).

1.4.3 The biophysical basis for arrays of heteromeric lipid complexes

When considering how one might apply array design to detecting heteromeric lipid complexes as N-Ab targets, the issue of scale requires foremost consideration. In excess of 300 different species of glycosphingolipids (GSLs) have been identified, based on their carbohydrate chain structure (Degroote, Wolthoorn, & van 2004). An array of all heteromeric complex permutations of these 300 GSLs in an equimolar ratio would generate almost 45,000 ($300 \times 299/2$) targets for screening. Even a simple screen of 20 GSLs generates 190 unique heteromeric complex targets. Inclusion of additional accessory lipids (e.g. cholesterol or sphingomyelin), or introducing a range of molar ratios massively expands the target size to unmanageable proportions using conventional ELISAs. In addition, heterogeneity is also present in the ceramide chain length, degree of unsaturation and hydroxylation of both the sphingoid base and the fatty acid moieties (Fantini, Maresca, Hammache, Yahj, & Delezay 2000; Fantini & Barrantes 2009). These physicochemical properties have the potential to influence *cis* interactions between neighbouring GSLs as well as cholesterol in the plasma membrane and therefore influence the shape of an antigenic determinant that might be a target for N-Abs. GSLs are enriched in the exoplasmic leaflet of neural cell membranes, and concentrated in nanoscale domains known as membrane rafts. The core components of these rafts are cholesterol and sphingomyelin, which together with GSLs form densely packed domains of variable size, composition and lifespan (Pike 2006). The transient nature of these platforms, as well as the lateral diffusion of molecules within the plasma membrane, allow for a myriad of potential *cis* interactions, resulting in either preferential presentation (complex-enhancement) or masking (complex inhibition) of constituent molecules through conformational modulation, steric hindrance and the generation of neoepitopes. It is this local microenvironment that has the potential to dramatically influence N-Ab/GSL interactions, as the molecular topography of the exofacial membrane leaflet visible to circulating ligands is the result not only of the properties of the single components but also of the interactions among them.

1.4.4 Conformational modulation of GSLs

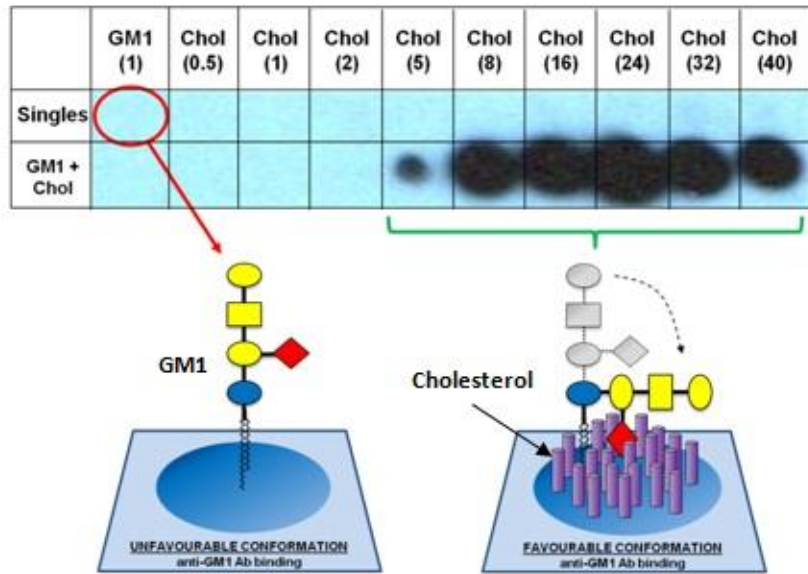
One accessory lipid that we have identified as a modulator of N-Ab binding to GM1 is cholesterol (see Figure 1.7 A). In other contexts, there has been intense interest in the modulating effects of cholesterol on GSLs including GM1 within the cell membrane (Fantini et al. 2013a; Fantini and Yahi 2010; Fantini and Yahi 2013; Lingwood et al. 2011; Mahfoud et al. 2010; Yahi et al. 2010). Cholesterol contains a rigid four ring hydrophobic structure with a short flexible chain and a polar hydroxyl headgroup (Bloom et al. 1991). It resides, almost completely submerged, in the plasma membrane and is a key component of the liquid ordered lipid raft domain in the exofacial leaflet. The rigid structure of cholesterol allows for the tight packing and orientational ordering of GSLs within the lipid raft. Only the hydroxylated polar headgroup is free to interact with the hydrophilic carbohydrate moieties of GSLs, through the formation of a hydrogen bond (H-bond) network (Hall et al. 2010). This series of interactions induces a tilt in the orientation of the carbohydrate headgroup from perpendicular to parallel to the membrane surface, thereby either enhancing or inhibiting ligand binding (Lingwood, Binnington, Rog, Vattulainen, Grzybek, Coskun, Lingwood, & Simons 2011). In liposomes, cholesterol interactions with the carbohydrate headgroup of neighbouring GM1 and globotriose (Gb3) reduces the binding of cholera toxin and verotoxin respectively. This inhibitory effect was also determined to be biologically relevant in toxin binding studies to human tissues (kidney, erythrocytes, sperm) and reversed under conditions of cholesterol depletion with methyl- β cyclodextrin (Lingwood, Binnington, Rog, Vattulainen, Grzybek, Coskun, Lingwood, & Simons 2011). Interestingly, when the cerebroside, galactocerebroside (GalC) or glucocerebroside (GlcC) were incorporated into detergent resistant membrane vesicles containing Gb3 and abundant cholesterol, verotoxin binding occurred. Gb3 was seen to bind GalC and GlcC on TLC overlay, however, cleavage or substitution of the fatty acid moiety of the ceramide tail, rendered this interaction void, indicating a pivotal role for this component in the interaction with Gb3 (Mahfoud, Manis, Binnington, Ackerley, & Lingwood 2010).

This scenario is reported to be reversed in models of Alzheimer's disease, where an increase in cholesterol enhances β -amyloid binding to GM1. In a description of this situation, cholesterol presents a hydroxyl group to form a H-bond with the

glycosidic bond of GM1 at the junction of the apolar ceramide tail and the polar headgroup. This induces a downwards tilt in the glycan orientation of GM1, allowing it to form homodimers in which both sugar headgroups are parallel to the membrane and orientated in opposite directions, thereby creating a 'chalice-shaped' receptacle for beta-amyloid binding (Fantini et al. 2013b).

The impact of cholesterol on the conformational modulation of GSLs is thought to be highly dependent upon the hydroxylation status of the C2 of the fatty acid chain of the GSL ceramide moiety (i.e. non hydroxylated/hydroxylated fatty acid, NFA/HFA). Whilst the hydroxylation status of the fatty acid C2 and its functional effect in neural gangliosides is debated (Hama 2010), this has been well documented for GalC. Since NFA and HFA GalC as a single antigen (see Figure 1.7 B) and in heteromeric complex with other GSLs (see Figure 1.7 C), are a target for N-Abs and highly abundant in myelin, this also requires consideration in combinatorial array design. It has been demonstrated that the galactose group of the HFA-GalC forms an intramolecular H-bond network which restricts the headgroup to the parallel conformation, whereas NFA-GalC is free to adopt a conformation perpendicular to the membrane surface (Nyholm et al. 1990). In this latter situation, cholesterol is able to fine tune the orientation of the NFA-GalC headgroup to the parallel conformation through the formation of intermolecular H-bonds (Fantini & Yahi 2010; Yahi, Aulas, & Fantini 2010), which has the potential to either enhance or reduce interactions with N-Abs. In addition to interacting with cholesterol, the galactose residue of GalC can form multiple H-bonds (4.5-5 H-bonds) (Hall, Rog, Karttunen, & Vattulainen 2010) with other GSL components, and in doing so mould the local membrane architecture. By inference, one might predict that other GSLs, whether in HFA or NFA forms (Hama 2010) and containing variable numbers of H-bond, donor/acceptor groups, to a greater or lesser extent, can form both intra- and inter-molecular H-bonds in a similar fashion.

A



B



C

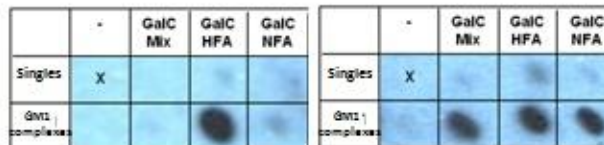


Figure 1.7. Inter- and intra-molecular modulation of GSL conformation. Glycoarray grids are presented in one dimension of each lipid and complex.

Panel A. The upper row contains cholesterol or GM1 as single lipids, and the lower row contains heteromeric complexes of cholesterol with GM1. The molar ratio of cholesterol relative to GM1 increases from left (0.5:1) to right (40:1). The grid was overlaid with a N-Ab serum that demonstrated heterodimer-dependent binding at molecular ratios equal to or greater than 5:1 cholesterol:GM1, in the absence of binding to either single component. Cholesterol can modulate the orientation of the glycan headgroup of GM1, from perpendicular to parallel to the membrane surface through the formation of intermolecular hydrogen bond (H-bonds) networks. By inference, this also appears to occur on the glycoarray platform, herein creating a GM1 conformation favourable to N-Ab binding.

Panel B. One N-Ab serum is profiled on a glycoarray comprising either hydroxylated or non-hydroxylated galactocerebroside (GalC-HFA or NFA). This sample showed preferential binding to GalC-HFA, with absence of binding to GalC-NFA. The presence of a hydroxyl group on the C2 of the ceramide moiety of GalC, is capable of forming intramolecular H-bonds networks, causing the galactose headgroup to tilt parallel towards the membrane surface. In comparison, the galactose headgroup of GalC-NFA (in the absence of any additional modulating GSLs or cholesterol), exists perpendicular to the membrane, creating unfavourable conditions for this N-Ab binding.

Panel C. Two different N-Ab sera were evaluated on combinatorial glycoarray. One N-Ab (left) bound exclusively to the GM1:GalC-HFA complex, in the absence of binding to GM1 GalC-NFA or GalC -NFA/HFA mixtures, or any single lipids. The second (right) indiscriminately bound to GalC-HFA, GalC-NFA and mixtures of both when in complex with GM1. The conformational modulation of GM1 by GalC, through both intra- and inter-molecular H-bond partnerships, can be recapitulated on a glycoarray platform, and different N-Ab possess varied preferences towards these glycan orientations.

1.4.5 *Cis*-interactions between GSLs result in the formation of neoepitopes or introduce steric hindrance

The concept of N-Abs that bind preferentially to heteromeric GSL complexes is now well established (Rinaldi 2013). After the initial demonstration of N-Abs that bound a GD1a/GD1b complex (Kaida, Morita, Kanzaki, Kamakura, Motoyoshi, Hirakawa, & Kusunoki 2004; Willison 2005) many other heteromeric pairings (e.g. GM1/GD1a, GM1/GQ1b, LM1/GM1) have now been identified (Kaida & Kusunoki 2010; Ogawa et al. 2013; Rinaldi 2013). N-Abs are defined as having undetectable or very low reactivity against either single species of GSL, but greatly enhanced reactivity in the presence of the heteromeric complex of both GSLs in equimolar amounts (Brennan et al. 2011; Galban-Horcajo, Fitzpatrick, Hutton, Dunn, Kalna, Brennan, Rinaldi, Yu, Goodyear, & Willison 2013; Kaida, Morita, Kanzaki, Kamakura, Motoyoshi, Hirakawa, & Kusunoki 2004; Kaida, Sonoo, Ogawa, Kamakura, Ueda-Sada, Arita, Motoyoshi, & Kusunoki 2008; Kaida & Kusunoki 2010; Rinaldi et al. 2009). For GM1/GD1a N-Abs, conformation of the requirement for both GSLs has been confirmed using a GM1-GD1a hybrid ganglioside derivative (Mauri, Casellato, Ciampa, Uekusa, Kato, Kaida, Motoyama, Kusunoki, & Sonnino 2012). In another context a monoclonal antibody (mAb) that reacts with the heteromeric GM2/GM3 dimer, but not to either partner, has been characterised (Todeschini et al. 2008). IgM N-Abs to heteromeric complexes of GM1/GalC and GM2/GalC are extensively found in multifocal motor neuropathy sera, including in samples negative for conventional anti-GM1 antibodies (Galban-Horcajo, Fitzpatrick, Hutton, Dunn, Kalna, Brennan, Rinaldi, Yu, Goodyear, & Willison 2013; Nobile-Orazio, Giannotta, Musset, Messina, & Leger 2013; Pestronk, Choksi, Blume, & Lopate 1997). However it has yet to be experimentally demonstrated at the structural level that the GSL interactions form new molecular shapes i.e. 'neoepitopes' identifiable by N-Abs that contain glycan elements of both GSL components within the antibody binding site.

Of equal importance is the reverse phenomenon of steric hindrance which appears prominent amongst N-Abs, having long been observed amongst other anti-GSL antibodies (Lloyd et al. 1992; Shichijo and Alving 1986). Herein, this is defined as the process in which the binding of an N-Ab to a single GSL is prevented by the spatial structure of a second GSL in near proximity. In lipid

rafts in which molecules are tightly packed in the liquid ordered phase, it is likely that the numerous interactions occurring at any given time will give rise to inhibitory partnerships, resulting in the masking of various membrane components. Indeed, Greenshields *et al* found that when examining the properties of mouse monoclonal anti-GM1 IgG antibodies with similar GM1 binding affinities that only one was able to bind to live plasma membranes, as was also the case for human anti-GM1 N-Abs. Further investigations revealed that this was due to steric hindrance resulting from the adjacent presence of GD1a in the neuronal membrane, which masked the specific GM1 epitope for one antibody but not the other (Figure 1) (Greenshields, Halstead, Zitman, Rinaldi, Brennan, O'Leary, Chamberlain, Easton, Roxburgh, Peditani, Furukawa, Furukawa, Goodyear, Plomp, & Willison 2009). Similar findings have been observed for anti-GD1b N-Abs that bind dorsal root ganglion neurons (Kusunoki et al. 1999).

Issues surrounding GSL packing and density are thus critical to N-Ab target binding. Monovalent interactions of anti-GSL antibodies or lectins with their target are typically very weak, even undetectable. Most ligands rely on engaging multiple binding sites and/or the formation of multivalent immune complexes to increase the avidity of the interaction. The density of GSL targets on any glycan array platform is thus fundamental to ensuring simultaneous binding of two or more epitopes, resulting in a net avidity enhancement. In addition to avidity, density can also influence antibody selectivity (Oyelaran, Li, Farnsworth, & Gildersleeve 2009a) and antigen presentation through an increased frequency of neoepitope formation, or steric hinderance of target epitopes. When screening polyreactive serum samples in which multiple antibodies may be directed against the same molecule, but with different epitope specificities, this becomes complex. A balance of these enhancing and inhibitory factors thus needs to be achieved that maximises N-Ab detection rates, which may not be achievable in a single array design.

1.4.6 Methodological developments of combinatorial glycoarrays

Traditional ELISA based methodologies for N-Ab detection are inappropriate for large scale screening of GSL complexes owing to impractical increases in requirement for volumes of sera and scarce lipid reagents (Bech, Jakobsen, &

Orntoft 1994;Carpo, Allaria, Scarlato, & Nobile-Orazio 1999;Cats et al. 2010b;Willison, Veitch, Swan, Baumann, Comi, Gregson, Illa, Zielasek, & Hughes 1999). This heightened the need for a HTS combinatorial array platform capable of screening single and complex epitopes simultaneously without an increase in sera and lipid usage. In 2006, adapting the principles of dot-blot assays (Chabraoui, Derrington, Mallie-Didier, Confavreux, Quincy, & Caudie 1993), a polyvinylidene difluoride (PVDF)-based non-covalent array comprising 200 lipids spotted using an automated TLC dispenser was used to probe multiple sclerosis (MS) sera for autoantibodies (Kanter et al. 2006). We further adapted this method to generate combinatorial arrays to screen single and complex lipid epitopes for MS-associated autoantibodies and N-Abs (Brennan, Galban-Horcajo, Rinaldi, O'Leary, Goodyear, Kalna, Arthur, Elliot, Barnett, Linington, Bennett, Owens, & Willison 2011;Galban-Horcajo, Fitzpatrick, Hutton, Dunn, Kalna, Brennan, Rinaldi, Yu, Goodyear, & Willison 2013;Rinaldi, Brennan, Goodyear, O'Leary, Schiavo, Crocker, & Willison 2009). The method has been described in detail (Rinaldi, Brennan, & Willison 2012), and multiple examples shown in Figures 1-3. Unmodified single lipids and complexes in methanol are spotted in duplicate onto a PVDF substrate via non-covalent, hydrophobic interactions and dried by evaporation. For complexes, GSLs and other lipids are pre-mixed in appropriate ratios prior to spotting. Arrays generally comprising 10 to 20 lipids and their heteromeric permutations are probed with neuropathy and control sera for N-Ab identification. For detection, we have extensively used HRP-labelled secondary antibodies and enhanced chemiluminescence (ECL plus). Although very sensitive, ECL plus suffers from a low dynamic range and is currently being replaced by fluorescently labelled secondary antibodies that generate a more dynamic intensity measurement with higher saturation threshold (Figure 3). This requires low fluorescence PVDF (PVDF-FL), to reduce the intrinsic auto-fluorescence of PVDF (Zhang and Zhou 2011). Furthermore, fluorescence based secondary antibodies labelled with different fluorophores (e.g anti-IgG-Alexafluor 647 and anti-IgM-Alexafluor 555) allow the simultaneous detection of different classes of antibodies in the same serum sample. Data readout is numerical and analysed using iterative cluster analysis, heat maps and graphical representation.

1.5 Summary

High throughput screening of human serum cohorts for N-Abs directed to heteromeric lipid complexes that approximate their native state in neural membranes has necessitated the development of new methodologies specifically tailored to this need. Herein we have described some theoretical issues underpinning this field and its practical application, illustrating the sensitivity, specificity and versatility of the methodology developed to date. Further automation and increases in scale to include a wider range of lipids admixed in greater complexity with variations in components and ratios are currently being developed. The major long-term goal for clinical diagnostics is to recapitulate the natural lipid landscape of neural membranes that might act as targets for N-Abs in their full molecular diversity; in doing so we expect that previously unidentified lipid complex targets for N-Abs will be discovered. The major gap in fundamental knowledge concerns the theoretical basis underpinning lipid complex formation resulting from *cis*-interaction in the lateral plane of the membrane which requires the application of advanced biophysical and imaging techniques.

The aims of this thesis were therefore:

1. Investigate the diversity and cryptic behaviour of anti-GM1 Abs in patient sera using non-immobilised artificial membranes and Ab affinity purification (Chapter 3).
2. Characterize anti-ganglioside complex antibodies in Multifocal Motor Neuropathy (MMN) (Chapter 4).
 - 2.1. Compare the diagnostic efficiency of Glycoarray and ELISA.
 - 2.2. Validate preliminary findings by the use of an external, double-blinded cohort including patients and controls.
3. Explore the existence of anti-ganglioside complex antibodies against targets containing three different GSL in Chronic Inflammatory Demyelinating Polyneuropathy (CIDP) (Chapter 5).

3.1. Pattern recognition antibodies.

3.2. Antibodies against heterotrimeric GSL complexes.

2 Chapter 2. Materials and Methods

Table 2.1. Lipids used in ELISA, Array and liposome experiments.

Lipid	Supplier
GM1	Sigma (UK)
GM2	Sigma (UK)
GM3	Sigma (UK)
GA1	Sigma (UK)
GD1a	Sigma (UK)
GD1b	Sigma (UK)
GQ1b	Matreya (Pennsylvania, USA)
GD3	Avanti Polar Lipids (Alabama, USA)
LM1	Professor RK Yu (Augusta, USA)
SGPG	Professor RK Yu (Augusta, USA)
Galactosylcerebroside (GalC)	Sigma (UK)
Phrenosin (Phre)	Matreya (Pennsylvania, USA)
Kerasin (Ker)	Matreya (Pennsylvania, USA)
Sulphatide (Sulph)	Sigma (UK)
Sphingomyelin (SM)	Sigma (UK)
Cholesterol (Chol)	Avanti Polar Lipids (Alabama, USA)
Phosphatidylcholine (PC)	Avanti Polar Lipids (Alabama, USA)
Coprostanol (Copr)	Avanti Polar Lipids (Alabama, USA)
Lanosterol (Lano)	Avanti Polar Lipids (Alabama, USA)
Cholestenol (Stan)	Avanti Polar Lipids (Alabama, USA)
Ergosterol (Ergo)	Avanti Polar Lipids (Alabama, USA)
Sitosterol (Sitos)	Avanti Polar Lipids (Alabama, USA)
Zymosterol (Zym)	Avanti Polar Lipids (Alabama, USA)
Diosgenin (Dios)	Avanti Polar Lipids (Alabama, USA)
Cholesterol sulphate (Chs)	Avanti Polar Lipids (Alabama, USA)
Dicetylphosphate	Sigma (UK)

2.1 Monoclonal antibody production from existing cell lines

SM1, BO3, DO1 and BR1 cell lines from MMN patients producing human anti-GM1 antibodies were cultured (O'Hanlon et al. 1996). Cell culture procedures were all conducted under sterile conditions using a class II hood and the cells were incubated at 37°C in 5%CO₂.

Previously cloned cells were retrieved from liquid nitrogen and thawed on a sterile water bath set at 37°C. Cells were then resuspended in 50 ml of RPMI (Invitrogen, UK) containing 10% Foetal Bovine Serum (FBS) (Invitrogen, UK) and spun down for 5 minutes at 200 g using a centaur 2 bench-top centrifuge (MSE, UK). The supernatant was removed and the cell pellet resuspended in 15 ml RPMI-FBS put into a T25 tissue culture flask (Corning, Netherlands) and transferred to a 3100 Forma Series II incubator at 37°C (Thermo Scientific, UK). Cells were subjected to regular viability assessment and expanded into larger

flasks when reaching confluence. Cells were removed from a confluent T25 culture flask, pelleted down as described previously resuspended in RPMI-FBS and split between several T175 flasks containing 50 ml fresh RPMI-FBS media. In order to assess the antibody production rate of the growing cell lines, regular supernatant aliquots were taken and tested on ELISA (see Methods 2.5) on a ganglioside panel containing GM1.

2.1.1 Antibody purification

When a minimum of 1 litre of supernatant was available, the monoclonal antibodies were purified using a HiTrap Protein M column (GE Healthcare, UK). Supernatants were removed from the flasks transferred to sorval RC5C centrifuge bottles (Fisher scientific, UK) and spun for 30 minutes at 10000 rpm at 4°C to remove particulate matter contained in the media on a Beckman (Beckman Coulter, UK). The supernatant was transferred to dialysis tubing of molecular weight cut-off <900,000 Daltons and placed in 10x the volume of antibody binding buffer (see appendices 1) to dialyse overnight at 4°C.

Following dialysis the supernatant was filtered through a 0.2 µm bottle top filtration unit (Milipore, UK) before loading onto the HiTrap protein M column using a peristaltic pump at 50 rpm. The flow through was kept to ensure no protein remained in it and for quantification purposes. Once the supernatant was loaded, the column was washed with 10x the column volume of binding buffer and the wash through collected in 10 fractions. The bound protein was eluted with 10x column volumes of 0.1M glycine at pH 2.7 (see appendices 1) into 10 fractions containing a precalculated volume of 1M Tris-HCL at pH 9 (see appendices 1) to neutralise the low pH. All fractions, including starting supernatant, flow through, wash and elution fractions were tested by ELISA and glycoarray for anti-GM1 IgM binding (see Methods 2.5 and 2.6).

Fractions showing antibody binding to GM1 were pooled and desalted using a Sephadex PD-10 column (Amersham Biosciences, Sweden) and eluted in phosphate buffered saline (PBS) (see appendices 7.1). Antibody concentration was calculated using spectrophotometric absorbance (Eppendorf, Germany) as follows:

Antibody concentration (mg/ml) = A280/1.43

Antibodies were then aliquoted and stored at -80°C.

2.2 Preparation of liposomes

Liposomes were prepared using a mole to mole 5:4:1:1 ratio of Cholesterol (Chol), Sphingomyelin (SM), dicetylphosphate and ganglioside respectively to a final ganglioside concentration of 2mM.

Lipid components dissolved in 1:1 chloroform:methanol were added to a 15 ml plastic tube (Corning, Netherlands) and dried under oxygen free nitrogen (BOC, UK) in order to form a thin lipid film. Five times the lipid volume of PBS was added to the falcon, rehydrating the thin lipid layers and allowing the formation of cave-like lipid structures which will finally fuse to generate multilamellar vesicles (MLVs). The size of the MLVs was then reduced by sonication (Ultrawave Ltd, UK) for 15 minutes at room temperature. After sonication, liposome preparations underwent five freeze-thaw cycles by submerging in liquid nitrogen and then thawing at 37°C in a water bath. Larger vesicles and aggregates were removed by centrifugation at 600 g in a B4 centrifuge (Jouan, France) at room temperature for 20 minutes. To create unilamellar vesicles, the supernatant underwent 11 cycles of extrusion using a Mini-extruder (Avanti Polar Lipids, USA) with supports and filters of 0.4 µm pore size (Whatman, UK). The unilamellar vesicles were then isolated by centrifugation in a Beckman at 38500 rpm (Beckman Coulter, UK) and 22°C for 1 hour. The resulting pellet was resuspended in 2.5 ml of PBS pH 7.4.

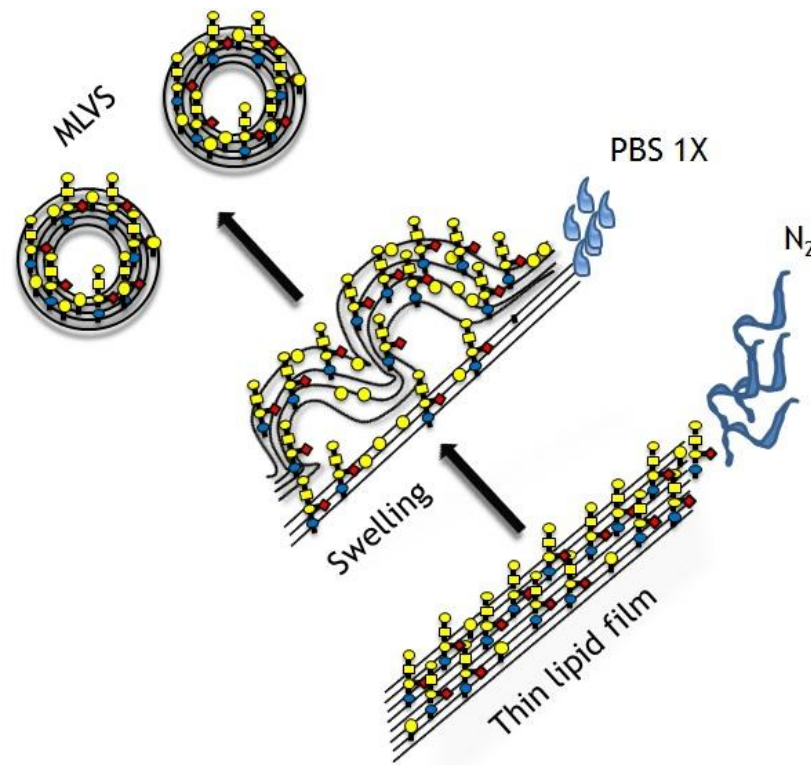


Figure 2.1. Diagram illustrating the formation of GM1-containing multilamellar vesicles (MLVs).

2.3 Quantification of antibody binding to liposomes using flow cytometry

A flow cytometry based assay was adapted to detect antibody binding to liposomes containing single gangliosides or heteromeric ganglioside complexes (Temmerman and Nickel 2009).

Liposomes were prepared as previously described with the exception of BODIPY labelled Cholesteryl FLC₁₂ (Invitrogen, UK) substituting Cholesterol (see Methods 2.2). Alternatively, for liposomes labelled with OVA albumin tagged with Alexa 488 (OVA488), during liposome preparation, the thin layer of lipid obtained after the application of nitrogen was reconstituted with a PBS solution containing OVA488. Liposome preparations were blocked for 1 hour at room temperature using 3% BSA (see appendices 7.1). Liposomes were then spun down (10 minutes at 16000g) and resuspended in 2 ml of PBS 1X. The suspensions were split in five different aliquots containing 300µl and spun down again under the same conditions. Pellets were reconstituted on a solution containing the primary antibody diluted in 0.1% BSA and incubated at 4°C for 30 minutes. Every

liposome aliquot will have a different antibody treatment including a negative control containing 0.1% BSA. After the incubation, liposomes solutions were pellet down as previously described and resuspended with 600 μ l of PBS 1X. This process was repeated twice before adding the Alexa647 labelled secondary antibody. The secondary antibody was diluted 1:100 in PBS 1X containing 0.1% BSA and incubated with the liposomes for 30 minutes at 4°C. The unbound secondary antibody was washed using three sequential PBS 1X washes spinning down the liposomes after every wash. After finalising the washes, liposomes were resuspended in PBS 1X and transferred onto flow cytometry tubes (Corning, Netherlands).

Latex beads ranging from 0.1 to 0.6 μ m (LB1-6, Sigma, UK) were used as size controls to set the gates on the flow cytometer and establish the compensation.

2.4 Affinity Purification using liposomes

Liposomes prepared at a ganglioside concentration of 2 mM (see Methods 2.2) were blocked overnight with 2.5 ml of 2% bovine serum albumin (Europa Bioproducts, UK) in PBS (BSA/PBS). The liposomes were then split between three microtubes and centrifuged for 15 minutes at 16000g at room temperature. After centrifugation the pellets were resuspended in 900 μ l PBS and the process repeated in order to eliminate the remaining BSA. Following the final centrifugation step, the first liposome pellet was resuspended with 70% patient sera diluted with 0.2% BSA/PBS and the mix incubated for 30 minutes at 4 °C. After incubation the sera/liposome mix was centrifuged for 15 minutes at 16000g at room temperature and the supernatant transferred to the second then third aliquot of liposomes and the process repeated each time. Two washes were performed on the pellets from each stage, comprising resuspension of the pellet in PBS and recentrifugation. The three pellets, containing the affinity purified antibodies from patient sera, were incubated with 0.83 ml glycine buffer (0.1M pH 2.5) for 2 minutes to elute them from the liposomes before neutralising the pH with 0.083 ml of Tris HCl (1mM pH9). Samples were then centrifuged for 15 minutes at 16000g and the supernatants containing the purified antibodies stored for further analysis.

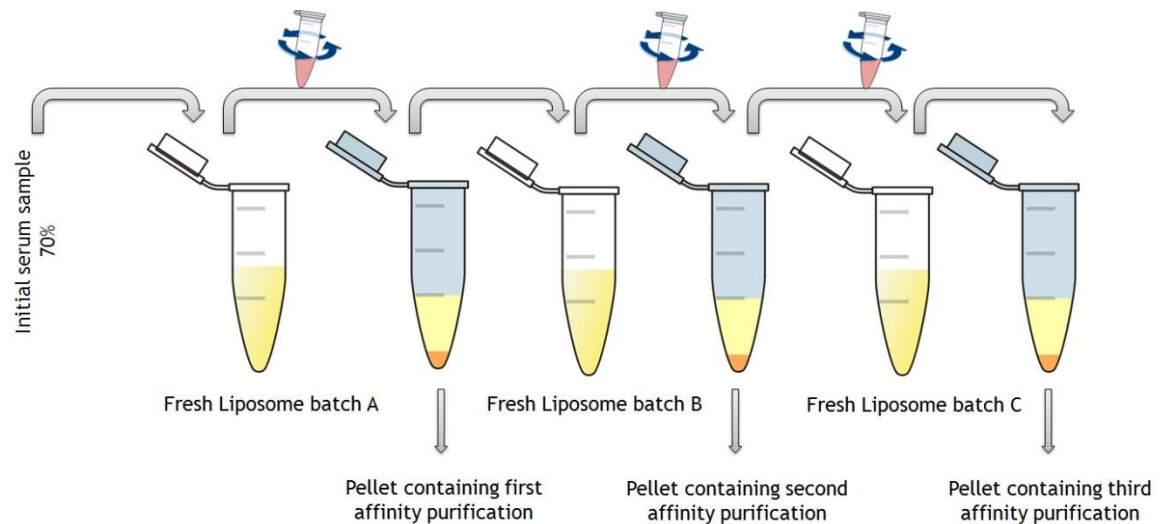


Figure 2.2. Diagramme illustrating the liposome-based methodology for antibody affinity purification from patient sera.

2.5 Enzyme linked immunosorbant assay (ELISA)

The enzyme linked immunosorbant assay (ELISA) method from the Glasgow Diagnostic Neuroimmunology Laboratory was used (Willison, Veitch, Swan, Baumann, Comi, Gregson, Illa, Zielasek, & Hughes 1999). Polystyrene plates (Immulon 2HB microtitre plates, Dynatech, UK) were coated with 200ng per well of glycolipid dissolved in methanol and allowed to dry leaving the glycolipid adhering to the ELISA plate. For preparation of heteromeric complexes comprising a 50:50 ratio of two glycolipids, 100ng of each glycolipid was admixed in methanol by sonication (3 min), and a total of 200ng of glycolipid mixture was applied per well. Following complete evaporation of the methanol the plates were stored at 4°C for a minimum of one hour before blocking with 150 µl per well of 2% BSA/PBS for one hour at 4°C. The blocking reagent was then discarded followed by five consecutive PBS washes before 100µl sera, diluted in 0.1% BSA/PBS, was applied to duplicate wells at 1:100, 1:500, 1:2500, 1:12500 dilutions and incubated for twelve hours at 4°C. After washing 5 times with PBS, 100µl per well of horse radish peroxidase-labelled secondary antibody (DakoCytomation, Denmark) diluted 1:3000 in 0.1% BSA/PBS was applied for one hour at 4°C. Detection was performed using 100 µl of substrate solution (see appendices 7.1) per well for 15 minutes at room temperature in the dark and the reaction terminated with 50 µl of 4 M H₂SO₄ (see appendices 1). Optical density (OD) was read at 492 nm using an automated plate reader (Sunrise™, Tecan Group Ltd, Männedorf, Switzerland). Background (methanol only coated wells)

OD values were subtracted to give final OD values. OD values >0.1 at 1:500 dilution were considered positive, based on previous assay validation data (Willison, Veitch, Swan, Baumann, Comi, Gregson, Illa, Zielasek, & Hughes 1999).

2.6 Glycoarray

2.6.1 Slide preparation

2.6.1.1 Slides for Chemiluminescence

For a lipid lay out containing 10 lipids and their corresponding heteromeric combinations, 0.2 µm polyvinylidene difluoride (PVDF) membranes (Invitrogen, UK) (2.8cm wide x 2.5 cm height) were fixed onto glass slides using UHU glue (UHU, UK). The dimensions of the PVDF were proportionally adapted to the dimensions of the lipid grid. After the membrane had fully adhered and the slides were fully dry (15-30 minutes) a hydrophobic sealing pen was applied on the border of the PVDF with the glass.

2.6.1.2 Slides for fluorescence

PVDF-FL (Immobilon®PVDF-FL, Milipore, UK) was affixed fully covering the glass slide (7.5cm wide x 2.5cm height) using a low fluorescence spray glue (3M photo mount, 3M, UK) (See Appendices 7.2.1). Any PVDF-FL outside the limits of the slide area was shaved off using a scalpel. The area containing lipids was then delimited using a hydrophobic sealing pen applied directly onto the PVDF-FL membrane.

2.6.2 Lipid preparation

2.6.2.1 For complexes containing two lipids

Screening of antibody binding by combinatorial array using chemiluminescence as a detection method was performed as follows. Individual glycolipid solutions were prepared at a concentration of 100µg/ml in methanol and added to chromacol vials (maximum capacity 300µl) (Chromacol, UK). In order to generate the 1:1 heteromeric glycolipid complexes, equal volumes of the individual glycolipid solutions were mixed in a chromacol vial the total volume of the mix

being equal to the individual glycolipid preparations. The final glycolipid density in the vials remained constant between single and complex lipid mixtures. Following preparation, samples were sonicated for 3 minutes (Ultrawave Ltd, UK).

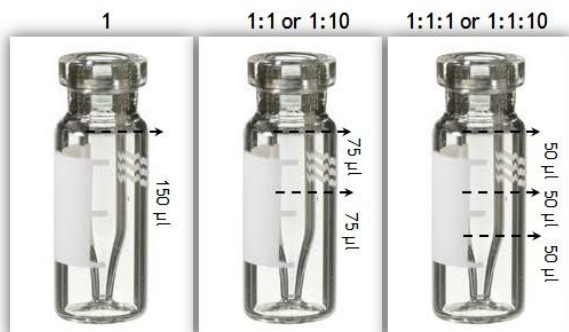


Figure 2.3. Chromacol vials illustrating the different lipid preparations.

2.6.2.2 For Complexes containing three lipids

In order to generate the 1:1:1 or 1:1:10 heteromeric glycolipid complexes, equal volumes of the individual glycolipid solutions were mixed in a chromacol vial the total volume of the mix being equal to the 1:1, 1:10 and individual glycolipid preparations. The final glycolipid density in the vials remained constant between single, dimeric and trimeric lipid mixtures. Following preparation, samples were sonicated for 3 minutes (Ultrawave Ltd, UK).

2.6.3 TLC Printing and program preparation

2.6.3.1 Program preparation

In order to print individual spots using the ATS4 TLC autosampler (Camag, Muttenz, Switzerland) it was necessary to write programs where the individual spots were defined by specific X and Y coordinates. Glycolipid singles and complexes were printed in duplicate in a grid formation. The first data point corresponding to the first single glycolipid on the initial slide was (15mm, 36mm) and its duplicate (17mm, 34mm). In order to complete print run of 6 PVDF slides, 31.4mm were sequentially added to all X coordinates while the Y coordinates remained the same. For programs containing 12 slides, 92mm were added to all the Y coordinates while X coordinates remained unchanged.

All PVDF printed slides contain a diagonal line composed of methanol only spots that are used as negative background controls. The initial coordinates for the first two methanol spots were (17mm,36mm) and (19mm,38mm). The same rule described above applies for methanol in printings containing 6 or 12 slides.

Spot number	Position x	Position y	Type	Width (x)	Height (y)	Volume (μ l)	Content
1	17	36	Band	0.4	0.4	0.1	metOH
2	19	38	Band	0.4	0.4	0.1	metOH
3	21	40	Band	0.4	0.4	0.1	metOH
4	23	42	Band	0.4	0.4	0.1	metOH
5	25	44	Band	0.4	0.4	0.1	metOH
6	27	46	Band	0.4	0.4	0.1	metOH
7	29	48	Band	0.4	0.4	0.1	metOH
8	31	50	Band	0.4	0.4	0.1	metOH
9	33	52	Band	0.4	0.4	0.1	metOH
10	35	54	Band	0.4	0.4	0.1	metOH
121	15	36	Band	0.4	0.4	0.1	GM1
122	17	34	Band	0.4	0.4	0.1	GM1
145	15	38	Band	0.4	0.4	0.1	GM2
146	19	34	Band	0.4	0.4	0.1	GM2
169	15	40	Band	0.4	0.4	0.1	GA1
170	21	34	Band	0.4	0.4	0.1	GA1
193	15	42	Band	0.4	0.4	0.1	GD1a
194	23	34	Band	0.4	0.4	0.1	GD1a
217	15	44	Band	0.4	0.4	0.1	GD1b
218	25	34	Band	0.4	0.4	0.1	GD1b
241	15	46	Band	0.4	0.4	0.1	LM1
242	27	34	Band	0.4	0.4	0.1	LM1
265	15	48	Band	0.4	0.4	0.1	SGPG
266	29	34	Band	0.4	0.4	0.1	SGPG
289	15	50	Band	0.4	0.4	0.1	GQ1b
290	31	34	Band	0.4	0.4	0.1	GQ1b
313	15	52	Band	0.4	0.4	0.1	Sulph
314	33	34	Band	0.4	0.4	0.1	Sulph
337	15	54	Band	0.4	0.4	0.1	GalC
338	35	34	Band	0.4	0.4	0.1	GalC

Figure 2.4. Example of a programme listing the coordinates for 10 single lipids and methanol only controls on the first slide.

2.6.3.2 TLC printing and settings

The ATS4 TLC autosampler (Camag, Muttenz, Switzerland) was used to apply 0.1 μ l per spot of single glycolipid or glycolipid complex at 100 μ g/ml in methanol to PVDF membranes affixed to glass slides. From 10 individual lipids, a total of 45

heteromeric lipid complexes were achieved, each duplicated in a mirror image against a diagonal control line of methanol.

Oxygen free Nitrogen (BOC, UK) was used for the spraying system within the ATS4 TLC, at an optimum pressure of 5 bars. Both 25 μl and 10 μl syringes were used with an optimized filling speed of 15 $\mu\text{l}/\text{s}$, a rinsing vacuum speed of 4 seconds and a general vacuum pressure of 1.2 MPa.

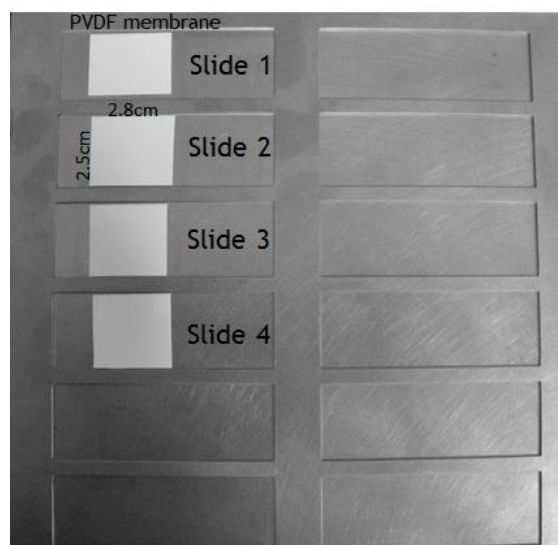


Figure 2.5. Glycoarray slide holder for TLC dispensing
Presenting four PVDF slides for an array dimension of 11x11.

2.6.4 Array probing and Analysis

The protocols described below have been adapted assuming an array area of 2.8cm x 2.5cm corresponding to a symmetrical lipid layout of 10 lipids by 10 lipids. The volumes of sera, secondary antibody and chemiluminescent reagents need to be proportionally adjusted to the dimension of the array.

2.6.4.1 Array probing using Chemiluminescence

Slides of the printed arrays were blocked for 1 hour in 2% BSA/PBS at room temperature in a staining dish on an orbital shaker, slides were then placed in a slide box containing moist paper and 250 μl of sera diluted 1 in 100 in was added and the slides incubated for 1 hour at 4°C. Slides were then washed twice for 15 minutes in 1% BSA/PBS with agitation before again transferring to the slide box and 250 μl of horseradish peroxidase conjugated secondary antibody (DakoCytomation, Denmark) prepared in 1% BSA/PBS at 1:25000 was applied and

the slides incubated for 30 minutes at 4°C. The slides were then tapped dry and washed twice for 30 minutes in 1% BSA/PBS and subsequently for 5 minutes in distilled water. Binding was detected by enhanced chemiluminescence, (ECL+; Amersham/GE Healthcare, UK) following application of 450 µl of ECL (40:1 Reagent A and B respectively) for 3 minutes slides were taped into an x-ray cassette and x-ray film (Kodak, UK) applied in the darkroom and the radiographs exposed for various times. Radiographs were then digitized by flatbed scanning (Epson DX 6000), and spot intensity calculated using TotalLab image analysis software (Nonlinear Dynamics Ltd, Newcastle upon Tyne, UK), and expressed as pixel intensity units of individual spots (IU).

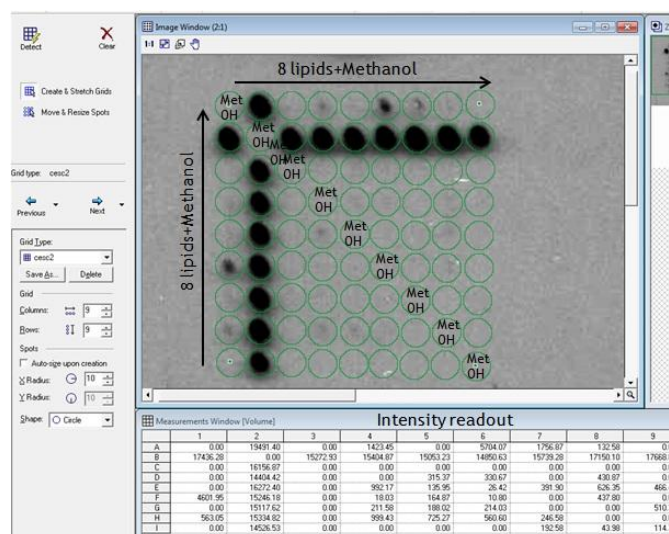


Figure 2.6. TotalLab software lay out depicting the measurement of a 9x9 lipid grid.

2.6.4.2 Array probing using fluorescent tags

Arrays were blocked in 2% BSA/PBS at room temperature on an orbital shaker. After one hour, slides were placed on a slides box containing moist paper and 250 µl of sera diluted 1 in 100 in 1% BSA/PBS added, leaving the slides to incubate for 1 hour at 4°C. Slides were then washed twice for 15 minutes in 1% BSA/PBS before application of 250 µl of fluorescently labelled secondary antibody (α-IgG Alexa 555 and/or α-IgM Alexa 647, Invitrogen, UK) prepared in 1% BSA/PBS at 1:1000 and incubation for 1 hour at 4°C. The slides were then tapped dry and washed twice for 30 minutes in 1% BSA/PBS and for 5 minutes in distilled water. Binding was detected by fluorescent reading of the slides using a flatbed scanner (ScanArray Express imaging system, Perkin Elmer, UK). Intensity

was measured as mean fluorescence intensity minus background using the software provided with the scanner. (See Appendices 7.2.22)

2.7 Microarray

2.7.1 Microarray generation

A sciFLEXARRAYER (Sciencion, Germany) non-contact piezoelectric array was used to generate combinatorial lipid arrays. Lipids stocks were prepared at 30 µg/ml in a 70:30 methanol/water mixture and sonicated for 2 min prior to loading onto the 384 well plate for dispensing. Unless indicated, the microarrays containing heteromeric complexes were produced over-spotting the two single lipid samples forming the complex. In order to increase the molarity of lipid spotted, each spot was generated by the addition of 6 droplets, adding up to a total of 0.003 µl, of lipid solution. Lipids were dispensed onto PVDF-FL membranes (Immobilon®PVDF-FL, Milipore, UK) affixed to glass slides (see Methods 2.6.1.2). The layout of the lipid grid, assuming spacing between spots of 390 µm and 10 single lipids and their correspondent heteromeric complexes, allowed the generation of eight sub-arrays per slide. After printing, the arrays were left to dry overnight at 4°C.

2.7.2 Microarray probing

Slides were first blocked for 1 hour at room temperature in 2% BSA/PBS in a 50ml Falcon tube on a rocker. Slides were then washed in 45 ml of PBS 1 for 20 minutes at room temperature. Following the wash step the slides were arranged and the FAST Frame multi slide plate (Whatman, UK) was placed on top of the slides in order to delineate the 8 sub-arrays generated per slide. Each sub-array was incubated with patient sera (1:100 dilution), monoclonal antibody or 0.2% BSA/PBS for 1 hour at 4°C. After incubation, the solution within each FAST frame was carefully removed by aspiration using a Gilson pipette, the frame removed and the slides washed four times (15 minutes per wash) with 45 ml of PBS in a 50ml falcon tube placed on a rocker. The slides were then transferred to the Fast frame and fluorescently labelled secondary antibody (diluted 1:500 in 0.2% BSA/PBS) added and incubated for 1 hour at 4°C. The secondary antibody solution was carefully aspirated by pipetting and the Fast frame removed. The

slides were then washed four times with PBS in a falcon tube with agitation. Following the final wash cycle the slides were left to dry overnight at room temperature in the dark before scanning using the ScanArray Express imaging system (Perkin Elmer, UK). Detection was carried out using the 633nm laser excitation wavelength corresponding to AlexFluor647. Slides were scanned at 10 μm resolution using 35% PMT with 90% laser power.

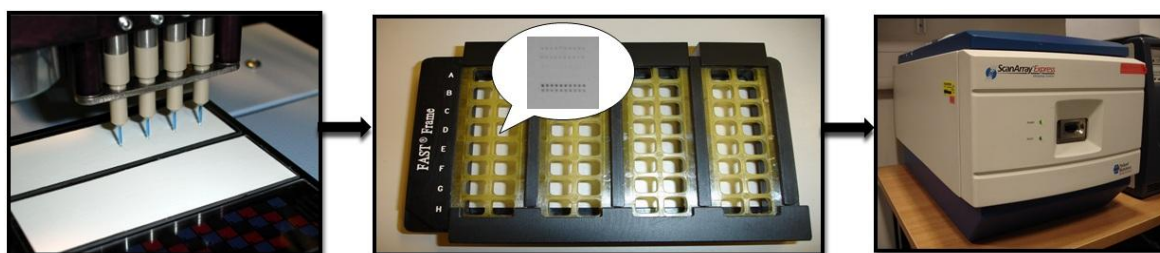


Figure 2.7. Diagram illustrating the process of printing, probing with the FAST Frame and scanning the arrays.

2.8 Mass spectrometry

The matrix assisted desorption/ionization (MALDI) in Silica P254 (Merck, Darmstadt, Germany) TLC plates (20 cm x10 cm) was performed as follows.

The TLC plate containing the combinatorial lipid arrays were attached to a MALDI sample plate with double-sided adhesive tape and coated with 40 layers of a matrix containing 2,5-dihydroxybenzoic acid (DHB) at 20 mg/ml dissolved in 50% acetonitrile (ACN) and 0.1% trifluoroacetic acid (TFA). The layers were applied at speeds of 5, 10, 15, 30 $\mu\text{l}/\text{min}$. The matrix, added in excess, was intended for maximising the absorption of the MALDI UV laser light.

The analysis was performed using a Bruker Ultraflex Extreme MALDI Tandem TOF Mass Spectrometer (Bruker, USA) with 50 Hz nitrogen laser. The extraction voltage was 20 KV. The calibration of the MALDI-TOF-MS's spectra was made by the use of a standard lipid mixture on DHB (positive ion mode). For calibration (negative ion mode) the signals originated from the DHB matrix were used.

TLC spot imaging and scanning was done using an ultraflex MALDI-TOF/TOF. Imaging settings were as follows: laser in reflector mode at 200 Hz, 25 KV

extraction voltage and matrix suppression $m/z < 200$. Spot images were taken at 200x200 μm resolution using flexImaging.

2.9 Statistical methodologies

All data presented from serology studies was originated in the course of three independent studies containing a minimum of two internal duplicates.

Throughout these studies the intra and inter-assay variability was monitored using sera samples of known reactivity and accepted as valid if the fluctuation of intensity was within 10-15% variation (Murray and Lawrence 1993). This variation was calculated as a coefficient of variation (CV) measured as follows:

$$\text{CV} = (\text{Standard Deviation (SD)} / \text{Mean}) * 100$$

2.9.1 Normality test

Descriptive statistics were used to determine the goodness of fit of our data to a normal distribution. Kolmogorov-Smirnov (KS) test and quantile-quantile plots (QQ) were the methodologies of choice to elucidate deviation from Gaussian distribution. (GRAPHPAD PRISM 5 software (GraphPad Software Inc., USA)).

2.9.2 Receiver Operator Characteristic (ROC) analysis

MEDCALC software using the Hanley & McNeil (Chapter 4.3) or DeLong (Chapter 4.7) approach with 95% confidence intervals was used to perform ROC analysis. The areas under the curve were analysed assuming a likelihood ratio of LR+2.0 and LR-0.5, corresponding to an area under the curve (AUC) of 0.75, as the accepted cut-off value for a clinically useful biomarker (Jones and Athanasiou 2005). AUC values from Jones and co-workers (Jones & Athanasiou 2005) were used for reference purposes, being as follows: ≥ 0.97 excellent, 0.93-0.96 very good and 0.75-0.92 good. Although these guidelines were followed, every study needs to be assessed individually, in a clinical context, and the AUC values are not to be taken as an absolute indicator of a biomarker's strength.

2.9.3 Heat map analysis

Raw intensity unit values or Log_{10} transformed data from glycoarrays and microarrays were used to generate heat maps, which underwent hierarchical clustering (HCL) and Pearson correlation for distance metric selection (MEV software; Dana-Farber Cancer Institute, Boston, MA, USA).

2.9.4 Clinical correlation studies

Correlation studies for upper limit of normal (ULN) calculation including Wilcoxon signed rank test for non-parametric data and box and whisker plots set within 5-95% intervals were calculated using MINITAB 15 software (Minitab 15 software, State College, PA, USA) and GRAPHPAD PRISM 5 software (GraphPad Software Inc., San Diego, CA, USA).

3 Chapter 3. Anti-GM1 antibody diversity.

3.1 Introduction

In 1976 GM1 ganglioside was first described to induce and/or mediate an experimental autoimmune neurologic disorder after being injected into rabbits (Nagai et al. 1976). A few years later, various studies finally associated GM1 as an antibody target in patients with motor neuron disease (Freddo et al. 1986; Latov et al. 1988) and Guillain-Barré syndrome (Ilyas, Willison, Quarles, Jungalwala, Cornblath, Trapp, Griffin, Griffin, & McKhann 1988b). Since then, anti-GM1 antibodies have not escaped controversy.

The inconsistency in anti-GM1 antibodies detection in patients has been pointed out as a major limitation in identifying these antibodies as causing agents of some neurological disorders (Parry 1994). Percentages of antibody positive patients have been found to be extremely diverse, depending on the technique used and disease evaluated, ranging from 30% to 60% (Adams, Kuntzer, Burger, Chofflon, Magistris, Regli, & Steck 1991; Pestronk 2000; Sadiq, Thomas, Kilidireas, Protopsaltis, Hays, Lee, Romas, Kumar, Van den Berg, Santoro, & . 1990). In the remainder antibodies are undetectable, although expected to be present as there is no clear distinction in phenotype characteristics or treatment responsiveness between antibody-positive and -negative cases amongst the distinct neurological disorders.

The single most striking observation to emerge from the study of anti-GM1 antibody mediated neuropathies is the existence of a clearly differentiated motor phenotype (Pestronk, Cornblath, Ilyas, Baba, Quarles, Griffin, Alderson, & Adams 1988). However, existing accounts fail to resolve the apparent contradiction between GM1 ganglioside location in both motor and sensory peripheral nerves and the distinct disease phenotype (Ogawa-Goto and Abe 1998).

Studies in tissue and solid-phase immunoassays have revealed that the GM1-epitope can be inaccessible for antibody binding due to a masking effect exerted by neighbouring gangliosides such as GD1a (complex mediated *cis*-inhibition). The most striking conclusion to emerge from the data is that unless GM1-epitope

is topologically available for antibody binding no axonal damage or conduction block would be induced due to a lack of antibody bound complement activation (Greenshields, Halstead, Zitman, Rinaldi, Brennan, O'Leary, Chamberlain, Easton, Roxburgh, Pediani, Furukawa, Furukawa, Goodyear, Plomp, & Willison 2009).

It can thus be suggested that heteromeric lipid complexes containing GM1 can be modulators, either enhancing or inhibiting antibody binding, thereby explaining the diversity found within anti-GM1 antibodies. For example, the presence of antibodies which exclusively bind lipid complexes formed by GM1 and GalC in the absence of antibody binding to the single components, highlights the importance of the neighbouring lipid environment in the formation of neoepitopes or the conformational modulation of the target epitope (Galban-Horcajo, Fitzpatrick, Hutton, Dunn, Kalna, Brennan, Rinaldi, Yu, Goodyear, & Willison 2013; Nobile-Orazio, Giannotta, Musset, Messina, & Leger 2013; Pestronk, Choksi, Blume, & Lopate 1997).

3.2 Aims

The aims of this study are:

- Evaluate lipid complex formation in a non-immobilised artificial membrane environment using a liposome-based model and Flow Cytometry analysis.
- Use the developed liposome model to affinity purify anti-GM1 antibodies from neuropathy patient sera.
- Characterise, through array technology, anti-GM1 antibody binding diversity in a complex lipid environment.

3.3 Results

3.3.1 Antibody binding to liposomes containing gangliosides

Two mouse anti-GM1 IgG monoclonal antibodies (mAb), DG1 and DG2, were used to model lipid complex formation in liposome membranes. These two mAb have

similar GM1 binding affinities, but have been described to exert a differential GM1 binding in the presence of GD1a ganglioside; DG1 binding was cis-inhibited in the presence of GD1a and binding of DG2 remained unaltered (Greenshields, Halstead, Zitman, Rinaldi, Brennan, O'Leary, Chamberlain, Easton, Roxburgh, Pediani, Furukawa, Furukawa, Goodyear, Plomp, & Willison 2009).

Liposomes were prepared as stated in Materials and Methods section 2.2. Prior to commencing the study, liposome staining with mAb was optimised.

All the studies presented here comprise three internal replicates per sample and were repeated three consecutive times.

3.3.1.1 Assessment of liposome labelling

In initial experiments, liposomes were labelled by inclusion of OVA conjugated Alexa-488 (OVA-488) during the preparation of MLVs (see Methods Preparation of Liposomes 2.2). This protocol was adapted from a mouse immunisation regime utilising liposomes incorporating OVA as a T-Cell response adjuvant (Habjanec et al. 2006).

Four different molarities of OVA-488, (0.05 μ mol, 0.1 μ mol, 0.5 μ mol and 1 μ mol) were tested and compared against unlabelled liposomes, which were used as an indication of background autofluorescence. Flow cytometry data (Figure 3.1) revealed a disappointingly weak fluorescence emission signal for all the concentrations of OVA employed when excited at 488nm. The low signal could be due to a poor incorporation efficiency of OVA by the liposomes or the use of an insufficient quantity of labelled OVA. Examination of the literature suggests that the low incorporation rate of OVA into MLVs may result from the hydration of the thin lipid layers with a PBS containing OVA solution (Taneichi et al. 2010). An alternative method for OVA incorporation would consist of coupling via disuccinimidyl suberate on the surface of the liposome (Taneichi et al. 2006). Although proven more efficient, this methodology was discarded due to the potential disruption that OVA presented on the surface of the liposome could cause to antibody binding to gangliosides contained on the outer membrane of the vesicles.

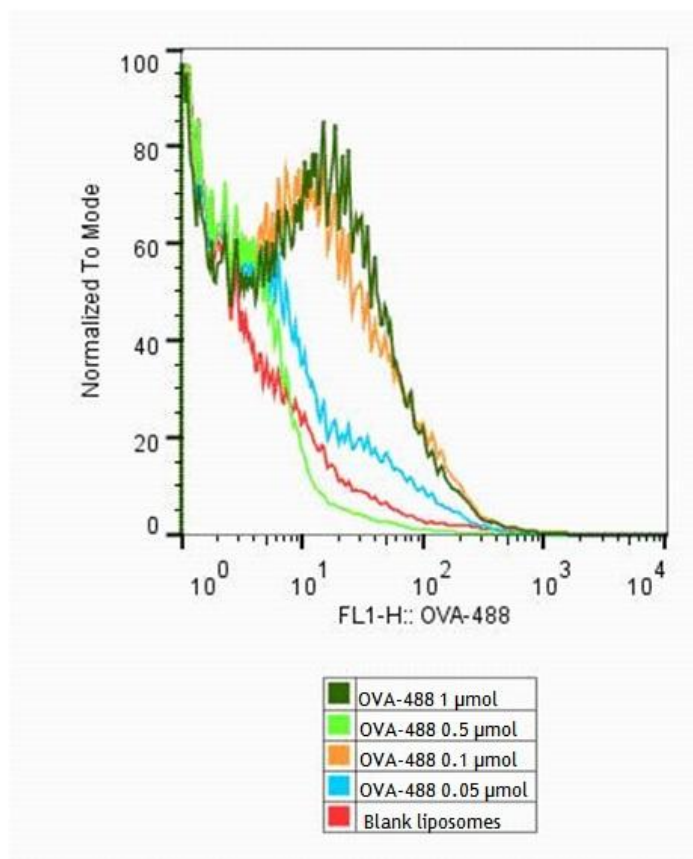


Figure 3.1. Histogram representing OVA-488 positive liposomes.

Flow cytometry data, plotted as a histogram. Data points represent fluorescent intensity from different liposome preparations. The liposome preparations included different quantities of Ova-488 introduced during the synthesis of liposome. The different preparations were as follows: 1 μmol of OVA-488 (Dark green), 0.5 μmol of OVA-488 (light green), 0.1 μmol of OVA-488 (orange), 0.05 μmol of OVA-488 (blue) and liposomes without including OVA as a test for liposome auto fluorescence (red). The X axis represents the size of the OVA-488 population and the Y axis represent the fluorescence intensity normalize to 100 using the highest intensity value.

Subsequently, BODIPY labelled Cholesteryl (a non-hydroxylated cholesterol molecule) was assessed for liposome labelling. In this scenario, liposome cholesterol was substituted for either 0.30 mg, 0.60mg or 0.90mg fluorescently conjugated cholesteryl. Due to the integral role of cholesterol/cholestreryl, 0.30 mg was the minimum amount of required for liposome formation.

Flow cytometry data showed a significant difference between all the cholesteryl labelled liposomes and the unlabelled liposomes (Figure 3.2B) revealing a successful labelling protocol. However, no significant difference was observed between liposomes containing different amounts of labelled cholesteryl, suggesting that the labelling already reached saturation with the inclusion of 0.30 mg.

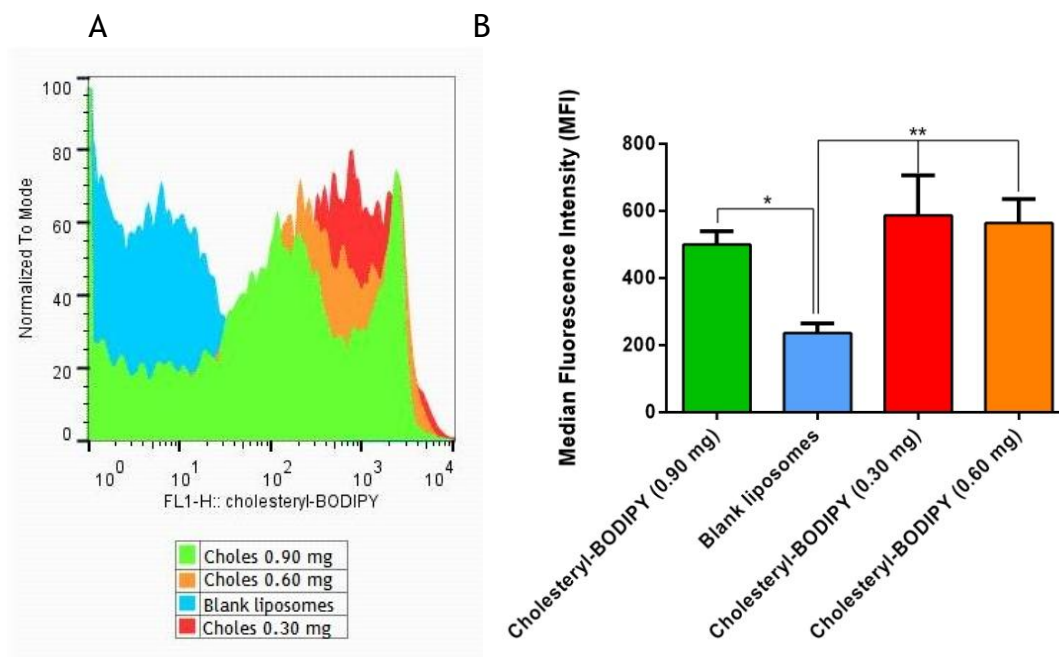


Figure 3.2. Cholesteryl BODIPY and liposome's fluorescence intensity.

Panel A shows the overlapped histograms of flow cytometry data for unlabelled liposomes (blank liposomes) (blue) and liposomes containing 0.30 mg (red), 0.60 mg (orange) and 0.90 mg (green) of cholesteryl. Blank liposomes were an indication of autofluorescence. Panel B. illustrates the median fluorescence intensity of all the liposome populations. Significance was analysed using Kolmogorov-Smirnov (K-S) test (Young 1977) (*p value \leq 0.05 and **p value \leq 0.01).

Much has been speculated as to how fluorescent labels might affect the way lipids diffuse across the membrane and interact with the neighbouring environment (Marks et al. 2008). In the case of antibody binding to glycolipid domains present on liposomes, the membrane lateral interactions could play a key role with the formation of glycolipid complexes. In this experiment the hydroxylated headgroup of naturally occurring cholesterol, is substitute by BODIPY in the cholesteryl molecule. It has recently been shown that the hydroxylated headgroup of cholesterol modulates the presentation of neighbouring glycolipid through the formation of hydrogen bonds. Therefore it could result in the disruption of lipid lateral flow within the membrane and alter the presentation of glycolipids. However, a study comparing the diffusion and sterol trafficking of natural radiolabelled [^3H]cholesterol and BODIPY cholesteryl in membranes of Chinese hamster ovary (CHO) cells demonstrated that both molecules exerted a similar behaviour, and no anomaly due to labelling was reported (Holttu-Vuori et al. 2008). However, it is currently unknown what affect fluorescently conjugated cholesteryl may have on glycolipid presentation and antibody binding.

In the light of these results, further flow cytometry experiments will be conducted using 0.30 mg of BODIPY-cholesteryl per liposome preparation.

3.3.1.2 Titration of DG2 mAb using GM1 liposomes

Increasing concentrations of DG2 (10, 20, 40, 60, 80 $\mu\text{g}/\text{ml}$) were applied to blank liposomes and liposomes containing GM1 ganglioside. Antibody binding was detected using Alexa647 conjugated anti-mouse IgG antibody, and the positive liposome subsets were selected as BODIPY/Alexa647 double positive (Figure 3.3.B).

DG2 binding to GM1 liposomes was significantly increased between 10 $\mu\text{g}/\text{ml}$ to 20 $\mu\text{g}/\text{ml}$ after which the fluorescent intensity plateaued. These data suggests that the antibody binding reached saturation at a concentration between 10-20 $\mu\text{g}/\text{ml}$.

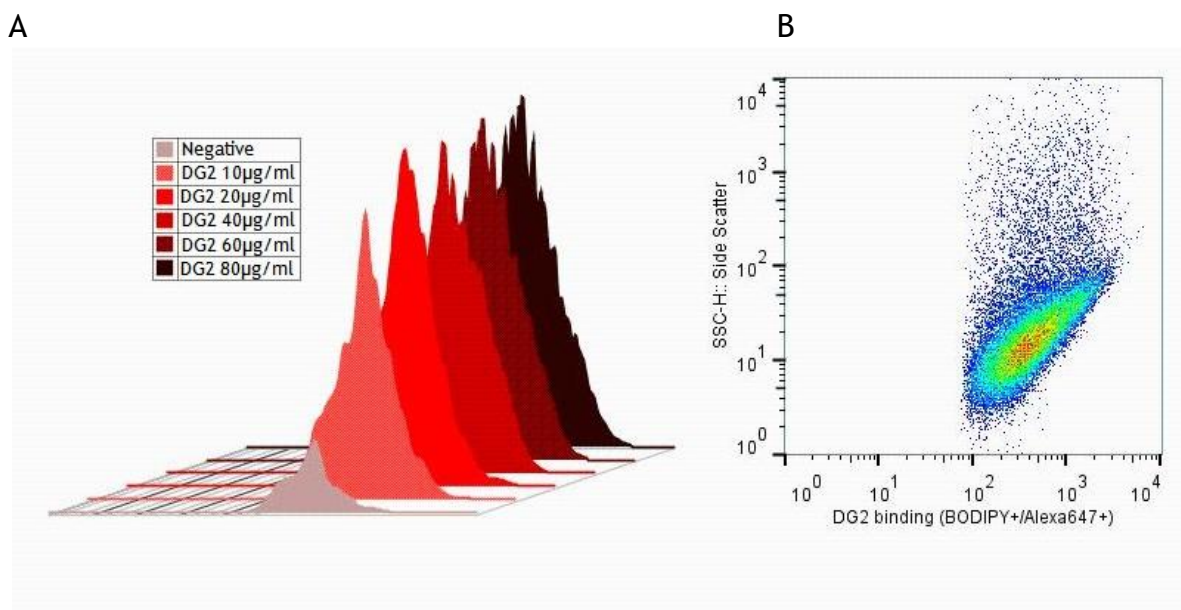


Figure 3.3. Flow Cytometry data corresponding to stained GM1-liposomes.

A. Stained with increasing concentrations of DG2 mAb and secondary Ab only (negative) and B. selected as BODIPY+/Alexa647+ liposome subset. The MFI data for these concentrations was: 10 $\mu\text{g}/\text{ml}$ 397, 20 $\mu\text{g}/\text{ml}$ 414, 40 $\mu\text{g}/\text{ml}$ 454, 60 $\mu\text{g}/\text{ml}$ 423 and 80 $\mu\text{g}/\text{ml}$ 387.

Therefore, the mAb concentration used for the subsequent liposome studies was 40 $\mu\text{g}/\text{ml}$ to ensure saturation.

3.3.1.3 Assessment of lipid complex formation in liposomes using DG1 and DG2 mAb

The GM1:GD1a ratio used in liposomes for Flow Cytometry studies was elucidated using the sera of a GBS patient (JK) which contained IgG antibodies against GM1:GD1a but no antibodies directed against the single epitopes (Figure 3.4 A).

For this study, GM1 was kept constant at 100 µg/ml and increasing concentrations of GD1a were premixed with GM1 in order to obtain nine different weight:weight ratios on a single array. Arrays probed with different dilutions of JK serum revealed that the highest peak of binding intensity was found when both GM1 and GD1a were at 100 µg/ml (1:1, w:w). The binding profile of this antibody acquired a Gaussian shape, progressively decreasing its binding intensity as GD1a concentration was increased (Figure 3.4 B).

The molecular weight of GM1 and GD1a are 1547 g/mol and 1838 g/mol respectively, therefore 100 µg are equivalent to $6.46 \cdot 10^{-8}$ moles of GM1 and $5.44 \cdot 10^{-8}$ moles of GD1a. The existence of an optimum molecular ratio of 1:1 GM1:GD1a, has been previously demonstrated by the construction of a dimeric GM1:GD1a hybrid ganglioside. In this study, a chemical construct formed by a 1:1 dimerisation of GM1 with GD1a was seen to be an optimum epitope for complex specific IgG antibodies contained in patient sera (Mauri, Casellato, Ciampa, Uekusa, Kato, Kaida, Motoyama, Kusunoki, & Sonnino 2012).

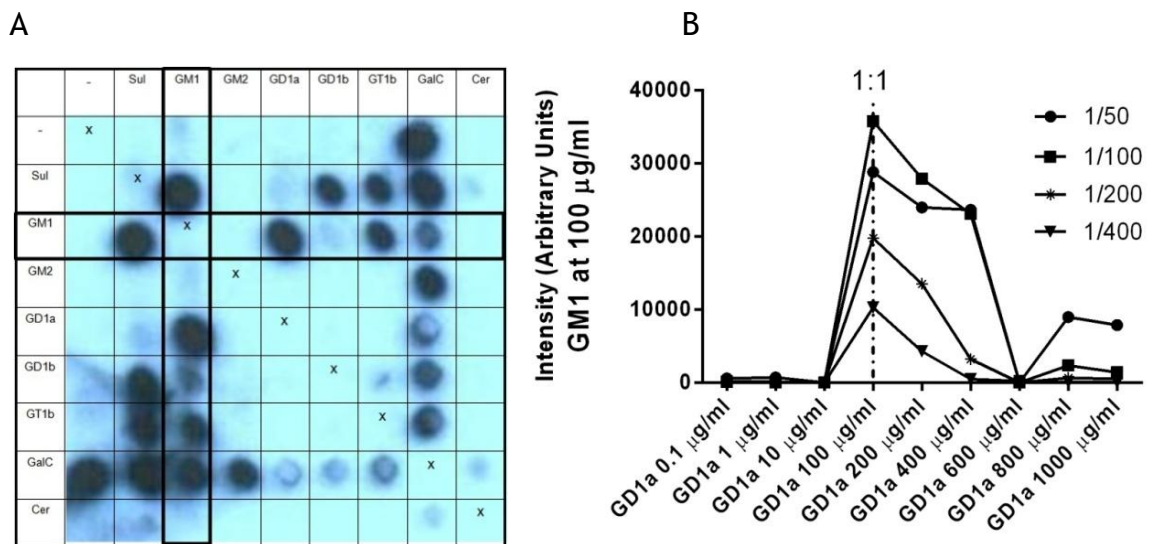


Figure 3.4. Analysis of GM1:GD1a IgG antibodies in the patient JK.

Panel A. Blot demonstrating JK's IgG antibody binding profile when diluted at 1:100. Combinatorial glycoarrays are designed to identify antibody reactivity to single glycolipids (duplicated in top row and left-hand row) and 1:1 glycolipid complexes (w/w) (remainder of grid). A line of symmetry runs top left to bottom right, representing analysis in duplicate. Panel B. Illustrates data from arrays containing GM1 ganglioside at a constant concentration (100µg/ml), forming heteromeric complexes with increasing concentrations of GD1a in blots probed with JK sera at various dilutions.

It is therefore likely, that the GM1:GD1a complexes will exist as 1:1 dimers on a liposome membrane and that the composition of these vesicles will contain a molecular ratio of 1:1 GM1:GD1a. As a result of this, all the subsequent studies were conducted including a 1:1 (mole to mole) ratio of both gangliosides.

Liposomes containing GM1, GD1a, GM1:GD1a and without gangliosides (blank liposomes) were prepared and stained with DG1, DG2, MOG35 (a GD1a specific mouse IgG mAb) and MOG1 (a GD1b specific mouse IgG mAb)

As shown in Figure 3.5, binding of DG1 to GM1 was cis-inhibited in the presence of equal moles of GD1a (A) , while the binding of DG2 was unaltered (B). Neither DG1 nor DG2 bound to liposomes containing GD1a only (data not shown). There was very weak nonspecific binding of these mouse mAb to the liposomes, as tested using liposomes containing no ganglioside, therefore the difference in binding profiles between the antibodies was due to the presence of GD1a (Figure 3.5 C).

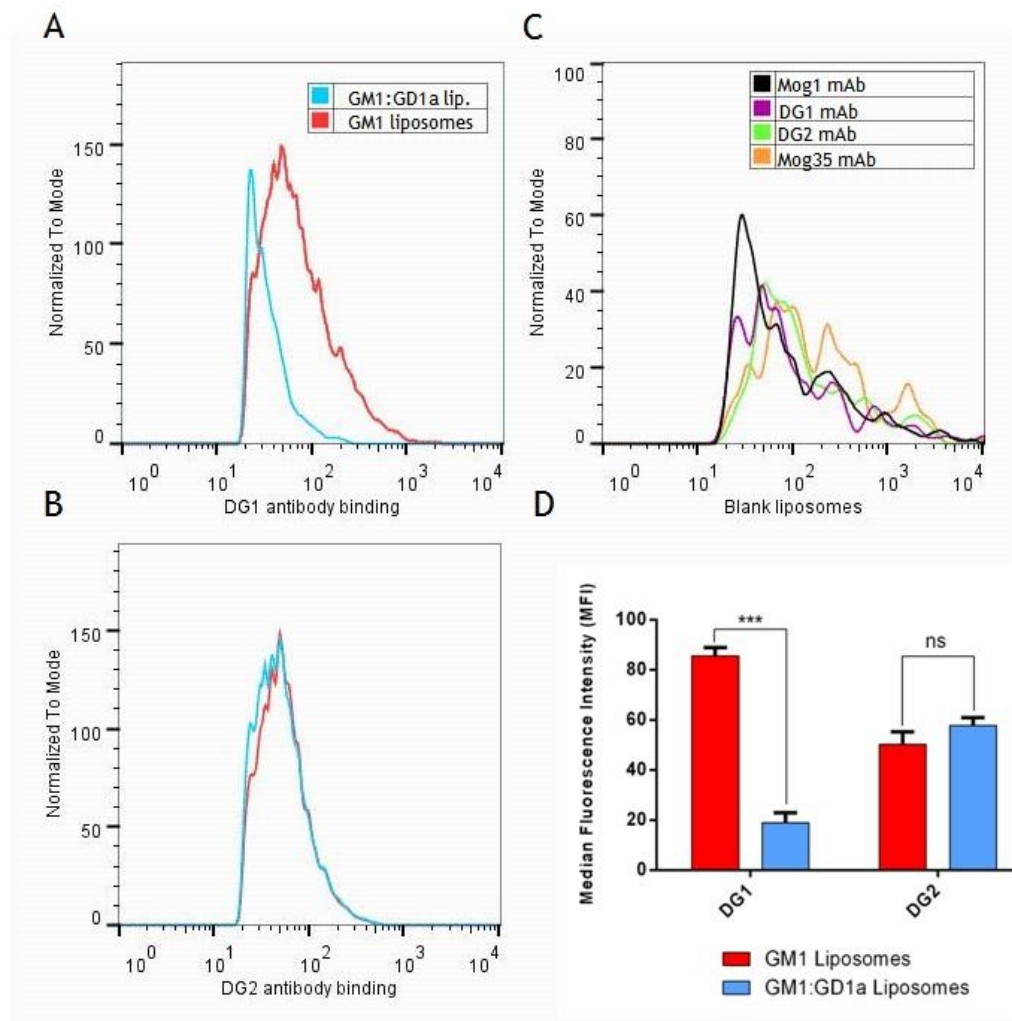


Figure 3.5. Histograms depicting DG1 and DG2 binding to liposomes.

A. Shows DG1 binding to GM1 (red) and GM1:GD1a (blue) liposomes. The scale has been automatically normalized up to 200. B. Shows DG2 binding to GM1 (red) and GM1:GD1a (blue). The scale has been automatically normalized up to 200. C. shows weak binding of ganglioside specific mAbs to liposomes containing no gangliosides. The scale has been automatically normalized up to 100. D. Graph bar representing the significance of difference in mAb binding to both GM1 and GM1:GD1a liposomes, expressed as mean fluorescence intensity (MFI). Analysis of histogram data was conducted using the Kolmogorov-Smirnov (K-S) test (Young 1977) (***) p value ≤ 0.001 .

From the data above we can see that the observations of Greenshields and co-workers (Greenshields, Halstead, Zitman, Rinaldi, Brennan, O'Leary, Chamberlain, Easton, Roxburgh, Pediani, Furukawa, Furukawa, Goodyear, Plomp, & Willison 2009) were successfully reproduced using a liposome-based format. Therefore, the decrease in DG1 binding intensity to GM1 in the presence of GD1a, indicated the formation of GM1:GD1a complexes in the liposomes.

3.3.2 Affinity purification of anti-GM1 antibodies from a GBS patient (BTN) serum

The affinity purification was performed as stated in Materials and Methods 2.4.

Due to the scarcity of sera availability, the following affinity purification studies were conducted using a GBS patient BTN, in which I explored GM1:Cholesterol IgG antibody binding.

Prior to commencing the study, the optimum molecular ratio of GM1:Cholesterol was determined. For this, an array containing nine different GM1:Cholesterol ratios were probed with BTN serum and stained using an anti-Human IgG antibody HRP labelled (Figure 3.6)

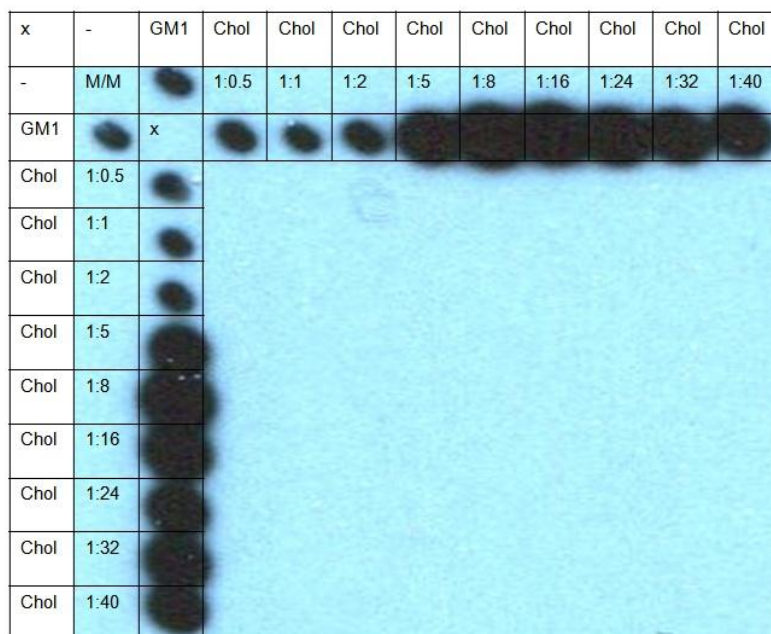


Figure 3.6. Array illustrating the IgG antibody binding profile of BTN serum.

The molarity of GM1 was kept constant while Cholesterol was increased from 1:0.5 to 1:40 (GM1:Cholesterol, M/M). Single glycolipids are duplicated in top row and left-hand row and GM1:Cholesterol complexes (M/M) are duplicated in second top row and second left-hand row. The array was probed with unpurified BTN serum at 1:100 dilution and detected using HRP conjugated anti-human IgG secondary antibody.

From the data in Figure 3.6 it is apparent that antibody binding intensity to GM1 increased with increasing amounts of cholesterol before reaching an intensity maximum at 1:8 GM1:Cholesterol.

These finding, while preliminary, suggests that a molecular ratio of 1:8 GM1:Cholesterol would be the optimum in order to affinity purify this antibodies

using liposomes. Therefore, further studies were conducted using liposomes containing this ratio.

GM1:Chol, GM1 and Cholesterol liposomes were prepared and used to isolate the anti-GM1 and/or Cholesterol antibody component of the serum. (Figure 3.7). For isolation of complex dependent antibody, three consecutive purifications of BTN serum with GM1:Chol liposomes was performed, to maximise antibody retrieval, as it was anticipated that the liposome antigen would be readily saturated with antibodies. Glycoarray analysis of the affinity purified fraction revealed the presence of a complex specific GM1:Chol IgG antibody. This affinity purified antibody did not bind GM1 or cholesterol single epitopes but a only complex of both (Figure 3.7 purification 1, 2 and 3). When a batch of the same serum was applied to liposomes containing only cholesterol, no antibodies were retrieved, confirming the absence of anti-cholesterol antibodies in this patient's serum.

The supernatant fraction (not bound by the liposomes) was analysed by glycoarray following the first and final round of liposome affinity purification. The results reveal the presence of anti-GM1/GM1:Chol antibodies, albeit at a reduced intensity, indicating that the efficiency of the affinity purification could be further improved (Figure 3.7 supernatant step 1 and 3).

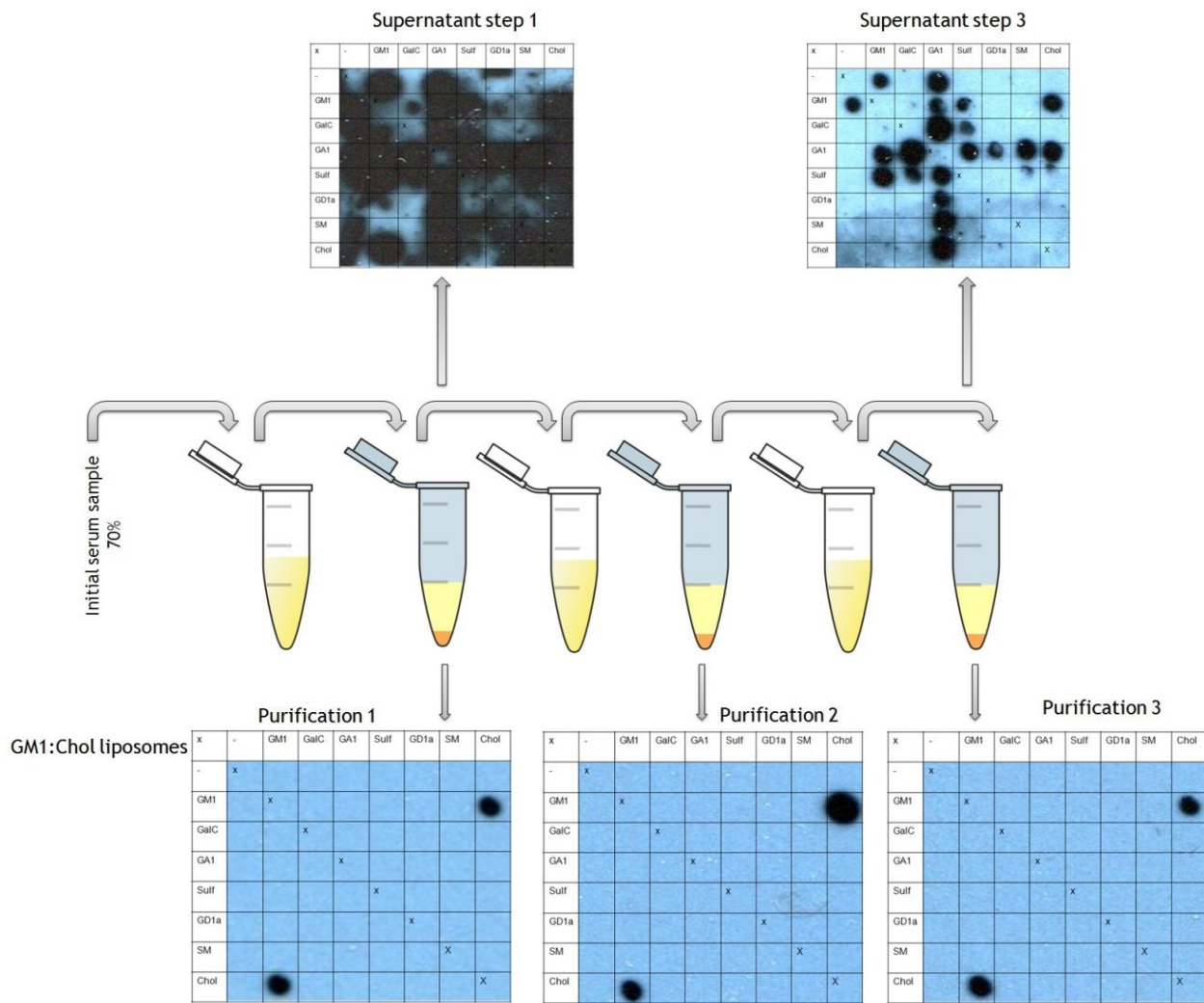


Figure 3.7. Affinity purification process.

GM1:Chol IgG antibodies from BTN serum were purified using a three steps purification as specified in Chapter 2 (Materials and methods 1.4). In every purification step an array was probed to qualitatively analyse antibody reactivity present in the eluted material and in the supernatant.

To establish whether antibody fractions remained attached to the liposomes after pH driven elution, liposomes from the last purification step were spotted onto PVDF-FL coated microscope slides using a piezoelectric driven, non-contact microarray spotter. The arrays were then stained using an anti-Human IgG antibody labelled with Alexa555.

The results obtained from the preliminary analysis of liposomes suggest that a significant amount of unknown specificity IgG antibodies remained bound to the liposomes (Figure 3.8).

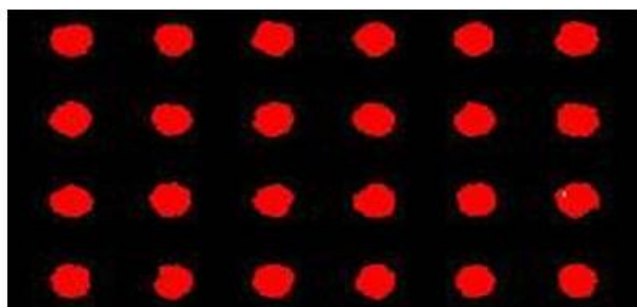


Figure 3.8. Liposomes spotted using microarray.

GM1:Chol liposomes were spotted onto PVDF-FL slides after being used for affinity purification of Abs with BTN serum. Liposomes were then probed using fluorescently labelled anti-human IgG secondary antibody to detect IgG antibodies still attached to the liposomes.

This finding has important implications for future development of a more efficient method to detach antibodies bound to liposomes and to improve any potential nonspecific binding.

To determine the binding profile of the antibody purified using GM1:Cholesterol liposomes, arrays identical to that presented in Figure 3.6 were probed with the affinity purified, eluted antibody. As anticipated, the GM1:Chol isolated antibody followed a similar enhancement pattern to that previously seen in whole patient serum (Figure 3.6), in which no antibody binding was detected at ratios of 1:0.5 up to 1:2, despite binding at a molecular ratio, at or greater than 1:5 (Figure 3.9 A). The antibody binding intensity was significantly increased at ratio 1:8 and greater (Figure 3.9 B). This data suggests the presence of one or more antibodies species, present in human serum, highly sensitive to specific molecular ratios which can be isolated using liposome model membranes and can be readily detected on array platforms.

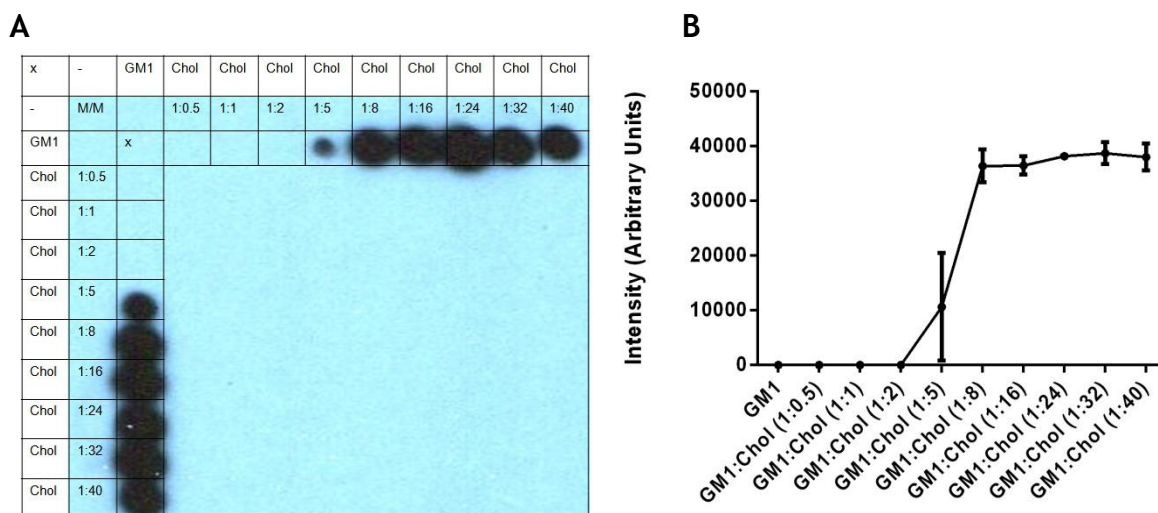


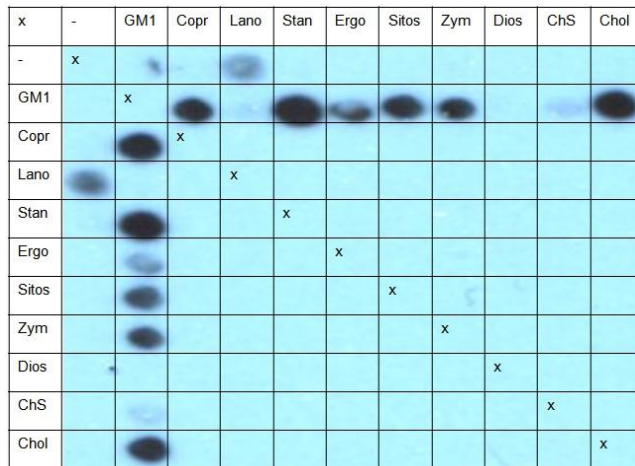
Figure 3.9. Glycoarray blots depicting GM1:Cholesterol mole to mole heteromeric complexes and singles lipids.

The molarity of GM1 was kept constant and the molarity of Cholesterol increased gradually up to 40 times higher the molarity of GM1. Single glycolipids are duplicated in top row and left-hand row and GM1:Cholesterol complexes (M/M) are duplicated in second top row and second left-hand row. A. the array was probed using GM1:Cholesterol antibodies affinity purified from BTN serum and detected using anti-human IgG HRP labelled secondary antibody. B. Intensity readout \pm SEM (n=3) of panel A.

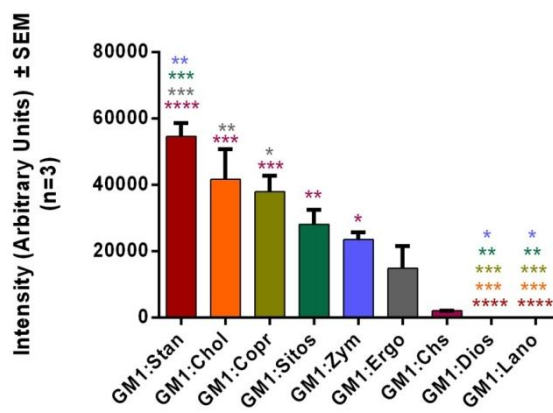
The nature of the heteromeric partnership between GM1 and cholesterol, and its ability to be detected by GM1:Cholesterol liposome isolated antibodies was further investigated by substituting cholesterol for various different sterol molecules on an array platform. A direct comparison was made between anti-GM1:Cholesterol antibody binding under these conditions.

Antibody binding to GM1 in the presence of Ergosterol (Ergo), Lanosterol (Lano), Cholesterol Sulphate (Chs) or Diosgenin (Dios) was very weak or absent when compared to GM1:Cholesterol binding intensity (Figure 3.10 B). Whereas, both Cholestenol (Stan) and Coprostanol (Copr) demonstrated equivalent binding intensities to GM1:Cholesterol complexes (Figure 3.10 C).

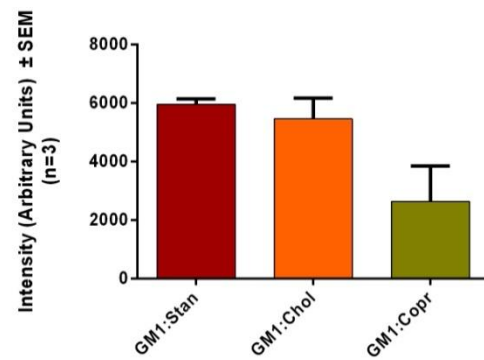
A



B



C



D

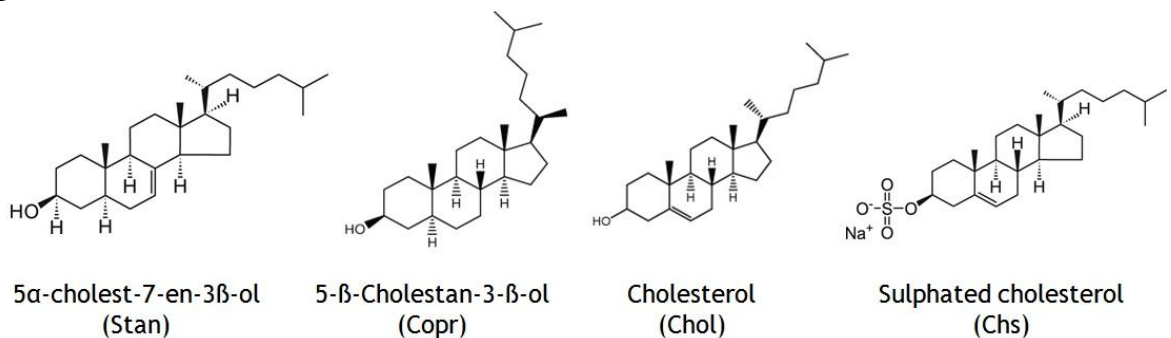


Figure 3.10. Arrays containing GM1 complexes with cholesterol variants probed with purified IgG GM1:Cholesterol antibody.

A. Antibody detection on glycoarrays using an HRP labelled secondary antibody. B. Intensity readout corresponding to arrays developed using ECL. Analysis was conducted with a one way anova using Tukey's multiple comparison test (*p value \leq 0.05, **p value \leq 0.01, ***p value \leq 0.001 and ****p value \leq 0.0001). C. Intensity readout corresponding to arrays developed using fluorescence. D. Structure of four of the different sterols examined in this study.

3.4 Discussion

3.4.1 Future technical improvements

There is considerable room for further progress in affinity purification of antibodies from patient sera. Firstly, a considerable amount of IgG antibodies remained bound to the liposomes after the final elution step (Figure 3.8). This result might be explained by a number of different factors. The most important factor which would require further analysis is the extraction/elution buffer composition. Alving and Richards demonstrated that glycine-HCl buffer was amongst the less efficient solutions for antibody-lipid dissociation (Alving and Richards 1977a; Alving and Richards 1977b). Instead, this study recommended CHCl_3 /Saline followed by elution using 1M NaI as the most effective methods of extraction. The method was proven so effective that the time for incubation with extraction buffer could be reduced down to 10 minutes. It could be expected then that a new extraction/elution buffer would reduce the concentration of antibody bound to the liposomes after final elution and increase antibody recovery.

3.4.2 Future prospectives

- Evaluation of the antibody binding diversity to GM1:Cholesterol epitope by assessing the polyclonality of the purified antibody using isoelectric focusing (IEF).
- Assess the effect of antibody binding to increasing concentrations of cholesterol complexed to GM1 compared to Cholesterol (Figure 3.9).
- Use 5- α -colestane, a cholesterol derivative lacking the A ring β -OH group.
- Test the potential tissue binding of the purified antibody in order to locate cholesterol-enriched GM1 domains in nerve preparations.

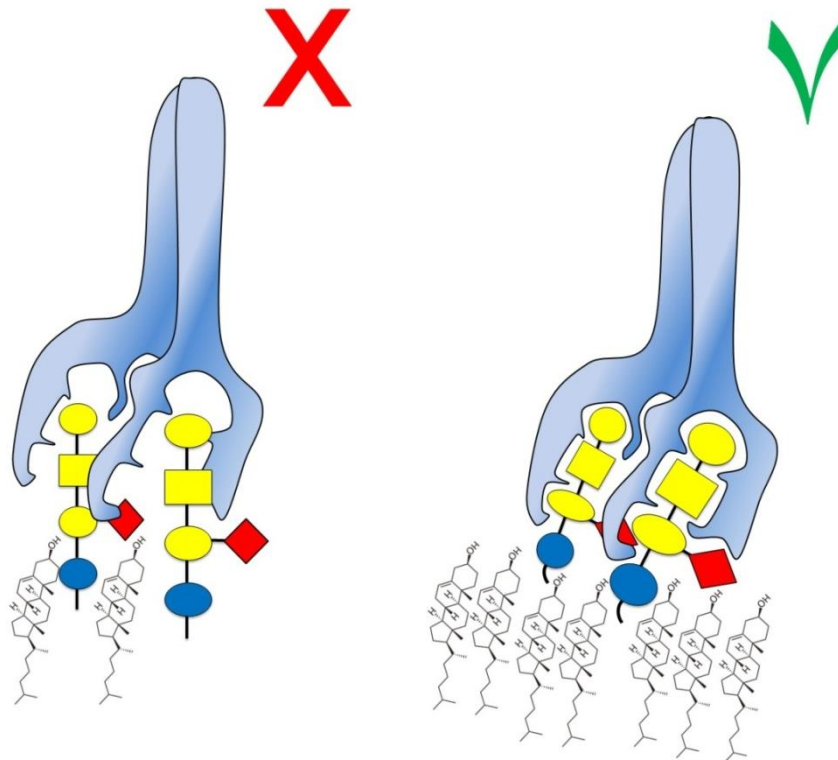
3.4.3 Conceptual development

The single most striking observation to emerge from the antibody isolation studies is the presence of an anti-GM1 antibody which solely binds GM1 in the presence of a high molar ratio of Cholesterol. However, the initial interpretation, derived from Figure 3.6, was that IgG antibodies binding GM1 single epitope are cis-enhanced by the presence of cholesterol. These studies to our knowledge are the first to demonstrate the existence of GM1:Cholesterol ratio-dependent, complex-specific antibodies. These findings stress the complexities of working with polyclonal serum samples in which multiple competing reactivities can mask individual binding patterns. Therefore it is essential to constantly re-evaluate the concept of cis-enhancement. The GM1:Cholesterol enhancement observed in the array using whole, unpurified BTN serum (Figure 3.6) was due to the presence of a different subset of antibodies all of which were complex specific. These observations highlight the polyclonality of the antibody repertoire and suggest an alternative interpretation of antibody binding cis-enhancements in the context of glycoarray analysis.

Having concluded that anti-GM1:Cholesterol antibodies are a different subset of antibodies from the single reactive anti-GM1 antibodies found in whole BTN serum, the question which arises is what makes the partnership between cholesterol and GM1 so different from GM1 alone clusters. Lingwood and co-workers described the structural modulation of GM1 by cholesterol enriched domains (Lingwood, Binnington, Rog, Vattulainen, Grzybek, Coskun, Lingwood, & Simons 2011). This article suggests that cholesterol is capable of altering the structure of GM1 by tilting its sugar headgroup orientation from perpendicular to parallel the membrane surface. This sterol induced structural change of GM1 made the glycolipid unavailable for cholera toxin binding. In addition to this, the necessary molar ratio of cholesterol to induce structural changes to GM1 was 50:1. This data demonstrates how heteromeric complexes may influence the presentation of antigen by either favouring or inhibiting ligand binding. In contrast to Lingwoods findings, BTN isolated antibody, exclusively binds GM1 epitopes containing abundant cholesterol, suggesting that this Ab binding would favour a specific structural orientation of the glycan epitope (Figure 3.9 and Figure 3.11). A more recent study using molecular dynamics simulation, has established that cholesterol may alter the structure of GM1 and GalC by creating

hydrogen bond networks between its donor OH group and GM1's glycosidic bond which links the ceramide to the glycan fraction (Figure 3.11 B). In addition, other stabilisation interactions were found between GM1 and cholesterol which were mediated by Van der Waals forces, interacting with the ganglioside's ceramide moiety (Di et al. 2013). This evidence support previous studies suggesting that the structure of cholesterol is relatively specific for an optimum formation of glycolipid complexes (Niedieck 1975a;Niedieck 1975b;Yahi, Aulas, & Fantini 2010). One of these studies, using anti-GalC sera which precipitated GalC micelles solely in the presence of cholesterol but not but not in its absence, reported a differential behaviour of these antibodies after substituting cholesterol by other sterols. However, molecules such as cholestanol and coprostanol exerted the same effect on the antibody binding to micelles as cholesterol. On the other hand, antibody binding did not occur in the presence of sterols in which the OH group at the 3 position of the A ring had been substituted (Niedieck and Kuck 1976). Our data suggests a similar behaviour of coprostanol and Cholestenol, showing a comparable effect to that of cholesterol in forming complexes with GM1 (Figure 3.10 B and C). Moreover, Cholesterol Sulphate (Chs) in which the OH group of the A ring is substituted by a sulphatide group, does not induce antibody binding in the presence of GM1. There is, however, a discrepancy; Diosgenin (Dios) and Lanosterol (Lan), sterol containing OH groups in the A ring, do not facilitate antibody binding when in complex with GM1 as seen our glycoarrays (Figure 3.10 C). According to Niedieck and Kuck (Niedieck & Kuck 1976), the nature of the domains formed by cholesterol is mainly conferred by the presence of an unaltered aliphatic side chain and an A ring OH group in B position. Therefore it could be hypothesised that our GM1:Cholesterol IgG antibody has other structural requirements apart from the OH group for optimum binding. Some of these requirements could include the presence of a planar ring system or the α and β position of the OH group in the A ring (Niedieck & Kuck 1976).

A



B

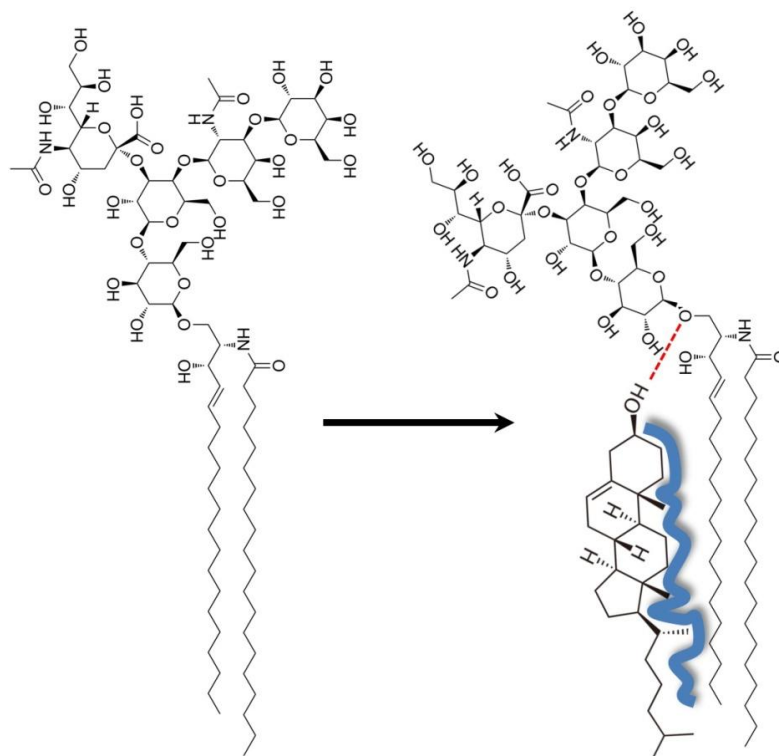


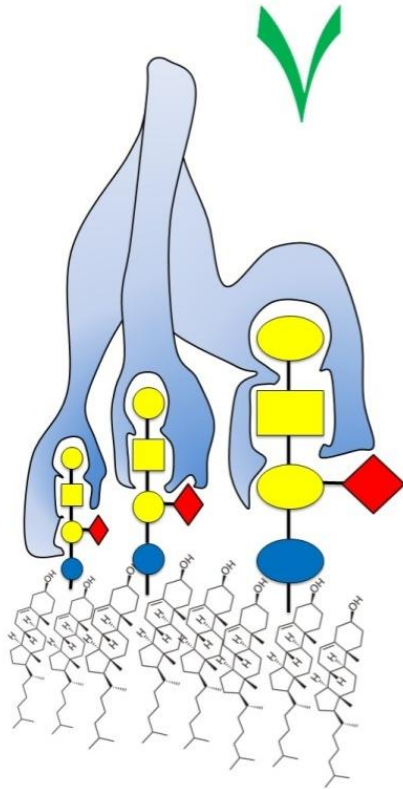
Figure 3.11. Diagram illustrating the Hypothesis of “GM1 structure change”.

A. Absence of antibody binding to GM1 in the presence of low cholesterol ratios (indicated by a red cross). High cholesterol ratios inducing a structural change to GM1 facilitating glycolipid-antibody recognition (indicated by a green tick). B. GM1 backbone structures illustrating the conformation change. Red dotted line represents hydrogen bonding and blue line around the cholesterol depicts the presence of Van der Waals forces.

Another plausible explanation for how cholesterol impacts on antibody binding to GM1 could be explained by considering high density GM1 clusters. In the case of Cholera Toxin, binding to GM1 in a liposome model membrane (MacKenzie et al. 1997) or on immobilised bilayers (Shi et al. 2007), it has been demonstrated that binding strength was almost exclusively dependent on ligand density, such that toxin binding was found to be weakened on high density domains of GM1. Monovalent interactions of most anti-carbohydrate antibody and lectins with their target are known to be very weak. To compensate they rely on engaging multiple binding arms to increase the avidity of the interaction and so, density of the antigen is crucial to ensure simultaneous binding event may occur. It is possible that cholesterol may act as a spacing molecule in which GM1 is dispersed at optimum distances to allow such interaction to occur.

This antibody screening approach could open up a hitherto unexplored and entirely novel area of biomarker discovery, where epitope structure and clustering could be tailored by using sterols and other highly abundant membrane molecules at different molecular ratios (Figure 3.12).

A



B

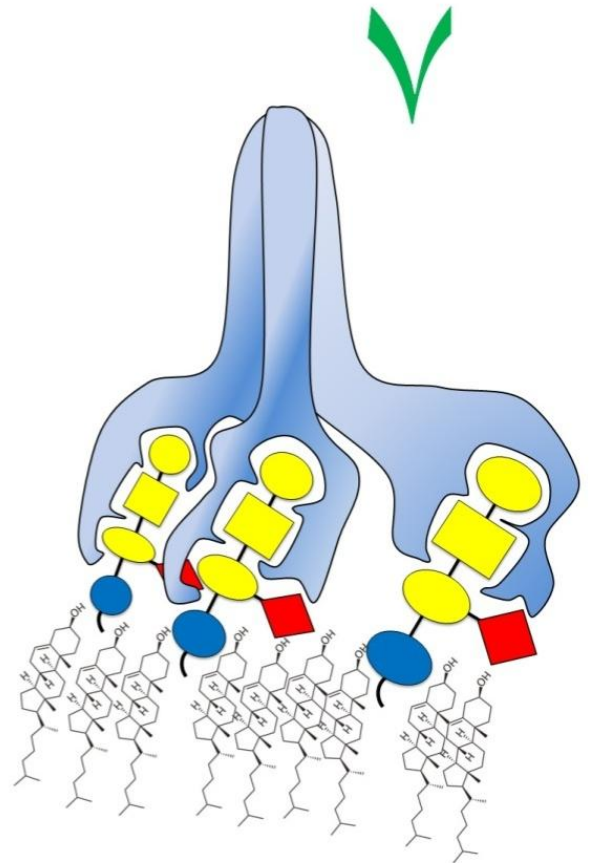


Figure 3.12. Two hypothesis for multivalent binding molecules.

A. Illustration highlighting the possibility of “spacing” as a key player for antibody binding stabilisation. B. “Spacing and structural change” as the factors potentially involved in multivalent binding stabilisation.

4 Chapter 4. Antibodies to heteromeric glycolipid complexes in Multifocal Motor Neuropathy.

4.1 Introduction

As outlined in Chapter 3, the interaction of GM1 with neighbouring GSLs can play a major role in modulating Ab binding. Recent observations (Nobile-Orazio, Giannotta, Musset, Messina, & Leger 2013) on an MMN cohort have confirmed the Ab binding enhancing effect of GalC over GM1 Ab binding (Pestronk, Choksi, Blume, & Lopate 1997). In contrast, other GSLs can inhibit Ab binding to GM1. A good example is GD1a which has been reported as cis-inhibitory when in complex with GM1 after sera profiling of MMN patients (Nobile-Orazio, Giannotta, & Briani 2010).

This chapter will attempt to describe the anti-GSL profile found in MMN patient sera, with particular emphasis on the enhancing or inhibitory effect of adjacent molecules to antibody binding.

4.2 Chapter aims

- Establish glycoarray as a robust method for routine diagnostic use in MMN.
- Identify new GM1 ganglioside complexes in MMN which might unmask previously undetected antibody reactivities.
- Investigate and characterise pattern recognition antibodies in MMN
- Validate the findings on an external, double blinded cohort containing equal number of patients and controls.

4.3 Southern General Hospital serology study

4.3.1 Study aims

- To investigate the antibody fingerprint of MMN sera using a recently developed combinatorial glycoarray, in which highly diverse repertoires of heteromeric complexes of lipids and glycolipids can be readily examined

for enhanced or attenuated antibody binding (Brennan, Galban-Horcajo, Rinaldi, O'Leary, Goodyear, Kalna, Arthur, Elliot, Barnett, Linington, Bennett, Owens, & Willison 2011; Rinaldi, Brennan, Goodyear, O'Leary, Schiavo, Crocker, & Willison 2009).

- Compare the performance of Glycoarray screening with conventional ELISA methodology.
- Using the same patient samples and MMN-derived monoclonal antibodies, further investigate antibody binding to epitopes consisting of specific molecular patterns, as described in the previous chapter.

4.3.2 Study design

Sera of 33 patients fulfilling diagnostic criteria for MMN were collected from the Southern General Hospital Glasgow, mostly undergoing treatment in our local clinical centre. 22 of these patients had undergone screening for a clinical trial of a complement inhibitor (Fitzpatrick et al. 2011).

Other neurological disease (OND) sera (n=30) comprised other neuropathies (n=6), multiple sclerosis (n=4), motor neurone disease (n=3), chronic fatigue syndrome (n=2), non-organic or undiagnosed neurological disorder (n=6), encephalopathy (n=1), cerebrovascular disease (n=1), optic neuritis (n=1), viral meningitis (n=1), migraine (n=2), headache (n=1), idiopathic intracranial hypertension (n=2).

Sera from healthy controls (HC) were obtained from 27 volunteers.

Sera was screened by glycoarray against an initial panel comprising the following lipids and glycolipids and their 1:1 (weight to weight) heteromeric complexes: GM1, GM2, GD1a, GT1b, GA1, galactocerebroside (GalC), 3-sulphated galactosylceramide (sulphatide, sulph), sulphated glucuronyl paragloboside (SGPG), sialosyl-lactoneotetraosylceramide (LM1) and phosphatidylserine (PS). The same sera was then screened using ELISA against GM1, GalC and GM1:GalC.

All sera were screened a minimum of three times (n=3).

4.3.3 Results

All MMN and control samples were screened by glycoarray comprising 10 single lipids and their 45 possible 1:1 complexes. Preliminary results showed 9 characteristic antibody binding fingerprints being shown in Figure 4.1, alongside 2 controls.

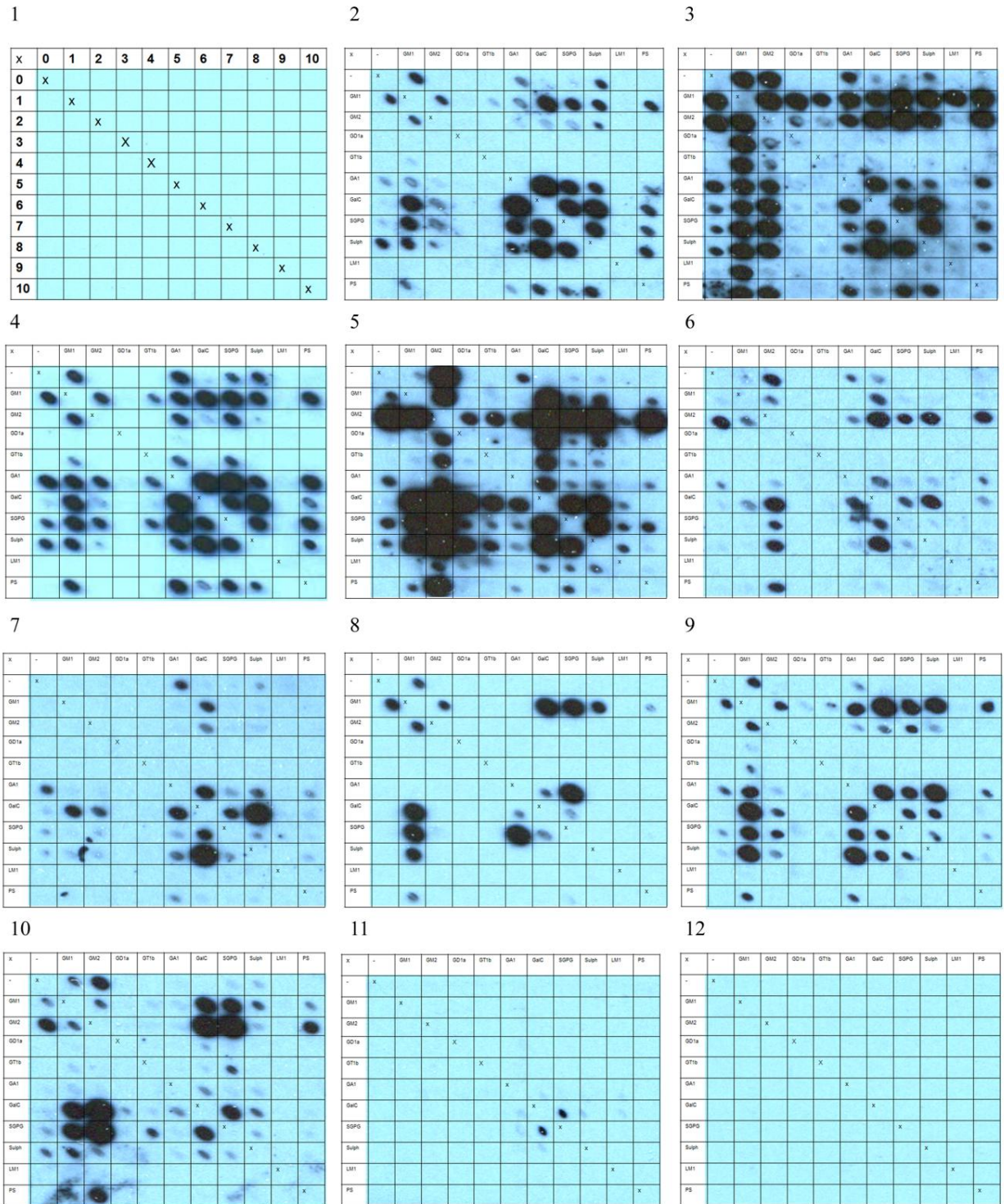


Figure 4.1. Representative blots from glycoarray.

Examples of glycoarrays from 9 MMN (2-10) and 2 control (11-12) cases, illustrating the different patterns of binding to individual glycolipids and their 1:1 complexes. Glycoarrays are printed in a grid, with the topmost row and far left hand column containing spots of 10 individual glycolipids, and the remaining spots comprising the complex formed from the combination of the glycolipids in the corresponding row and column. The template is shown in Array 1 as follows: 0, methanol; 1, GM1; 2, GM2, 3, GD1a; 4, GT1b; 5, GA1; 6, GaC; 7, SGPG; 8, sulphatide; 9, LM1; 10, PS. Each glycolipid and complex is thus printed in duplicate per array. A line of symmetry runs top left to bottom right, in which no antigen is spotted (marked with X). The intricacy of antibody binding patterns to single glycolipids and complexes can be readily appreciated.

4.3.3.1 Determining a cut-off value for positivity

As the glycoarray had not previously been systematically applied to an MMN population, there was no pre-determined upper limit of normal range (ULN) prior to the start of this study. Two proposed methods for determining ULN were compared. Firstly, the median and 95% confidence interval of GM1 spot intensity signal in the healthy control population was calculated by Wilcoxon signed rank test (as data were not normally distributed) giving an estimated median of 460 intensity units (IU), with a 95% confidence interval of 341 to 654 IU. Secondly, as the correlation coefficient for ELISA and glycoarray was high (0.78) (Figure 4.6 A), the regression equation was used to directly calculate the glycoarray value equivalent to 0.1 OD units on ELISA, yielding an ULN for the glycoarray of 4365 IU. This latter, more restrictive, value (4365 IU) was used as the cut-off value for positivity for GM1 and all other single lipids and heteromeric complexes studied in the glycoarray.

Using this cut-off value, 19/33 MMN samples were positive for anti-GM1 IgM by glycoarray. 3 of the samples positive for anti-GM1 IgM by ELISA were negative when screened by glycoarray (Figure 4.6 A).

4.3.3.2 Analysis of combinatorial glycoarray data

Array data from all MMN cases, OND and healthy controls were subjected to cluster analysis that yielded a heat map comprising spot intensities for 40/55 glycolipids and glycolipid complexes amongst cases and controls (Figure 4.2 A). For the remaining 15 targets, no detectable array signal was obtained from any of the samples (cases or controls), and these were excluded from further analysis. Spot intensities were categorised as either positive (>4365 AU) or negative (<4365 AU) and each of the 40 remaining glycolipid and glycolipid complexes were then individually subjected to ROC analysis, comparing MMN cases (n=33) with the combined OND and healthy control groups (n=57). The areas under the ROC curve (AUC, used as a summary measure of diagnostic accuracy) were ranked according to value (Figure 4.2 B). Through this process, the best performing glycolipid complex combinations for diagnostic accuracy were identified as GM1, GA1 and GM2, all in complex with GalC. Another high performing complex was GM1:SGPG. Although ranked 3rd, this marker was not

considered further in this study as SGPG is scarcely available and thus impractical for routine diagnostic use in most laboratories.

ROC graphs for GM1, GA1 and GM2, individually and in complex with GalC are shown in Figure 4.2 C, and all the individual sample intensity values in Figure 4.2 D.

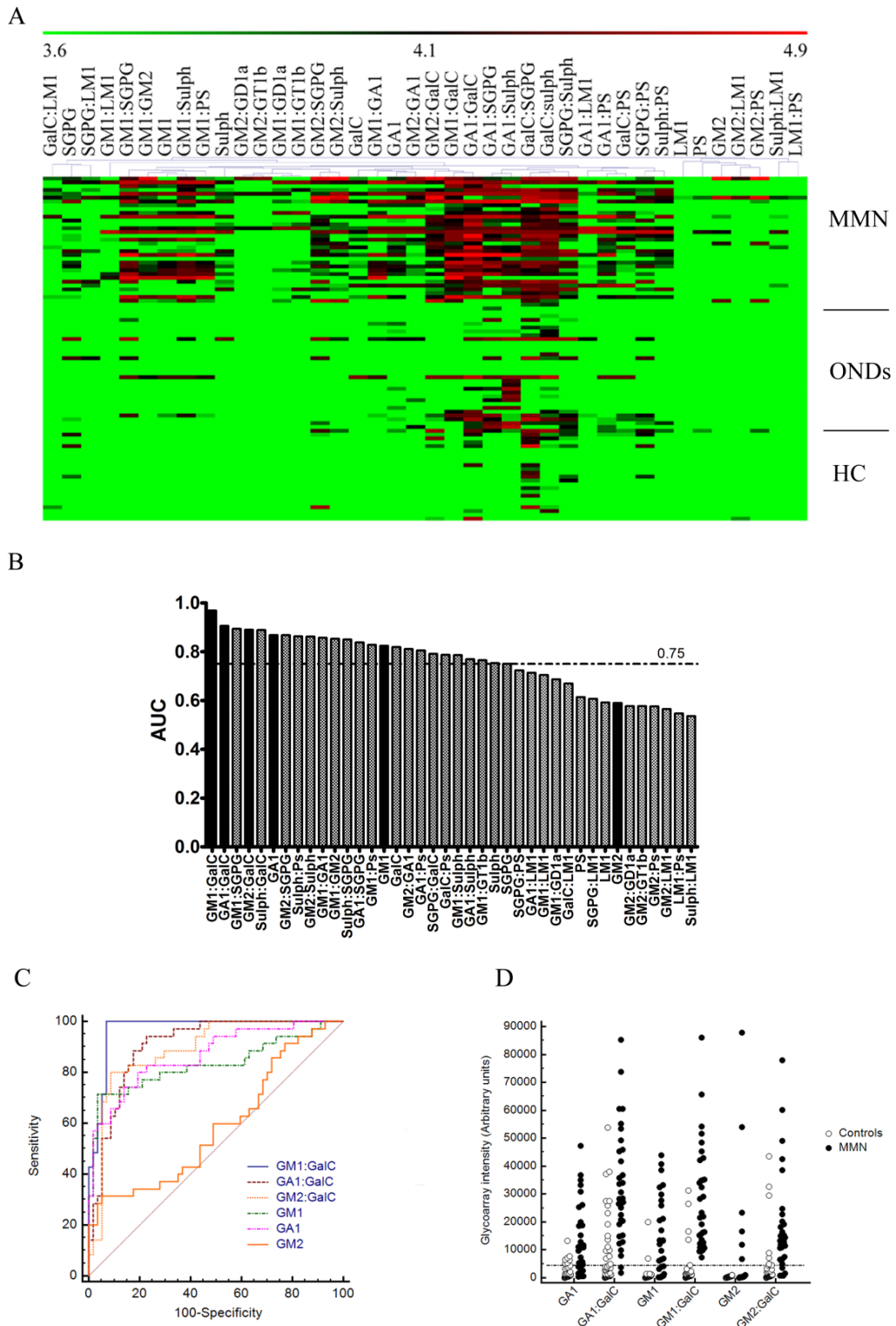


Figure 4.2. Quantitative and statistical analysis of glycoarray data.

Panel A. Heat map showing the values (logarithmic scale) of antibody binding intensity to the 40/55 single glycolipids and complexes that returned a detectable signal for 33 MMN patient sera, 27 healthy controls and 30 ONDs. The 15 lipids or lipid complexes that returned no signal in any samples are excluded from the heat map. The minimal value assigned to any sample was set at 3.6 IU, corresponding to \log_{10} ULN (4365 AU). Thus, pale green corresponds to antibody negative signals (<4365 AU), darker green and black to mid-range signals and red to high value signals. Panel B. ROC analysis was applied to rank signals by sensitivity/specificity ratio as a summary measure of assay performance, the highest values representing the best performing glycolipids and lipid complexes. Black bars highlight datasets plotted in Panels C and D. Panel C. Individual ROC curves for 3 single glycolipids (GM1, GM2 and GA1) and their complexes with GalC. Panel D. Individual glycoarray intensity values for MMN cases and all controls against 3 single glycolipids (GM1, GM2 and GA1) and their complexes with GalC.

Examining these data, GM1:GalC is the best performing complex for diagnostic sensitivity and specificity in this MMN population. Non parametric testing also revealed GM1:GalC as the lipid complex most significantly differentiating the MMN group from the combined control group ($p=6.4 \times 10^{-17}$) (Table 4.1).

Table 4.1. Sensitivity and specificity values for GM1, GM2, GA1 and representative complexes.

Antigen	MMN (n=33)	Controls (n=57)	Sensitivity	Specificity	AUC
GM1	19	2	58%	96.5%	0.824
GM1:GalC	33	4	100%	93.0%	0.979
GM1:Sulph	22	3	67%	95.0%	0.889
GM1:SGPG	24	6	73%	89.5%	0.894
GA1	24	7	73%	87.7%	0.868
GA1:GalC	31	17	94%	70.2%	0.938
GA1:Sulph	31	15	94%	73.7%	0.769
GA1:SGPG	28	15	85%	73.7%	0.838
GM2	6	0	18%	100%	0.590
GM2:GalC	28	6	85%	89.5%	0.890
GM2:Sulph	21	2	64%	96.5%	0.863
GM2:SGPG	26	6	79%	89.5%	0.868

A characteristic of the glycoarrays as described here are the readily observable patterns of enhancement and attenuation seen with different complexes, in comparison with antibody binding intensity to the single lipid. Thus, the median signal intensity of antibody binding to GM1 in the MMN group was 13394 IU (IQR 5213 - 28801). When GM1 is in complex with other glycolipids, the signal intensity may increase (complex enhanced), decrease (complex attenuated) or remain unchanged (complex independent) (Figure 4.3).

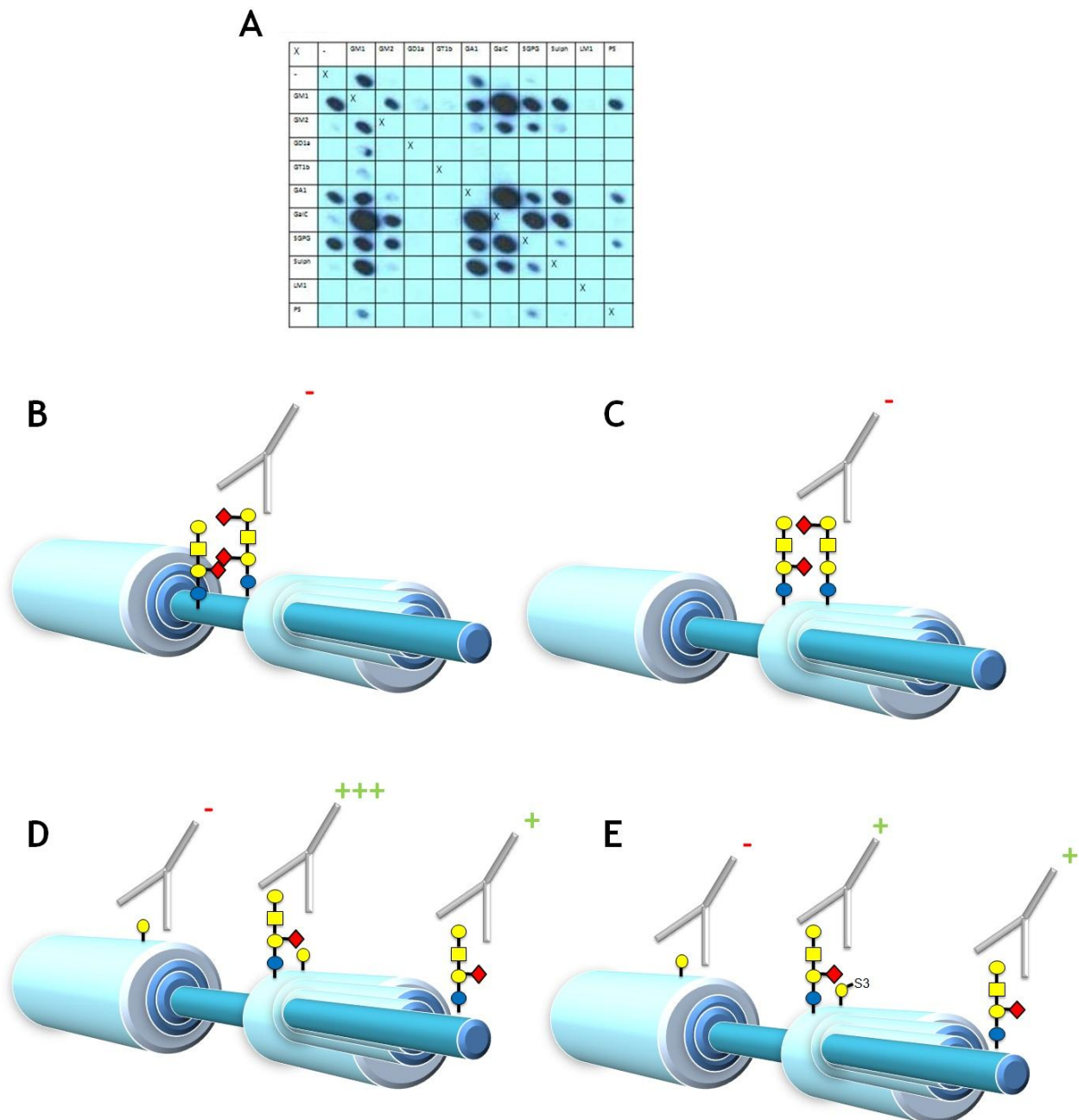


Figure 4.3. Diagram illustrating Ab binding profiles found in MMN sera.

A. Illustrative blot from MMN sera. Nerve illustration showing inhibition by GD1a (B) and LM1 (C) of GM1 antibody binding. D. GalC mediated enhancement of GM1 antibody binding. E. Complex independent antibody binding to GM1.

These data are quantified in the MMN group for GM1, GM2 and GA1 in complex with the 9 other antigens spotted in this glycoarray, where the single glycolipid signal intensity is set to zero for each sample as follows:

Complex A:B Single A Single B

$A:B-(A+B)$

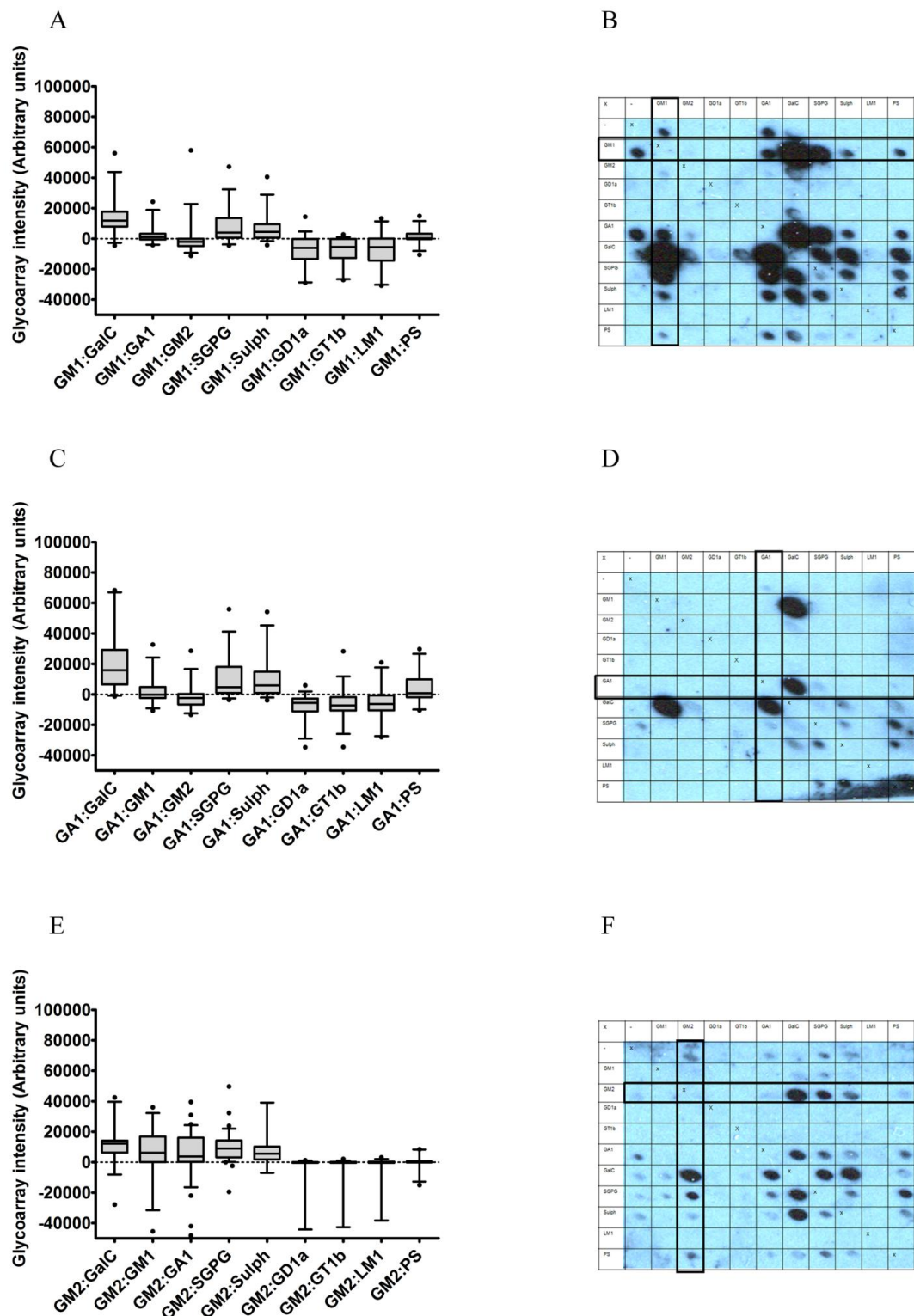


Figure 4.4. Patterns of antibody binding in MMN sera.

GM1 (Panel A), GA1 (Panel C) and GM2 (Panel E) binding for MMN sera showing complex enhancement and/or attenuation with other glycolipids. Data are shown as box and whisker plots (median and interquartile ranges) depicting signal intensities above (complex enhancement) or below (complex attenuation) the intensity value for the single glycolipid which is set at zero. Panels B (GM1), D (GA1) and F (GM2) show representative glycoarrays from individual patients binding to each of the three glycolipids. For all MMN cases ($n=33$), datasets were derived in duplicate from the boxed coordinates comprising each of the single glycolipids and the 9 possible complexes. Most MMN sera bind to more than one complex; thus in Panels B and D, the 2 MMN sera are binding strongly to GM1:GalC and GA1:GalC; and in Panel F, the MMN serum is binding strongly to GM2:GalC and GA1:GalC. Other complex reactivities are also often seen (e.g. sulphatide:GalC and SGPG:GalC in Panels B and F) but were not subjected to further enhancement and attenuation analysis.

Illustrative arrays from individual patients are shown in the adjacent panels (Figure 4.4). From these data sets, it is evident that GalC always provides the greatest complex enhancement for GM1, GA1 and GM2. Thus for GM1 in complex with GalC, the mean intensity of the GM1:GalC complex was significantly higher (paired t-test, $p=0.008$) by 8797 IU (95% CI, 2538 - 15056), compared with the intensity of the sum of each single spot (GM1 single + GalC single). A similar pattern was observed for GM2 and GA1. Other enhancing glycolipids for GM1, GM2 and GA1 are sulfatide and SGPG, a finding supported by data shown in Table 4.1. By contrast the complex-inhibiting glycolipids for antibody binding to GM1, GM2 or GA1 were LM1, GD1a, and GT1b.

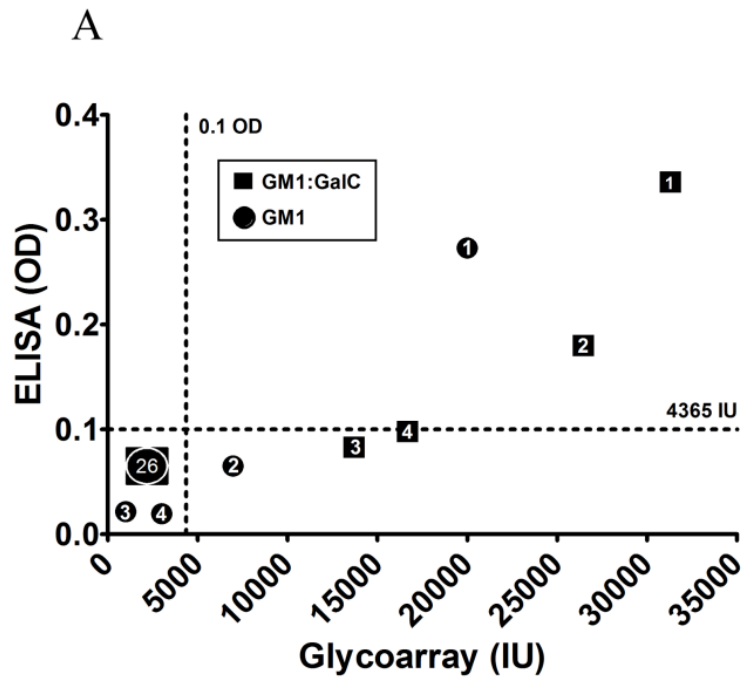
4.3.3.3 Analysis of Control population

From visual observation of the heat map for the array data (Figure 4.2 A), (4365=3.6 therefore all values represented are positive), it is clear that IgM antibodies to certain individual glycolipids and their complexes are present in a proportion of both OND and normal controls in addition to MMN samples, GalC:SGPG being prominent in this respect. Individual data values in control samples for 6 antigens shown in Figure 4.2 D indicate that for some glycolipids sensitivity is low but specificity is high (e.g. GM2), whereas for others (e.g. GA1:GalC) high sensitivity is offset by lower specificity, as summarised in the ROC analyses (Figure 4.2 B). Quantified examples for GM1 and GM2 in complex with GalC, sulfatide or SGPG are shown in Table 4.1.

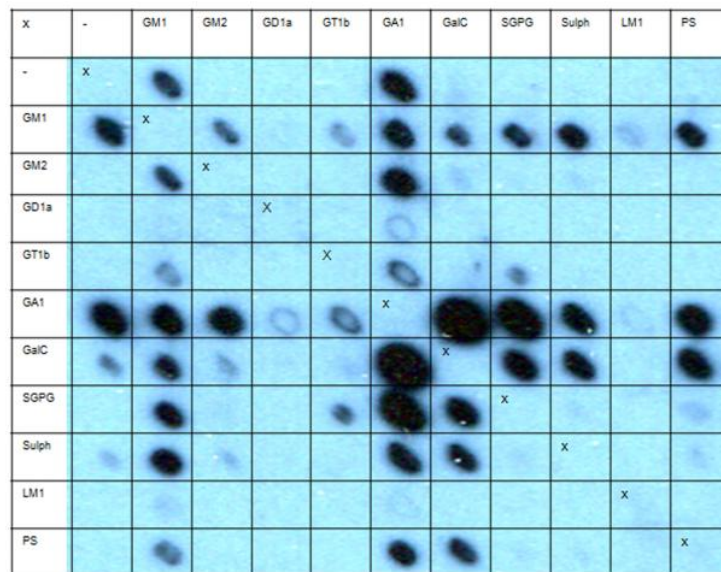
Evaluation of these findings is, by definition, dependent upon the statistical methodology used for setting assay thresholds; thus had we used the upper 95% confidence interval of the median control value as the ULN in glycoarray, 25/33 of the MMN population would be positive for anti-GM1 antibodies, equating to 76%, as opposed to 19/33 (58%), when the ULN of 4365 was applied. By corollary, lowering the threshold for sensitivity also decreases the specificity.

Since the GM1:GalC complex assessed by glycoarray appears from this study to be a highly sensitive marker for MMN, careful attention was paid to the 4 positive samples for this complex in the control population (data points as shown in Figure 4.2 D). These data are plotted for the OND group ($n=30$) in Figure 4.5 A, for both ELISA and glycoarray in comparison with data for GM1 alone. Of the 4

OND samples, one was positive for both GM1 and GM1:GalC by both ELISA and glycoarray (sample 1). The remainder were either negative for GM1 by ELISA (samples 2, 3, 4) and glycoarray (samples 3, 4) or negative for GM1:GalC by ELISA (samples 3, 4). The glycoarray for sample 1 is shown in Figure 4.5 B and shows a range of antibodies to single glycolipids and complexes in addition to GM1 and GM1:GalC, most notably GA1 and GA1:GalC. Clinically, sample 1 was catalogued as having 'idiopathic peripheral neuropathy' but on review of the clinical notes had presented with multifocal upper limb motor and sensory symptoms affected ulnar and radial nerves with median nerve motor conduction block in a forearm segment. When previously assayed for anti-GM1 IgM by ELISA as part of routine diagnostic workup, this serum sample contained anti-GM1 antibodies just below the ULN for the assay, and thus had been reported as negative at the time. In retrospect, this patient may have fulfilled diagnostic criteria for MMN or Lewis-Sumner syndrome but this was not evaluated further, and the sample was retained in the OND group.



B



Control sample 1

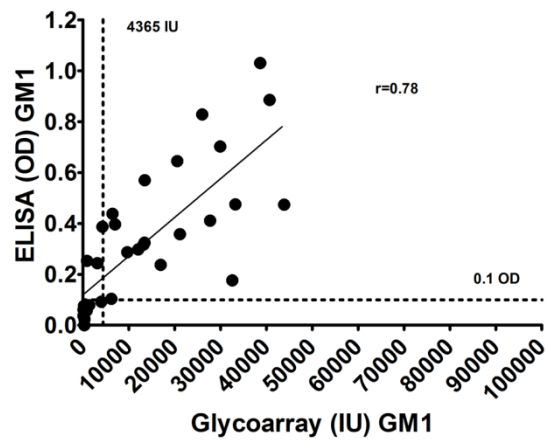
Figure 4.5. Analysis of positive controls.

Panel A. Analysis of the OND samples registering low positive intensity values for either GM1 and/or GM1:GalC by either ELISA and/or glycoarray. One sample (numbered 1) is positive for GM1 and GM1:GalC by both ELISA and glycoarray, and the corresponding glycoarray is shown in Panel B.

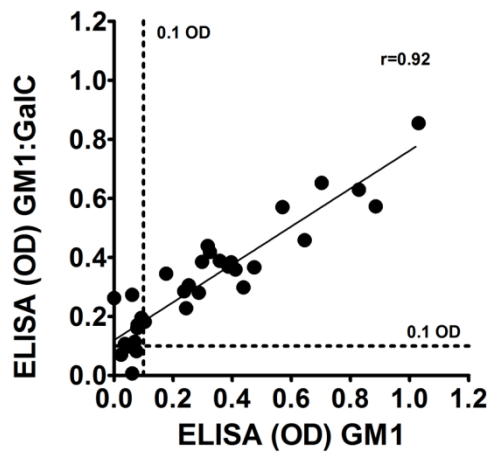
4.3.3.4 Comparative analysis of ELISA and glycoarray data for MMN samples

ELISA and glycoarray values for GM1 and GM1:GalC complex were determined to have high correlation coefficients by regression analysis (Figure 4.6 and Figure 4.7). Thus, comparison of ELISA and glycoarray for determining anti-GM1 IgM Ab yields a correlation coefficient of 0.78 (Figure 4.6 A). The correlation coefficients for GM1 versus GM1:GalC (Figure 4.6 B-C) were also high, whether assaying by ELISA or glycoarray (0.92 and 0.72 respectively). Focusing on samples at the lower end of the assay range in ELISA, 7/11 anti-GM1 Ab negative MMN samples were either very weakly or borderline positive for GM1:GalC complexes (Figure 4.6 B). Using the glycoarray in the same comparative analysis between GM1 and GM1:GalC complex (Figure 4.6 C), average IU values were in general higher for GM1:GalC than for GM1 alone, and all 33 MMN samples were GM1:GalC positive (i.e. above the 4365 IU threshold), compared with 19/33 for GM1 alone. Data from more detailed examination of the GM1:GalC complex is shown in Figure 4.7.

A



B



C

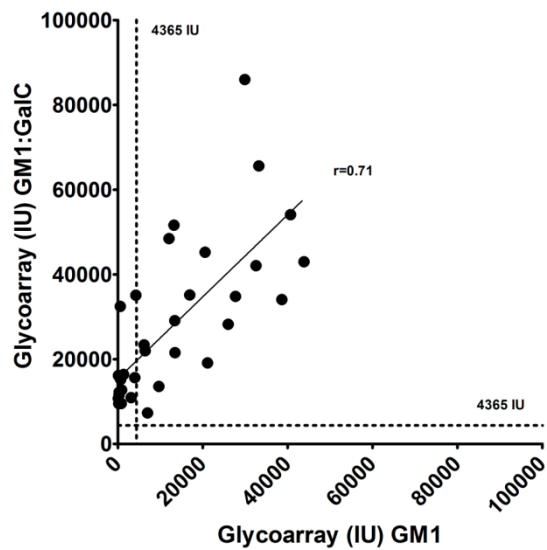


Figure 4.6. Regression analysis of GM1 and/or GM1:GalC for both glycoarray and ELISA. Panel A. Correlation coefficient, $r=0.78$ between ELISA and glycoarray for GM1 antibody binding. Panel B. Correlation coefficient, $r=0.92$, between GM1 and GM1:GalC intensity values for ELISA data. Panel C. Correlation coefficient, $r=0.71$, between GM1 and GM1:GalC intensity values for glycoarray data.

Using the assay cut-off criteria described above and including all control samples (n=57), ROC analysis was used to assess the overall sensitivity and specificity of the glycoarray and ELISA techniques and showed no significant difference in diagnostic performance ($p=0.59$) (Figure 4.7 A). Examining the data sets for individual MMN sera from both assays (Figure 4.7 B), the correlation coefficient is 0.57. Four MMN samples negative for anti-GM1:GalC complex IgM antibodies by ELISA were positive by glycoarray (Figure 4.7 C, an expansion of bottom left corner of Figure 4.7 B). The corresponding glycoarrays for these 4 samples are shown in Figure 4.7 D. In each of these 4 samples, reactivity with other glycolipids or complexes are also seen, including GM2, GM2:GalC, GA1 and GA1:GalC.

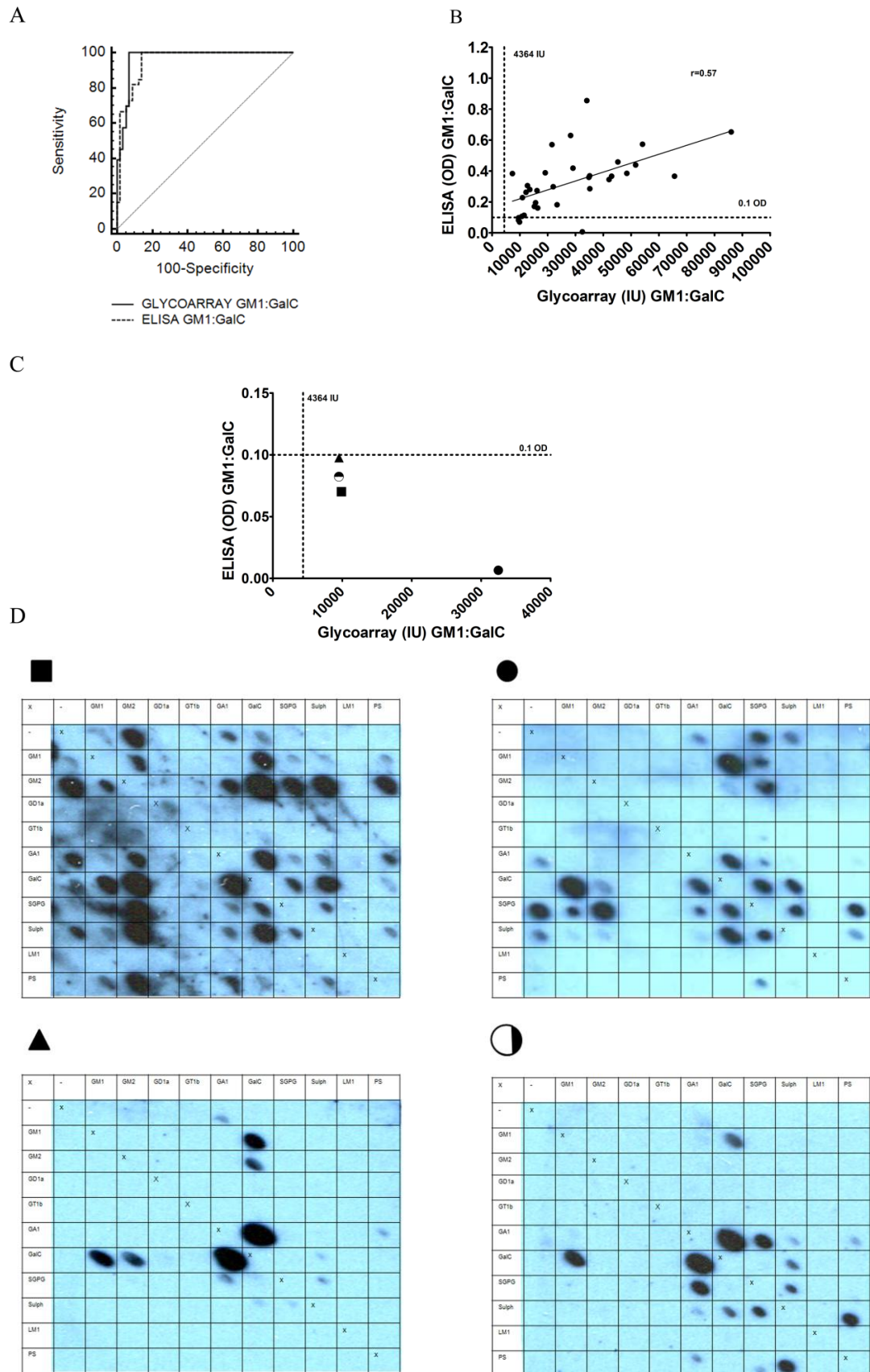


Figure 4.7. Comparative data of ELISA and glycoarray performance for MMN serum binding to GM1:GalC.

Panel A. ROC curves show high performance for the two methods, that are insignificantly different ($p=0.59$). Panel B. Correlation analysis shows a coefficient of 0.57 between the 2 methods. Panel C. Magnified view of ELISA-negative values ($n=4$) that were positive by glycoarray. Panel D. Individual glycoarray blots of the 4 ELISA-negative, glycoarray- positive MMN samples shown in Panel C.

4.3.4 Study remarks

It may be assumed that the strength of the correlation between ELISA and Glycoarray methodologies negates the need to replace a well established technique such as ELISA with glycoarray for routine diagnostics for MMN in the hospital setting. Whilst ELISA remains an excellent technique for detecting antibodies to single or complexed lipids present in serum at medium to high titre, our data suggest that the glycoarray method may be more sensitive at the lower end of the detection range.

Although being equally sensitive and specific than ELISA at medium to high titres, this new method has several strong advantages over ELISA:

- It permits simultaneous screening of an extensive complex ganglioside panel with no increment on the amount of sera employed. Containing within the same panel an internal duplicate for every epitope.
- Allows the identification of an antibody binding fingerprint, specific for every disease. Being characterised by complex dependent enhancements and inhibitions.
- Visual location of spots facilitates differential analysis of background and genuine antibody binding.
- There is a significant reduction in sample and reagent volume.

This study provides strong support for the long-standing observation by Pestronk and colleagues that a complex of GM1:GalC constitutes a very sensitive antigen for screening MMN sera (Pestronk, Choksi, Blume, & Lopate 1997). Indeed, in this cohort of 33 MMN cases, all sera were reactive against the GM1:GalC complex in glycoarray screening, including those that were not reactive to either GM1 or GalC alone. In addition, 4 cases whose sera were negative for antibodies to the GM1:GalC complex by ELISA, were positive by glycoarray. These findings need to be viewed cautiously until the overall conclusions can be validated in an independent, blinded cohort containing a randomised selection of MMN cases and appropriate controls.

Although the 33 cases from our national area were randomly selected for inclusion in this survey, referral bias to both our diagnostic neuroimmunology laboratory and clinical service may have been a factor in increasing the proportion of antibody positive cases. Moreover, the lack of an automated quantification process of spot intensity could somehow contribute to an increase on the bias.

The principle clinical point emerging from this study is that the diagnostic yield of the standard anti-GM1 antibody ELISA can be improved upon through use of the combinatorial glycoarray.

The finding of antibodies to GM1 in complex with other glycolipids influences our ideas about the immunopathogenesis of MMN by providing further support for an antibody-mediated autoimmune hypothesis. What remains unknown is whether any complexes that are capable of binding antibody exist in the living nerve environment, and where they might be localised. Equally, inhibitory complexes, such as GM1:GD1a, may play important roles in attenuating antibody binding and subsequent tissue injury, as has been shown experimentally (Greenshields, Halstead, Zitman, Rinaldi, Brennan, O'Leary, Chamberlain, Easton, Roxburgh, Padiani, Furukawa, Furukawa, Goodyear, Plomp, & Willison 2009). Further information about this will come from isolating anti-complex antibodies for use in more detailed pathogenesis studies.

4.4 Cryptic behaviour of GBS/MMN-derived human monoclonal antibodies.

4.4.1 Study aims

GBS/MMN-derived human monoclonal antibodies were used to investigate the effect of neighbouring lipids to GM1 single binding.

4.4.2 Results

The binding pattern of previously cloned GBS/MMN-derived human monoclonal antibodies (Willison, Paterson, Kennedy, & Veitch 1994) was first evaluated on the lipid panel used in the original SGH MMN study. MAbs BO1 and BO3 were

excluded from the current study because of their preferential binding to GA1 over GM1.

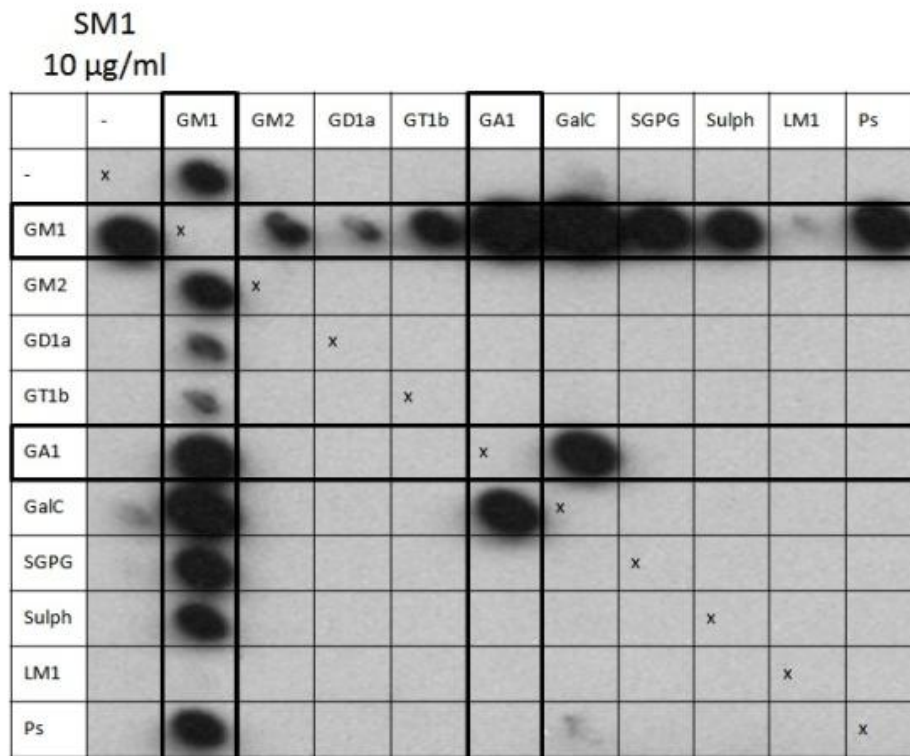


Figure 4.8. Glycoarray binding fingerprint of human mAb SM1 .

The glycolipid panel comprised GM1, GM2, GD1a, GT1b, GA1, GalC, SGPG, Sulph, LM1 and PS.

Data corresponding to the SM1 binding fingerprint revealed a similar pattern to that observed in SGH MMN patients. GM1 complex binding was characterised by GD1a and LM1 inhibition and GalC moderate enhancement (Figure 4.8). In addition to this, SM1 presented complex dependent binding to GA1:GalC (Figure 4.9). GA1 and GM1 molecular structures are identical, except GM1 contains a sialic acid group attached to the internal galactose molecule. It is possible that binding signal seen for both GM1:GalC and Ga1:GalC represents one or more antibodies binding to the same epitope, shared by both heteromeric complexes, or different antibody species binding to unique complex dependent epitopes.

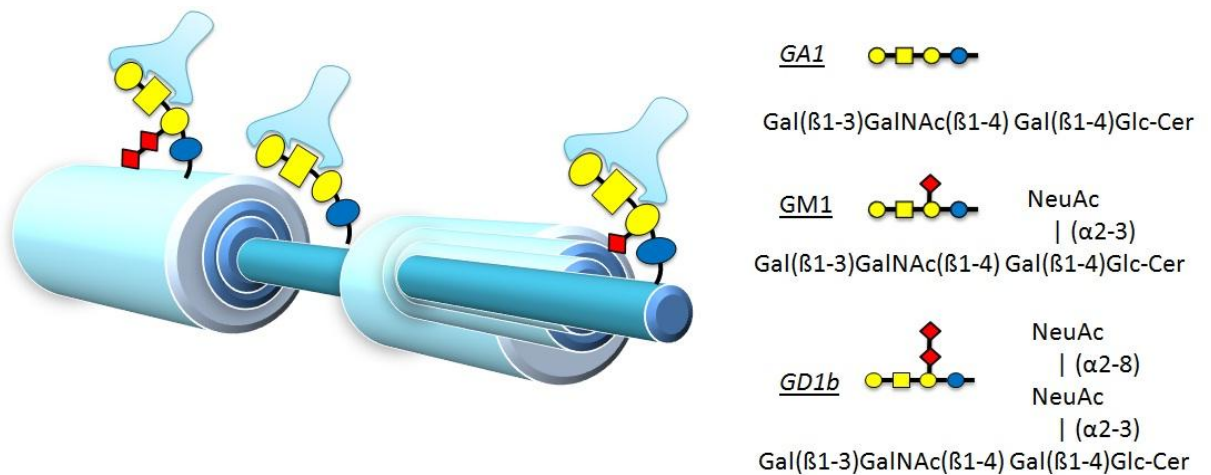


Figure 4.9. Diagram illustrating ganglioside molecular mimicry.

Monoclonal antibodies SM1 (MMN), BR1 (MMN) and DO1 (GBS) were then probed against arrays containing different molecular ratios of GM1:GalC, as previously done for MMN sera.

An unexpected finding was that the binding intensity of all three mAb was significantly decreased for GM1:GalC complex at a 1:1 ratio, when compared with the summed binding intensity of the single lipid components (Figure 4.10 A). SM1 binding was constant for GM1:GalC ratios between 1:1 and 1:120 (w/w) exerting an average intensity of 25954.44 ± 1093.8 (Figure 4.10 A). In contrast, BR1 and DO1 were unable to bind GM1:GalC complexes at molecular ratios equal to or greater than 1:10 and 1:40 (w/w) respectively (Figure 4.10 A).

Human monoclonal antibody BR1 was derived from a patient included in the SGH MMN study previously described. Interestingly, the antibody binding pattern described for BR patient serum comprised a strong enhancement of GM1 binding in the presence of GalC at a 1:1 w/w ratio (Figure 4.10 B). This data was in contrast with the GM1 binding inhibition exerted by BR1 mAb in the presence of GalC at any molecular ratio. There are several possible explanations for this results, all explained by the polyclonal nature of patient sera. First, the data may be explained by the presence of several different anti-GM1 single antibodies in BR serum. Among this highly diverse antibody subset some would be binding GM1 in the presence of GalC (independent or enhanced) and others would not (inhibited). BR1 mAb would belong to the group of anti-GM1 antibodies which are inhibited by the presence of GalC. Although BR serum would be representing

all the spectrum of GM1 reactivity. A second possible explanation would be the presence of complex dependent GM1:GalC (1:1 w/w) antibodies and GM1 single specific antibodies. The first antibody subset would recognise GM1 exclusively in the presence of GalC but not GM1 alone and the second subset would only recognise GM1 when presented as a single epitope. BR mAb would therefore have been cloned from a subset of GM1 antibodies which only recognise GM1 when presented as a single epitope. These findings highlight the fact that in polyclonal serum multiple antibodies may be targeted to different epitopes on the same molecule and that these antibodies respond differently to the presence of a secondary lipid (i.e. enhanced, attenuated or independent). It is these unique antibody fingerprints that are frequently obscured when examining whole sera, due to the competing nature of the various antibodies, and can only be discriminated when using mAb.

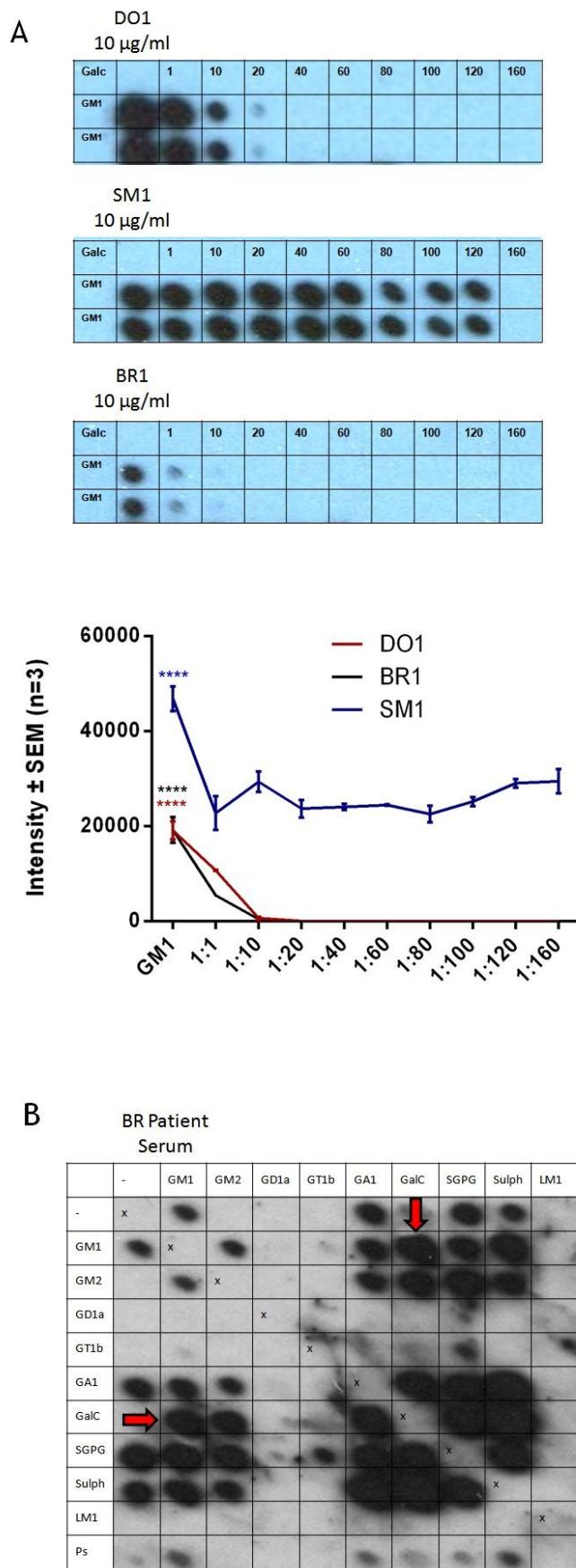


Figure 4.10. Human monoclonal antibodies binding profile.

Panel A. Arrays depicting antibody binding to GM1 single or in complex with increasing amounts of GalC (w/w) followed by a graphic representation of antibody binding intensity. Analysis was conducted with a one way anova using Tukey's multiple comparison test (****p value ≤ 0.0001)

Panel B. Ab binding profile of MMN patient sera BR, highlighting the presence of a GM1:GalC binding enhancement.

4.5 Dutch MMN validation cohort (first screen)

4.5.1 Results

Array data from MMN cases and controls, including ALS cases and healthy individuals, were subjected to cluster analysis generating a heat map comprising spot intensities for 8 single lipid and 28 lipid complex epitopes (Figure 4.11).

No threshold of positivity was applied to categorise the numerical data thus the intensities were expressed as intensity units.

The strength of each biomarker was then assessed by ROC analysis comparing MMN cases (n=100) and controls (n=200). Complex lipids were analysed after intensity from each individual component was subtracted from the complex intensity. According to this evaluation, the best performing biomarkers were GA1:Sulph, GM1, SGPG:GalC, GM1:Sulph, GM2:GalC and GM2 with AUC of 0.807, 0.775, 0.709, 0.654, 0.606 and 0.570 respectively (Figure 4.12 A).

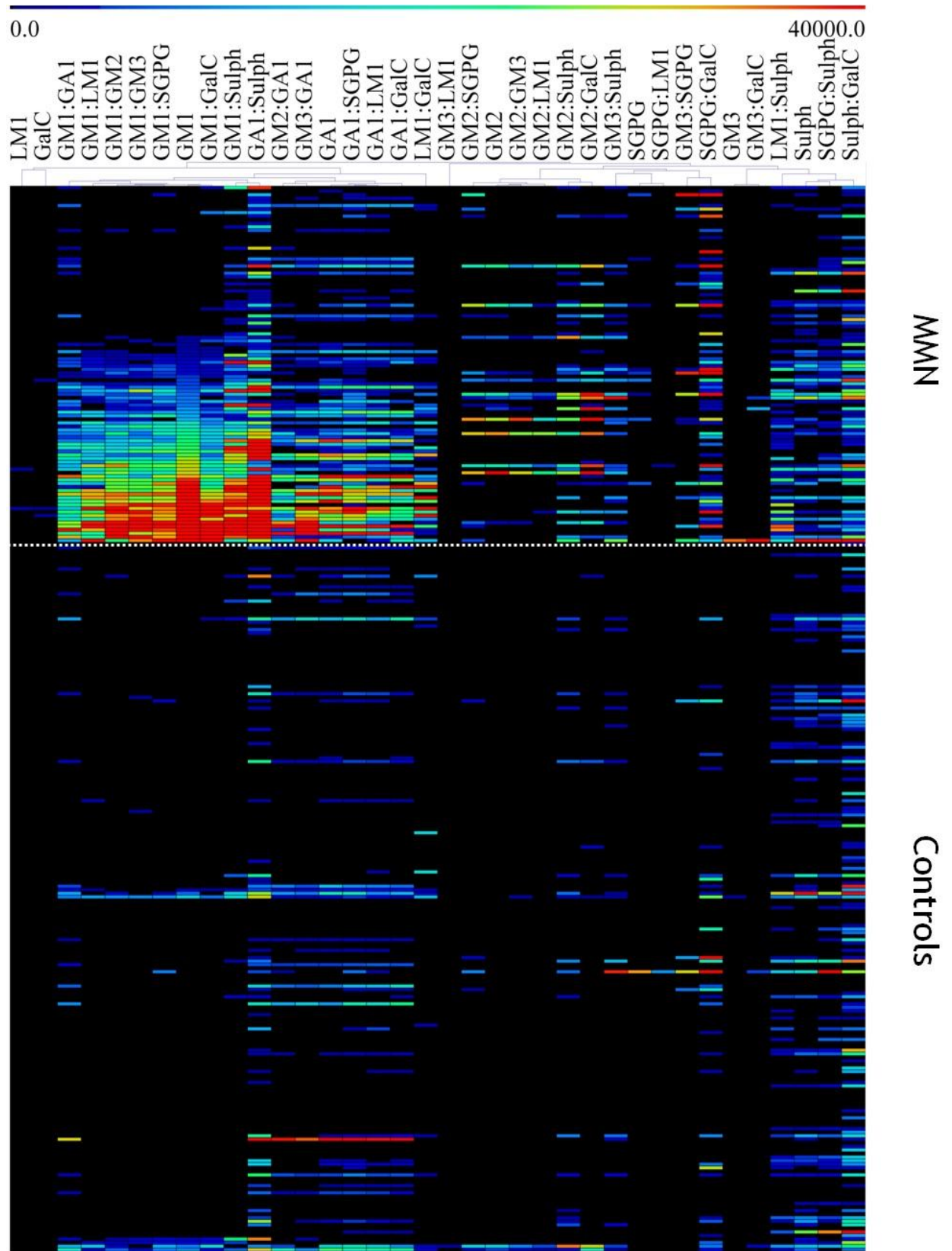


Figure 4.11. Quantitative analysis of glycoarray data.

Heat map showing the values (AU) of antibody binding intensity to the 8 single glycolipids and 28 complexes for 100 MMN patient sera and 200 controls (100 ALS controls and 100 healthy individuals). The minimal value assigned to any sample was set at 0 IU. The rainbow scale was applied to categorised the wide range of different intensities. Thus, black corresponds to antibody negative signals, with signal intensity increasing from pale blue to red.

Unlike the original SGH MMN cohort, no individual glycolipid or complex was identified as a conclusive biomarker of this disease. However, The combination of the top biomarkers (overall markers), excluding SGPG:GalC, as diagnostic tool significantly improved the sensitivity of the test (84%) with a slight decrease of the specificity (81%) yielding an overall AUC of 0.865. The overall markers were proven to perform significantly better than GA1:Sulph alone ($p=0.05$). Although accompanied by an improvement of the diagnostic performance, the addition of SGPG:GalC to the overall markers was considered not significant ($p=0.54$)(Figure 4.12 B).

A

Lipid epitope (Singles subtracted from complexes)	Sensitivity (%)	Specificity (%)
GA1:Sulph	74	83
GM1:Sulph	32	99
GM1	58	96
GM2	15	99
GM2:GalC	24	97
Combined diagnostic efficiency (overall markers)	84	81

B

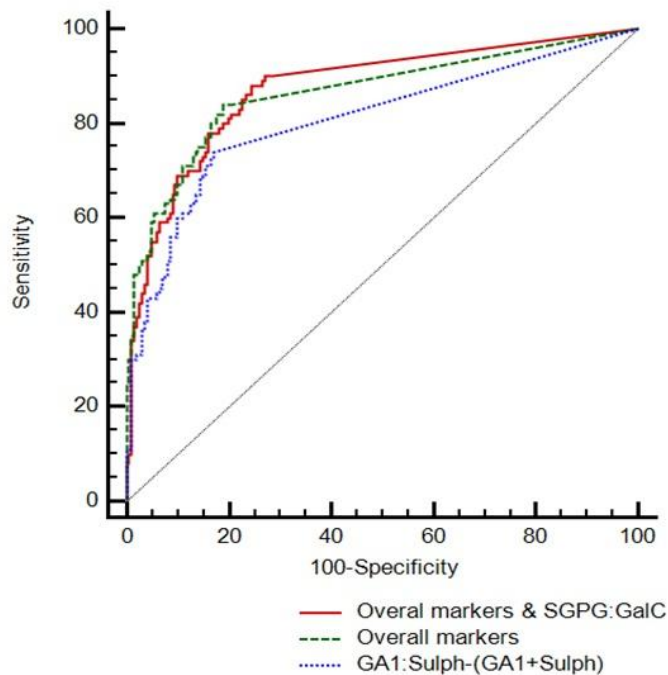


Figure 4.12. Statistical analysis of best performing biomarkers.

Panel A. Table containing the sensitivity and specificity for the best five performing biomarkers and their combined diagnostic efficiency (overall markers). Panel B. ROC analysis depicting the differences in assay performance between GA1:Sulph (AUC 0.807), overall markers (AUC 0.865) and overall markers plus SGPG:GalC (AUC 0.874).

The enhancing effect of GalC, when complexed with a secondary lipid which was widely documented in my previous study (4.3) was not replicated in this current study, except for GM2:GalC. The surprising failure of GalC complex binding enhancement when screening this cohort was exemplified by the lack of GM1:GalC enhanced reactivity, where only three patient sera measured a

significant increase of intensity unexplained by GM1 single reactivity. Out of these three MMN patients, only one (IU 8968.70) was above the 4365 AU set as positivity threshold on the SGH serology study, the other two presented intensities of 1586.60 IU and 1130.00 IU respectively (Figure 4.13 B).

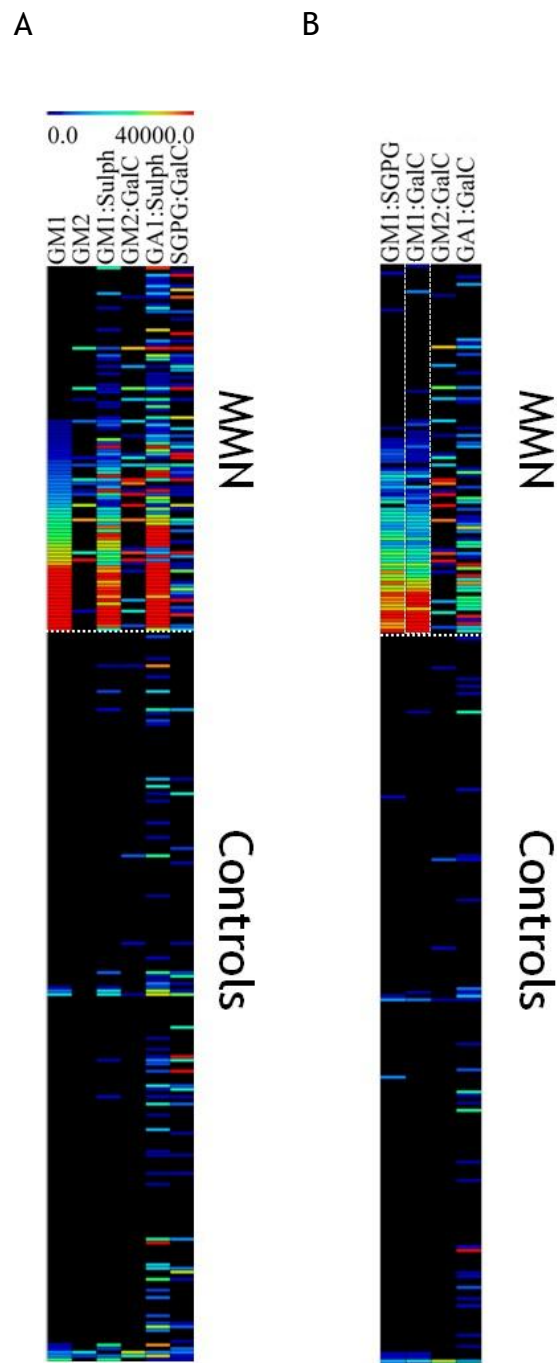


Figure 4.13. Heat map representation of Dutch serology data.

Highlighting the best performing biomarkers on the Dutch cohort (A) and the previously found on the SGH serology study (B).

Out of the 16 MMN patients negative for the overall markers depicted on Figure 4.12 A, 7 were positive for SGPG:GalC (Figure 4.14 A). This increase of overall sensitivity explains the mild increase of the overall markers AUC after the inclusion of SGPG:GalC (from 0.865 to 0.874). However, the specificity for this biomarker was seen to be extremely poor, due to 13% of the controls containing IgM antibodies against SGPG:GalC (Figure 4.14 B).

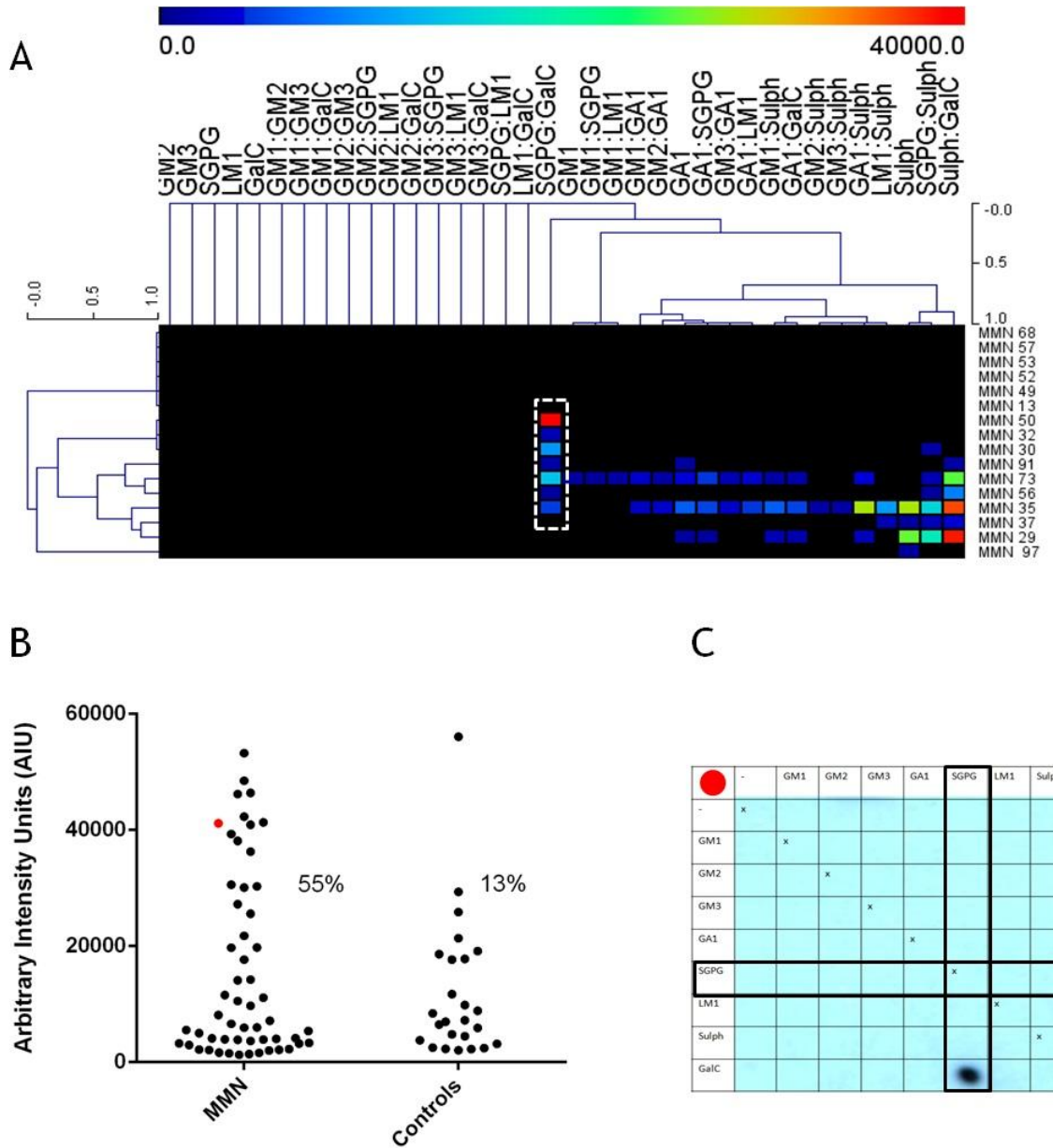


Figure 4.14. Analysis of negative patients for overall markers.

Panel A. Heat map presenting the 16 MMN patients negative for 'overall markers'. Panel B. Dot plot illustrating the antibody reactivity for SGPG:GalC in MMN patients versus controls. Highlighted as a red dot is the MMN patient whose glycoarray blot is represented in panel C.

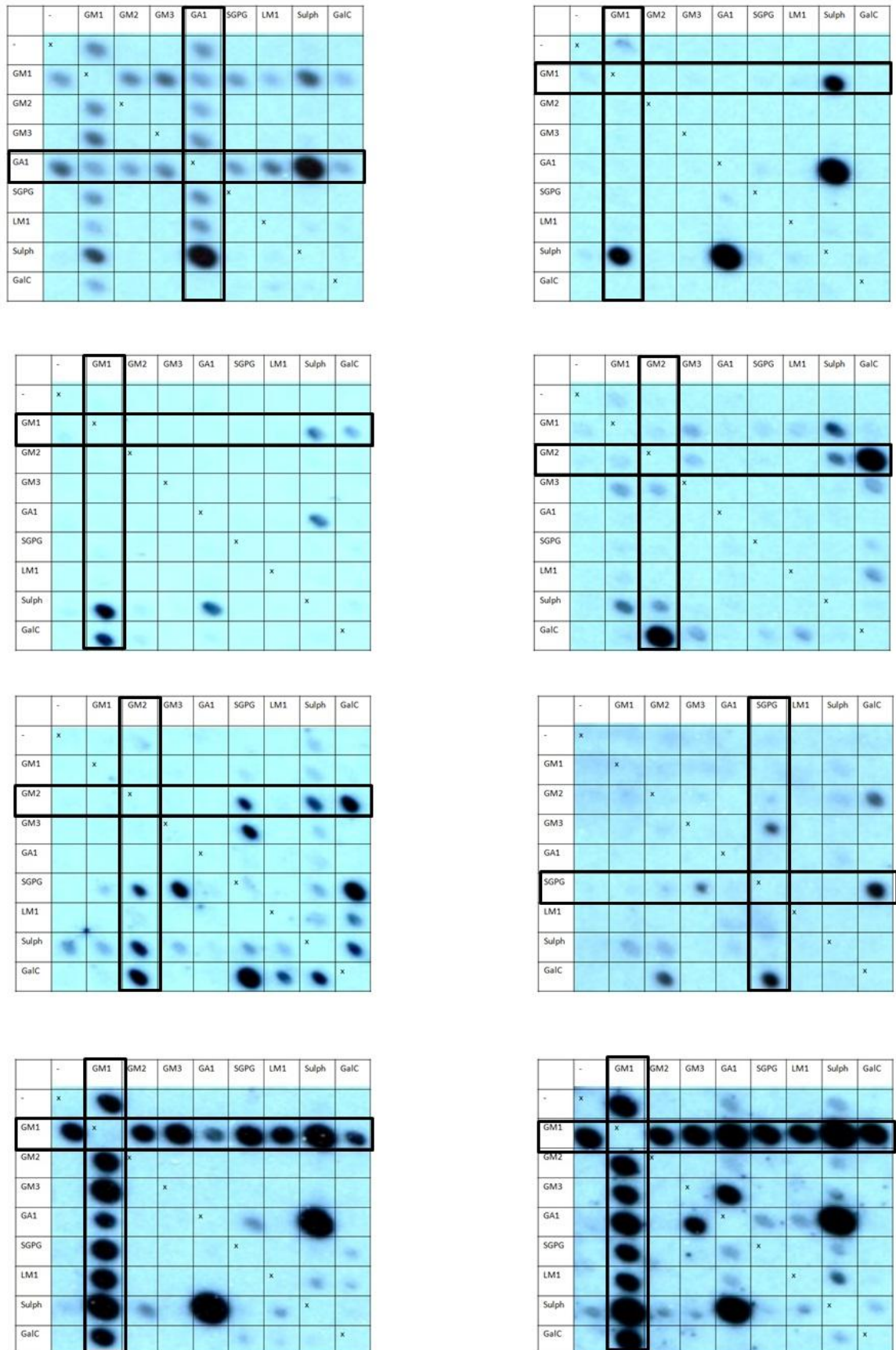


Figure 4.15. Representative glycoarray blots.

Examples of glycoarrays from 8 MMN cases, illustrating the different patterns of binding to individual glycolipids and their 1:1(w:w) complexes. Glycoarrays are printed in a grid, with the topmost row and far left hand column containing spots of 8 individual glycolipids, and the remaining spots comprising the complex formed from the combination of the glycolipids in the corresponding row and column.

4.5.1.1 Comparison of assay performance between ELISA and Glycoarray

The sensitivity/specificity ratio of anti-GM1 antibody detection originated from ELISA and glycoarray was used to evaluate their assay performance. Sera samples were concurrently tested on ELISA (GM1) (screening done by Carolyn Watt, Southern General Hospital) and values were correlated with glycoarray values.

The correlation curve with an R^2 of 0.84 indicated an extremely robust fit between the performances of both techniques, with a slight tendency in favour of glycoarray due to its higher sensitivity (Figure 4.16 A).

Further statistical analysis using ROC highlights a significantly better performance of glycoarray (AUC 0.775) compared to ELISA (0.673) ($p=0.0016$). ELISA while maintaining a really high specificity (99.5%) presented a really low sensitivity (35%). On the other hand, glycoarray demonstrated improved sensitivity (58%) with just a slight reduction in specificity (96%) (Figure 4.16 B).

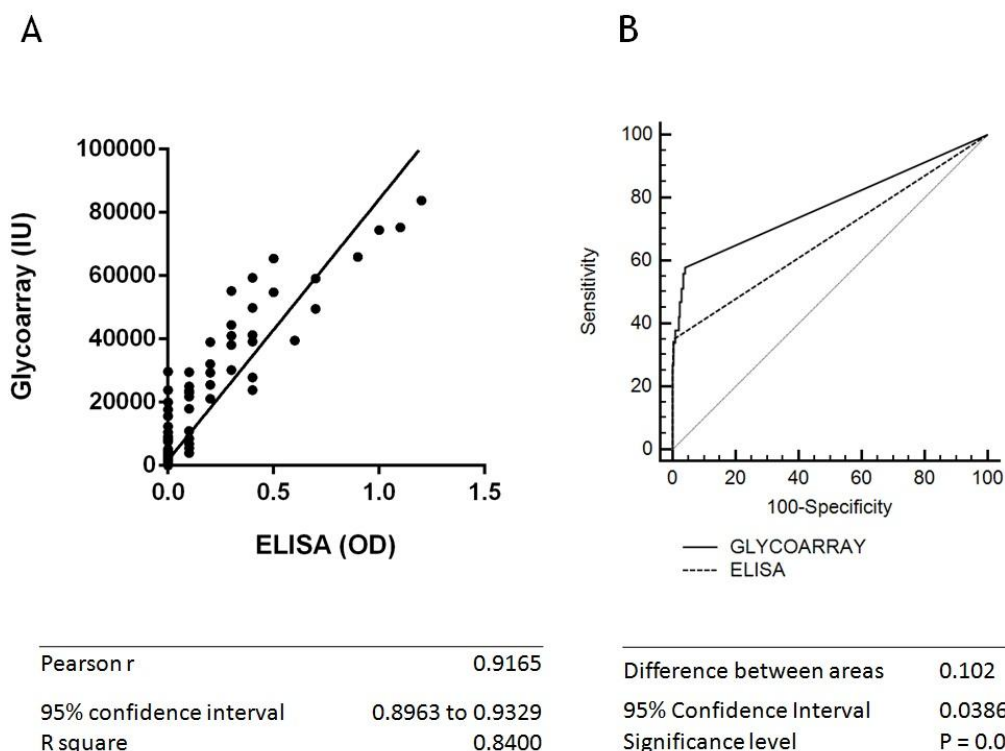


Figure 4.16 Glycoarray and ELISA performance comparison.

4.5.1.2 Coefficient of variation (CV)

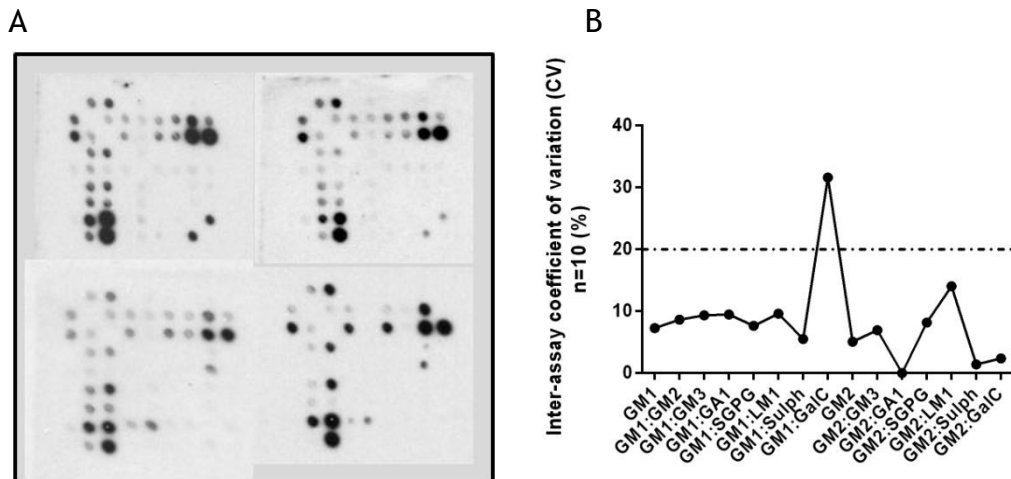


Figure 4.17. Inter-assay variability of a control sera used during a serology study.

A. depicts the arrays containing GM1, GM2, GM3, GA1, SGPG, LM1, Sulph and GalC and their corresponding combinations originated from ten independent studies using a neuropathy control sera mainly reactive for GM2:GalC, GM1:GalC, GM2:Sulph and GM1:Sulph. B. shows the percentage of variation of GM1 and GM2 single and lipid combinations for ten independent studies.

A patient previously screened within the SGH MMN study (4.3) was included as a positive control in every screening. This serum was selected due to its complex dependent reactivity with GM1:GalC and remarkable GalC mediated enhancement of GM2 signal. The known median intensities for GM1:GalC and GM2:GalC after single reactivity subtraction were 15558 IU and 25802 IU respectively.

Figure 4.17 demonstrates that the inter-assay variability in glycoarray was frequently within the normal range of 10% for high and mid reactive lipid epitopes such as GM2:GalC, GM2:Sulph and GM1:Sulph. In addition to this, the median intensity for GM2:GalC for the current study was insignificantly different than the previously established with a value of 24935 IU. Values which would support the strength of the results obtained for this biomarker. CV percentages exceeding 10% in serology studies have been associated with epitopes presenting low antibody binding levels, denoting the detection limit for this technique (Reed et al. 2002).

In our particular case, the high intensity units previously presented by GM1:GalC associated binding for this serum would be above the detection limit for this technique, previously established between 1000-2000 IU. Therefore, in this case the exceedingly high CV (>30 %) presented by GM1:GalC would indicate an

unusual fluctuation on the intensity signal for this biomarker which could not be explained by limitations on the array technique.

4.5.2 Summary

- The enhancing effect of GalC found in the SGH serology study (Chapter 4.3.3.2) could not be replicated for any ganglioside with the exception of GM2 which presented a mild enhancement.
- The enhancement in this cohort was predominantly mediated by sulphatide.
- Glycoarray showed a better overall performance than ELISA detecting anti-GM1 antibodies.
- The high CV on the house-keeping serum presented by GM1:GalC reactivity throughout this study could be due to:
 - A GalC reagent failure exclusively dependent on GM1.
 - An aliquot consistency failure of the house-keeping serum.

4.5.3 Future recommendations

- Investigate the integrity of the GalC stock, including: Batch to batch variation, stock solubility, difference in branding and molecular composition.
- In order to avoid aliquot inconsistencies, prepare all the house-keeping sera with a mix of a minimum of three different aliquots of the same serum.
- The selection criteria used for positive control serum samples is crucial. For all future studies three different types of sera controls should be used: a control with high antibody titre, one with moderate and one with low antibody titres.

4.6 GalC investigations

The main objective of this study was to evaluate any potential change on GalC stocks which may explain the loss of GM1:GalC enhancement detected in the first screening of the Dutch cohort. The loss of GM1:GalC Ab reactivity in our positive control, lead us to believe in the possibility of a GalC reagent failure. For this study, sera previously screened in the SGH MMN cohort were used.

4.6.1 Qualitative differences

Our initial assumption was that GalC (Sigma) was not fully solubilised when resuspended in chloroform/methanol 1:1. This hypothesis was supported by the appearance of precipitate in the GalC and GM1:GalC upon preparation of the working solutions. For this reason, I will investigate GalC derived from different commercial suppliers. In addition to this, I will investigate whether the hydroxylation status of GalC stocks has an effect in antibody binding.

An array containing GalC (Sigma), GalC (Matreya), hydroxylated GalC (Phrenosin) and non hydroxylated GalC (Kerasin) was printed and screened using mass spectrometry. Filters for Phrenosin and Kerasin were applied in order to discriminate between the most abundant species. Mass spectrometry studies were performed by Joanna Cappell. This technique allowed us to directly identify the presence of the species contained within the array without the need of antibody staining. At the same time, we were capable of identifying the hydroxylation profile of GalC.

Contrary to expectations, mass spectrometry confirmed the presence of GalC spotted onto the array. Although a slight difference in quantity spotted between the stocks could be appreciated, indicated by the slight decrease in brightness of the Kerasin containing spots, this technique did not allow any detailed quantification (Figure 4.18 A).

The most striking result to emerge from mass spectrometry data was the existence of a significant quantitative difference of Phrenosin and Kerasin between the single glycolipid stocks. Thus, GalC Sigma was seen to contain mainly Kerasin in both stocks and on the other hand GalC from Matreya was seen

to contain mainly Phrenosin. Although mass spectrometry data would only give an indication of the predominant species, in order to appear as predominant the quantitative difference between species needs to be significant (Figure 4.18 A).

In order to investigate the effect of these GalC species in Ab binding, arrays containing these species as single epitopes and in complex with gangliosides were printed and probed with MMN patient sera. Results were inconclusive when some sera were screened on an array containing the different species of GalC (Figure 4.18 B, C and D). It did not show an apparent antibody binding correlation between GalC Sigma, which according to mass spectrometry data mainly contains Kerasin, and Kerasin and GalC Matreya, which according to mass spectrometry data mainly contains Phrenosin, and Phrenosin. Moreover, it did not recover the GM1:GalC enhancement previously seen in these samples.

The only exception was GM2:GalC which seem to maintain the enhancement but only when in complex with Sigma GalC (Figure 4.18 B and D). This data partially explains why the GM2:GalC enhancement was not lost during the Dutch MMN screening which was exclusively performed using Sigma GalC.

No firm conclusions can be drawn from these results, but it could be postulated that the optimum composition of GalC for a GM1 binding enhancement could be a specific molecular ratio of both Phrenosin and Kerasin. This might explain the lack of correlation between GM2:GalC (Sigma) antibody binding with the binding to GM2:Kerasin (Figure 4.18 B). This theory would speculate that the optimum antibody binding to GM2 would take place on an environment mainly containing Kerasin but including a minor component of Phrenosin.

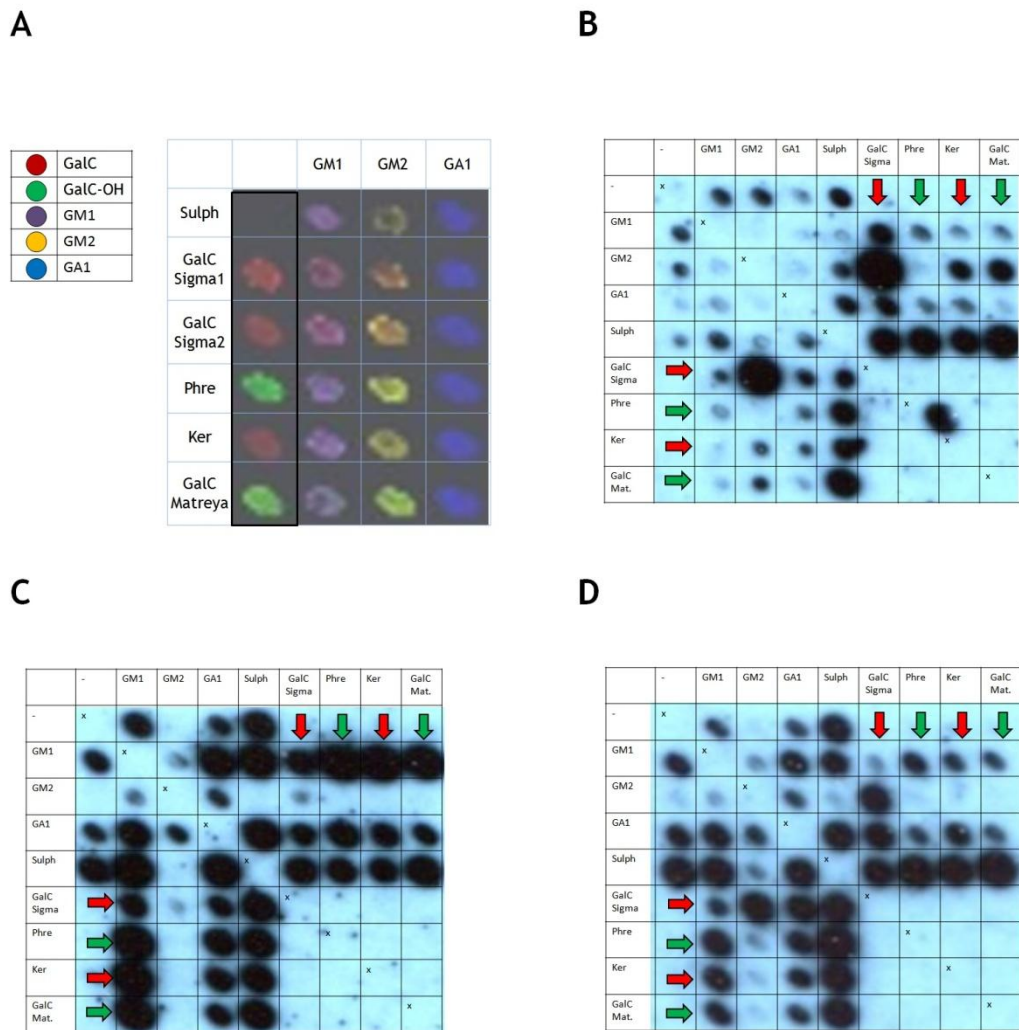


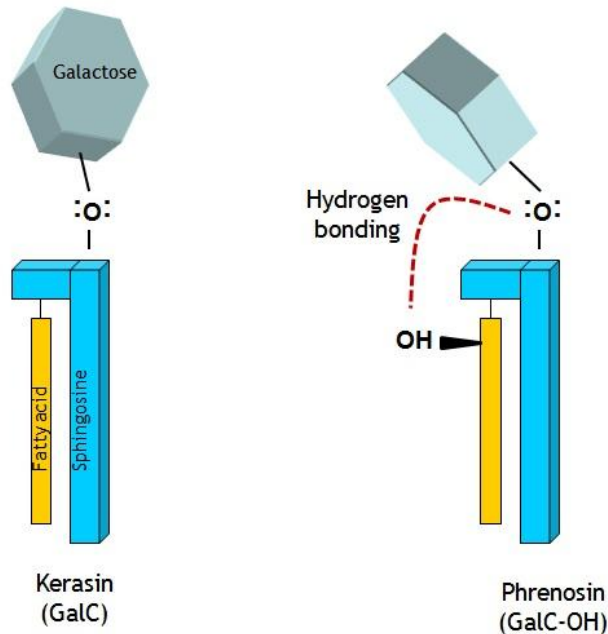
Figure 4.18. Phrenosin and Kerasin content of commercial GalC stocks.

Panel A. Mass spectrometry data depicting the dominant GalC species, Phrenosin (green) and Kerasin (red) within the GalC commercial stocks. Panel B, C and D. Arrays highlighting the diversity of Ab binding to complexes containing different GalC species.

4.6.1.1 Differential antibody binding to complexes containing Phrenosin and Kerasin

It has been previously documented that proteins are selective when binding to either hydroxylated GalC (Phrenosin) or non-hydroxylated GalC (Kerasin) (Fantini, Maresca, Hammache, Yah, & Delezay 2000; Hammache et al. 1998; Yah et al. 1992). The presence of the hydroxylated group on the C2 of the fatty acid chain induces a conformational change in the molecule through the formation of an intra-molecular hydrogen bond network. This alters the orientation of the sugar head group from perpendicular to parallel to the membrane surface (Fantini, Maresca, Hammache, Yah, & Delezay 2000). Proteins such as Beta amyloid bind preferentially to GalC when presented in the parallel orientation, whereas some antibodies recognise the perpendicular conformation (Yah,

Aulas, & Fantini 2010) (Figure 4.19). However, the impact of these conformational changes on ganglioside complexes has never been explored, but it is postulated to have a major impact in the formation of GSL complex epitopes.



	-	Sul	Phre	Ker	GalC
-	x				
Sul		x			
Phre			x		
Ker				x	
GalC					x

Figure 4.19. Kerasin and Phrenosin structure.

Diagram illustrating Phrenosin structure change due to hydrogen bonding network, followed by an array probed with a recombinant protein with preferential binding to Kerasin.

Strong evidence of differential mAb binding to ganglioside complexes containing hydroxylated and non hydroxylated GalC species was found after screening of a CANOMAD derived human mAb (HA1) on ELISA. As can be seen from Figure 4.20 , HA1 bound GM2 only when in complex with Phrenosin. The binding of HA1 to GM2:Phre was significantly different from Ab binding to GM2:Ker and GM2:GalC sigma ($p \text{ value} \leq 0.0001$). As previously demonstrated using mass spectrometry (Figure 4.18 A), GalC (Sigma) mainly contains Kerasin. Therefore, the resemblance in HA1 binding intensities between GM2:GalC (Sigma) and GM2:Kerasin complexes indicates that the dominant species in GalC (Sigma) is

Kerasin. After addition of Kerasin in the GM2:Phre complex, a significant decrease on HA1 binding intensity was observed ($p \text{ value} \leq 0.01$). In summary, these findings indicate that HA1 preferentially binds GM2 when in complex with Phrenosin. Thus, it could be postulated that the hydroxylation profile of GalC and its subsequent impact in glycolipid structure influences in the formation of GSL complexes and that translates in complex specific Ab binding. Therefore, these data heightened the need of a more in depth analysis on the impact of GalC hydroxylation status in the formation of complex epitopes.

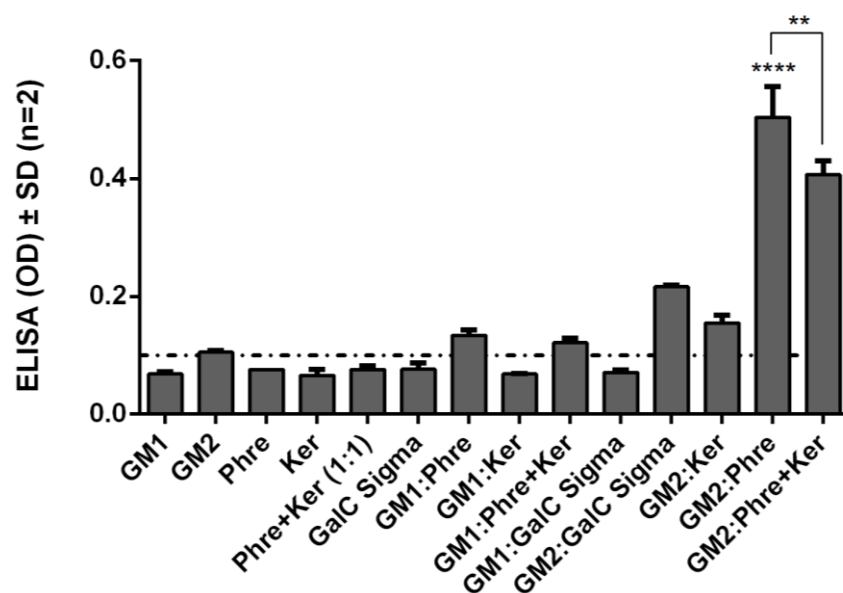


Figure 4.20. Monoclonal antibody binding profile on ELISA.

MAB (HA1) binding profile, at a concentration of 20 $\mu\text{g/ml}$, to GM1 and GM2 complexes with GalC, Phrenosin, Kerasin, GalC sigma and Phrenosin+Kerasin. The assay consisted on two independent repeats with two internal duplicates within every repeat. Significance was obtained after one-way ANOVA analysis with Tukey's multiple comparison test (** $p \text{ value} \leq 0.01$ and **** $p \text{ value} \leq 0.0001$). Horizontal dotted line represents the threshold of positivity set at 0.1 OD.

4.6.2 Quantitative differences

As a means to further investigate the potential issues derived from GalC solubility, lipids were solubilised both in chloroform:methanol (2:1) and chloroform:methanol:water (2:1:0.5). GM1 single concentration remained constant at 100 $\mu\text{g/ml}$ and was premixed with GalC (Sigma) at 100, 200, 400 and 800 $\mu\text{g/ml}$ to form heteromeric complexes, containing half the initial concentration of each lipid (Figure 4.21 A). Arrays were then probed with MMN sera previously investigated in the SGH MMN study.

Data from Figure 4.21 B revealed the recovery of GM1 intensity enhancement, but only at increasing concentrations of GalC (Sigma). 1:1 W/W proportion, as previously used in the SGH MMN study failed to demonstrate an enhancement. The highest enhancement was at a GM1:GalC W/W ratio of 1:8. Moreover, this enhancement was partially attenuated when the lipids had been solubilised with the addition of water.

Under these experimental conditions GM1 enhancement is dependent upon increased ratio of GalC which may indicate quantitative issues.

A

x	-	GM1 100	GalC 100	GalC 200	GalC 400	GalC 800	GalC 100	GalC 200	GalC 400	GalC 800
-	x	GM1: GalC 100	GM1: GalC 200	GM1: GalC 400	GM1: GalC 800					
GM1 100	GM1: GalC 100	x	GM1: GalC 100	GM1: GalC 200	GM1: GalC 400	GM1: GalC 800				
GalC 100	GM1: GalC 200	GM1: GalC 100	x							
GalC 200	GM1: GalC 400	GM1: GalC 200		x						
GalC 400	GM1: GalC 800	GM1: GalC 400			x					
GalC 800		GM1: GalC 800				x				
GalC 100										
GalC 200										
GalC 400										
GalC 800										

GalC dissolved as 2:1:0.5 Chloroform/Methanol/dH2O
 GalC dissolved as 2:1 Chloroform/Methanol

B

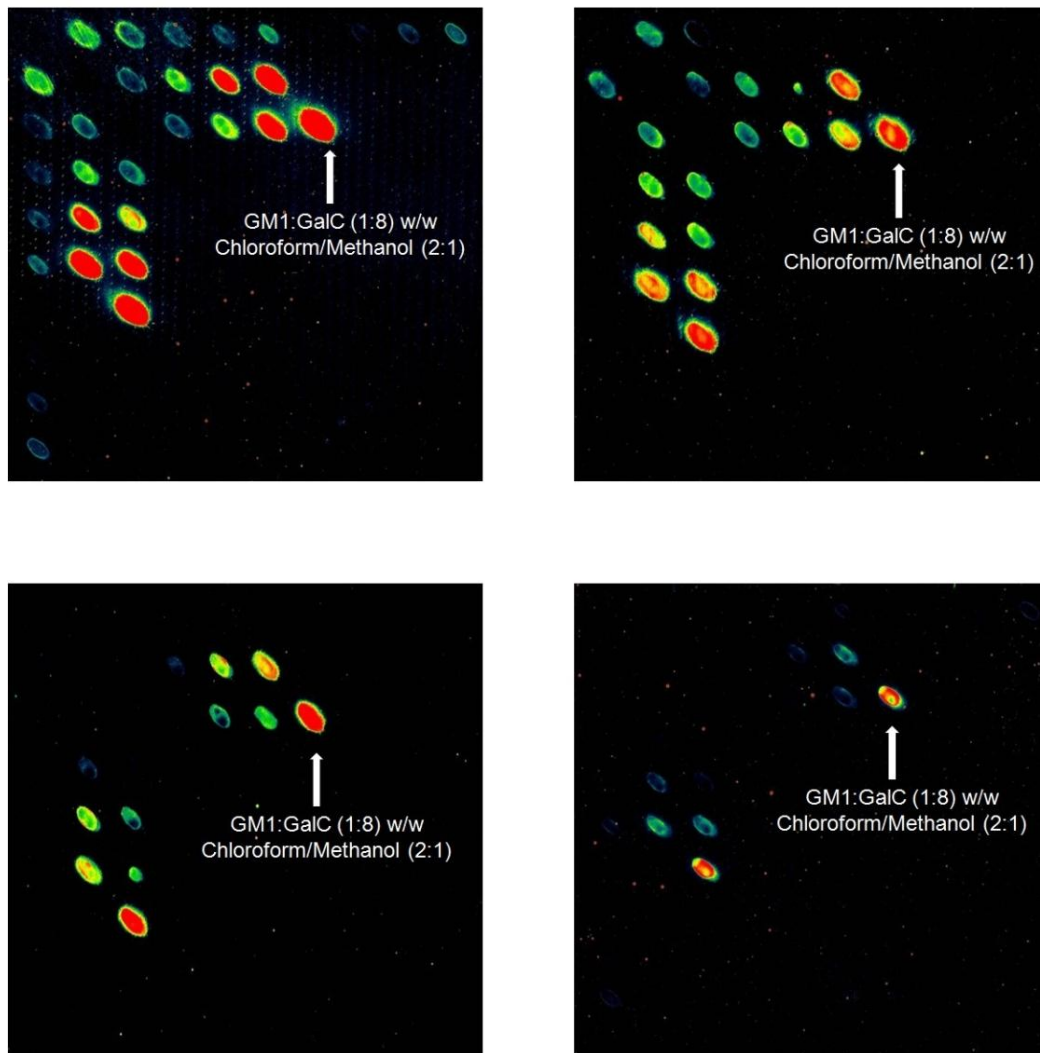


Figure 4.21. The effect of GalC concentration and solubilisation in GM1:GalC complexes. Panel A. Shows the lay out used for this study. Panel B. Presents characteristic fluorescent glycoarrays for 4 different MMN patients.

To solve this quantitative issue, the concentrations of GM1 as well as GalC were increased from 100 µg/ml up to 200 µg/ml, using as a stock solvent Chloroform:Methanol (2:1). It is worth pointing out that the W/W ratio between GM1 and GalC will be maintained constant and equivalent to the one used for the SGH sera screen (1:1 W/W).

Arrays comparing GM1 at 200 µg/ml and GM1:GalC complexes, both at 200 µg/ml, showed a significant intensity enhancement for GM1:GalC complexes in both ECL (Figure 4.22 A) and fluorescence (Figure 4.22 B). Further analysis revealed an insignificant difference between different GalC stocks and between stocks at 200 µg/ml and 400 µg/ml. All the data analysis was done using one-way ANOVA with Tukey's multiple comparison test from independent triplicates of one single MMN patient sera.

On a larger data set (n=4), MMN sera was tested against an array containing GM1, GM2, GA1 and their complexes with GalC. Both singles and complexes were tested at 100 µg/ml and 200 µg/ml. The only complex showing a significant increase in intensity enhancement after comparing complexes at 100 µg/ml and 200 µg/ml was GM1:GalC (two-way ANOVA with Bonferroni correction for multiple comparison $p \text{ value} \leq 0.01$). Thus GM1:GalC presented a higher intensity enhancement at 200 µg/ml even recovering the signal of borderline negative sera (Figure 4.22 C).

No significant difference was found between GM2:GalC complexes at 100 µg/ml and complexes at 200 µg/ml (Figure 4.22 C). This lack of difference might explain why during the Dutch cohort first screening the GM2:GalC signal was maintained constant throughout the study, presenting a CV within acceptable range (Figure 4.17). It is apparent that the GalC mediated GM2 enhancement is less sensitive to fluctuations in the GalC content than the GM1:GalC enhancement.

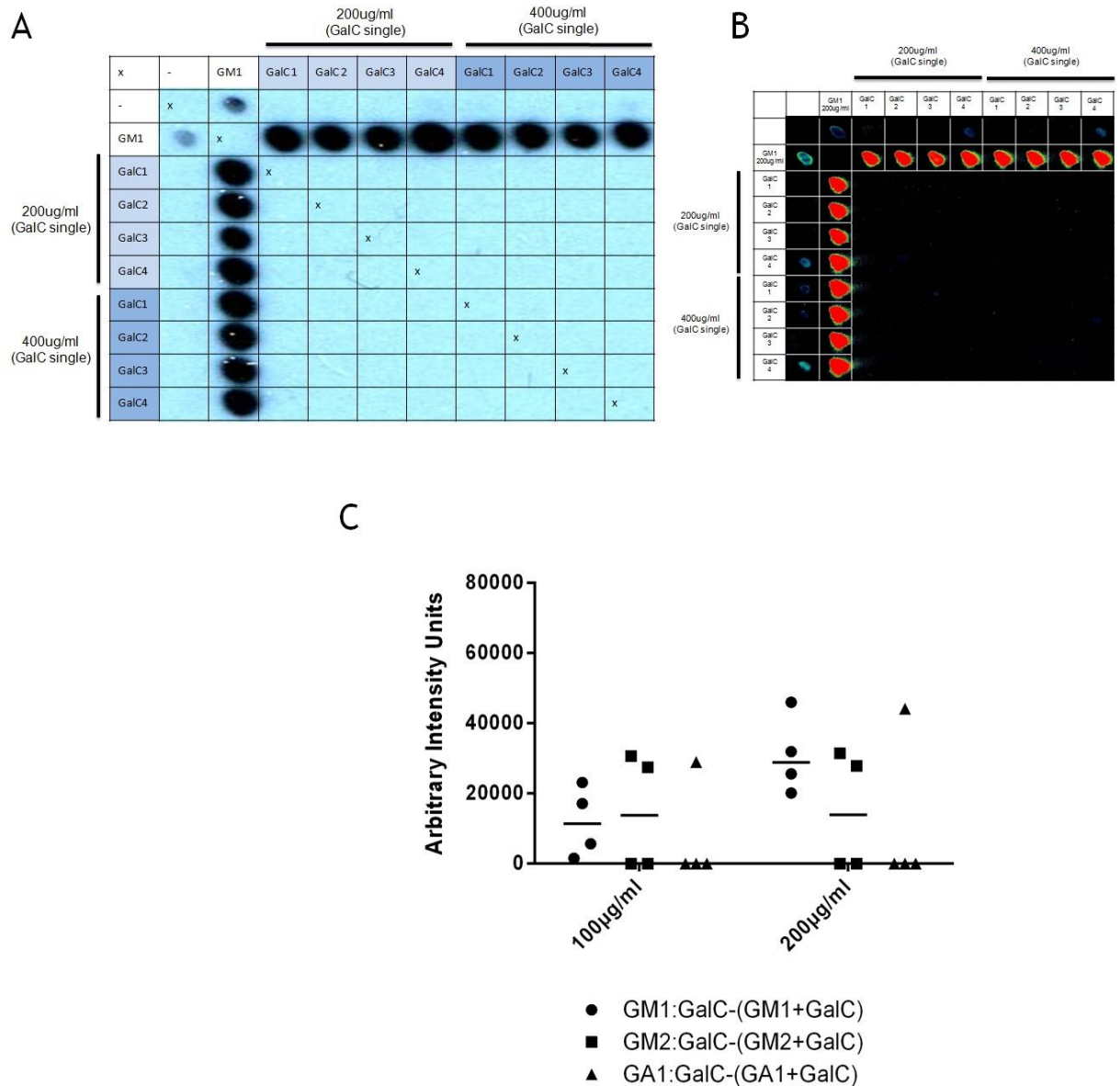


Figure 4.22. Comparison of different GM1 and GalC concentration.

ECL (A) and fluorescence (B) array comparing GM1 at 200 µg/ml with GM1:GalC complexes containing GalC at 200 µg/ml and 400 µg/ml. (C) evaluation of GM1, GM2 and GA1 antibody binding enhancement due to GalC. All single lipids were tested at two different concentrations, 100 µg/ml and 200 µg/ml.

4.6.3 Future recommendations

- All the lipids included within the array will be solubilised using a chloroform:methanol (2:1) solution.
- 200 µg/ml will be the working concentration for the lipids included in the array.

- The four MMN patients characterised in Figure 4.22 C will be used as positive controls for the next MMN serology screening. For assay validation, positive control must maintain a CV no greater than 20%.

4.7 Dutch MMN validation cohort (repeat)

4.7.1 Study design

- All lipids were reconstituted in chloroform:methanol 2:1 (Future recommendations 4.6.3).
- New coded samples were used.
- Samples were then screened (n=3) using the lipid panel as follows: GM1, GM2, GM3, GA1, SGPG, LM1, Sulph and GalC.
- The lipid concentration for every lipid was increased up to 200 µg/ml, maintaining the molecular proportion used on the SGH screening.

4.7.2 Results

4.7.2.1 ROC analysis

The strength of each biomarker was assessed by ROC analysis comparing MMN cases (n=100) and controls (n=200). Complex lipids were analysed after intensity from each individual component was subtracted from the complex intensity. According to this evaluation, the best performing biomarkers were GM1:GalC, GM1, GA1, GM2:GalC and GA1:GalC, as indicated by the AUC value (Figure 4.23 A and Table 4.2). GM1:GalC presented a significantly better performance than GM1 (p=0.0047), the second highest performing biomarker.

Combinations of various biomarkers increased the sensitivity of diagnosis compared to individual biomarkers. However, combined biomarkers resulted in a significant decrease in specificity. Due to this decrease in specificity there is no significant difference between the diagnostic performance of GM1:GalC and any of the different combination of biomarkers (Table 4.2).

Table 4.2. Top markers.

	Sensitivity (%)	Specificity (%)	AUC
GM1:GalC	81	80	0.834
GM1	67	80.5	0.762
GA1	56	72.5	0.654
GM2:GalC	33	90.5	0.621
GA1:GalC	54	67	0.601
GM2	25	91.5	0.579
GM1:GalC+GM1	84	77.2	0.842
GM1:GalC+GM2:GalC	85	77.2	0.845
GM1:GalC+GM2:GalC+GM1	86	74	0.851
GM1:GalC+GM2:GalC+GM1+GM2	86	73	0.851

4.7.2.2 GM1 and GM1:GalC analysis

81 MMN patients (81%) contained IgM antibodies against GM1:GalC. Out of the 19 (19%) GM1:GalC negative patients, there was 3 GM1 positive, 3 GA1 positive, 3 GA1:GalC positive, 1 GA1:Sulph positive, 3 SGPG:GalC positive and 6 patients with no observable antibody reactivity. 23 ALS controls (23%) and 17 Healthy controls (17%), adding up to a total of 20% of the overall control population, had IgM antibodies against GM1:GalC. Thus GM1:GalC yielded a sensitivity of 81% and a specificity of 80% (Table 4.2 and Figure 4.23 B).

67 MMN patients (67%) contained IgM antibodies against GM1. Out of the 33 (33%) GM1 negative patients, there was 17 GM1:GalC positive, 3 GA1 positive, 3 GA1:GalC positive, 1 GA1:Sulph positive, 3 SGPG:GalC positive and 6 patients with no observable antibody reactivity. 24 ALS controls and 15 Healthy controls, adding up to a total of 19.5% of the overall control population, had IgM antibodies against GM1. Thus GM1 yielded a sensitivity of 67% and a specificity of 80.5% (Table 4.2 and Figure 4.23 B).

The addition of 17 GM1:GalC positive MMN patients (Figure 4.23 C and D) which were GM1 negative conferred a significant increase in the test sensitivity without a detriment on the specificity. The presence of 3 MMN patients positive for GM1 but negative for GM1:GalC left the sensitivity increase achieved by the addition of GalC at a total of 14%.

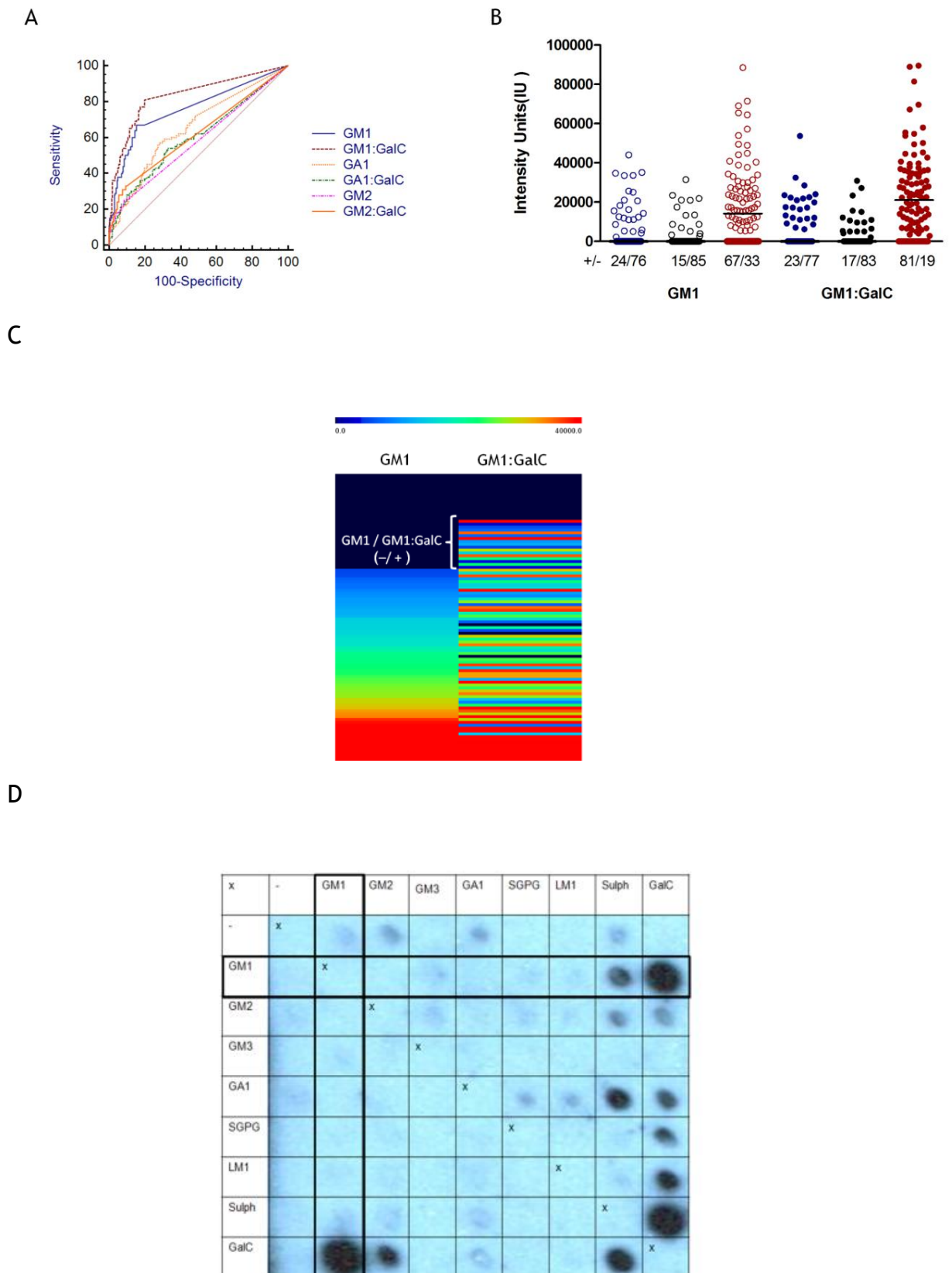


Figure 4.23. Quantitative and statistical analysis of glycoarray data.

Panel A. Individual ROC curves for 3 single glycolipids (GM1, GM2 and GA1) and their complexes with GalC. Panel B. Individual glycoarray intensity values for MMN cases and all controls against GM1 and GM1:GalC. Panel C. Heat map in rainbow scale showing the raw intensity values sorted through antibody binding to GM1, and corresponding GM1:GalC reactivities. Highlighted are the 17 MMN patients negative for GM1 and positive for GM1:GalC. The colour scale is as follows: dark blue corresponds to antibody negative signals, pale blue and green low to mid-range signals and red high value signals. Panel D. Example of a glycoarray depicting patient sera with complex dependent GM1:GalC Ab binding.

4.7.2.3 First and second screening compared: GM1:GalC enhancement recovery

The repeat screening of MMN positive control sera demonstrated GM2:GalC and GM1:GalC reactivities with CVs within the normal range (<20%). The average CV for the four MMN positive control sera was 18.35% for GM1:GalC and 12.87% for GM2:GalC. This major improvement in the CV of GM1:GalC reactivities would suggest a consistent behaviour of GalC epitopes.

Correlation of data collected for GM1:GalC reactivities for the first and the second screening, demonstrated that the GalC mediated enhancement was recovered in the second screening (Figure 4.24 B) with a minor variability in the GM1 data (Figure 4.24 A). In the repeat screen, 14 MMN patients previously described as GM1 negative in the first study were subsequently positive. The increase in lipid concentration on the second screen could account for the slight increase in GM1 single reactivity (Figure 4.24 A). However, contrary to the notion of a generalised increase all lipid reactivities is that 3 patients which were GM1 positive on the initial screen, were found to be GM1 negative on repeat.

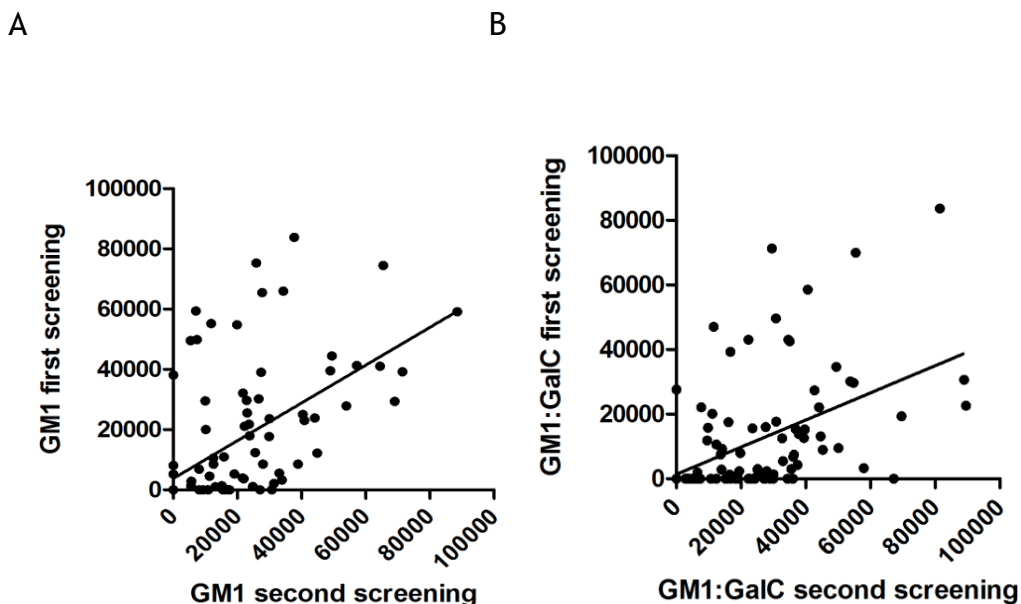


Figure 4.24. First and second screening correlation studies.

GM1 (A) and GM1:GalC (B) data from the first and second screening were compared, obtaining a Pearson correlation index of $r=0.60$ and $r=0.49$ respectively.

4.7.3 Summary

- CV data confirmed the consistency of our assay throughout the study.
- Correlation studies between GM1:GalC data from the first and second screening, it can be confirmed that GalC mediated GM1 enhancement was majorly recovered.
- Results confirmed the significantly higher sensitivity of GM1:GalC (81%) compared to GM1 (67%).
- This major increase of sensitivity was accompanied by an insignificant decrease in specificity (from 80.5% to 80%).
- Combinations of biomarkers including GM1:GalC did increase the sensitivity (from 81% to 86%) but at the cost of a significant decrease in specificity (from 80% to 74%).

4.7.4 Future recommendations

- The optimum ratio of Phrenosin:Kerasin in GalC preparations needs to be further explored. This study could eventually define the antibody profile of the 19 MMN patients negative for GM1:GalC.
- A comparative study between ELISA and glycoarray, focusing on the diagnostic strength of GM1:GalC, would be required before adapting this test into ELISA-based routine diagnostics in a hospital setting.
- The ELISA clinical validation sample set could consist on the Dutch cohort (300 samples), newly blinded, including the top targets from our previous study (GM1, GM2, GA1 and their GalC complexes).
- Based on our current findings we would strongly recommend the introduction of GM1:GalC to the routine serology diagnostic test for MMN.

4.8 Discussion

Initial findings on MMN serology corroborate the ideas of Pestronk and co-workers (Pestronk, Choksi, Blume, & Lopate 1997), who postulated an enhancing effect of GalC in anti-GM1 antibody binding. The idea that GM1:GalC complexes compared to single GM1 significantly increase the antibody detection sensitivity in MMN has been recently confirmed (Nobile-Orazio, Giannotta, Musset, Messina, & Leger 2013). Our assay, although similar in principle to those of Nobile-Orazio and Pestronk highly differs in methodology. Pestronk's assay included a complex mixture of lipids, which he described as MAG-associated lipid fraction, consisted of GM1, GalC, and Cholesterol sulphate (GSC) at a proportion of 1:10:10. The initial results, obtained from a cohort including 21 MMN patients and 525 controls, revealed that 19% of the patients presented elevated titres specific to GM1:GSC yielding an overall sensitivity of 62%, in contrast to the 43% of GM1 alone. The specificity for GM1:GSC was 100%. Under the same principle Nobile-Orazio tested MMN sera on a panel containing GM1:GalC at a 1:10 ratio. In this study, 75% of MMN patients showed a GM1:GalC specific reactivity, a 28% increase in sensitivity respect that of GM1 alone. This GM1:GalC increase in sensitivity was accompanied by a mild decrease in specificity (8%). The main featured differences between our assay and those described above are the array platform and the epitope composition. We used glycoarray as opposed to conventional ELISA. Our technique by incorporating the combinatorial factor allowed the identification of an antibody binding profile common to a majority of the MMN samples of the SGH serology test. This MMN antibody binding fingerprint consisted on GM1:GalC enhancement and GM1:GD1a/GM1:LM1 cis-inhibition. Prior studies had already reported the presence of a GD1a cis-inhibition of GM1 binding in MMN patient sera (Nobile-Orazio, Giannotta, & Briani 2010). Another key feature of our assay was the use of GM1:GalC at a 1:1 weight to weight ratio. Under these conditions, our first study revealed that GM1:GalC complexes increased by a 42% the anti-GM1 detection sensitivity with just a 3.5% drop in specificity (Galban-Horcajo, Fitzpatrick, Hutton, Dunn, Kalna, Brennan, Rinaldi, Yu, Goodyear, & Willison 2013). Our double blinded validation study came to confirm the significant increase in MMN diagnostic sensitivity conferred by the use of GM1:GalC complexes. 81% of MMN patients had anti-GM1:GalC antibodies accounting for a 14% increase compared to GM1 alone

diagnostic sensitivity. All these preliminary evidence indicate the necessity of introducing GalC in partnership with GM1 as a diagnostic test for MMN in a clinical setting.

The comparison of anti-GM1:GalC antibody detection efficiency between ELISA and glycoarray during the SGH study, showed a strong correlation between both techniques. This comparative study highlights the potential adaptability of glycoarray in routine diagnostics. However, further comparisons based on anti-GM1 detection during the Dutch first screening, indicated a significantly better sensitivity/specificity balance for glycoarray. Therefore, the conflicting results would be a reflection of the existing inter-laboratory variability and could not be accounted as variability between different methodologies. These inconsistencies stress the need for a standardised protocol which would strongly benefit from an internationally coordinated meta-analysis to identify the source and magnitude of inter-laboratory variability.

In Pestronk's article, several of the MMN patients presenting high titers for anti-GM1 Abs had low titers for anti-GM1:GalC Abs (Pestronk, Choksi, Blume, & Lopate 1997). This observation was then confirmed by the finding in the Dutch cohort, second screening, of three GM1 positive patients which were GM1:GalC negative. A more detailed analysis of this apparent paradox has been attempted throughout this chapter. An array containing GM1 as a single epitope and in complex with increasing amounts of GalC was used to probe neuropathy-derived human anti-GM1 IgM monoclonal antibodies. Results from these arrays revealed a high binding diversity among these mAbs. Although some antibodies (e.g. SM1) bound GM1 independently of GalC presence in any concentration, some mAb were unable to bind GM1 when in the presence of specific concentrations of GalC, confirming Pestronk's initial observations (e.g. BR1) (Figure 4.10). Furthermore, this binding diversity could be found within the antibody repertoire of a single patient. Interestingly, while the antibody profile of patient BR (Figure 4.10 B) was characterised by GM1 single binding followed by a GM1:GalC binding enhancement, BR1 the mAb derived from BR was unable to bind GM1 in the presence of GalC (Figure 4.10 A). This striking single observation could be explained by the presence within the same patient of three different types of anti-GM1 antibodies:

- Abs which bind GM1 single epitope with or without the presence of GalC (cis-independent)
- Abs which exclusively bind GM1 when in heterodimeric partnership with GalC (complex dependent)
- Abs which do not bind GM1 when in the presence of GalC (cis-inhibited)

Therefore, when BR1 was cloned from BR patient's blood (O'Hanlon, Paterson, Wilson, Doyle, McHardie, & Willison 1996), the antibody subset which was isolated corresponded to the third type, GM1:GalC cis-inhibited.

This combination of findings provides some support for the conceptual premise that GM1 neighbouring lipids play a major role in modulating antibody binding. The cryptic nature of these epitopes highlights the enormous diversity of anti-GM1 antibodies and strengthens the belief that cis-inhibitions and cis-enhancements could modulate antibody binding in tissue and eventually define disease phenotypes.

The initial finding of a high proportion of GM1:GalC specific patients at 1:1 ratio redefined to a great extent the concept of antibody-negative patients. It seems apparent from this data that the epitope presentation and thus its composition has played a major role in unmasking antibody subsets believed to be involved in the development of the disease.

The past twenty years have seen increasingly rapid advances in the field of antibody detection in neuropathy patient sera. Throughout these years of development, arrays in PNS neuropathies have conceptually shifted from the simplicity of a single epitope to the combinatorial factor introduced by heterodimeric ganglioside complexes. Despite its initial diagnostic success, most of these array studies do not conceive antibody epitopes as lipid domains. The importance of this chapter relies on proving that by increasing the complexity of the epitope, some cryptic antibodies can now be detected.

5 Chapter 5. Antibodies to heterotrimeric glycolipid complexes in Chronic Inflammatory Demyelinating Polyradiculoneuropathy.

5.1 Introduction

As outlined in chapter 4, some neuropathy patients present antibodies with high specificity for highly cryptic epitopes. These epitopes, characterised by specific molecular arrangements and ratios between different glycolipids, have helped to unmask reactivities in patients previously described as antibody-negative. In order to test the diagnostic potential of these cryptic epitopes, a cohort of patients with CIDP, an inflammatory neuropathy where traditionally a small proportion of patients show anti-ganglioside antibodies (Hughes et al. 2006), was screened using this approach.

5.2 Aims

5.2.1 Conceptual aims

- Investigate the presence of pattern recognition antibodies and antibodies against heterotrimeric complexes in CIDP.

5.2.2 Experimental aims

The initial experimental aim was to design an array formed by heterotrimeric complexes of three different glycolipids. In order to achieve this level of molecular complexity I:

- Look for the optimum molecular ratio between gangliosides and glycolipids for enhanced antibody binding. GalC at increasing concentrations will be used as the paradigmatic molecule.
- Compare the Ab binding enhancement properties of different adjuvant molecules at a set molecular ratio.

- The optimum adjuvant molecule at the set molecular ratio will be included into heterodimeric complexes forming arrays containing heterotrimeric epitopes.
- The antibody binding properties of these newly developed arrays will be tested onto a cohort comprising CIDP patients and controls.

5.3 Study design

- Samples were tested exclusively for IgM reactivities by ECL and fluorescence. Numerical analysis was performed using ECL data.
- Experiments were repeated 3 times with internal duplicates.
- Pilot studies were performed with 19 CIDP patients randomly selected. The arrays on the pilot study were conceived as asymmetrical and horizontally laid out.
- For the definitive screening, 51 CIDP patients and 93 controls (71 multiple sclerosis and 22 rheumatoid arthritis) were included.
- All of the 144 samples were probed against an array consisting of two 11x11 grids placed next to each other on the same PVDF/PVDF-FL membrane. On the left, the grid consisted of single lipids and their corresponding heterodimeric complexes at a working concentration of 100 µg/ml each. The grid on the right hand side of the array consisted of the same target epitopes but containing in all of them a third glycolipid, Phrenosin at a working concentration of 1000 µg/ml. Both 11x11 grids were therefore probed simultaneously, as a single array, with the same sera (Figure 5.1).
- The lipids included in the array were as follows: GM1, GM2, GM3, GD1a, GD1b, LM1, SGPG, GD3, GT1b and Sulph.

Array left (without Phrenosin) Array right (with Phrenosin)

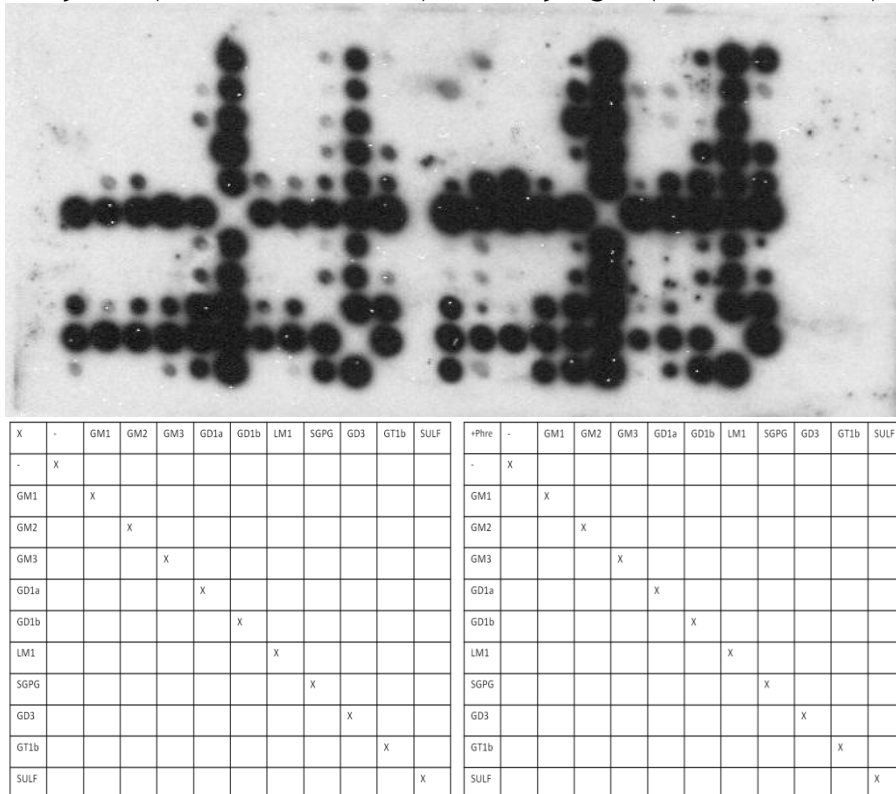


Figure 5.1. Array lay out for CIDP cohort screen.

5.4 Results

5.4.1 Pilot Studies

5.4.1.1 Determination of the optimum complex molecular ratio

The initial pilot studies aimed to validate the ratio 1:10 (ganglioside:GalC) as the optimum lipid platform for pattern recognition antibody binding. As seen in Figure 5.2 the ratio 1:10 (w/w) in CIDP patients revealed a complex dependent IgM antibody binding. The use of a complex molecular ratio between gangliosides and GalC unmasked Ab reactivity undetected at lower molecular ratios (e.g. 1:1 or 1:5).

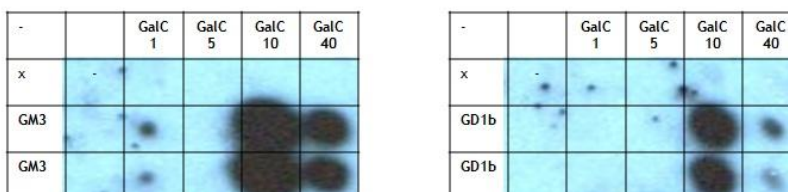


Figure 5.2. Ganglioside complexes containing different GalC ratios.

The array was printed horizontally and asymmetrically, and contain the GalC singles at different concentration on the top first row, and their duplicated complexes with gangliosides on the second and third rows. Ganglioside singles were duplicated on the intersection between the first column and second and third rows.

5.4.1.2 Determination of the optimum adjuvant molecule

Further analyses were conducted to determine the optimum adjuvant molecule to be used in complex with the glycolipid heterodimers on the final CIDP screening. The molecular ratio established as the optimal in section 5.4.1.1 for GalC was adapted to all the adjuvant molecules. Thus, for this study the following molecules were tested in complex with gangliosides at 1:10 ratio (ganglioside:adjuvant molecule w/w): GalC, Phre, Ker, GluC, SM, Cer, PC, DGDG and Chol.

Although specific epitope variability was observed, data revealed an increased Ab binding to epitopes containing GalC species (Figure 5.3).

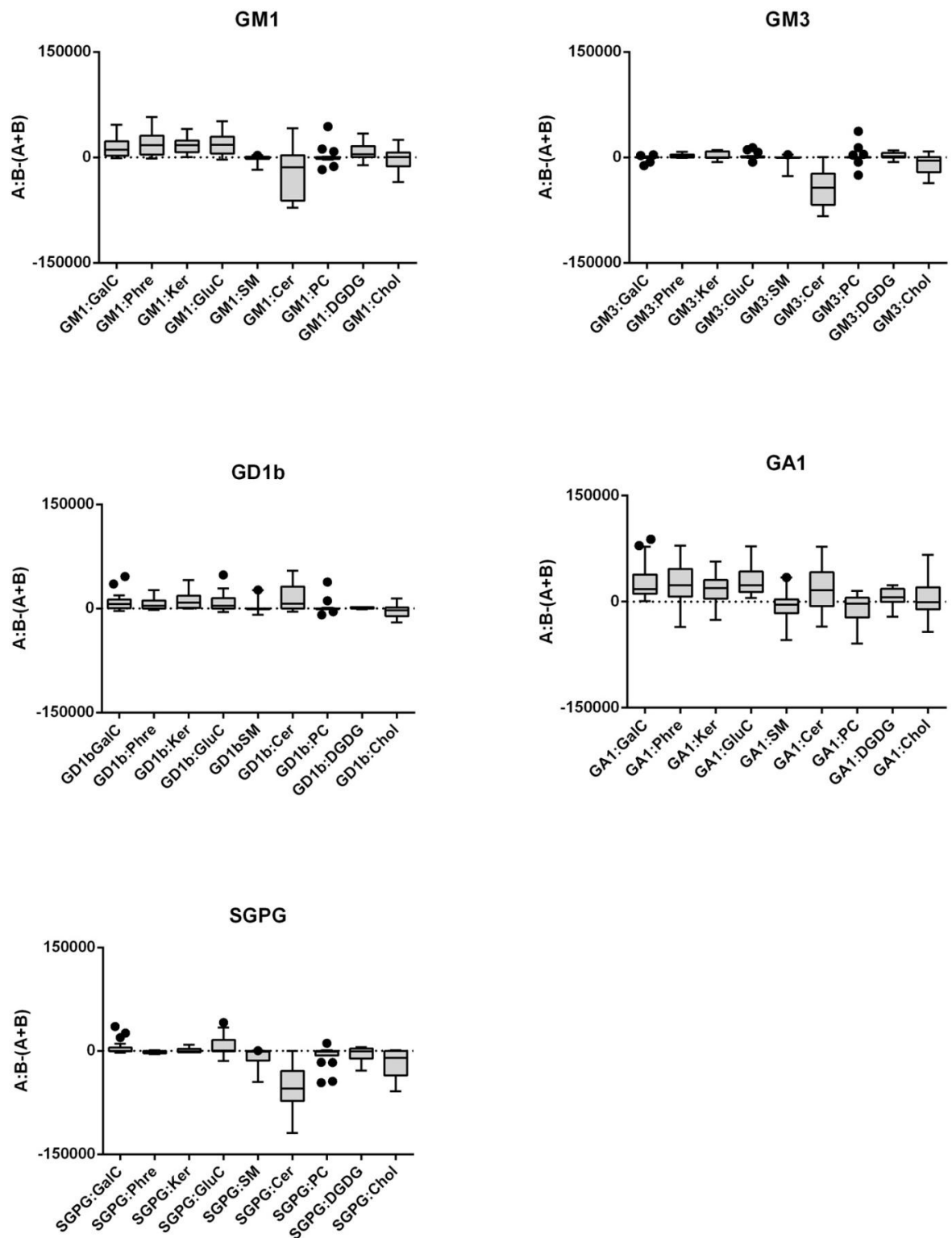


Figure 5.3 Patterns of antibody binding in CIDP sera.

CIDP sera binding to GM1, GM3, GD1b, GA1 and SGPG can show complex enhancement and/or attenuation with adjuvant molecules. Data are shown as box and whisker plots (median and interquartile ranges) depicting signal intensities above (complex enhancement) or below (complex attenuation) the intensity value for the single glycolipid which is set at zero.

Individual analysis of CIDP patients highlighted the presence of patients with exclusively Phre dependent reactivities which were GalC complex negative (Figure 5.4). This finding, in addition to the fact that all the patients reactive

for GalC epitopes were also reactive for Phre complexes, made us choose Phre as the adjuvant molecule for the final screen.

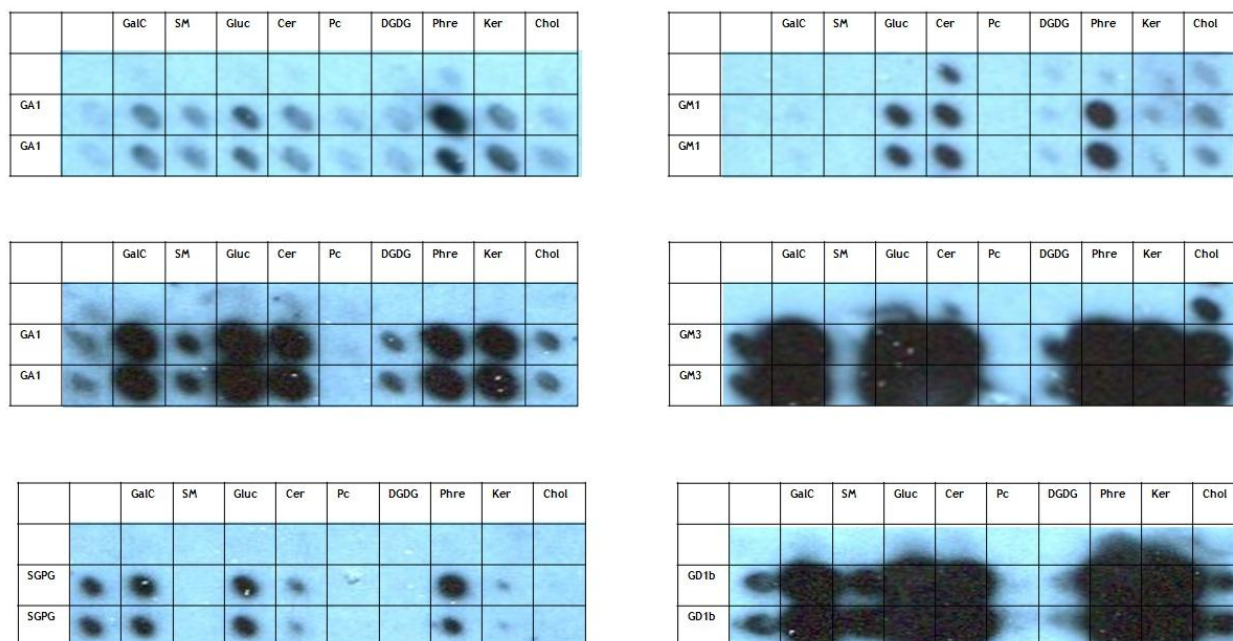


Figure 5.4. Ganglioside complexes with different adjuvant molecules.

Samples were prepared containing gangliosides at 100 $\mu\text{g}/\text{ml}$ and adjuvant molecules including GalC, SM, Gluc, Cer, Pc, DGDG, Phre, Ker and Chol at 1000 $\mu\text{g}/\text{ml}$. The array was conceived horizontally and asymmetrically, containing the adjuvant molecules as single epitopes on the top first row, and their duplicated complexes with gangliosides on the second and third rows. Ganglioside singles were duplicated on the intersection between the first column and second and third rows.

Therefore, ganglioside complexes and single epitopes will be mixed with ten times Phre in a weight to weight proportion. The layout of the grid containing two 11x11 arrays (Figure 5.1) will allow direct comparison between arrays with and without adjuvant glycolipid.

5.4.2 CIDP cohort screening

Array data from all CIDP cases (Figure 5.5) and controls (Figure 5.6) were subjected to cluster analysis that yielded a heat map comprising spot intensities for all the complexes with and without Phre. Spot intensities were categorised according to their arbitrary intensity raw values.

A significant increase in intensity signal can be seen when including Phre for both CIDP and control populations (Figure 5.5 and Figure 5.6). In some cases, the increase in signal translated into a saturated signal in ECL. This was later re-evaluated a descriptive study by fluorescence analysis (Figure 5.7).

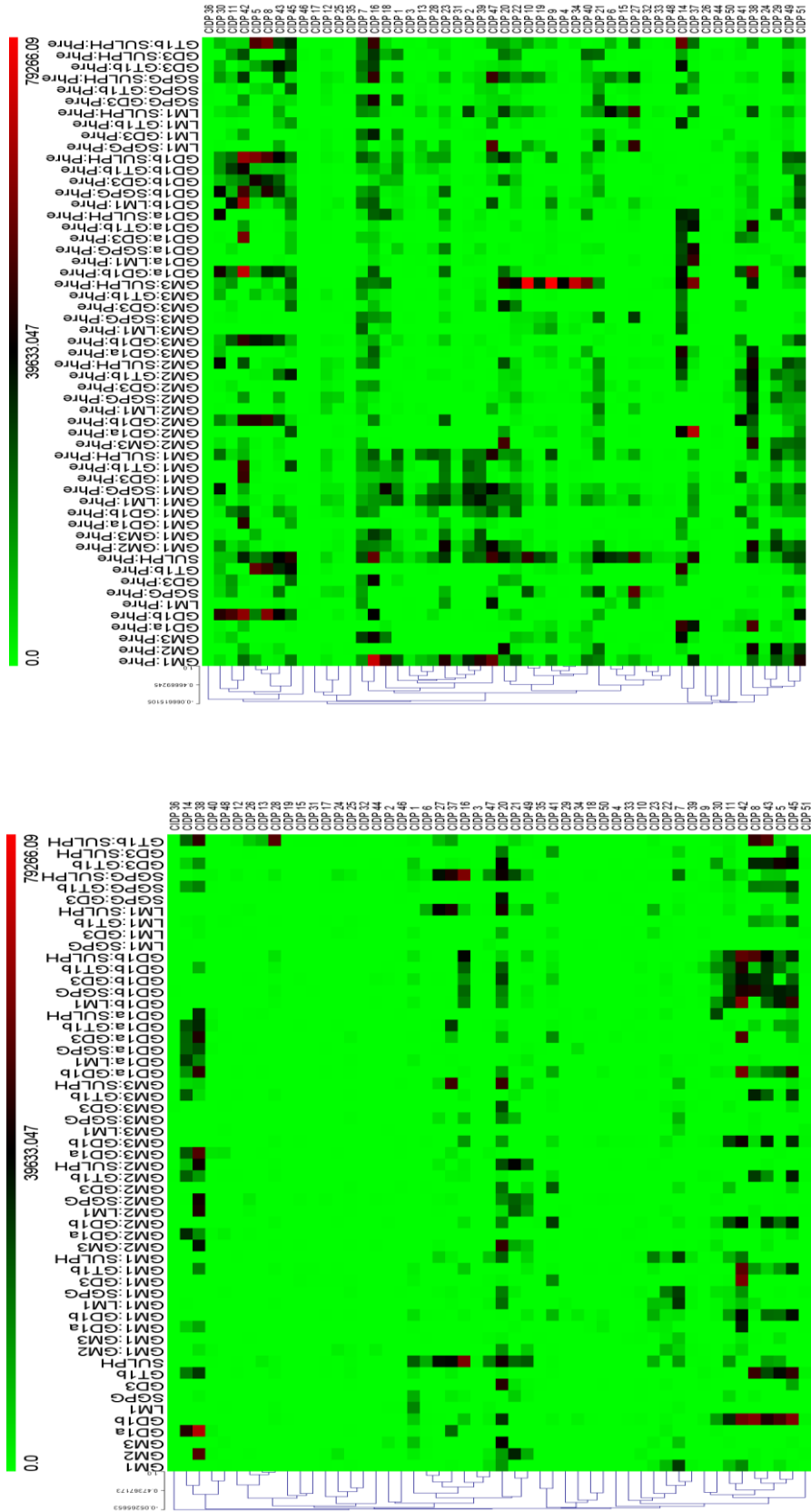
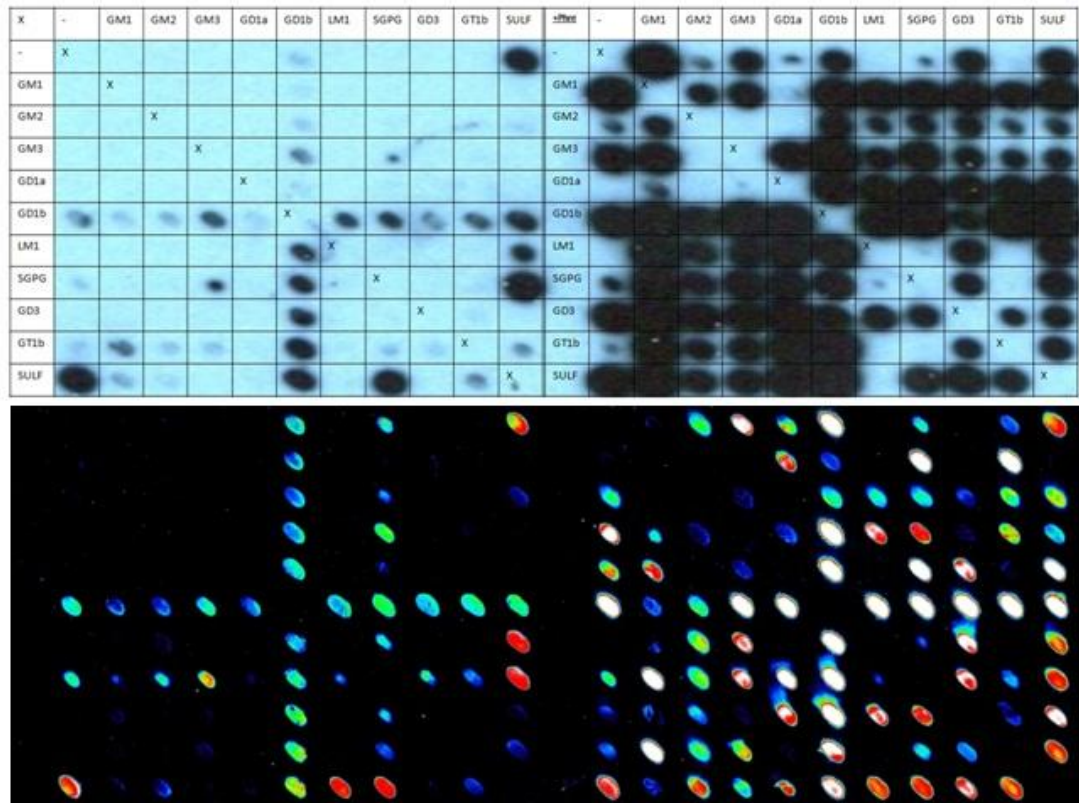


Figure 5.5. Data from the CIDP population presented as a clustered Heat map. Heat maps were created using the raw data recorded for each lipid antigen (rows) depicting serum IgM reactivity per patient (columns). The highest intensity value (79266.09 IU) was set as the upper limit intensity. Thus, pale green corresponds to antibody-negative signals, darker green and black to mid-range signals and red to high value signals

A



B

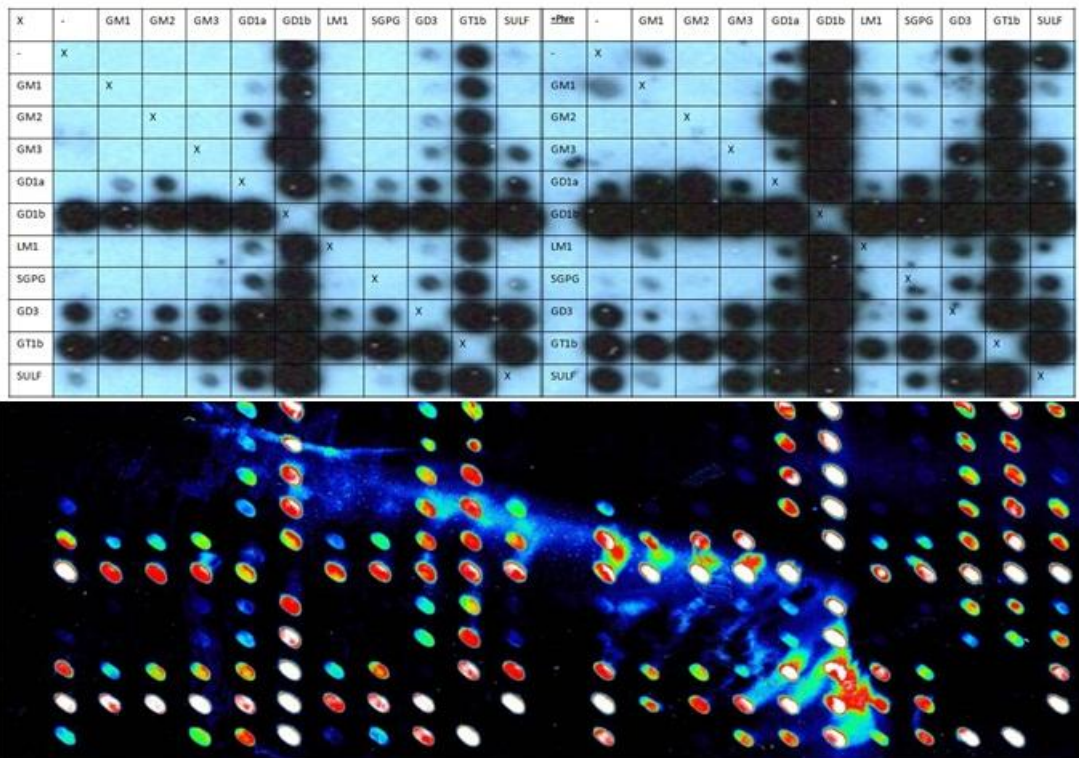


Figure 5.7. Representative blots from glycoarray.

Blots corresponding to two (A and B) representative patients screened using both ECL (above) and fluorescence (below). These comparative blots demonstrate the level of saturation existing within ECL intensity quantification, which might lead to understating the relevance of complex epitopes in Ab binding enhancement.

5.4.2.1 CIDP versus Controls

Further statistical analysis comparing CIDP and control populations, revealed that only 9 markers presented higher intensity binding in the CIDP group than in the control population prior to the addition of Phre. After the addition of Phre as an adjuvant molecule, an extra 12 epitopes presented significantly higher Ab binding in the CIDP group (Table 5.1). No epitope lost significance after the addition of Phre, suggesting that the specificity was kept constant although the sensitivity increased. Sensitivity/specificity data for these 12 epitopes after the addition of Phre can be found in Table 5.1.

Table 5.1. Comparison of CIDP and Control populations.

Bonferroni's multiple comparison of markers with or without the addition of Phre. (ns=not significant; *p value \leq 0.05, **p value \leq 0.01, ***p value \leq 0.001 and ****p value \leq 0.0001). Sensitivity and specificity corresponds to the complexes containing Phre.

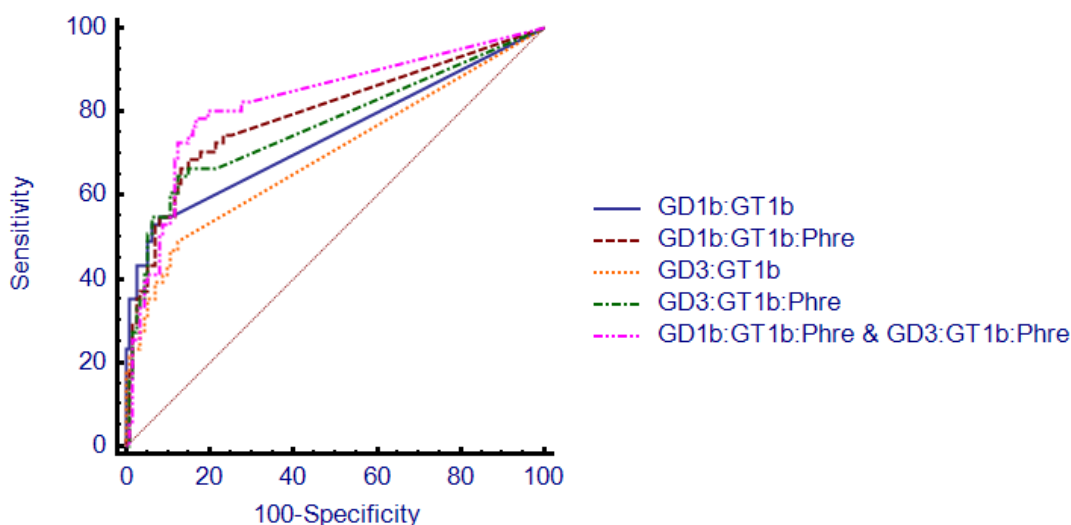
	- Phre	+ Phre	Sensitivity (%)	Specificity (%)
GM1	ns	****	66.7	80.4
GM1:GM2	ns	****	76.5	75
GM1:GD1b	ns	****	74.5	75
GM1:LM1	ns	****	72.5	70.5
GM1:SGPG	ns	****	82.4	47.3
GM1:Sulph	ns	****	70.6	79.5
GM2:GD1b	ns	***	21.6	95.5
GM3:GD1b	ns	****	66.7	82.1
GM3:Sulph	ns	****	47	88.39
GD1a:Sulph	ns	***	33.3	90.2
GD1b:GD3	ns	*	66.7	73.2
GD3:Sulph	ns	**	51	84.8
GD1b	****	****	70.6	75
SULPH	**	****	84.3	42
GD1a:GD1b	**	****	58.8	74.1
GD1b:Sulph	****	****	52.9	76.8
GT1b:Sulph	***	****	51	87.5
GD1b:LM1	**	**	70.6	71.4
GD3:GT1b	*	**	64.7	87.5
GD1b:GT1b	*	*	68.6	84.8
GD1b:SGPG	**	*	39.2	79.5

5.4.2.2 Top markers: GD1b:GT1b:Phre and GD3:GT1b:Phre

Ranking of markers for diagnostic accuracy using ROC, established GD1b:GT1b:Phre and GD3:GT1b:Phre as among the top markers with AUCs of 0.793 and 0.767 respectively (Figure 5.8 B). Although scoring a higher AUC when in complex with Phre, GD1b:GT1b:Phre and GD3:GT1b:Phre were not significantly different than their equivalent without Phre ($p=0.2880$ and $p=0.1614$ respectively) (Figure 5.8 A).

After combining the diagnostic efficiency of both markers (GD1b:GT1b:Phre & GD3:GT1b:Phre), the overall AUC increased up to 0.824. This increase although insignificant when compared to GD1b:GT1b:Phre and GD3:GT1b:Phre as independent epitopes ($p=0.2229$ and $p=0.1655$ respectively), represented a significant improvement when compared to both heterodimeric complexes without Phre (Figure 5.8 A).

A



B

	AUC	Sensitivity (%)	Specificity (%)
GD1b:GT1b:Phre	0.793	68.6	84.8
GD1b:GT1b	0.740	55	92
GD3:GT1b:Phre	0.767	64.7	87.5
GD3:GT1b	0.694	49	87.5
GD3:GT1b:Phre & GD1b:GT1b:Phre	0.824	78.4	83

Figure 5.8. Statistical analysis of glycoarray data for top markers.

A. Individual ROC curves for two heterodimeric complexes (GD1b:GT1b and GD3:GT1b), their complexes with Phre (GD1b:GT1b:Phre and GD3:GT1b:Phre) and the overall overall diagnosis efficiency of both markers together. B. Table summarising the equivalent AUCs, Sensitivity and specificity for every each one of the individual ROC curves.

5.4.2.3 Antibody binding fingerprint: GM3:Sulph:Phre

After individual analysis of patient arrays, a marker which did not rank among the most efficient diagnostic epitopes was considered for multivariable fingerprint profiling. 22% of the patients presented GM3:Sulph:Phre complex enhanced binding, 4 % of those binding exclusively to GM3:Sulp:Phre, suggesting the potential use of this marker as part of a larger biomarker fingerprint for CIDP (Figure 5.9). In addition to this, the presence of Ab binding to GM3:Sulph:Phre heterotrimeric complexes but not to GM3, Sulph, Phre, Sukph:Phre, GM3:Sulph or GM3:Phre suggests the presence of an antibody subset specific for epitopes composed of three different glycolipids.

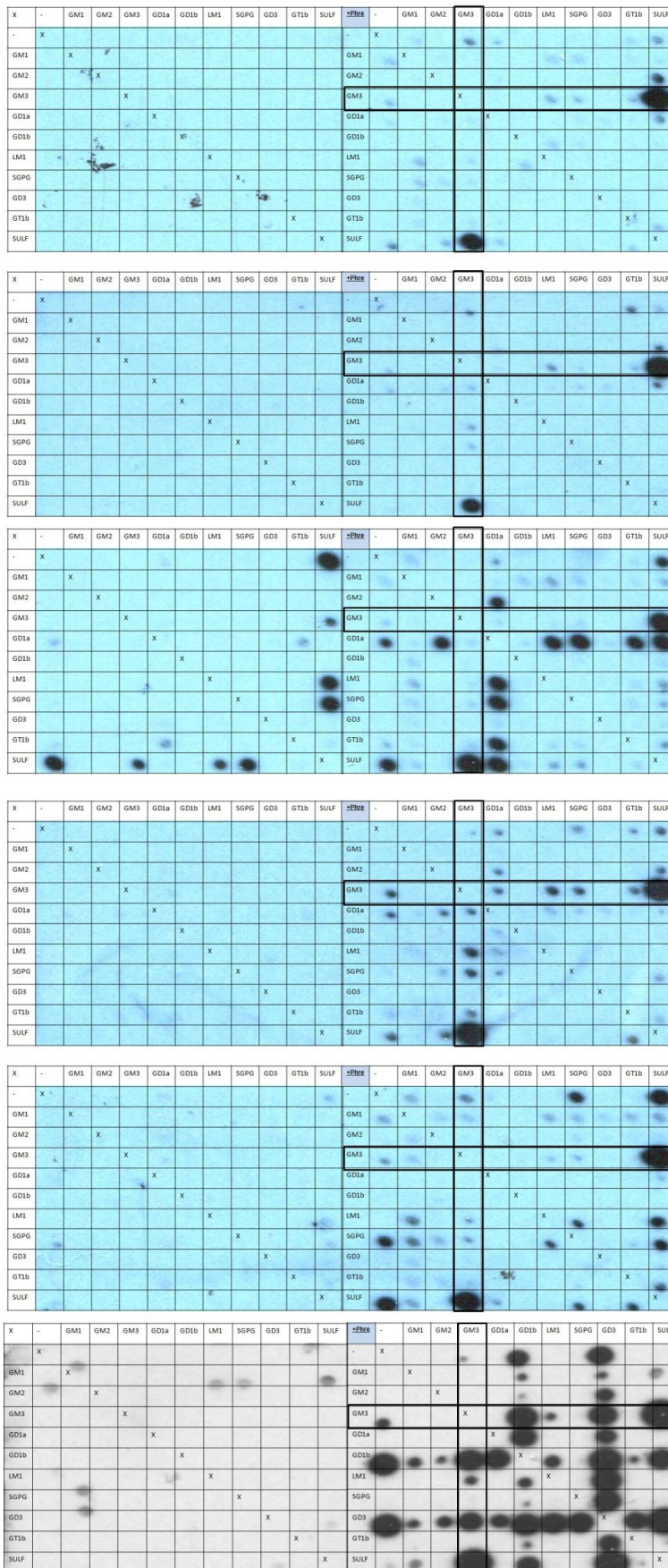


Figure 5.9. Characteristic blots depicting enhanced or complex specific GM3:Sulph:Phre reactivities.

11x11 grids placed next to each other within the same PVDF membrane. On the left, the grid consisted of single lipids and their corresponding heterodimeric complexes at a working concentration of 100 µg/ml. The grid on the right hand side of the array consisted of the same target epitopes but containing in all of them a third glycolipid, Phrenosin.

The addition of GM3:Sulph:Phre to GD1b:GT1b:Phre and GD3:GT1b:Phre marginally improved the AUC, from 0.824 to 0.853. A more in depth analysis revealed a 4% increase in sensitivity with a 0.9% decrease in specificity (Figure 5.10 and Figure 5.11 B).

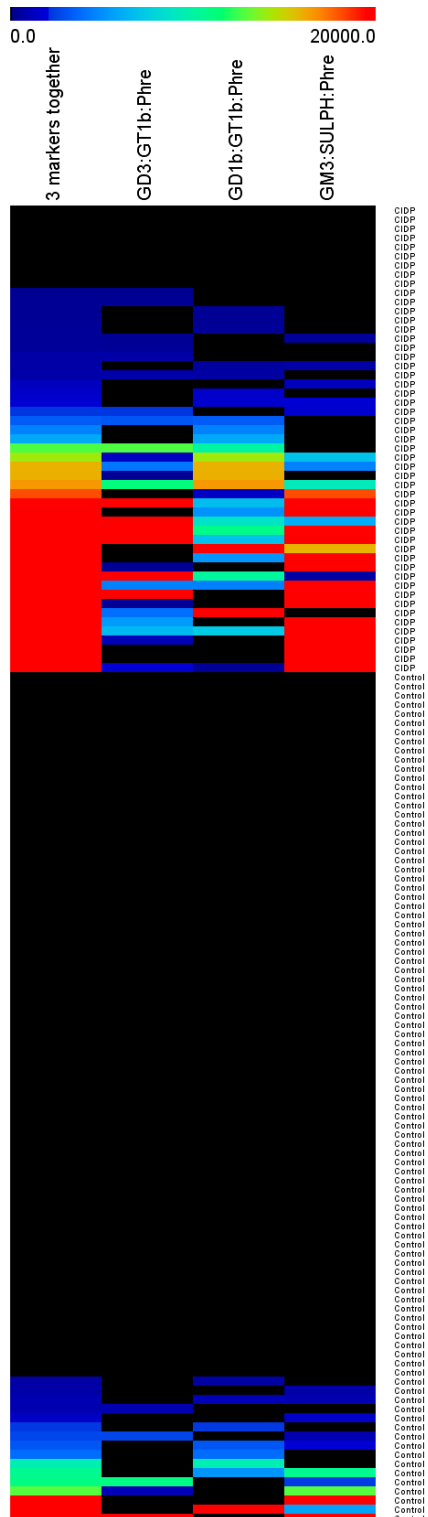
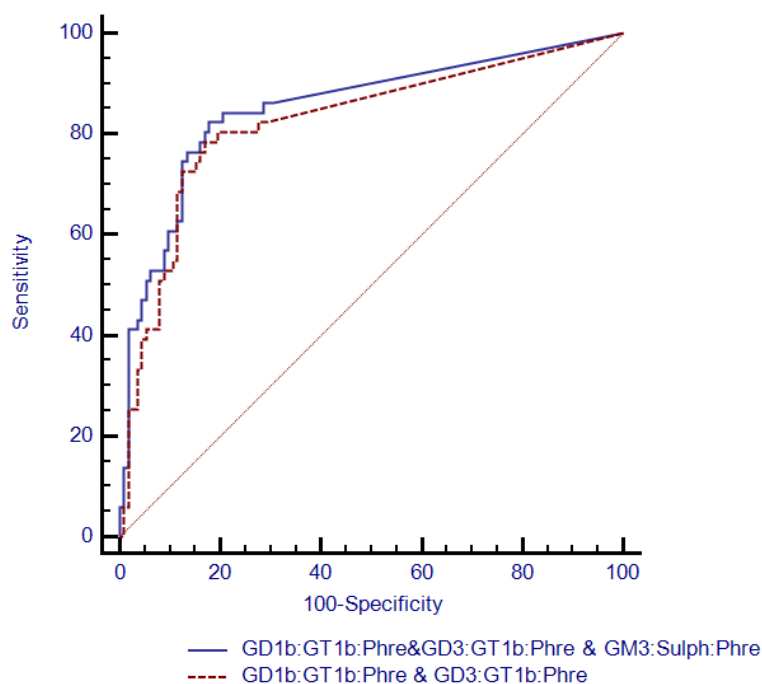


Figure 5.10. Heat map depicting the top markers.

Heat map representing the Ab binfing fingerprint for the CIDP and control population (rows). The rainbow scale representation has been adapted to a maximum threshold of 20000 intensity units. Under this scale the CIDP patients for the three markers together have been classified as: low intensity (n=17), mid intensity (n=6) and high intensity (n=19).

Although this slight improvement did not prove significant after ROC analysis ($p=0.1236$), the 4% increase in sensitivity and the stability of specificity highlights the beneficial effect of adding GM3:Sulph:Phre as a test marker for CIDP (Figure 5.11 A).

A



B

	AUC	Sensitivity (%)	Specificity (%)
GD3:GT1b:Phre & GD1b:GT1b:Phre & GM3:Sulph:Phre	0.853	82.4	82.1
GD3:GT1b:Phre & GD1b:GT1b:Phre	0.824	78.4	83

Figure 5.11. Statistical analysis of glycoarray data for overall markers.

A. Individual ROC curves for the diagnosis efficiency of GD1b:GT1b+GD3:GT1b and , GD1b:GT1b+GD3:GT1b+GM3:Sulph:Phre. B. Table summarising the equivalent AUCs, Sensitivity and specificity for every each one of the individual ROC curves.

After establishing GD1b:GT1b:Phre + GD3:GT1b:Phre+ GM3:Sulph:Phre as the most efficient biomarker fingerprint for CIDP, the significance of Phre within the complexes was evaluated using ROC analysis.

The comparison between the heterodimeric complexes with and without Phre, demonstrated the relevance of Phre as a potent adjuvant for antibody binding. The markers conforming the CIDP fingerprint without Phre scored an AUC of

0.730, being significantly lower than the AUC of 0.853 for the same markers including Phre ($p=0.0065$) (Figure 5.12).

Although the addition of Phre to these markers decreases the specificity by a 5.4%, the sensitivity experiences a significant 25.5% increase. Therefore, the overall diagnostic efficiency depends to a great extent on the epitope content of Phre.

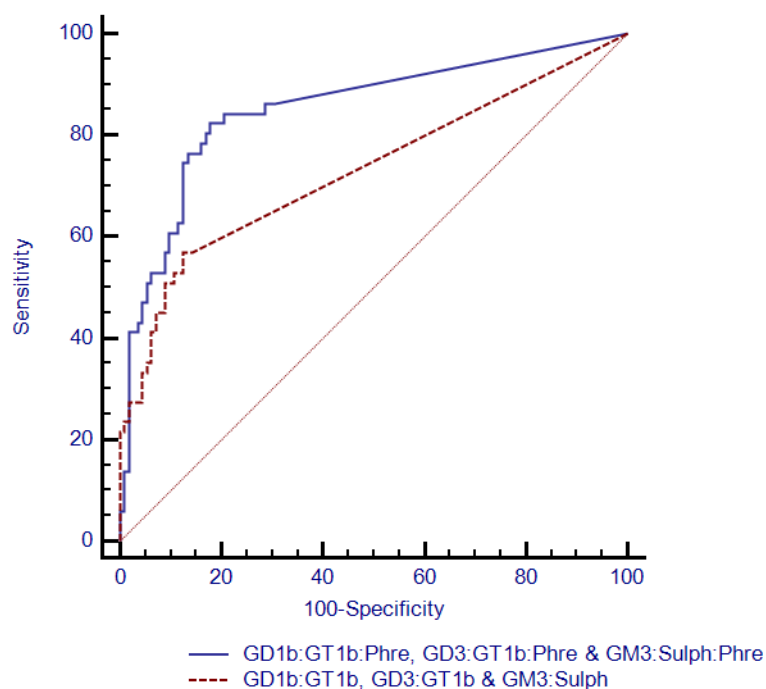


Figure 5.12. Ab binding fingerprint after the inclusion of Phre. Individual ROC curves comparing the Ab binding fingerprint for CIDP (GD1b:GT1b:Phre+GD3:GT1b:Phre+GM3:Sulph:Phre) with and without Phre.

5.5 Future work

- Look for characteristic clinical correlations between the IgM markers identified and disease phenotypes.
- Investigate the IgG reactivity present within this cohort of patients and controls.
- Include another control group consisting of healthy subjects.

- Validate the markers found in this study on a double blinded cohort of CIDP patients and controls.

5.6 Discussion

42 of 51 CIDP patients demonstrated IgM binding to glycolipid antigens defined by a cluster of three different reactivities: GD1b:GT1b:Phre, GD3:GT1b:Phre and GM3:Sulph:Phre. The remaining 9 CIDP patients did not present any glycolipid binding, and were classified as antibody-negative for this study. 16 of 93 controls demonstrated IgM binding to the cluster of three different epitopes specified above. The rest of the controls were either antibody-negative or presented low levels of GM1:Phre and mid to high levels of Sulph:Phre.

Reactivities found in previous serology studies with CIDP patients, such as anti-SGPG IgM antibodies (Yuki et al. 1996) were slightly underrepresented in our test. In our study 13% of CIDP patients presented antibodies against SGPG in contrast to the 40% reported by Yuki and co-workers (Yuki, Tagawa, & Handa 1996). LM1, a myelin glycolipid with similar structure to that of SGPG, differing only in the presence of a sialic acid as opposed to a 3-sulfated glucuronic acid, was also marginally represented by a 6% antibody binding.

In order to generate an animal model of CIDP, rabbits have been traditionally immunised with galactocerebroside (Saida, Saida, Brown, & Silberberg 1979). Therefore, a hypothesis from this study would be that antibodies to this glycolipid could be involved in the development of the disease and thus found in high titres in CIDP patients. In agreement with previous findings (Hughes et al. 1984; McCombe et al. 1988), our study did not find IgM reactivity against single galactosylceribrosides or its sulphated form.

The addition of complexity within the epitope, after incorporating Phre, considerably improved IgM antibody binding in this study. Phrenosin has been proven to increase the sensitivity of the arrays at the same time as maintaining the specificity. One representative case of the cryptic behaviour of antibodies has been the discovery of antibodies against GM3:Sulph:Phre. This subset of antibodies found in a greater proportion and higher levels in CIDP patients, exclusively bound GM3 when in complex with Sulphatide and Phrenosin. This

antibody binding to heterotrimeric complex is the first description to date of an antibody binding to 3 different lipids but not the singles or the heterodimers alone. IgM antibodies are known for their intrinsic capability to form multivalent interactions. As it has been previously demonstrated (Niedieck & Kuck 1976; Oyelaran, Li, Farnsworth, & Gildersleeve 2009a), the use of a complex lipid platform for antibody detection enhances the affinity and avidity of these antibodies which are per se low affinity. Although, little is understood about the molecular rearrangement which takes place within the epitope, the generation of these cryptic domains has shown a promising testing improvement for CIDP serology diagnostics. After the discovery of heterodimers as Ab epitopes (Kaida, Morita, Kanzaki, Kamakura, Motoyoshi, Hirakawa, & Kusunoki 2004), much has been speculated on the possibility of a more complex scenario. This new GM3:Sulph:Phre heterotrimer moves the epitope complexity a step forward and sets the final goal for array screening on developing a dynamic membrane-like platform for HTS.

6 Chapter 6. Discussion

6.1 Modulation of antibody binding to GM1

Anti-GM1 antibodies have been previously described as having a highly diverse binding profile in tissue (O'Hanlon, Paterson, Wilson, Doyle, McHardie, & Willison 1996; O'Hanlon et al. 1998) and arrays (Greenshields, Halstead, Zitman, Rinaldi, Brennan, O'Leary, Chamberlain, Easton, Roxburgh, Peditani, Furukawa, Furukawa, Goodyear, Plomp, & Willison 2009). This diversity, present even within antibodies derived from the same patient (e.g. BO1 and BO3), cannot be solely explained by differences in epitope distribution. Therefore, it seems apparent that factors other than single presentation of GM1 clusters might be influencing the binding diversity of this highly cryptic epitope.

In Chapter 3 we have seen how anti-GM1 Abs can be modulated by the presence of neighbouring molecules. The presence of Cholesterol in complex with GM1, allowed Ab recognition in a complex-dependent manner. Ab in BTN sera recognised GM1 in liposomes containing cholesterol (1:5 M/M) and exclusively bound GM1 when in complex with cholesterol. The array binding data also revealed the importance of molecular ratios in Ab binding. Isolated anti-GM1 Ab from BTN serum started binding GM1:Chol in molecular ratios of 1:5 and greater. As previously discussed, the formation of this epitope could be induced by a GM1 conformation change. The change induced by cholesterol through a hydrogen bond network with GM1, would modify GM1's sugar moiety to a more planar conformation, closer to the membrane surface (Lingwood 1996; Mahfoud, Manis, Binnington, Ackerley, & Lingwood 2010).

This chapter also highlights the relevance of GD1a in forming complexes with GM1. Antibodies against GM1:GD1a complexes were first described in 2004 (Kaida, Morita, Kanzaki, Kamakura, Motoyoshi, Hirakawa, & Kusunoki 2004) and later characterised as a 1:1 molecular complex (Mauri, Casellato, Ciampa, Uekusa, Kato, Kaida, Motoyama, Kusunoki, & Sonnino 2012). Our study using JK sera also determined GM1:GD1a 1:1 as the optimal molecular ratio for antibody binding.

Chapter 4 first describes data from a local cohort of MMN patients. In this study, 19/33 contain Ab against GM1 alone however 33/33 MMN patients exhibited Ab reactivity against GM1:GalC (Galban-Horcajo, Fitzpatrick, Hutton, Dunn, Kalna, Brennan, Rinaldi, Yu, Goodyear, & Willison 2013). These results support those of Pestronk and co-workers (Pestronk, Choksi, Blume, & Lopate 1997) where they found a significant enhancement of GM1 Ab binding in the presence of a GalC mix. Recently, these observations have been further confirmed demonstrating a 27% increase in anti-GM1 Ab detection when in complex with GalC (Nobile-Orazio, Giannotta, Musset, Messina, & Leger 2013).

The initial validation cohort study revealed the complete disappearance of GM1:GalC reactivity. Further investigations identified a quantitative and qualitative failure of our GalC reagent. We discovered a decrease in the solubility of our GalC stock. That decrease in solubility accompanied the disappearance of the GalC enhancing effect over GM1 reactivity. After re-adapting the solubilisation methodology, by increasing the chloroform content in the solvent mix, and increasing the lipid concentration from 100 µg/ml to 200 µg/ml, the enhancing effect was recovered. At the same time, mass spectrometry data suggested a qualitative difference between the commercially procured GalC stocks. Each lot contained variable proportions of different GalC species. According to GalC's hydroxylation profile, there are two different species: Phrenosin (HFA-GalC) and Kerasin (NFA-GalC). The hydroxylation of GalC has been seen to affect the conformation of its sugar moiety that ultimately alters anti-GalC Ab binding (Chapter 4.6.1). Studies based on HIV's mechanism of cell anchoring proved how the anchor protein gp120 preferentially bound Phrenosin but not kerasin due to a preference for the kinked conformation of Phrenosin's galactose (Coffin et al. 1997; Hammache, Pieroni, Yahi, Delezay, Koch, Lafont, Tamalet, & Fantini 1998; Yahi, Baghdiguian, Moreau, & Fantini 1992). The structural constraints of GalC could influence the way they form complexes with GM1. The qualitative variability in GalC stocks translated into a differential Ab binding when in complex with GM1 and/or GM2 (Chapter 4.6.1).

A validation study, using a blinded cohort of MMN patients and controls, confirmed the anti-GM1 Ab detection enhancement conferred by the addition of

GalC. This study detected antibodies against GM1:GalC in 81/100 MMN patients, a 14% increase in Ab detection compared to GM1 alone. However, the 100% sensitivity could not be replicated in this study. One issue which needs to be addressed is the affect Phrenosin/Kerasin molecular ratios have on Ab binding to GM1:GalC complexes. The difference in Phrenosin/Kerasin ratios between GalC stocks could explain the variability between the SGH study and the Dutch validation cohort of MMN patients positive for GM1:GalC Abs. Similarly, this variability could account for the inter-assay and inter-laboratory variability of the GM1:GalC assay. In order to find the optimum GalC reagent for this Ab test, an array should be designed containing GM1 as a single epitope and in complex with different Phrenosin/Kerasin molecular ratios. The Dutch cohort could then be re-screened and each of the GM1:GalC complexes evaluated for sensitivity and specificity.

Several studies have singled out the inhibitory effect of GD1a over GM1 Ab binding (Greenshields, Halstead, Zitman, Rinaldi, Brennan, O'Leary, Chamberlain, Easton, Roxburgh, Pediani, Furukawa, Furukawa, Goodyear, Plomp, & Willison 2009; Nobile-Orazio, Giannotta, & Briani 2010). In our SGH MMN screening a significant majority of the patients presented cis-inhibition of GM1 Ab binding in the presence of GD1a and LM1 (Chapter 4.3.3). The existence of anti-GM1 Abs with enhanced or cis-inhibited binding to the same epitope (GM1:GD1a) reflects the wide diversity existing among these antibodies. The Dutch validation cohort further confirmed the inhibitory effect of GM1:LM1 complexes over GM1 Ab binding.

Contrary to expectations, when we analysed anti-GM1 mAb binding to GM1:GalC complexes, GalC was found to be detrimental to Ab binding in a concentration dependent manner. Anti-GM1 mAbs DO1 and BR1 did not bind GM1 when in complex with GalC while at the same time SM1 GM1 binding remained unaltered in the presence of GalC (Chapter 4.4.2). In support of this data, Pestronk and co-workers found several patients with high titres of anti-GM1 abs with a significant titre reduction when GM1 was in complex with GalC (Pestronk, Choksi, Blume, & Lopate 1997). A similar observation was noted in the second screening of the Dutch validation cohort (Chapter 4.7.2). In this screening three MMN patients with anti-GM1 Abs had cis-inhibition of Ab binding when GM1 was in complex

with GalC. This phenomenon highlights, once again, the high reactivity diversity among anti-GM1 antibodies and the major role played by adjacent molecules in GM1 Ab binding.

As previously discussed, BR1, the MMN-derived human anti-GM1 mAb, was inhibited from binding GM1 in the presence of GalC. Initial serology data from BR, the patient origin of the BR1 mAb clone, revealed the presence of anti-GM1:GalC Abs within the patient serum (Chapter 4.4.2). These findings may help us to have a deeper understanding of the polyclonal nature of patient sera and the huge diversity existing among antibodies against the same target. Although, the diversity of a patient's anti-GM1 Ab repertoire can be determined by the way these antibodies behave in the presence of neighbouring lipids such as GalC, their individual contribution to GSLs complex binding can only be fully dissected by the use of mAb.

6.1.1 GM1:GD1a complex inhibition as potential modulator of clinical phenotypes

Serology studies detecting anti-GM1 antibodies have been used for many years as a diagnostic tool for several neuropathies (Kaida, Morita, Kanzaki, Kamakura, Motoyoshi, Hirakawa, & Kusunoki 2004; Kaida, Sonoo, Ogawa, Kamakura, Ueda-Sada, Arita, Motoyoshi, & Kusunoki 2008; Latov, Hays, Donofrio, Liao, Ito, McGinnis, Konstadoulakis, Freddo, Shy, & . 1988; Pestronk, Cornblath, Ilyas, Baba, Quarles, Griffin, Alderson, & Adams 1988). Even though the techniques employed have ranged from ELISA-based studies (Adams, Kuntzer, Burger, Chofflon, Magistris, Regli, & Steck 1991; Willison, Veitch, Swan, Baumann, Comi, Gregson, Illa, Zielasek, & Hughes 1999) to surface Plasmon resonance (Alaedini and Latov 2001) and more recently a methodology based on combinatorial glycoarrays (Brennan, Galban-Horcajo, Rinaldi, O'Leary, Goodyear, Kalna, Arthur, Elliot, Barnett, Linington, Bennett, Owens, & Willison 2011; Galban-Horcajo, Fitzpatrick, Hutton, Dunn, Kalna, Brennan, Rinaldi, Yu, Goodyear, & Willison 2013; Rinaldi, Brennan, Goodyear, O'Leary, Schiavo, Crocker, & Willison 2009), the objective has always been to link the antibody reactivity to clinical phenotype allowing a more accurate diagnosis followed by a more precise treatment than relatively non-specific treatments such as plasma exchange or intravenous immunoglobulin (IVIG).

Serology does not necessarily infer clinical indicators, for example with antibodies targeting the same ganglioside, GM1, clinical features can be variable depending on antibody specificity and affinity (Lardone et al. 2010; Lopez et al. 2010) and in many cases can be reversible (Koga et al. 2003). Various studies have attempted to link a specific antibody reactivity profile to clinical features in many cohorts of patients suffering from a wide range of neuropathies (Kinsella, Lange, Trojaborg, Sadiq, Younger, & Latov 1994), based exclusively on multi-focal motor neuropathy (MMN) patients (Cats, Jacobs, Yuki, Tio-Gillen, Piepers, Franssen, van Asseldonk, van den Berg, & van der Pol 2010b) or on cases of Guillain-Barré syndrome (GBS) (Kuwabara et al. 1998a; Kuwabara et al. 1998b). The first two studies reported a significant correlation between high anti-GM1 antibody titres and a clinical phenotype characterized by a more severe weakness. Kuwabara and co-workers (Kuwabara, Yuki, Koga, Hattori, Matsuura, Miyake, & Noda 1998b) reported the main feature consisting of conduction failure and axonal degeneration. This evidence shows a possible correlation between anti-GM1 antibodies and the presence of certain clinical features in a range of neuropathies; however it does not entirely explain the nature of the difference in clinical phenotypes.

In the case of MMN, neuropathy of peripheral nerves characterized by the presence of asymmetric distal weakness, conduction block along motor axons and often the presence of IgM anti-GM1 antibodies, the clinical features correspond to an exclusive motor nerve disorder leaving the sensory nerves unaffected (Pestronk, Cornblath, Ilyas, Baba, Quarles, Griffin, Alderson, & Adams 1988) (Parry & Clarke 1988) surprisingly both motor and sensory nerves contain a similar proportion of GM1 ganglioside (Svennerholm 1994; Svennerholm et al. 1994). In 1994, and later in 1998 published as a review article, Ogawa-Goto brought attention to differences in GM1 ganglioside structures as determinants of antibody binding in patients with GBS. In his article Ogawa-Goto postulated that it was the difference in the carbon length of the fatty acid containing ceramide of GM1 which determined the differences in anti-GM1 antibody binding. The results showed decreases in binding respectively in the presence of motor nerve GM1, sensory nerve GM1 and brain GM1 (Ogawa-Goto et al. 1992; Ogawa-Goto & Abe 1998). This finding, while preliminary, suggests that slight differences in ganglioside structure could lead to high affinity antibody

binding in certain regions of the peripheral nervous system (PNS), such as motor nerves, where a specific form of GM1 is more abundant, causing motor neuropathies with no clinical sensory features (eg. MMN and acute motor axonal neuropathy (AMAN)).

One question to be addressed, however, is whether the membrane environment is going to play a role in the way the GM1-epitope will be presented for antibody recognition (Li and Pestronk 1991; Marcus et al. 1989). Perhaps the most serious disadvantage of the methods employed by Ogawa-Goto and co-workers is that solid-phase assays do not take into account the complexity of a cryptic membrane environment. Strong evidence of the complexity of the GM1-epitope was found when antibodies from MMN patients which were unreactive to either GM1 ganglioside or galactocerebroside (GalC) as single lipid epitopes were shown to be reactive to a complex mixture (GM1:GalC) and that the detection efficiency was significantly increased when cholesterol was introduced to the lipid complex mixture (Galban-Horcajo, Fitzpatrick, Hutton, Dunn, Kalna, Brennan, Rinaldi, Yu, Goodyear, & Willison 2013; Nobile-Orazio, Giannotta, Musset, Messina, & Leger 2013; Pestronk, Choksi, Blume, & Lopate 1997). Supporting these findings, antibody binding to complex gangliosides was found in patients suffering GBS (Kaida, Morita, Kanzaki, Kamakura, Motoyoshi, Hirakawa, & Kusunoki 2004; Kaida, Sonoo, Ogawa, Kamakura, Ueda-Sada, Arita, Motoyoshi, & Kusunoki 2008) and antibodies targeting GM1 mediated lipid complexes (eg. GM1:GalNac-GD1a) could be playing an important role in the development of pure motor GBS (Kaida, Sonoo, Ogawa, Kamakura, Ueda-Sada, Arita, Motoyoshi, & Kusunoki 2008; Kaida & Kusunoki 2010). Difficulties arise, however, when an attempt is made to extrapolate these findings to the “living membrane”. Recently, studies in tissue and solid-phase immunoassays have revealed that the GM1-epitope can be inaccessible for antibody binding due to a masking effect exerted by neighbouring gangliosides such as GD1a (Complex mediated *cis*-inhibition) (Greenshields, Halstead, Zitman, Rinaldi, Brennan, O'Leary, Chamberlain, Easton, Roxburgh, Pediani, Furukawa, Furukawa, Goodyear, Plomp, & Willison 2009; Nobile-Orazio, Giannotta, & Briani 2010). The most striking conclusion to emerge from the data is that unless the GM1-epitope is topologically available for antibody binding no axonal damage or conduction block would be induced due to a lack of antibody bound complement activation

(Greenshields, Halstead, Zitman, Rinaldi, Brennan, O'Leary, Chamberlain, Easton, Roxburgh, Padiani, Furukawa, Furukawa, Goodyear, Plomp, & Willison 2009).

It can thus be suggested that lipid complexes containing GM1 could be modulators, either enhancing or inhibiting antibody binding, and play a key role in producing different clinical phenotypes within the same neuropathy. For example, the presence of antibodies which exclusively bind lipid complexes formed by GM1, a major ganglioside of axons of both the motor and sensory spinal roots (Gong, Tagawa, Lunn, Laroy, Heffer-Lauc, Li, Griffin, Schnaar, & Sheikh 2002;Kusunoki et al. 1993;O'Hanlon, Paterson, Veitch, Wilson, & Willison 1998) and GalC, a major component of myelin (Garbay et al. 2000), could conceivably indicate a more nodal lesion, the specialised area where this complex is more likely to be found.

If we now turn our attention to the capability of some gangliosides, such as GD1a, to inhibit antibody binding to GM1 in MMN (Cats, Jacobs, Yuki, Tio-Gillen, Piepers, Franssen, van Asseldonk, van den Berg, & van der Pol 2010b;Galban-Horcajo, Fitzpatrick, Hutton, Dunn, Kalna, Brennan, Rinaldi, Yu, Goodyear, & Willison 2013;Nobile-Orazio, Giannotta, & Briani 2010) and IgG monoclonal antibodies (Greenshields, Halstead, Zitman, Rinaldi, Brennan, O'Leary, Chamberlain, Easton, Roxburgh, Padiani, Furukawa, Furukawa, Goodyear, Plomp, & Willison 2009) we might be able to find a possible explanation for what seems an apparent inconsistency between GM1 distribution in PNS and the existence of exclusively motor neuropathies. According to previous reports there are no quantitative differences in the distribution of GD1a between dorsal (containing afferent sensory axons) and ventral (containing efferent motor axons) roots (Svennerholm et al. 1992;Svennerholm, Bostrom, Fredman, Jungbjer, Lekman, Mansson, & Rynmark 1994). However, qualitative differences in GD1a structure, possibly consisting of differences in fatty acid chain length, between motor and sensory nerves have been reported. Two forms of GD1a are expressed in motor nerves as opposed to sensory nerves which just contain one variant of GD1a ganglioside. These results suggest the presence of an alternative form of GD1a strictly expressed in motor nerves (Gong, Tagawa, Lunn, Laroy, Heffer-Lauc, Li, Griffin, Schnaar, & Sheikh 2002). It could be hypothesized then

that in motor nerves the alternative form of GD1a would be unable to *cis*-inhibit antibody binding to GM1 or could form a complex with GM1 which would compete with the conventional inhibitory GM1:GD1a complex, enhancing antibody binding and giving the disease a pure motor phenotype. Another plausible explanation for the appearance of two different forms of GD1a in the previous study is the presence of GalNac-GD1a in peripheral nerves (Ilyas et al. 1988a; Ilyas, Willison, Quarles, Jungalwala, Cornblath, Trapp, Griffin, Griffin, & McKhann 1988b), which would only be expressed by motor neurons and axons (Gong, Tagawa, Lunn, Laroy, Heffer-Laue, Li, Griffin, Schnaar, & Sheikh 2002). Together this data suggests that in motor nerves GalNac-GD1a would not exert an inhibitory effect on antibody binding to GM1 when in complex, and could be targeted by IgM antibodies as a single epitope or in complex with GM1 (Tatsumoto et al. 2006) causing the profile of a pure motor neuropathy whereas GM1:GD1a has a *cis*-inhibitory effect in sensory nerves. Although this theory can be supported in the case of MMN, caution must be applied when considering pure motor forms of GBS (AMAN). In patients suffering AMAN, GM1:GalNac-GD1a lipid complexes have been identified as a main target for high affinity antibodies (Kaida, Sonoo, Ogawa, Kamakura, Ueda-Sada, Arita, Motoyoshi, & Kusunoki 2008). Although this could again indicate the role of complex *cis*-enhancement/inhibition in modulating a disease phenotype, it cannot be forgotten that in GBS GD1a, present in both motor and sensory nerves, has not been reported as inhibiting antibody binding to GM1 when in lipid complex form *in vitro* (Kaida, Morita, Kanzaki, Kamakura, Motoyoshi, Hirakawa, & Kusunoki 2007) although there is some conflicting *in vivo* data (Greenshields, Halstead, Zitman, Rinaldi, Brennan, O'Leary, Chamberlain, Easton, Roxburgh, Pediani, Furukawa, Furukawa, Goodyear, Plomp, & Willison 2009).

6.1.2 Molecular ratios of GalC as modulators of antibody binding to GM1

Chapter 4 has given an account of the high diversity existing among anti-GM1 antibodies in MMN. It has also described how neighbouring lipids can substantially affect antibody binding to GM1 ganglioside. The results of this work contribute to the existing knowledge that the binding of anti-GM1 antibodies can be inhibited by the presence of GD1a and LM1. It also contributes additional

evidence that suggests the key role played by GalC in enhancing antibody binding to GM1 epitopes in a clinical cohort.

Whilst confirming the effect of neighbouring lipids on modulating antibody binding to GM1, this study partially substantiates the idea that molecular ratios between lipid complexes could also be a key factor. These molecular patterns defining GM1 epitopes would potentially form highly specific antibody binding platforms. This newly described antibody behaviour would be capable of unmasking anti-GM1 antibodies in patients previously described as antibody-negative.

Despite its exploratory nature, work with MMN-derived human monoclonal antibodies offers some insight into the inhibitory effect which GM1:GalC driven molecular patterns might have on anti-GM1 antibodies. This apparent paradox, where GM1 antibodies in patient sera see their binding enhanced in the presence of GalC and in contrast MMN-derived monoclonal antibodies are potentially inhibited by GalC molecular patterns, emphasises the diverse and obscure nature of these antibodies.

In studies using rodent and human tissue, binding diversity in vitro translated into differential tissue binding profiles for each of these human monoclonal antibodies (O'Hanlon, Paterson, Wilson, Doyle, McHardie, & Willison 1996; O'Hanlon, Paterson, Veitch, Wilson, & Willison 1998). SM1 and WO1 for example, were the only mAb presenting nodal staining in human teased fibre preparations. When comparing this observation with array studies where SM1 is the only antibody that binds GM1 in the presence of high concentrations of GalC, it could be hypothesised that exclusive binding of SM1 in certain nerve regions could indicate the presence of GalC enriched GM1 domains. Array data on WO1 has not been acquired for this study due to antibody availability. In order to further support this theory, the GM1 binding behaviour of WO1 in the presence of high concentrations of GalC should be tested on array to ascertain if it mimics SM1 behaviour.

Cautious interpretation must be applied when translating concepts from solid-phase assays onto tissue and vice versa. This merely speculative work should be further tested on a definitive in vivo platform. The relevance of GalC as binding

modulator of GM1 could be tested using PC12 cells containing GalC. PC12, a cell line derived from rat adrenal medulla allows easy modification and engineering of its lipid membrane profile (Mutoh et al. 1998). The role played by GD1a on antibody binding could be elucidated by regulating its presence by treating the tissue with sialidases. This family of enzymes hydrolyse terminal sialic acid residues converting GD1a into GM1 (Monti et al. 2010). If our initial hypothesis was correct, and GM1 was found in complex with GalC on a living membrane, the only mAb staining PC12 cells containing GalC would be SM1 and/or WO1. Further studies for confirmation could be done on murine tissue lacking GalC.

6.1.3 Cholesterol as potential modulator of GM1 antibody binding

So far we have hypothesised how GM1:GalC clusters can determine tissue binding of certain mAb but not others. This would potentially determine the distribution of SM1 staining in specific tissue preparations. Although GM1 complexes with GD1a could explain the absence of SM1 binding in certain tissue samples (Greenshields, Halstead, Zitman, Rinaldi, Brennan, O'Leary, Chamberlain, Easton, Roxburgh, Padiani, Furukawa, Furukawa, Goodyear, Plomp, & Willison 2009), it could not explain the binding difference between SM1 and other human mAb (O'Hanlon, Paterson, Wilson, Doyle, McHardie, & Willison 1996; O'Hanlon, Paterson, Veitch, Wilson, & Willison 1998), being as they are all equally inhibited by the presence of GD1a according to array data.

In light of the capability of Cholera Toxin (CT) to inhibit the binding in human tissue of these mABs, they were broadly classified into two groups: CT like (SM1, WO1 and BO3) and CT unlike (BR1, DO1 and BO1) (O'Hanlon, Paterson, Veitch, Wilson, & Willison 1998). As described in chapter 3, the binding of CT to GM1 is affected by the presence of cholesterol enriched domains. These domains would induce a conformational change upon GM1 making it unavailable for CT recognition (Lingwood, Binnington, Rog, Vattulainen, Grzybek, Coskun, Lingwood, & Simons 2011; Mahfoud, Manis, Binnington, Ackerley, & Lingwood 2010). If one assumes cholesterol as the only modulator of GM1-CT binding, the degree of correlation of CT binding with the binding of these human mAb could then suggest the presence of GM1:Cholesterol domains in human tissue. Therefore, mAbs such as SM1 characterised as CT like would be unable to recognise the crooked form of GM1 found in the presence of cholesterol, and by

corollary CT unlike mAbs would mainly bind the GM1 form found within cholesterol clusters.

Although it could offer an alternative explanation for differential tissue binding due to anti-GM1 antibody diversity, the above is merely hypothetical.

Preliminary studies on arrays containing GM1:Cholesterol probed with MMN-derived mAbs would need to be conducted to confirm the validity of this hypothesis on solid-phase platforms. Further investigations using cyclodextrin treated tissue could be performed to confirm the extent of cholesterol involvement in the modulation of Ab binding to GM1.

6.1.4 Standardisation of the GM1:GalC assay

The final goal of a diagnostic marker is to contribute to the definitive clinical diagnosis of a patient. The high variability in results for anti-GM1 Abs has in effect devalued its use as diagnostic test for MMN. Since the first description of anti-GM1 Abs as potential biomarkers for MMN (Pestronk, Cornblath, Ilyas, Baba, Quarles, Griffin, Alderson, & Adams 1988) there have been a huge number of publications reporting different diagnostic potentials for anti-GM1 in MMN. These studies have differed methodologically and conceptually from each other. The techniques vary from ELISA (Carpo, Allaria, Scarlato, & Nobile-Orazio 1999) to dot-blot (Chabraoui, Derrington, Mallie-Didier, Confavreux, Quincy, & Caudie 1993) and most recently to glycoarray (Galban-Horcajo, Fitzpatrick, Hutton, Dunn, Kalna, Brennan, Rinaldi, Yu, Goodyear, & Willison 2013). The controls used within the assays also differ and include ALS (Carpo, Allaria, Scarlato, & Nobile-Orazio 1999), CIDP and Healthy controls (Nobile-Orazio, Giannotta, Musset, Messina, & Leger 2013), undiagnosed neurological disorders and multiple sclerosis (Galban-Horcajo, Fitzpatrick, Hutton, Dunn, Kalna, Brennan, Rinaldi, Yu, Goodyear, & Willison 2013). Over the years, there has been little attempt to methodologically standardise anti-GM1 testing. This has created confusion within clinical practice and has substantially diminished the strength of anti-GM1 Abs as a possible marker for MMN diagnosis. Although there have been attempts to identify patterns among the various studies by the use of metanalysis (van Schaik et al. 1995), no simultaneous inter-laboratory study on assay variability has been attempted.

With GM1:GalC as a recently emerging marker for MMN, and the existence of only three publications to date (Galban-Horcajo, Fitzpatrick, Hutton, Dunn, Kalna, Brennan, Rinaldi, Yu, Goodyear, & Willison 2013;Nobile-Orazio, Giannotta, Musset, Messina, & Leger 2013;Pestronk, Choksi, Blume, & Lopate 1997), the same questions arise once again: What is the inter-laboratory/methodology testing variability, which is the optimal method for testing and therefore what is the real diagnostic value of GM1:GalC antibodies in MMN.

Among the existing studies on GM1:GalC Ab testing, the methodological discrepancies are already significant:

- The use of ELISA (Nobile-Orazio, Giannotta, Musset, Messina, & Leger 2013;Pestronk, Choksi, Blume, & Lopate 1997) and Glycoarray (Galban-Horcajo, Fitzpatrick, Hutton, Dunn, Kalna, Brennan, Rinaldi, Yu, Goodyear, & Willison 2013).
- The solubilisation of the working lipid solutions using methanol (Galban-Horcajo, Fitzpatrick, Hutton, Dunn, Kalna, Brennan, Rinaldi, Yu, Goodyear, & Willison 2013;Pestronk, Choksi, Blume, & Lopate 1997) and ethanol (Nobile-Orazio, Giannotta, Musset, Messina, & Leger 2013).
- Potential solubilisation of the lipid stocks using chloroform:methanol 1:1 (Galban-Horcajo, Fitzpatrick, Hutton, Dunn, Kalna, Brennan, Rinaldi, Yu, Goodyear, & Willison 2013) and 2:1 (Chapter 4, Dutch cohort repeat).
- The use of GM1:GalC at w/w ratios of 1:10 (Nobile-Orazio, Giannotta, Musset, Messina, & Leger 2013;Pestronk, Choksi, Blume, & Lopate 1997) and 1:1 (Galban-Horcajo, Fitzpatrick, Hutton, Dunn, Kalna, Brennan, Rinaldi, Yu, Goodyear, & Willison 2013).
- The use of Cholesterol sulphate as part of the GM1:GalC mix (Pestronk, Choksi, Blume, & Lopate 1997)or GM1:GalC alone (Galban-Horcajo, Fitzpatrick, Hutton, Dunn, Kalna, Brennan, Rinaldi, Yu, Goodyear, & Willison 2013;Nobile-Orazio, Giannotta, Musset, Messina, & Leger 2013).

- Secondary antibody dilutions 1:20000 (Pestronk, Choksi, Blume, & Lopate 1997) and 1:25000 (Galban-Horcajo, Fitzpatrick, Hutton, Dunn, Kalna, Brennan, Rinaldi, Yu, Goodyear, & Willison 2013).

Before the volume of research on GM1:GalC Abs in MMN expands and the overall message on any anti-GM1:GalC predictive value becomes diluted by data inconsistency, an international multi-centre cooperative study would be necessary to standardise and validate this test.

The design of the aforementioned international GM1:GalC predictive value validation study in MMN could consist of:

- International collection of sera samples from MMN patients and controls (including other neurological diseases and healthy controls) and creation of a centralised sera bank. The MMN patients included in the study would have been diagnosed using clinical criteria other than their GM1 Ab reactivity in sera. This cohort of serum samples will then be coded and double-blinded.
- Aliquots from this sera cohort would then be distributed to all the international laboratories collaborating in the study.

The screening of these samples would comply with several requirements:

- All participating laboratories would use ELISA, as it is currently the standard technique for sera screening within a hospital setting.
- The sera dilutions for titration should be standardised and agreed between all participating laboratories prior to commencement of screening.
- Sera screening would be repeated a minimum of three times ($n=3$) to account for the intra-assay variability.

- Lipid samples (e.g. GM1 and GalC) and HRP labelled secondary Ab would be sourced from the same commercial supplier and consist of the same batch, if possible.
- The totality of the data would be analysed by one laboratory designated as the data coordination centre.

These data, originating from the same set of samples, would allow a meta-analysis where the only inter-assay variability would originate from methodological divergences. Identifying these divergences would allow the optimal conditions for GM1:GalC Ab testing to be determined and finally elucidate the real diagnostic value of these Abs in MMN.

6.2 Antibodies to heterotrimeric glycolipid complexes in CIDP

Chapter 5 introduced a new methodology for Ab screening. It combined the concepts of pattern recognition antibodies (Dam and Brewer 2010a; Dam and Brewer 2010b) and heterotrimeric lipid complexes. The results, from initial pilot studies, suggested Phre at a ratio of 1:10 (GSL:Phre w/w) as the ideal adjuvant molecule for Ab-GSL binding enhancement. A first crude analysis of the data proved a significant overall sensitivity improvement for complexes containing Phre (Chapter 5.4.2.1).

ROC analysis ranked GD1b:GT1b:Phre and GD3:GT1b among the top diagnostic markers with an overall sensitivity ranging from 65% to 69% and the specificity from 85% to 87%. The use of both GSL epitopes as a composite disease marker increased the test's sensitivity up to 78% with a marginal specificity decrease. In this case, the addition of two markers strengthened the sensitivity of the assay and indicated the beneficial effect of using multivariable array analysis in CIDP diagnosis.

22% of all the CIDP patients showed an Ab binding enhancement with GM3:Sulph:Phre, 4% of which had complex specific Ab binding. Upon the inclusion of GM3:Sulph:Phre to the overall markers specified above, the test sensitivity was raised to 82.4% with an insignificant decrease in specificity.

60% of the CIDP patients positive for the addition of the three markers yielded mid to high Ab binding intensities (12709-79266 IU), the other 40% rendered low to mid intensities (900-5976 IU).

In conclusion, the introduction of epitope complexity has helped unmask Ab reactivities previously undetected in neuropathy patients. This chapter first describes the diagnostic potential of a novel screening methodology based on a complex lipid landscape as Ab epitope.

6.3 Final remarks

Through the use of glycoarray, previously developed by Rinaldi and co-workers (Rinaldi, Brennan, & Willison 2012), this thesis has explored and extended the concept of complex glycolipid landscapes in the context of neuropathy associated antibodies. Using the well-established concept of anti-glycolipid complex antibodies, where the Ab binding intensity to a single glycolipid element is lower than the binding intensity to a complex of epitopes, we have demonstrated the presence and diagnostic relevance of highly cryptic antibodies in GBS, MMN and CIDP.

Although no inference could be made between clinical phenotype and serological Ab profiling, the decay of Ab titres in convalescent GBS patients would suggest an Ab drive of the disease. In support of this notion several serological studies have associated severe weakness to high titres of anti-GM1 antibodies (Cats et al. 2010a) and the presence of severe disability with anti-GD1b:GT1b antibodies (Kusunoki and Kaida 2011). However, to date there is no direct evidence linking anti-glycolipid complex antibodies and the development of the disease.

The origin and development of these neuropathy associated antibodies is far from clear. Several studies have suggested the role played by viral and bacterial infections in the development of GBS. Infections such as mycoplasma pneumoniae and campylobacter jejuni have been seen to precede cases of GBS (Yuki and Hartung 2012). These infections induce an IgA Ab response against the bacterial lipo-oligosaccharides (LOSs) and due to a phenomenon known as molecular mimicry the Abs target gangliosides, present in nerve, due to their structural similarities with LOSs (Young et al. 2007). Recognition of membrane

structures by self Ab implies that a break in the immune tolerance needs to take place (Bowes et al. 2002). Research to date highlights the interaction of bacterial LOSs with toll like receptors, dendritic cell stimulation and subsequent B cell proliferation as the most plausible mechanism inducing an Ab response targeting sialic acid containing glycolipids (Geleijns et al. 2004;Huizinga et al. 2012;Kuijf et al. 2010).

If we accept post-infectious molecular mimicry as the causal factor for GBS and assume the involvement of complex antibodies in the development of the disease, there has to be an LOS structure mimicking ganglioside complexes. Addressing this paradigm, studies using sera with GM1:GD1a complex Abs were found to bind campylobacter jejuni preparations containing GM1-like and GD1a-like LOSs (Kuijf et al. 2007). This finding suggested the presence of complex oligosaccharide structures mimicking ganglioside complexes, strengthening the notion of GBS as a post-infectious disease. However, it has yet to be demonstrated whether complex ganglioside structures, such as the ones described throughout this thesis, have an equivalent LOS mimic.

This thesis has attempted to replicate a membrane-like environment, in a solid-phase assay, in an endeavour to unmask self-antibodies. To date these complex Ab platforms had only been reproduced by the use of liposomes (Townson, Boffey, Nicholl, Veitch, Bundle, Zhang, Samain, Antoine, Bernardi, Arosio, Sonnino, Isaacs, & Willison 2007). Although liposomes are an efficient approach to generate membrane domains, they prove challenging to work with and extremely time costly. The use of combinatorial arrays, containing complex glycolipid platforms, has most definitely enhanced the exploratory nature of these assays. The relevance of combinatorial glycoarrays has proven important in diseases such as AIDP where self-Ab detection rates have traditionally yielded very low sensitivity. A recent study, using complex epitopes immobilised on a combinatorial array platform, identified antibodies targeting complex glycolipids in more than 60% of AIDP cases (Rinaldi et al. 2013;Rinaldi 2013). These new Ab targets formed by gangliosides and the neutral lipids contained in myelin significantly increased Ab detection.

In an attempt to shed light over the so called “antibody-negative” GBS and MMN cases, this thesis has demonstrated the diagnostic value of Abs to complex

glycolipid epitopes; Thus narrowing the gap between the association of clinical phenotypes and serological screenings. Further technique standardisation studies need to take place to fully understand the clinical application of combinatorial glycoarrays, however, we can now confirm the enormous potential that complex glycolipid platforms have in the context of self-Ab detection.

6.4 In conclusion

This thesis has attempted to explore the extent and relevance of Abs to complex GSL epitopes as diagnostic markers for PNS neuropathies. In the case of MMN, a great proportion of patients have been identified as bearing Abs to the novel target GM1:GalC, although several questions, such as the influence of GalC hydroxylation profile on complex formation and Ab binding, still remain unanswered, combinatorial array research has facilitated a substantial improvement in MMN diagnosis. This diagnostic improvement could eventually lead to a more refined treatment intervention. The ultimate goal of GM1:GalC testing is to become an internationally standardised highly robust diagnostic tool directly influencing treatment decision-making.

Furthermore, the increase in array complexity has permitted identifying two classes of Abs to GSL: pattern recognition Abs and Abs to heterotrimeric lipid complexes. The construction of arrays containing a combined approach of molecular patterns and heterotrimeric epitopes has allowed us to substantially improve CIDP diagnosis. The combination of three different complex biomarkers led to significant Ab detection enhancement.

As part of a larger effort to improve prognosis and treatment course, Abs against complex GSLs have been proven specific markers for differential diagnosis and have pushed forward the notion of PNS neuropathies as Ab driven diseases.

7 Appendices

7.1 Buffers and solutions

PBS 10X

NaCl	80g
KH ₂ PO ₄	2g
Na ₂ HPO ₄ ·12H ₂ O	29g
KCl	2g

Make up to 1000ml with dH₂O.

Dilute 1:10 to use. pH to 7.4.

1% 2% 3% BSA

Add 1g, 2g or 3g bovine serum albumin in 100ml PBS

ELISA detection buffer

14ml 0.1M Citrate (10.507g to 500ml dH₂O)
16ml 0.2M Na₂HPO₄ (14.196g to 500ml dH₂O)
30ml dH₂O
1x OPD tablet (Sigma)
20µl H₂O₂

ELISA stop solution

4M H₂SO₄ (54ml to 500ml dH₂O, perform in hood, add acid slowly to water)

Binding Buffer

A. 0.2M NaH₂PO₄ 2H₂O (31.2g/L), pH 7.0
B. 0.2M Na₂HPO₄ (28.39g/L)

Elution buffer

0.1M glycine-HCl pH 2.7 (3.75g glycine to 500ml dH₂O)
Tris-HCl pH 9.0 (30.285g +250ml dH₂O)

10% RPMI-FBS

500ml RPMI with L-glutamine
100ml / 50ml foetal bovine serum
10ml penicillin / streptomycin solution

7.2 Methodological development

7.2.1 Fluorescent slides development

In order to test the most suitable spray glue to be used for fluorescent staining, two different 3M models were used. Three independent studies were conducted, generating arrays containing a full panel of gangliosides plus secondary antibody control spots. These arrays were probed with an antibody-negative serum from a healthy control and the auto fluorescence of the glue was evaluated after the images were scanned.

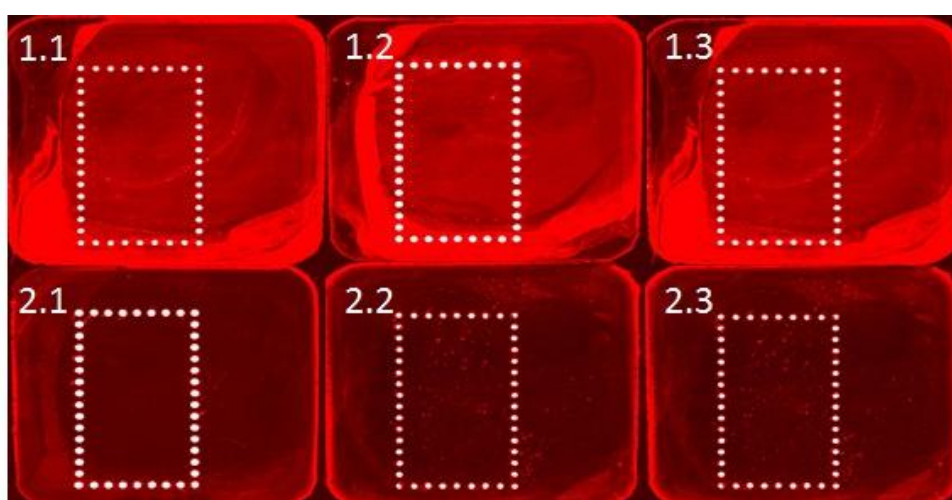


Figure 7.1. Arrays showing the differential auto fluorescent profile of two commercial 3M glues.

Panel 1 represent three independent studies using 3M commercial glue A. Panel 2 represent three independent studies using 3M commercial glue B.

The only methodological difference between the assays presented in panel 1 and panel 2 was the use of different commercial glue. As can be seen in Figure 7.1, 3M commercial glue B presented a cleaner array surface due to the lower auto fluorescence background originating from the glue. The signal to noise ratio of 3M commercial glue B was significantly higher (2-fold) than the ratio resulting from 3M commercial glue A.

7.2.2 Fluorescence-ECL comparison

The detection system employed on a serology study is going to influence to a great extent the interpretation of antibody binding enhancements and cis-inhibitions. In glycoarray, the commonly used ECL detection system (Brennan, Galban-Horcajo, Rinaldi, O'Leary, Goodyear, Kalna, Arthur, Elliot, Barnett,

Linington, Bennett, Owens, & Willison 2011; Galban-Horcajo, Fitzpatrick, Hutton, Dunn, Kalna, Brennan, Rinaldi, Yu, Goodyear, & Willison 2013; Rinaldi, Brennan, Goodyear, O'Leary, Schiavo, Crocker, & Willison 2009) has as limiting factors the capacity of the photographic film to absorb light and the availability of substrate to enable the chemoluminescent reaction. Therefore the plateau of intensity saturation will be reached for reasons other than antibody binding affinity and avidity. In the case of detection by fluorescently labelled secondary antibodies the detection directly depends on reading antibody binding and sensitivity of the fluorescence signal. This detection method offers a greater linear dynamic range of variation on the upper scale of intensity, allowing discriminating between high intensity signals.

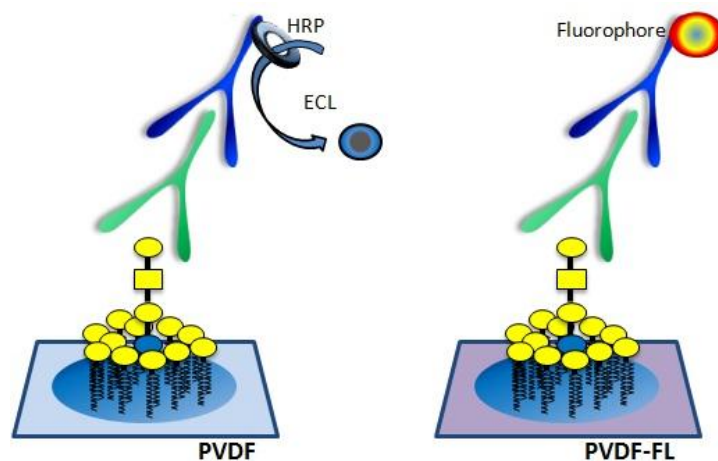


Figure 7.2. Experimental outline of combinatorial arrays using Chemoluminescence or Fluorescence as detection systems.

GA1 ganglioside is attached to the PVDF hydrophobic membrane. Primary antibody recognises the lipid. Secondary antibody HRP labelled or fluorescently labelled will then bound the primary antibody. In the case of fluorescent arrays, the array will be ready to be read after application of secondary antibody. For HRP arrays, slides will need to be incubated with ECL substrate to obtain a chemiluminescent reaction which will develop a radiographic film.

Using inter and intra-assay variability calculations allows to illustrate how fluorescence detection presents a wider range of intensities, translated into a higher coefficient of variation in contrast to ECL detection.

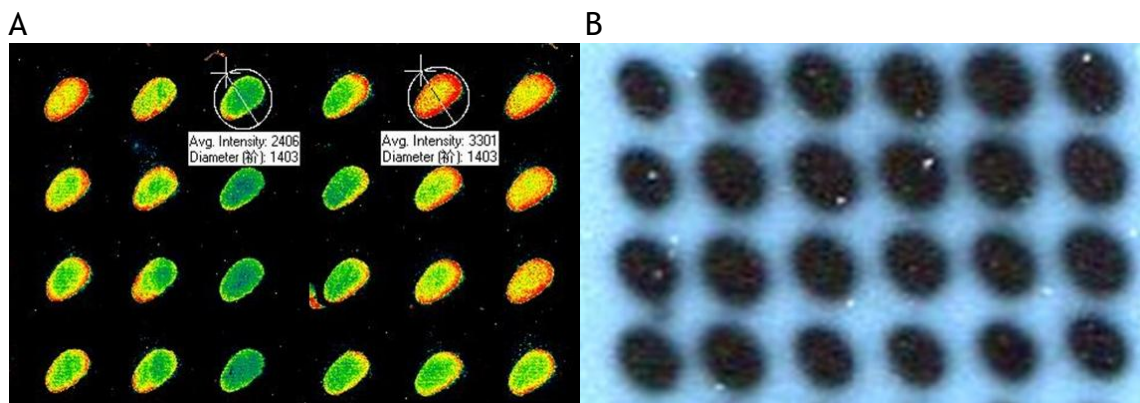


Figure 7.3. Fluorescence and ECL assay variability.

Glycoarrays containing GM1 ganglioside spots probed using the same patient sera of known reactivity. A was probed using Alexa647 labelled anti-Human IgM antibodies and B was probed using HRP labelled anti-Human IgM antibodies detected using ECL.

Table 7.1. Coefficient of variation (CV) for Fluorescence and ECL.

	Fluorescence (AlexaFluor 647)	ECL
Intra-assay variability (%)	14.58	9.54
Inter-assay variability (%)	12.81	9.98

The only difference between the arrays in Figure 7.3 is the detection method employed; therefore the differences in assay variability between both arrays are due to the nature of the probe. As seen in Table 7.1, fluorescently labelled antibodies as detection probes present a significantly higher intra and inter-assay variability. This difference comes to illustrate the wider spectrum of detection in the upper limit of the intensity scale presented by fluorescent probes in contrast to ECL dependent probes.

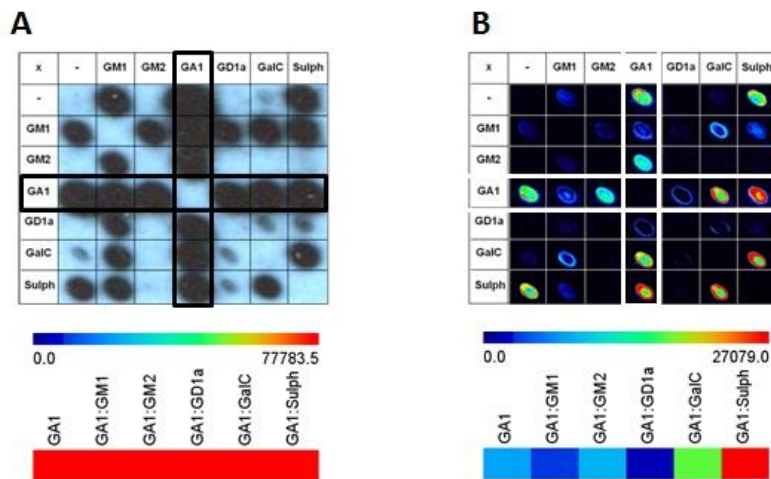


Figure 7.4 Detection methods employed in combinatorial glycoarrays.

Secondary antibodies conjugated to either HRP, which catalyses the 'ECL plus' reaction, or fluorophore have both been employed to visualise antibody binding on combinatorial glycoarrays. In this example binding of the same N-Ab containing sera was quantitatively compared using either detection method. Heatmaps are scaled to the highest intensity value of an individual spot in any one array. Panel A ECL autoradiography is a very sensitive detection system; however it has a narrow linear dynamic range and thus does not easily facilitate comparative analysis, as demonstrated here by the saturation of intensity measurements of GA1 and its complexes (black boxes). Panel B. Fluorophore-labelled secondary antibodies for N-Ab detection accommodate multiplexed analysis (different antibody classes and subclasses can be assessed in a single assay), resulting in increased experimental throughput, with improved linearity during quantitative analysis. This is demonstrated here by the range of intensity measurements of GA1 and its complexes (white boxes).

7.3 Publications

Antibodies to GM1: galactocerebroside complexes in multifocal motor neuropathy: it takes two to tango.

Willison HJ, Galban-Horcajo F, Halstead SK.

Institute of Infection, Immunity and Inflammation, College of Medical, Veterinary and Life Sciences, University of Glasgow, Glasgow, UK.

J Neurol Neurosurg Psychiatry. 2013 Sep 4. [Epub ahead of print]

Anti-GM2 ganglioside antibodies are a biomarker for acute canine polyradiculoneuritis.

Rupp A, Galban-Horcajo F, Bianchi E, Dondi M, Penderis J, Cappell J, Burgess K, Matiasek K, McGonigal R, Willison HJ.

Neuroimmunology Group, Institute of Infection, Immunity and Inflammation, College of Medical, Veterinary and Life Sciences, University of Glasgow, Glasgow, UK.

J Peripher Nerv Syst. 2013 Mar;18(1):75-88.

Antibodies to heteromeric glycolipid complexes in multifocal motor neuropathy.

Galban-Horcajo E, Fitzpatrick AM, Hutton AJ, Dunn SM, Kalna G, Brennan KM, Rinaldi S, Yu RK, Goodyear CS, Willison HJ.

Glasgow Biomedical Research Centre, College of Medical, Veterinary and Life Science, Institute of Infection, Immunity and Inflammation, University of Glasgow, Glasgow, UK.

Eur J Neurol. 2013 Jan; 20(1):62-70.

Lipid arrays identify myelin-derived lipids and lipid complexes as prominent targets for oligoclonal band antibodies in multiple sclerosis.

Brennan KM, Galban-Horcajo E, Rinaldi S, O'Leary CP, Goodyear CS, Kalna G, Arthur A, Elliot C, Barnett S, Linington C, Bennett JL, Owens GP, Willison HJ.

Institute of Infection, Immunity and Inflammation, College of Medical, Veterinary and Life Sciences, Glasgow Biomedical Research Centre, University of Glasgow, Glasgow, G12 8TA, UK.

J Neuroimmunol. 2011 Sep 15; 238(1-2):87-95.

Bibliography

- Adams, D., Kuntzer, T., Burger, D., Chofflon, M., Magistris, M.R., Regli, F., & Steck, A.J. 1991. Predictive value of anti-GM1 ganglioside antibodies in neuromuscular diseases: a study of 180 sera. *J.Neuroimmunol.*, 32, (3) 223-230 available from: PM:2033117
- Alaedini, A. & Latov, N. 2000. Detection of anti-GM1 ganglioside antibodies in patients with neuropathy by a novel latex agglutination assay. *J.Immunoassay*, 21, (4) 377-386 available from: PM:11071254
- Alaedini, A. & Latov, N. 2001. A surface plasmon resonance biosensor assay for measurement of anti-GM(1) antibodies in neuropathy. *Neurology*, 56, (7) 855-860 available from: PM:11294921
- Alving, C.R. & Richards, R.L. 1977a. Immune reactivities of antibodies against glycolipids--I. Properties of anti-galactocerebroside antibodies purified by a novel technique of affinity binding to liposomes. *Immunochemistry.*, 14, (5) 373-381 available from: PM:598864
- Alving, C.R. & Richards, R.L. 1977b. Immune reactivities of antibodies against glycolipids--II. Comparative properties, using liposomes, of purified antibodies against mono-, di- and trihexosyl ceramide haptens. *Immunochemistry.*, 14, (5) 383-389 available from: PM:598865
- Ang, C.W., Jacobs, B.C., & Laman, J.D. 2004. The Guillain-Barre syndrome: a true case of molecular mimicry. *Trends Immunol.*, 25, (2) 61-66 available from: PM:15102364
- Aranzamendi, C., Tefsen, B., Jansen, M., Chiumiento, L., Bruschi, F., Kortbeek, T., Smith, D.F., Cummings, R.D., Pinelli, E., & van Die, I. 2011. Glycan microarray profiling of parasite infection sera identifies the LDNF glycan as a potential antigen for serodiagnosis of trichinellosis. *Experimental Parasitology*, 129, (3) 221-226 available from: <http://www.sciencedirect.com/science/article/pii/S0014489411002669>
- Baumann, N., Harpin, M.L., Marie, Y., Lemerle, K., Chassande, B., Bouche, P., Meininger, V., Yu, R.K., & Leger, J.M. 1998. Antiglycolipid antibodies in motor neuropathies. *Ann.N.Y.Acad.Sci.*, 845, 322-329 available from: PM:9668365
- Bech, E., Jakobsen, J., & Orntoft, T.F. 1994. ELISA-type titertray assay of IgM anti-GM1 autoantibodies. *Clin.Chem.*, 40, (7 Pt 1) 1331-1334 available from: PM:8013109
- Bittman, R., Kasireddy, C.R., Mattjus, P., & Slotte, J.P. 1994. Interaction of cholesterol with sphingomyelin in monolayers and vesicles. *Biochemistry*, 33, (39) 11776-11781 available from: PM:7918394
- Bjorkbom, A., Ramstedt, B., & Slotte, J.P. 2007. Phosphatidylcholine and sphingomyelin containing an elaidoyl fatty acid can form cholesterol-rich lateral domains in bilayer membranes. *Biochim.Biophys.Acta*, 1768, (7) 1839-1847 available from: PM:17499576

- Bjorkbom, A., Rog, T., Kaszuba, K., Kurita, M., Yamaguchi, S., Lonnfors, M., Nyholm, T.K., Vattulainen, I., Katsumura, S., & Slotte, J.P. 2010. Effect of sphingomyelin headgroup size on molecular properties and interactions with cholesterol. *Biophys.J.*, 99, (10) 3300-3308 available from: PM:21081078
- Bloom, M., Evans, E., & Mouritsen, O.G. 1991. Physical properties of the fluid lipid-bilayer component of cell membranes: a perspective. *Q.Rev.Biophys.*, 24, (3) 293-397 available from: PM:1749824
- Bowes, T., Wagner, E.R., Boffey, J., Nicholl, D., Cochrane, L., Benboubetra, M., Conner, J., Furukawa, K., Furukawa, K., & Willison, H.J. 2002. Tolerance to self gangliosides is the major factor restricting the antibody response to lipopolysaccharide core oligosaccharides in *Campylobacter jejuni* strains associated with Guillain-Barre syndrome. *Infect.Immun.*, 70, (9) 5008-5018 available from: PM:12183547
- Brennan, K.M., Galban-Horcajo, F., Rinaldi, S., O'Leary, C.P., Goodyear, C.S., Kalna, G., Arthur, A., Elliot, C., Barnett, S., Linington, C., Bennett, J.L., Owens, G.P., & Willison, H.J. 2011. Lipid arrays identify myelin-derived lipids and lipid complexes as prominent targets for oligoclonal band antibodies in multiple sclerosis. *J.Neuroimmunol.*, 238, (1-2) 87-95 available from: PM:21872346
- Carlson, R.O., Masco, D., Brooker, G., & Spiegel, S. 1994. Endogenous ganglioside GM1 modulates L-type calcium channel activity in N18 neuroblastoma cells. *J.Neurosci*, 14, (4) 2272-2281 available from: PM:7512636
- Carpo, M., Allaria, S., Scarlato, G., & Nobile-Orazio, E. 1999. Marginally improved detection of GM1 antibodies by Covalink ELISA in multifocal motor neuropathy. *Neurology*, 53, (9) 2206-2207 available from: PM:10599811
- Cats, E.A., Jacobs, B.C., Yuki, N., Tio-Gillen, A.P., Piepers, S., Franssen, H., van Asseldonk, J.T., van den Berg, L.H., & van der Pol, W.L. 2010a. Multifocal motor neuropathy Association of anti-GM1 IgM antibodies with clinical features. *Neurology*, 75, (22) 1961-1967 available from: ISI:000284685800008
- Cats, E.A., Jacobs, B.C., Yuki, N., Tio-Gillen, A.P., Piepers, S., Franssen, H., van Asseldonk, J.T., van den Berg, L.H., & van der Pol, W.L. 2010b. Multifocal motor neuropathy: association of anti-GM1 IgM antibodies with clinical features. *Neurology*, 75, (22) 1961-1967 available from: PM:20962291
- Chabraoui, F., Derrington, E.A., Mallie-Didier, F., Confavreux, C., Quincy, C., & Caudie, C. 1993. Dot-blot immunodetection of antibodies against GM1 and other gangliosides on PVDF-P membranes. *J.Immunol.Methods*, 165, (2) 225-230 available from: PM:8228272
- Chad, D.A., Hammer, K., & Sargent, J. 1986. Slow resolution of multifocal weakness and fasciculation: a reversible motor neuron syndrome. *Neurology*, 36, (9) 1260-1263 available from: PM:3748396
- Chaudhry, V. 1998. Multifocal motor neuropathy. *Semin.Neurol.*, 18, (1) 73-81 available from: PM:9562669
- Chiba, A., Kusunoki, S., Obata, H., Machinami, R., & Kanazawa, I. 1993. Serum anti-GQ1b IgG antibody is associated with ophthalmoplegia in Miller Fisher

syndrome and Guillain-Barre syndrome: clinical and immunohistochemical studies. *Neurology*, 43, (10) 1911-1917 available from: PM:8413947

Chiba, A., Kusunoki, S., Obata, H., Machinami, R., & Kanazawa, I. 1997. Ganglioside composition of the human cranial nerves, with special reference to pathophysiology of Miller Fisher syndrome. *Brain Res.*, 745, (1-2) 32-36 available from: PM:9037391

Coffin, J.M., Hughes, S.H., & Varmus, H.E. 1997. The Interactions of Retroviruses and their Hosts. available from: PM:21433350

Dam, T.K. & Brewer, C.F. 2010a. Lectins as pattern recognition molecules: the effects of epitope density in innate immunity. *Glycobiology*, 20, (3) 270-279 available from: PM:19939826

Dam, T.K. & Brewer, C.F. 2010b. Maintenance of cell surface glycan density by lectin-glycan interactions: a homeostatic and innate immune regulatory mechanism. *Glycobiology*, 20, (9) 1061-1064 available from: PM:20548106

de Geus, E.D., Tefsen, B., van Haarlem, D.A., van Eden, W., van Die, I., & Vervelde, L. 2013. Glycans from avian influenza virus are recognized by chicken dendritic cells and are targets for the humoral immune response in chicken. *Molecular Immunology*, 56, (4) 452-462 available from: <http://www.sciencedirect.com/science/article/pii/S0161589013004264>

Degroote, S., Wolthoorn, J., & van, M.G. 2004. The cell biology of glycosphingolipids. *Semin.Cell Dev.Biol.*, 15, (4) 375-387 available from: PM:15207828

Di, S.C., Troadec, J.D., Lelievre, C., Garmy, N., Fantini, J., & Chahinian, H. 2013. Mechanism of cholesterol-assisted oligomeric channel formation by a short Alzheimer beta-amyloid peptide. *J.Neurochem.* available from: PM:23919567

Dick, K.J., Eckhardt, M., Paisan-Ruiz, C., Alshehhi, A.A., Proukakis, C., Sibtain, N.A., Maier, H., Sharifi, R., Patton, M.A., Bashir, W., Koul, R., Raeburn, S., Gieselmann, V., Houlden, H., & Crosby, A.H. 2010. Mutation of FA2H underlies a complicated form of hereditary spastic paraplegia (SPG35). *Hum.Mutat.*, 31, (4) E1251-E1260 available from: PM:20104589

Disney, M.D. & Seeberger, P.H. 2004. Carbohydrate arrays as tools for the glycomics revolution. *Drug Discovery Today: TARGETS*, 3, (4) 151-158 available from: <http://www.sciencedirect.com/science/article/pii/S1741837204024430>

Dobrowsky, R.T. 2000. Sphingolipid signalling domains floating on rafts or buried in caves? *Cell Signal.*, 12, (2) 81-90 available from: PM:10679576

Dobrowsky, R.T. & Gazula, V.R. 2000. Analysis of sphingomyelin hydrolysis in caveolar membranes. *Methods Enzymol.*, 311, 184-193 available from: PM:10563324

Dyck, P.J., Daube, J., O'Brien, P., Pineda, A., Low, P.A., Windebank, A.J., & Swanson, C. 1986. Plasma exchange in chronic inflammatory demyelinating polyradiculoneuropathy. *N.Engl.J.Med.*, 314, (8) 461-465 available from: PM:3511382

- Eckhardt, M., Yaghoofam, A., Fewou, S.N., Zoller, I., & Gieselmann, V. 2005. A mammalian fatty acid hydroxylase responsible for the formation of alpha-hydroxylated galactosylceramide in myelin. *Biochem.J.*, 388, (Pt 1) 245-254 available from: PM:15658937
- Fantini, J. 2003. How sphingolipids bind and shape proteins: molecular basis of lipid-protein interactions in lipid shells, rafts and related biomembrane domains. *Cell Mol.Life Sci.*, 60, (6) 1027-1032 available from: PM:12866532
- Fantini, J. & Barrantes, F.J. 2009. Sphingolipid/cholesterol regulation of neurotransmitter receptor conformation and function. *Biochim.Biophys.Acta*, 1788, (11) 2345-2361 available from: PM:19733149
- Fantini, J., Maresca, M., Hammache, D., Yahi, N., & Delezay, O. 2000. Glycosphingolipid (GSL) microdomains as attachment platforms for host pathogens and their toxins on intestinal epithelial cells: activation of signal transduction pathways and perturbations of intestinal absorption and secretion. *Glycoconjugate Journal*, 17, (3 -4) 173-179 available from: PM:11201788
- Fantini, J. & Yahi, N. 2010. Molecular insights into amyloid regulation by membrane cholesterol and sphingolipids: common mechanisms in neurodegenerative diseases. *Expert.Rev.Mol.Med.*, 12, e27 available from: PM:20807455
- Fantini, J. & Yahi, N. 2013. The driving force of alpha-synuclein insertion and amyloid channel formation in the plasma membrane of neural cells: key role of ganglioside- and cholesterol-binding domains. *Adv.Exp.Med.Biol.*, 991, 15-26 available from: PM:23775688
- Fantini, J., Yahi, N., & Garmy, N. 2013a. Cholesterol accelerates the binding of Alzheimer's beta-amyloid peptide to ganglioside GM1 through a universal hydrogen-bond-dependent sterol tuning of glycolipid conformation. *Front Physiol*, 4, 120 available from: PM:23772214
- Fantini, J., Yahi, N., & Garmy, N. 2013b. Cholesterol accelerates the binding of Alzheimer's beta-amyloid peptide to ganglioside GM1 through a universal hydrogen-bond-dependent sterol tuning of glycolipid conformation. *Frontiers in Physiology*, 4, available from: http://www.frontiersin.org/Journal/Abstract.aspx?s=664&name=membrane_physiology_and_biophysics&ART_DOI=10.3389/fphys.2013.00120
- Fastenberg, M.E., Shogomori, H., Xu, X., Brown, D.A., & London, E. 2003. Exclusion of a transmembrane-type peptide from ordered-lipid domains (rafts) detected by fluorescence quenching: extension of quenching analysis to account for the effects of domain size and domain boundaries. *Biochemistry*, 42, (42) 12376-12390 available from: PM:14567699
- Finean, J.B. 1954a. The effects of osmium tetroxide fixation on the structure of myelin in sciatic nerve. *Exp.Cell Res.*, 6, (2) 283-292 available from: PM:13173481
- Finean, J.B. 1954b. X-ray diffraction and electron microscope studies on the brain lipid strandin. *Arch.Biochem.Biophys.*, 52, (1) 38-47 available from: PM:13198236

Fishman, P.H. & Atikkan, E.E. 1980. Mechanism of action of cholera toxin: effect of receptor density and multivalent binding on activation of adenylate cyclase. *J.Membr.Biol.*, 54, (1) 51-60 available from: PM:6259358

Fishman, P.H., Pacuszka, T., Hom, B., & Moss, J. 1980. Modification of ganglioside GM1. Effect of lipid moiety on cholera toxin action. *J.Biol.Chem.*, 255, (16) 7657-7664 available from: PM:7400139

Fitzpatrick, A.M., Mann, C.A., Barry, S., Brennan, K., Overell, J.R., & Willison, H.J. 2011. An open label clinical trial of complement inhibition in multifocal motor neuropathy. *J.Peripher.Nerv.Syst.*, 16, (2) 84-91 available from: PM:21692905

Freddo, L., Yu, R.K., Latov, N., Donofrio, P.D., Hays, A.P., Greenberg, H.S., Albers, J.W., Alessi, A.G., & Keren, D. 1986. Gangliosides GM1 and GD1b are antigens for IgM M-protein in a patient with motor neuron disease. *Neurology*, 36, (4) 454-458 available from: PM:3960319

Fredman, P., Vedeler, C.A., Nyland, H., Aarli, J.A., & Svennerholm, L. 1991. Antibodies in sera from patients with inflammatory demyelinating polyradiculoneuropathy react with ganglioside LM1 and sulphatide of peripheral nerve myelin. *J.Neurol.*, 238, (2) 75-79 available from: PM:1856740

Galban-Horcajo, F., Fitzpatrick, A.M., Hutton, A.J., Dunn, S.M., Kalna, G., Brennan, K.M., Rinaldi, S., Yu, R.K., Goodyear, C.S., & Willison, H.J. 2013. Antibodies to heteromeric glycolipid complexes in multifocal motor neuropathy. *Eur.J.Neurol.*, 20, (1) 62-70 available from: PM:22727042

Garbay, B., Heape, A.M., Sargueil, F., & Cassagne, C. 2000. Myelin synthesis in the peripheral nervous system. *Prog.Neurobiol.*, 61, (3) 267-304 available from: PM:10727776

Geleijns, K., Jacobs, B.C., Van, R.W., Tio-Gillen, A.P., Laman, J.D., & van Doorn, P.A. 2004. Functional polymorphisms in LPS receptors CD14 and TLR4 are not associated with disease susceptibility or *Campylobacter jejuni* infection in Guillain-Barre patients. *J.Neuroimmunol.*, 150, (1-2) 132-138 available from: PM:15081257

Gieselmann, V., Matzner, U., Klein, D., Mansson, J.E., D'Hooge, R., DeDeyn, P.D., Lullmann, R.R., Hartmann, D., & Harzer, K. 2003. Gene therapy: prospects for glycolipid storage diseases. *Philos.Trans.R.Soc.Lond B Biol.Sci.*, 358, (1433) 921-925 available from: PM:12803926

Godula, K. & Bertozzi, C.R. 2012. Density Variant Glycan Microarray for Evaluating Cross-Linking of Mucin-like Glycoconjugates by Lectins. *Journal of the American Chemical Society*, 134, (38) 15732-15742 available from: <http://dx.doi.org/10.1021/ja302193u>

Gong, Y., Tagawa, Y., Lunn, M.P., Laroy, W., Heffer-Lauc, M., Li, C.Y., Griffin, J.W., Schnaar, R.L., & Sheikh, K.A. 2002. Localization of major gangliosides in the PNS: implications for immune neuropathies. *Brain*, 125, (Pt 11) 2491-2506 available from: PM:12390975

- Greenshields, K.N., Halstead, S.K., Zitman, F.M., Rinaldi, S., Brennan, K.M., O'Leary, C., Chamberlain, L.H., Easton, A., Roxburgh, J., Padiani, J., Furukawa, K., Furukawa, K., Goodyear, C.S., Plomp, J.J., & Willison, H.J. 2009. The neuropathic potential of anti-GM1 autoantibodies is regulated by the local glycolipid environment in mice. *J.Clin.Invest*, 119, (3) 595-610 available from: PM:19221437
- Habjanec, L., Frkanec, R., Halassy, B., & Tomasic, J. 2006. Effect of liposomal formulations and immunostimulating peptidoglycan monomer (PGM) on the immune reaction to ovalbumin in mice. *J.Liposome Res.*, 16, (1) 1-16 available from: PM:16556546
- Hadden, R.D. & Hughes, R.A. 1998. Guillain-Barre syndrome: recent advances. *Hosp.Med.*, 59, (1) 55-60 available from: PM:9798567
- Hakomori, S. & Igarashi, Y. 1995. Functional role of glycosphingolipids in cell recognition and signaling. *J.Biochem.*, 118, (6) 1091-1103 available from: PM:8720120
- Hall, A., Rog, T., Karttunen, M., & Vattulainen, I. 2010. Role of glycolipids in lipid rafts: a view through atomistic molecular dynamics simulations with galactosylceramide. *J.Phys.Chem.B*, 114, (23) 7797-7807 available from: PM:20496924
- Halstead, S.K., O'Hanlon, G.M., Humphreys, P.D., Morrison, D.B., Morgan, B.P., Todd, A.J., Plomp, J.J., & Willison, H.J. 2004. Anti-disialoside antibodies kill perisynaptic Schwann cells and damage motor nerve terminals via membrane attack complex in a murine model of neuropathy. *Brain*, 127, (Pt 9) 2109-2123 available from: PM:15289269
- Hama, H. 2010. Fatty acid 2-Hydroxylation in mammalian sphingolipid biology. *Biochim.Biophys.Acta*, 1801, (4) 405-414 available from: PM:20026285
- Hammache, D., Pieroni, G., Yahy, N., Delezay, O., Koch, N., Lafont, H., Tamalet, C., & Fantini, J. 1998. Specific interaction of HIV-1 and HIV-2 surface envelope glycoproteins with monolayers of galactosylceramide and ganglioside GM3. *J.Biol.Chem.*, 273, (14) 7967-7971 available from: PM:9525894
- Harris, L.G., Schofield, W.C.E., Doores, K.J., Davis, B.G., & Badyal, J.P.S. 2009. Rewritable Glycochips. *Journal of the American Chemical Society*, 131, (22) 7755-7761 available from: <http://dx.doi.org/10.1021/ja901294r>
- Holtta-Vuori, M., Uronen, R.L., Repakova, J., Salonen, E., Vattulainen, I., Panula, P., Li, Z., Bittman, R., & Ikonen, E. 2008. BODIPY-cholesterol: a new tool to visualize sterol trafficking in living cells and organisms. *Traffic.*, 9, (11) 1839-1849 available from: PM:18647169
- Hughes, R.A., Allen, D., Makowska, A., & Gregson, N.A. 2006. Pathogenesis of chronic inflammatory demyelinating polyradiculoneuropathy. *J.Peripher.Nerv.Syst.*, 11, (1) 30-46 available from: PM:16519780
- Hughes, R.A., Gray, I.A., Gregson, N.A., Kadlubowski, M., Kennedy, M., Leibowitz, S., & Thompson, H. 1984. Immune responses to myelin antigens in

Guillain-Barre syndrome. *J.Neuroimmunol.*, 6, (5) 303-312 available from: PM:6746894

Huizinga, R., Easton, A.S., Donachie, A.M., Guthrie, J., Van, R.W., Heikema, A., Boon, L., Samsom, J.N., Jacobs, B.C., Willison, H.J., & Goodyear, C.S. 2012. Sialylation of *Campylobacter jejuni* lipo-oligosaccharides: impact on phagocytosis and cytokine production in mice. *PLoS.One.*, 7, (3) e34416 available from: PM:22470569

Ilyas, A.A., Li, S.C., Chou, D.K., Li, Y.T., Jungalwala, F.B., Dalakas, M.C., & Quarles, R.H. 1988a. Gangliosides GM2, IV4GalNAcGM1b, and IV4GalNAcGC1a as antigens for monoclonal immunoglobulin M in neuropathy associated with gammopathy. *J.Biol.Chem.*, 263, (9) 4369-4373 available from: PM:2450092

Ilyas, A.A., Mithen, F.A., Dalakas, M.C., Chen, Z.W., & Cook, S.D. 1992. Antibodies to acidic glycolipids in Guillain-Barre syndrome and chronic inflammatory demyelinating polyneuropathy. *J.Neurol.Sci.*, 107, (1) 111-121 available from: PM:1578228

Ilyas, A.A., Willison, H.J., Quarles, R.H., Jungalwala, F.B., Cornblath, D.R., Trapp, B.D., Griffin, D.E., Griffin, J.W., & McKhann, G.M. 1988b. Serum antibodies to gangliosides in Guillain-Barre syndrome. *Annals of Neurology*, 23, (5) 440-447 available from: PM:3133978

Jones, C.M. & Athanasiou, T. 2005. Summary receiver operating characteristic curve analysis techniques in the evaluation of diagnostic tests. *Ann.Thorac.Surg.*, 79, (1) 16-20 available from: PM:15620907

Kaida, K. & Kusunoki, S. 2010. Antibodies to gangliosides and ganglioside complexes in Guillain-Barre syndrome and Fisher syndrome: mini-review. *J.Neuroimmunol.*, 223, (1-2) 5-12 available from: PM:20172612

Kaida, K. & Kusunoki, S. 2013. [Immune-mediated neuropathy and anti-glycolipid antibodies]. *Brain Nerve*, 65, (4) 413-423 available from: PM:23568989

Kaida, K., Morita, D., Kanzaki, M., Kamakura, K., Motoyoshi, K., Hirakawa, M., & Kusunoki, S. 2004. Ganglioside complexes as new target antigens in Guillain-Barre syndrome. *Annals of Neurology*, 56, (4) 567-571 available from: PM:15389898

Kaida, K., Morita, D., Kanzaki, M., Kamakura, K., Motoyoshi, K., Hirakawa, M., & Kusunoki, S. 2007. Anti-ganglioside complex antibodies associated with severe disability in GBS. *J.Neuroimmunol.*, 182, (1-2) 212-218 available from: PM:17113161

Kaida, K., Sonoo, M., Ogawa, G., Kamakura, K., Ueda-Sada, M., Arita, M., Motoyoshi, K., & Kusunoki, S. 2008. GM1/GalNAc-GD1a complex: a target for pure motor Guillain-Barre syndrome. *Neurology*, 71, (21) 1683-1690 available from: PM:19015484

Kanter, J.L., Narayana, S., Ho, P.P., Catz, I., Warren, K.G., Sobel, R.A., Steinman, L., & Robinson, W.H. 2006. Lipid microarrays identify key mediators of autoimmune brain inflammation. *Nature Medicine*, 12, (1) 138-143 available from: ISI:000234419000064

- Kaufmann, S., Sobek, J., Textor, M., & Reimhult, E. 2011. Supported lipid bilayer microarrays created by non-contact printing. *Lab on a Chip*, 11, (14) 2403-2410 available from: <http://dx.doi.org/10.1039/C1LC20073A>
- Kenworthy, A.K. & Edidin, M. 1998. Distribution of a glycosylphosphatidylinositol-anchored protein at the apical surface of MDCK cells examined at a resolution of <100 Å using imaging fluorescence resonance energy transfer. *J.Cell Biol.*, 142, (1) 69-84 available from: PM:9660864
- Kinsella, L.J., Lange, D.J., Trojaborg, W., Sadiq, S.A., Younger, D.S., & Latov, N. 1994. Clinical and electrophysiologic correlates of elevated anti-GM1 antibody titers. *Neurology*, 44, (7) 1278-1282 available from: PM:8035930
- Klenk, E. 1970. On the discovery and chemistry of neuraminic acid and gangliosides. *Chem.Phys.Lipids*, 5, (1) 193-197 available from: PM:4920302
- Koga, M., Yuki, N., Hirata, K., Morimatsu, M., Mori, M., & Kuwabara, S. 2003. Anti-GM1 antibody IgG subclass: a clinical recovery predictor in Guillain-Barre syndrome. *Neurology*, 60, (9) 1514-1518 available from: PM:12743241
- Kornberg, A.J. & Pestronk, A. 1994. The clinical and diagnostic role of anti-GM1 antibody testing. *Muscle Nerve*, 17, (1) 100-104 available from: PM:8264687
- Koumanov, K.S., Momchilova, A.B., Quinn, P.J., & Wolf, C. 2002. Ceramides increase the activity of the secretory phospholipase A2 and alter its fatty acid specificity. *Biochem.J.*, 363, (Pt 1) 45-51 available from: PM:11903045
- Kuijf, M.L., Godschalk, P.C., Gilbert, M., Endtz, H.P., Tio-Gillen, A.P., Ang, C.W., van Doorn, P.A., & Jacobs, B.C. 2007. Origin of ganglioside complex antibodies in Guillain-Barre syndrome. *J.Neuroimmunol.*, 188, (1-2) 69-73 available from: PM:17604126
- Kuijf, M.L., Samsom, J.N., Van, R.W., Bax, M., Huizinga, R., Heikema, A.P., van Doorn, P.A., van, B.A., van, K.Y., Burgers, P.C., Luijck, T.M., Endtz, H.P., Nieuwenhuis, E.E., & Jacobs, B.C. 2010. TLR4-mediated sensing of *Campylobacter jejuni* by dendritic cells is determined by sialylation. *J.Immunol.*, 185, (1) 748-755 available from: PM:20525894
- Kusunoki, S., Chiba, A., Tai, T., & Kanazawa, I. 1993. Localization of GM1 and GD1b antigens in the human peripheral nervous system. *Muscle Nerve*, 16, (7) 752-756 available from: PM:7685064
- Kusunoki, S., Hitoshi, S., Kaida, K., Arita, M., & Kanazawa, I. 1999. Monospecific anti-GD1b IgG is required to induce rabbit ataxic neuropathy. *Annals of Neurology*, 45, (3) 400-403 available from: PM:10072058
- Kusunoki, S. & Kaida, K. 2011. Antibodies against ganglioside complexes in Guillain-Barre syndrome and related disorders. *J.Neurochem.*, 116, (5) 828-832 available from: PM:21214559
- Kusunoki, S., Kaida, K., & Ueda, M. 2008. Antibodies against gangliosides and ganglioside complexes in Guillain-Barre syndrome: new aspects of research. *Biochim.Biophys.Acta*, 1780, (3) 441-444 available from: PM:17976386

- Kusunoki, S., Kaida, K.I., & Ueda, M. 2007. Antibodies against gangliosides and ganglioside complexes in Guillain-Barre syndrome: New aspects of research. *Biochim.Biophys.Acta* available from: PM:17976386
- Kuwabara, S., Asahina, M., Koga, M., Mori, M., Yuki, N., & Hattori, T. 1998a. Two patterns of clinical recovery in Guillain-Barre syndrome with IgG anti-GM1 antibody. *Neurology*, 51, (6) 1656-1660 available from: PM:9855518
- Kuwabara, S., Yuki, N., Koga, M., Hattori, T., Matsuura, D., Miyake, M., & Noda, M. 1998b. IgG anti-GM1 antibody is associated with reversible conduction failure and axonal degeneration in Guillain-Barre syndrome. *Annals of Neurology*, 44, (2) 202-208
- Lardone, R.D., Yuki, N., Odaka, M., Daniotti, J.L., Irazoqui, F.J., & Nores, G.A. 2010. Anti-GM1 IgG antibodies in Guillain-Barre syndrome: fine specificity is associated with disease severity. *J.Neurol.Neurosurg.Psychiatry*, 81, (6) 629-633 available from: PM:19965859
- Latov, N., Hays, A.P., Donofrio, P.D., Liao, J., Ito, H., McGinnis, S., Konstadoulakis, M., Freddo, L., Shy, M.E., & . 1988. Monoclonal IgM with unique specificity to gangliosides GM1 and GD1b and to lacto-N-tetraose associated with human motor neuron disease. *Neurology*, 38, (5) 763-768 available from: PM:2452383
- Li, F. & Pestronk, A. 1991. Autoantibodies to GM1 ganglioside: different reactivity to GM1-liposomes in amyotrophic lateral sclerosis and lower motor neuron disorders. *J.Neurol.Sci.*, 104, (2) 209-214 available from: PM:1940974
- Lingwood, C.A. 1996. Aglycone modulation of glycolipid receptor function. *Glycoconjugate Journal*, 13, (4) 495-503 available from: PM:8872104
- Lingwood, D., Binnington, B., Rog, T., Vattulainen, I., Grzybek, M., Coskun, U., Lingwood, C.A., & Simons, K. 2011. Cholesterol modulates glycolipid conformation and receptor activity. *Nat.Chem.Biol.*, 7, (5) 260-262 available from: PM:21460830
- Lloyd, K.O., Gordon, C.M., Thampoe, I.J., & DiBenedetto, C. 1992. Cell surface accessibility of individual gangliosides in malignant melanoma cells to antibodies is influenced by the total ganglioside composition of the cells. *Cancer Res.*, 52, (18) 4948-4953 available from: PM:1516051
- Lopez, P.H., Zhang, G., Zhang, J., Lehmann, H.C., Griffin, J.W., Schnaar, R.L., & Sheikh, K.A. 2010. Passive transfer of IgG anti-GM1 antibodies impairs peripheral nerve repair. *J.Neurosci.*, 30, (28) 9533-9541 available from: PM:20631181
- Lunn, M.P. & Willison, H.J. 2009. Diagnosis and treatment in inflammatory neuropathies. *J.Neurol.Neurosurg.Psychiatry*, 80, (3) 249-258 available from: PM:19228670
- MacKenzie, C.R., Hiramata, T., Lee, K.K., Altman, E., & Young, N.M. 1997. Quantitative analysis of bacterial toxin affinity and specificity for glycolipid receptors by surface plasmon resonance. *J.Biol.Chem.*, 272, (9) 5533-5538 available from: PM:9038159

Mahfoud, R., Manis, A., Binnington, B., Ackerley, C., & Lingwood, C.A. 2010. A major fraction of glycosphingolipids in model and cellular cholesterol-containing membranes is undetectable by their binding proteins. *J.Biol.Chem.*, 285, (46) 36049-36059 available from: PM:20716521

Marcus, D.M., Perry, L., Gilbert, S., Preud'homme, J.L., & Kyle, R. 1989. Human IgM monoclonal proteins that bind 3-fucosyllactosamine, asialo-GM1, and GM1. *J.Immunol.*, 143, (9) 2929-2932 available from: PM:2572647

Marks, D.L., Bittman, R., & Pagano, R.E. 2008. Use of Bodipy-labeled sphingolipid and cholesterol analogs to examine membrane microdomains in cells. *Histochem.Cell Biol.*, 130, (5) 819-832 available from: PM:18820942

Mauri, L., Casellato, R., Ciampa, M.G., Uekusa, Y., Kato, K., Kaida, K., Motoyama, M., Kusunoki, S., & Sonnino, S. 2012. Anti-GM1/GD1a complex antibodies in GBS sera specifically recognize the hybrid dimer GM1-GD1a. *Glycobiology*, 22, (3) 352-360 available from: PM:21921061

McCombe, P.A., Pollard, J.D., & McLeod, J.G. 1987. Chronic inflammatory demyelinating polyradiculoneuropathy. A clinical and electrophysiological study of 92 cases. *Brain*, 110 (Pt 6), 1617-1630 available from: PM:3427403

McCombe, P.A., Pollard, J.D., & McLeod, J.G. 1988. Absence of antimyelin antibodies and serum demyelinating factors in most patients with chronic inflammatory demyelinating polyradiculoneuropathy. *Clin.Exp.Neurol.*, 25, 53-60 available from: PM:3267485

Milhiet, P.E., Domec, C., Giocondi, M.C., Van, M.N., Heitz, F., & Le, G.C. 2001. Domain formation in models of the renal brush border membrane outer leaflet. *Biophys.J.*, 81, (1) 547-555 available from: PM:11423436

Milhiet, P.E., Giocondi, M.C., & Le, G.C. 2002. Cholesterol is not crucial for the existence of microdomains in kidney brush-border membrane models. *J.Biol.Chem.*, 277, (2) 875-878 available from: PM:11717303

Monti, E., Bonten, E., D'Azzo, A., Bresciani, R., Venerando, B., Borsani, G., Schauer, R., & Tettamanti, G. 2010. Sialidases in vertebrates: a family of enzymes tailored for several cell functions. *Adv.Carbohydr.Chem.Biochem.*, 64, 403-479 available from: PM:20837202

Munro, S. 2003. Lipid rafts: elusive or illusive? *Cell*, 115, (4) 377-388 available from: PM:14622593

Murray, A. & Lawrence, G.P. 1993. How should the repeatability of clinical measurements be analysed? An assessment of analysis techniques with data from cardiovascular autonomic function tests. *Q.J.Med.*, 86, (12) 831-836 available from: PM:8108540

Mutoh, T., Tokuda, A., Inokuchi, J., & Kuriyama, M. 1998. Glucosylceramide synthase inhibitor inhibits the action of nerve growth factor in PC12 cells. *J.Biol.Chem.*, 273, (40) 26001-26007 available from: PM:9748278

- Nagai, Y., Momoi, T., Saito, M., Mitsuzawa, E., & Ohtani, S. 1976. Ganglioside syndrome, a new autoimmune neurologic disorder, experimentally induced with brain gangliosides. *Neurosci.Lett.*, 2, (2) 107-111 available from: PM:19604825
- Narla, S.N. & Sun, X.L. 2012. Glyco-macroligand microarray with controlled orientation and glycan density. *Lab on a Chip*, 12, (9) 1656-1663 available from: <http://dx.doi.org/10.1039/C2LC21224B>
- Niedieck, B. 1975a. On a glycolipid hapten of myelin. *Prog.Allergy*, 18, 353-422 available from: PM:807919
- Niedieck, B. 1975b. On the function of lecithin and lecithin substitutes in the immune precipitation reaction of galactosyl lipids. *Immunochemistry.*, 12, (10) 807-812 available from: PM:812798
- Niedieck, B. & Kuck, U. 1976. Comparative studies of galactosyl lipid immune reactions with and without cholesterol and cholesterol derivatives. *Immunochemistry.*, 13, (9) 765-769 available from: PM:825444
- Nobile-Orazio, E., Cappellari, A., & Priori, A. 2005. Multifocal motor neuropathy: current concepts and controversies. *Muscle Nerve*, 31, (6) 663-680 available from: PM:15770650
- Nobile-Orazio, E., Giannotta, C., & Briani, C. 2010. Anti-ganglioside complex IgM antibodies in multifocal motor neuropathy and chronic immune-mediated neuropathies. *J.Neuroimmunol.*, 219, (1-2) 119-122 available from: PM:20006388
- Nobile-Orazio, E., Giannotta, C., Musset, L., Messina, P., & Leger, J.M. 2013. Sensitivity and predictive value of anti-GM1/galactocerebroside IgM antibodies in multifocal motor neuropathy. *J.Neurol.Neurosurg.Psychiatry* available from: PM:23907602
- Nyholm, P.G., Pascher, I., & Sundell, S. 1990. The effect of hydrogen bonds on the conformation of glycosphingolipids. Methylated and unmethylated cerebroside studied by X-ray single crystal analysis and model calculations. *Chem.Phys.Lipids*, 52, (1) 1-10 available from: PM:2306786
- O'Hanlon, G.M., Paterson, G.J., Veitch, J., Wilson, G., & Willison, H.J. 1998. Mapping immunoreactive epitopes in the human peripheral nervous system using human monoclonal anti-GM1 ganglioside antibodies. *Acta Neuropathol.*, 95, (6) 605-616 available from: PM:9650753
- O'Hanlon, G.M., Paterson, G.J., Wilson, G., Doyle, D., McHardie, P., & Willison, H.J. 1996. Anti-GM1 ganglioside antibodies cloned from autoimmune neuropathy patients show diverse binding patterns in the rodent nervous system. *J.Neuropathol.Exp.Neurol.*, 55, (2) 184-195 available from: PM:8786377
- Ogawa, G., Kaida, K., Kuwahara, M., Kimura, F., Kamakura, K., & Kusunoki, S. 2013. An antibody to the GM1/GalNAc-GD1a complex correlates with development of pure motor Guillain-Barre syndrome with reversible conduction failure. *J.Neuroimmunol.*, 254, (1-2) 141-145 available from: PM:23000056

- Ogawa-Goto, K. & Abe, T. 1998. Gangliosides and glycosphingolipids of peripheral nervous system myelins--a minireview. *Neurochem.Res.*, 23, (3) 305-310 available from: PM:9482242
- Ogawa-Goto, K., Funamoto, N., Ohta, Y., Abe, T., & Nagashima, K. 1992. Myelin gangliosides of human peripheral nervous system: an enrichment of GM1 in the motor nerve myelin isolated from cauda equina. *J.Neurochem.*, 59, (5) 1844-1849 available from: PM:1402926
- Oldfield, E. & Chapman, D. 1971. Effects of cholesterol and cholesterol derivatives on hydrocarbon chain mobility in lipids. *Biochem.Biophys.Res.Commun.*, 43, (3) 610-616 available from: PM:4327446
- Oldfield, E. & Chapman, D. 1972. Dynamics of lipids in membranes: Heterogeneity and the role of cholesterol. *FEBS Lett.*, 23, (3) 285-297 available from: PM:11946637
- Oyelaran, O., Li, Q., Farnsworth, D., & Gildersleeve, J.C. 2009a. Microarrays with Varying Carbohydrate Density Reveal Distinct Subpopulations of Serum Antibodies. *Journal of Proteome Research*, 8, (7) 3529-3538 available from: ISI:000267694600027
- Oyelaran, O., McShane, L.M., Dodd, L., & Gildersleeve, J.C. 2009b. Profiling Human Serum Antibodies with a Carbohydrate Antigen Microarray. *Journal of Proteome Research*, 8, (9) 4301-4310 available from: <http://dx.doi.org/10.1021/pr900515y>
- Parry, G.J. 1994. Antiganglioside antibodies do not necessarily play a role in multifocal motor neuropathy. *Muscle Nerve*, 17, (1) 97-99 available from: PM:8264709
- Parry, G.J. & Clarke, S. 1988. Multifocal acquired demyelinating neuropathy masquerading as motor neuron disease. *Muscle Nerve*, 11, (2) 103-107 available from: PM:3343985
- Paterson, G., Wilson, G., Kennedy, P.G., & Willison, H.J. 1995. Analysis of anti-GM1 ganglioside IgM antibodies cloned from motor neuropathy patients demonstrates diverse V region gene usage with extensive somatic mutation. *J.Immunol.*, 155, (6) 3049-3059 available from: PM:7673721
- Pestronk, A. 2000. Testing for serum IgM binding to GM1 ganglioside in clinical practice. *Neurology*, 54, (12) 2353-2354 available from: PM:10881275
- Pestronk, A. & Choksi, R. 1997. Multifocal motor neuropathy. Serum IgM anti-GM1 ganglioside antibodies in most patients detected using covalent linkage of GM1 to ELISA plates. *Neurology*, 49, (5) 1289-1292 available from: PM:9371910
- Pestronk, A., Choksi, R., Blume, G., & Lopate, G. 1997. Multifocal motor neuropathy: serum IgM binding to a GM1 ganglioside-containing lipid mixture but not to GM1 alone. *Neurology*, 48, (4) 1104-1106 available from: PM:9109910
- Pestronk, A., Cornblath, D.R., Ilyas, A.A., Baba, H., Quarles, R.H., Griffin, J.W., Alderson, K., & Adams, R.N. 1988. A treatable multifocal motor neuropathy with

antibodies to GM1 ganglioside. *Annals of Neurology*, 24, (1) 73-78 available from: PM:2843079

Pestronk, A. & Li, F. 1991. Motor neuropathies and motor neuron disorders: association with antiglycolipid antibodies. *Adv.Neurol.*, 56, 427-432 available from: PM:1649544

Pike, L.J. 2006. Rafts defined: a report on the Keystone Symposium on Lipid Rafts and Cell Function. *J.Lipid Res.*, 47, (7) 1597-1598 available from: PM:16645198

Plomp, J.J. & Willison, H.J. 2009. Pathophysiological actions of neuropathy-related anti-ganglioside antibodies at the neuromuscular junction. *J.Physiol*, 587, (Pt 16) 3979-3999 available from: PM:19564393

Prenner, E., Honsek, G., Honig, D., Mobius, D., & Lohner, K. 2007. Imaging of the domain organization in sphingomyelin and phosphatidylcholine monolayers. *Chem.Phys.Lipids*, 145, (2) 106-118 available from: PM:17188673

Radhakrishnan, A. 2010. Phase separations in binary and ternary cholesterol-phospholipid mixtures. *Biophys.J.*, 98, (9) L41-L43 available from: PM:20441733

Ramstedt, B. & Slotte, J.P. 1999. Interaction of cholesterol with sphingomyelins and acyl-chain-matched phosphatidylcholines: a comparative study of the effect of the chain length. *Biophys.J.*, 76, (2) 908-915 available from: PM:9929492

Rebolj, K., Ulrih, N.P., Macek, P., & Sepcic, K. 2006. Steroid structural requirements for interaction of ostreolysin, a lipid-raft binding cytolysin, with lipid monolayers and bilayers. *Biochim.Biophys.Acta*, 1758, (10) 1662-1670 available from: PM:16857161

Reed, G.F., Lynn, F., & Meade, B.D. 2002. Use of coefficient of variation in assessing variability of quantitative assays. *Clin.Diagn.Lab Immunol.*, 9, (6) 1235-1239 available from: PM:12414755

Rinaldi, S. 2013. Update on Guillain-Barre syndrome. *J.Peripher.Nerv.Syst.*, 18, (2) 99-112 available from: PM:23781958

Rinaldi, S., Brennan, K.M., Goodyear, C.S., O'Leary, C., Schiavo, G., Crocker, P.R., & Willison, H.J. 2009. Analysis of lectin binding to glycolipid complexes using combinatorial glycoarrays. *Glycobiology*, 19, (7) 789-796 available from: PM:19349623

Rinaldi, S., Brennan, K.M., Kalna, G., Walgaard, C., van, D.P., Jacobs, B.C., Yu, R.K., Mansson, J.E., Goodyear, C.S., & Willison, H.J. 2013. Antibodies to heteromeric glycolipid complexes in guillain-barre syndrome. *PLoS.One.*, 8, (12) e82337 available from: PM:24358172

Rinaldi, S., Brennan, K.M., & Willison, H.J. 2012. Combinatorial glycoarray. *Methods Mol.Biol.*, 808, 413-423 available from: PM:22057541

Rinaldi, S. & Willison, H.J. 2008. Ganglioside antibodies and neuropathies. *Curr.Opin.Neurol.*, 21, (5) 540-546 available from: PM:18769247

- Roth, G., Rohr, J., Magistris, M.R., & Ochsner, F. 1986. Motor neuropathy with proximal multifocal persistent conduction block, fasciculations and myokymia. Evolution to tetraplegia. *Eur.Neurol.*, 25, (6) 416-423 available from: PM:3024989
- Sadiq, S.A., Thomas, F.P., Kilidireas, K., Protopsaltis, S., Hays, A.P., Lee, K.W., Romas, S.N., Kumar, N., Van den Berg, L., Santoro, M., & . 1990. The spectrum of neurologic disease associated with anti-GM1 antibodies. *Neurology*, 40, (7) 1067-1072 available from: PM:2162499
- Saida, K., Saida, T., Brown, M.J., & Silberberg, D.H. 1979. In vivo demyelination induced by intraneural injection of anti-galactocerebroside serum: a morphologic study. *Am.J.Pathol.*, 95, (1) 99-116 available from: PM:434114
- Sandhoff, K. & Kolter, T. 2003. Biosynthesis and degradation of mammalian glycosphingolipids. *Philos.Trans.R.Soc.Lond B Biol.Sci.*, 358, (1433) 847-861 available from: PM:12803917
- Shi, J., Yang, T., Kataoka, S., Zhang, Y., Diaz, A.J., & Cremer, P.S. 2007. GM1 clustering inhibits cholera toxin binding in supported phospholipid membranes. *Journal of the American Chemical Society*, 129, (18) 5954-5961 available from: PM:17429973
- Shichijo, S. & Alving, C.R. 1986. Inhibitory effects of gangliosides on immune reactions of antibodies to neutral glycolipids in liposomes. *Biochim.Biophys.Acta*, 858, (1) 118-124 available from: PM:3707956
- Shogomori, H. & Brown, D.A. 2003. Use of detergents to study membrane rafts: the good, the bad, and the ugly. *Biol.Chem.*, 384, (9) 1259-1263 available from: PM:14515986
- Simons, K. & Ikonen, E. 1997. Functional rafts in cell membranes. *Nature*, 387, (6633) 569-572 available from: PM:9177342
- Singer, S.J. & Nicolson, G.L. 1972. The fluid mosaic model of the structure of cell membranes. *Science*, 175, (4023) 720-731 available from: PM:4333397
- Sonnino, S., Mauri, L., Chigorno, V., & Prinetti, A. 2007. Gangliosides as components of lipid membrane domains. *Glycobiology*, 17, (1) 1R-13R available from: PM:16982663
- Spiegel, S., Foster, D., & Kolesnick, R. 1996. Signal transduction through lipid second messengers. *Curr.Opin.Cell Biol.*, 8, (2) 159-167 available from: PM:8791422
- Sumner, A.J., Saida, K., Saida, T., Silberberg, D.H., & Asbury, A.K. 1982. Acute conduction block associated with experimental antiserum-mediated demyelination of peripheral nerve. *Annals of Neurology*, 11, (5) 469-477 available from: PM:6285800
- Svennerholm, L. 1956a. Composition of gangliosides from human brain. *Nature*, 177, (4507) 524-525 available from: PM:13321892

- Svennerholm, L. 1956b. On the isolation and characterization of N-acetyl-sialic acid. *Acta Soc.Med.Ups.*, 61, (1-2) 74-85 available from: PM:13339505
- Svennerholm, L. 1994. Designation and schematic structure of gangliosides and allied glycosphingolipids. *Prog.Brain Res.*, 101, XI-XIV available from: PM:8029441
- Svennerholm, L., Bostrom, K., Fredman, P., Jungbjer, B., Lekman, A., Mansson, J.E., & Rynmark, B.M. 1994. Gangliosides and allied glycosphingolipids in human peripheral nerve and spinal cord. *Biochim.Biophys.Acta*, 1214, (2) 115-123 available from: PM:7918590
- Svennerholm, L., Bostrom, K., Fredman, P., Jungbjer, B., Mansson, J.E., & Rynmark, B.M. 1992. Membrane lipids of human peripheral nerve and spinal cord. *Biochim.Biophys.Acta*, 1128, (1) 1-7 available from: PM:1390872
- Taneichi, M., Ishida, H., Kajino, K., Ogasawara, K., Tanaka, Y., Kasai, M., Mori, M., Nishida, M., Yamamura, H., Mizuguchi, J., & Uchida, T. 2006. Antigen chemically coupled to the surface of liposomes are cross-presented to CD8+ T cells and induce potent antitumor immunity. *J.Immunol.*, 177, (4) 2324-2330 available from: PM:16887993
- Taneichi, M., Tanaka, Y., Kakiuchi, T., & Uchida, T. 2010. Liposome-coupled peptides induce long-lived memory CD8 T cells without CD4 T cells. *PLoS.One.*, 5, (11) e15091 available from: PM:21264321
- Tatsumoto, M., Koga, M., Gilbert, M., Odaka, M., Hirata, K., Kuwabara, S., & Yuki, N. 2006. Spectrum of neurological diseases associated with antibodies to minor gangliosides GM1b and GalNAc-GD1a. *J.Neuroimmunol.*, 177, (1-2) 201-208 available from: PM:16844234
- Temmerman, K. & Nickel, W. 2009. A novel flow cytometric assay to quantify interactions between proteins and membrane lipids. *J.Lipid Res.*, 50, (6) 1245-1254 available from: PM:19144996
- Tettamanti, G., Bonali, F., Marchesini, S., & Zambotti, V. 1973a. A new procedure for the extraction, purification and fractionation of brain gangliosides. *Biochim.Biophys.Acta*, 296, (1) 160-170 available from: PM:4693502
- Tettamanti, G., Preti, A., Lombardo, A., Bonali, F., & Zambotti, V. 1973b. Parallelism of subcellular location of major particulate neuraminidase and gangliosides in rabbit brain cortex. *Biochim.Biophys.Acta*, 306, (3) 466-477 available from: PM:4726869
- Todeschini, A.R., Dos Santos, J.N., Handa, K., & Hakomori, S.I. 2008. Ganglioside GM2/GM3 complex affixed on silica nanospheres strongly inhibits cell motility through CD82/cMet-mediated pathway. *Proc.Natl.Acad.Sci.U.S.A*, 105, (6) 1925-1930 available from: PM:18272501
- Townson, K., Boffey, J., Nicholl, D., Veitch, J., Bundle, D., Zhang, P., Samain, E., Antoine, T., Bernardi, A., Arosio, D., Sonnino, S., Isaacs, N., & Willison, H.J. 2007. Solid phase immunoadsorption for therapeutic and analytical studies on neuropathy-associated anti-GM1 antibodies. *Glycobiology*, 17, (3) 294-303 available from: PM:17145744

- van Asseldonk, J.T., Franssen, H., Van den Berg-Vos RM, Wokke, J.H., & van den Berg, L.H. 2005. Multifocal motor neuropathy. *Lancet Neurol.*, 4, (5) 309-319 available from: PM:15847844
- van Doorn, P.A., Ruts, L., & Jacobs, B.C. 2008. Clinical features, pathogenesis, and treatment of Guillain-Barre syndrome. *Lancet Neurol.*, 7, (10) 939-950 available from: PM:18848313
- van Schaik, I.N., Bossuyt, P.M., Brand, A., & Vermeulen, M. 1995. Diagnostic value of GM1 antibodies in motor neuron disorders and neuropathies: a meta-analysis. *Neurology*, 45, (8) 1570-1577 available from: PM:7644057
- van, M.G., Voelker, D.R., & Feigenson, G.W. 2008. Membrane lipids: where they are and how they behave. *Nat.Rev.Mol.Cell Biol.*, 9, (2) 112-124 available from: PM:18216768
- Veatch, S.L. & Keller, S.L. 2005a. Miscibility phase diagrams of giant vesicles containing sphingomyelin. *Phys.Rev.Lett.*, 94, (14) 148101 available from: PM:15904115
- Veatch, S.L. & Keller, S.L. 2005b. Seeing spots: complex phase behavior in simple membranes. *Biochim.Biophys.Acta*, 1746, (3) 172-185 available from: PM:16043244
- Wang, D., Carroll, G.T., Turro, N.J., Koberstein, J.T., Kováčik, P., Saksena, R., Adamo, R., Herzenberg, L.A., Herzenberg, L.A., & Steinman, L. 2007. Photogenerated glycan arrays identify immunogenic sugar moieties of Bacillus anthracis exosporium. *PROTEOMICS*, 7, (2) 180-184 available from: <http://dx.doi.org/10.1002/pmic.200600478>
- Wehner, J.W., Hartmann, M., & Lindhorst, T.K. 2013. Are multivalent cluster glycosides a means of controlling ligand density of glycoarrays? *Carbohydrate Research*, 371, (0) 22-31 available from: <http://www.sciencedirect.com/science/article/pii/S0008621513000463>
- Willison, H.J. 2005. Ganglioside complexes: new autoantibody targets in Guillain-Barre syndromes. *Nat.Clin.Pract.Neurol.*, 1, (1) 2-3 available from: PM:16932482
- Willison, H.J., Paterson, G., Kennedy, P.G., & Veitch, J. 1994. Cloning of human anti-GM1 antibodies from motor neuropathy patients. *Annals of Neurology*, 35, (4) 471-478 available from: PM:8154875
- Willison, H.J., Townson, K., Veitch, J., Boffey, J., Isaacs, N., Andersen, S.M., Zhang, P., Ling, C.C., & Bundle, D.R. 2004. Synthetic disialylgalactose immunoabsorbents deplete anti-GQ1b antibodies from autoimmune neuropathy sera. *Brain*, 127, (Pt 3) 680-691 available from: PM:14960498
- Willison, H.J., Veitch, J., Swan, A.V., Baumann, N., Comi, G., Gregson, N.A., Illa, I., Zielasek, J., & Hughes, R.A. 1999. Inter-laboratory validation of an ELISA for the determination of serum anti-ganglioside antibodies. *Eur.J.Neurol.*, 6, (1) 71-77 available from: PM:10209353

- Willison, H.J. & Yuki, N. 2002. Peripheral neuropathies and anti-glycolipid antibodies. *Brain*, 125, (Pt 12) 2591-2625 available from: PM:12429589
- Wolf, C., Koumanov, K., Tenchov, B., & Quinn, P.J. 2001. Cholesterol favors phase separation of sphingomyelin. *Biophys.Chem.*, 89, (2-3) 163-172 available from: PM:11254209
- Yahi, N., Aulas, A., & Fantini, J. 2010. How cholesterol constrains glycolipid conformation for optimal recognition of Alzheimer's beta amyloid peptide (Abeta1-40). *PLoS.One.*, 5, (2) e9079 available from: PM:20140095
- Yahi, N., Baghdiguan, S., Moreau, H., & Fantini, J. 1992. Galactosyl ceramide (or a closely related molecule) is the receptor for human immunodeficiency virus type 1 on human colon epithelial HT29 cells. *J.Virol.*, 66, (8) 4848-4854 available from: PM:1378511
- Young, I.T. 1977. Proof without prejudice: use of the Kolmogorov-Smirnov test for the analysis of histograms from flow systems and other sources. *J.Histochem.Cytochem.*, 25, (7) 935-941 available from: PM:894009
- Young, K.T., Davis, L.M., & Dirita, V.J. 2007. Campylobacter jejuni: molecular biology and pathogenesis. *Nat.Rev.Microbiol.*, 5, (9) 665-679 available from: PM:17703225
- Yuki, N. & Hartung, H.P. 2012. Guillain-Barre syndrome. *N.Engl.J.Med.*, 366, (24) 2294-2304 available from: PM:22694000
- Yuki, N., Tagawa, Y., & Handa, S. 1996. Autoantibodies to peripheral nerve glycosphingolipids SPG, SLPG, and SGPG in Guillain-Barre syndrome and chronic inflammatory demyelinating polyneuropathy. *J.Neuroimmunol.*, 70, (1) 1-6 available from: PM:8862128
- Zhang, J. & Zhou, X. 2011. Novel 3-dimensional dendrimer platform for glycolipid microarray. *Biosensors and Bioelectronics*, 28, (1) 355-361 available from: <http://www.sciencedirect.com/science/article/pii/S0956566311004726>
- Zhang, Y., Campbell, C., Li, Q., & Gildersleeve, J.C. 2010. Multidimensional glycan arrays for enhanced antibody profiling. *Molecular BioSystems*, 6, (9) 1583-1591 available from: <http://dx.doi.org/10.1039/C002259D>
- Zidar, J., Merzel, F., Hodoscek, M., Rebolj, K., Sepcic, K., Macek, P., & Janezic, D. 2009. Liquid-ordered phase formation in cholesterol/sphingomyelin bilayers: all-atom molecular dynamics simulations. *J.Phys.Chem.B*, 113, (48) 15795-15802 available from: PM:19929009
- Zoller, I., Meixner, M., Hartmann, D., Bussow, H., Meyer, R., Gieselmann, V., & Eckhardt, M. 2008. Absence of 2-hydroxylated sphingolipids is compatible with normal neural development but causes late-onset axon and myelin sheath degeneration. *J.Neurosci.*, 28, (39) 9741-9754 available from: PM:18815260